ABSTRACT

MCCULLOCH, RYAN STERLING. Differential Chondrocyte Gene Expression Subsequent to *In Vitro* Shear and Axial Impactions in an Articular Cartilage Injury Model of Osteoarthritis. (Under the direction of Peter L. Mente.)

Osteoarthritis (OA) is a degenerative disease of the articular joints. OA leads to fibrillation, degradation, and lesions of the articular joint surfaces, resulting in pain and decreased mobility. A prior joint injury is a known risk factor for the development of OA. Therefore, this study used *in vitro* impact injuries to porcine patellae to model the early degenerative process. The goal was to examine gene expression levels in a panel of 18 OA associated genes related to: the cartilage matrix, degradative enzymes and their inhibitors, inflammatory response and signaling, and cell apoptosis and proliferation. Gene expression changes were evaluated by comparing axial or shear impact specimens to non-impacted control specimens. Identifying the gene expression changes following an injury may help identify potential targets for future intervention to slow disease progression.

Seventy-two patellae were randomly assigned to one of three treatments: axial impaction (2000 N compressive load), shear impaction (500N compressive load by 10mm tangential displacement), or a non-impacted control. Impactions were conducted in a hydraulic load frame with a stainless steel impactor. After the impaction, the patellae were placed in organ culture and full-thickness cartilage tissue specimens were harvested at 0, 3, 7, or 14 days post-injury. Total RNA was extracted from each specimen, and expression levels

were measured using quantitative real-time PCR. Differential gene expression was then evaluated by computing fold changes and evaluating statistical differences with a mixed model.

Using both Best Keeper and geNorm software, four reference genes were identified as having the most stable expression in porcine articular cartilage specimens exposed to these loading scenarios and culture conditions : *actb*, *gapdh, sdha*, and *ppia*. The geometric mean of these four genes was used to normalize the results for the 18 genes of interest.

Both the relative rise in *col2a1* at day 3 in shear vs. axial specimens, and the higher expression of *agc* and *sox-9* (a transcription factor for *agc* and *col2a1*) at the later time points may signify that the shear specimens are mounting a stronger repair attempt. However, the relative increase in *col1a1*, a collagen not normally expressed in articular cartilage, may indicate a less effective repair by the shear impaction specimens. The higher initial *mmp* levels in both axial and shear specimens as compared to control specimens suggests that the initial matrix breakdown following injury tapers off by the later time points. Increased expression of *timp-2*, an *mmp* inhibitor, indicates that cells in the shear specimens make a stronger attempt, relative to axial specimens, to limit matrix breakdown. The lowered expression levels of the genes associated with inflammatory response and signaling at the later time points may imply less inflammation for both

shear and axial treatments. Increased expression of *casp-8* may indicate that apoptosis is initiated at the later time points in the shear specimens.

The higher expression levels of cartilage matrix components in shear specimens compared to axial specimens signifies a more aggressive repair effort underway in the shear specimens, although the expression of *col1a1* indicates this repair effort may not be correct. The decreased levels of degradative enzymes in shear specimens at the later time points denote an attempt to preserve the cartilage matrix. The shear impaction model provides an *in vitro* method of studying the early degenerative changes associated with OA progression.

Differential Chondrocyte Gene Expression Subsequent to *In Vitro* Shear and Axial Impactions in an Articular Cartilage Injury Model of Osteoarthritis

by
Ryan Sterling McCulloch

A dissertation submitted to the Graduate Faculty of
North Carolina State University
in partial fulfillment of the
requirements for the Degree of
Doctor of Philosophy

Biomedical Engineering

Raleigh, North Carolina

2011

APPROVED BY:

_____	_____
Melissa S. Ashwell	Simon C. Roe
_____	_____
Ola L.A. Harrysson	Paul S. Weinhold

_____
Peter L. Mente
Chair of Advisory Committee

DEDICATION

This dissertation is dedicated to my wonderful wife, Danielle. She has shared in the many challenges, sacrifices, and triumphs of this endeavor, and without her support it would not have been possible.

BIOGRAPHY

Ryan S. McCulloch attended NCSU as an undergraduate on a Navy academic scholarship. Upon graduating with a B.S. in Mechanical Engineering, he received a commission as an Officer in the United States Navy. After completing the Naval Nuclear Power Training Program, Ryan was stationed on the USS Charlotte, a fast-attack submarine. While on board he held numerous engineering managerial positions and also received a Masters in Engineering Management from Old Dominion University.

Following the completion of his Naval service, Ryan moved to St. Paul, MN where he joined Guidant Corporation as part of the Clinical Application Research Studies department. There he was able to use his engineering background to achieve medical benefits for patients by developing studies for Guidant's pacemaker and internal cardiac defibrillator business.

After getting married, Ryan and his wife traveled around the world on a shoestring budget. Upon their return to the US, Ryan entered the joint Biomedical Engineering program at UNC/NCSU to pursue his long-time goal of developing his engineering skills to improve medical outcomes for patients. He obtained a MS in Biomedical Engineering for work studying hip implants. Upon completion of his PhD work, he plans to pursue his interests in the biomedical field.

ACKNOWLEDGEMENTS

While a PhD is awarded to one individual, its completion is not possible without the help and contributions of numerous people. Although it is not possible to list everyone, I would like to thank those who have had a significant impact on my education.

- Dr. Peter Mente, my advisor, provided endless amounts of discussion, taught me a tremendous amount about biomechanics, and was always ready to supply guidance. His unselfish devotion to his work was refreshing.
- Dr. Melissa Ashwell taught me all that I know about molecular biology. She was an instrumental advisor for my doctoral work.
- Dr. Simon Roe served as an excellent advisor for my MS, was on my PhD committee, and was the individual most responsible for starting and encouraging me on a research path. He has always been available for discussion, guidance, and support.
- Dr. Ola Harrysson has been instrumental in my education and development in the biomedical field. His excitement about his field of work is contagious.
- Dr. Paul Weinhold has provided guidance along my PhD path and has provided me with valuable exposure to the clinical side of the field.
- Audrey O'Nan, was critical to my success. She very patiently guided me through the development, trials, and difficulties of the methods used in this work, and she was always good-natured about my infinite questions.

- Dr. Richard Shoge, a fellow graduate student, was a good friend and was critical the impactions conducted for this study.
- There are numerous professors who motivated me to achieve new intellectual goals in my coursework. I cannot name them all here, but one in particular made a tremendous impact on my education, Dr. Robert Grossfeld. He exposed me to the world of physiology over two semesters. His course was extremely challenging, yet the most rewarding I have ever taken. His dedication to his students is unrivaled.
- The American taxpayers made this research possible with financial support via the NIAMS/NIH grant number: 1 R03 AR054557-01A1. I appreciate their implicit trust in those of us who conduct research and endeavor to use their funding wisely and responsibly.
- My parents, Richard and Joan McCulloch, are responsible for encouraging my engineering interests and teaching me the importance of an education from very early in my life. The taught me the value of hard work, persistence, and independence. I would never have started down this path without them.
- My son, Tate, has earned my gratefulness for so often being the bright spot at the end of a long day and for his encouragement as I worked on what he termed my "big paper."

- Most importantly, I would like to thank my wife, Danielle McCulloch, for her years of support as I pursued this dream. Her continuous understanding, patience, and encouragement are what made this pursuit possible. She equally shares in the attainment of this PhD.

TABLE OF CONTENTS

LIST OF TABLES

Page

LIST OF FIGURES

Page

1. INTRODUCTION

1.1 Motivation

Osteoarthritis (OA) is a debilitating degenerative joint disease that affects an estimated 27 million people in the United States [1]. The number of individuals who suffer from OA is predicted to increase over the coming decades as a function of population growth, obesity, and aging [1, 2]. While OA is a disease of the whole joint, the most traumatic effect is its progressive destruction of the load bearing surfaces results in pain and debilitation. As the disease progresses, the cartilage surface becomes fibrillated, the matrix constituents break down, and eventually cartilage lesions develop. These changes affect the ability of the joints to smoothly articulate and can cause severe pain and lack of mobility for the sufferer. Because cartilage is avascular (no blood supply), the chondrocytes have a low metabolism and therefore, there is little hope of successful self-repair.

A prior joint injury or trauma is a known predisposing factor for the development of OA [3]. A vehicular accident or a sports-related injury may be the cause of the impact and may lead to later OA development in the joint. Many prior studies have evaluated impact injuries to articular cartilage as a method of studying early-stage OA changes [4-6]. Primarily these studies have evaluated loads delivered normal to the cartilage surface and have neglected shear loads at the articular surface [7-9]. It is likely that a real physiologic injury will generate multiple axes of loading beyond just normal compressive forces, and will include damaging shear forces in the joint.

Evaluating the gene expression changes in the days and weeks following an impact injury will provide a more complete picture of the early changes leading to OA. Identifying gene expression changes that lead to OA development will provide targets for future therapeutic intervention before OA progresses to the point of causing debilitation.

1.2 Experimental Outline

This study utilized a mechanical impact model to study early changes in cartilage following an injury which may lead to OA. The articular surface of porcine patellae were impacted with either an axial compressive load, (normal to the surface) or an axial load combined with a transverse shear load that included both compressive loads and larger tangential shear loading. Following impacts patellae were maintained in culture for up to two weeks so that changes could be followed over time. Full thickness cartilage specimens were collected from directly beneath the impacted area, and areas adjacent to the impact site, at 0, 3, 7, and 14 days following the impaction. Total RNA was extracted from the cartilage specimens and gene expression levels were evaluated with quantitative real time reverse transcriptase polymerase chain reaction (qRT-PCR). A panel of genes identified from relevant reports in literature and our previous research related to OA were evaluated.

The *in vitro* impact model provided a means of generating OA symptoms in a controlled laboratory setting. The impact methods utilized allowed for an evaluation of results from both a more traditional normal loading model and a more complex shear loading model

compared to a non-impacted control. Changes in the gene expression reflected the response of the chondrocytes to the loading event, and those changes were measured over a two-week time period as an indication of the progression of very early-stage OA.

1.3 Specific Aim

Specific Aim:

Evaluate differential chondrocyte gene expression levels following axial and shear impaction injuries to articular cartilage to develop an understanding of the early cellular changes that initiate the degenerative process. In this model gene expression was evaluated in patellae over the first two weeks post-impact. The two types of impaction treatments (axial and shear) were compared to each other and non-impacted control specimens.

Hypothesis 1a:

Early gene expression changes in genes associated with OA progression can be detected over the 2 weeks following an impact trauma to articular cartilage.

Chondrocytes in normal and shear impacted tissue will show significant changes in gene expression relative to the non-impacted control tissue in many areas of biological activity, including increased matrix repair efforts, higher degradative enzyme activity, an increased inflammatory response and elevated levels of apoptosis.

Hypothesis 1b:

The higher shear stresses in the shear impaction model will cause more mechanical tissue damage to the chondrocytes and the cartilage matrix than the compressive loads of the axial impactions. Gene transcription of degradative enzymes, and indicators of biological stress will be more highly expressed in the shear specimens than in the axial or control specimens.

Hypothesis 2:

Due to the higher levels of loading beyond the immediate impact area that arise as a result of the shear loading, impactions with larger shear forces will cause more mechanical tissue damage in the cartilage areas adjacent to the impact site than an axial (compressive) impaction alone. Due to the induced damage, these shear specimens will have higher expression of genes related to cartilage degradation, inflammation, and biological stress signaling.

2. BACKGROUND

2.1 Articular Cartilage Components and Structure

Articular cartilage is an avascular, aneural, and alymphatic tissue covering the bones in the joint surfaces of the human body. It provides a lubricious bearing surface for articulating joints, and some shock absorption capability during movement. Additionally, because of its ability to deform at bearing locations, cartilage provides distribution of contact stresses. Cartilage is composed of cells embedded in a matrix, or scaffold. Chondrocytes are the only cells found in cartilage, and are found spread sparsely through the material. Chondroblasts are the precursor cells (early stage chondrocytes) that produce the matrix. In the matrix they occupy spaces referred to as lacunae and are referred to as chondrocytes [10]. The cartilage matrix is a complex material and consists water and electrolytes, collagen, proteoglycans, and other proteins [11].

Cartilage micro-structure:

Collagen is the most prevalent protein group in the human body. Type II collagen is the primary collagen in articular cartilage and is the most prevalent, accounting for > 90% of the collagen in articular cartilage [12]. Type II collagen is made up of three $\alpha 1$ protein chains in a right-handed helix. Type II collagen forms long fibers that provide structure for the cartilage matrix, resist tensile forces, and restrain the swelling pressure generated proteoglycans.

Proteoglycans are the next major constituent of articular cartilage. They are large molecules made up of a core protein and covalently attached glycosaminoglycan (GAG) chains. In articular cartilage, the GAG chains are primarily chondroitin and keratin sulfate [13]. Proteoglycans can exist as monomers 200 to 400nm long. Importantly for cartilage properties, though, proteoglycans also exist as large aggregating proteoglycans in the matrix, known as aggrecan. Approximately 90% of the proteoglycan in cartilage is in the form of aggrecan [13]. Aggrecan is composed of up to 150 proteoglycan monomers attached to a hyaluronan backbone (hyaluronic acid – HA). The large size of the aggrecan molecules keeps them relatively stable in the matrix, making it difficult for them to diffuse out. GAGs have a large negative charge that repulses other GAGs in the aggrecan molecule and attracts water molecules. Therefore the negative charge creates a swelling effect in the matrix by pulling in water, and repelling other GAGs.

Cartilage macro-structure:

Articular cartilage consists of both water and solid components. In its natural state, water makes up between 70 and 85% of the weight of cartilage, collagen makes up between 10 to 20% of the wet weight, and proteoglycans make up 5-10% of the wet weight of cartilage. Cartilage consists of three distinct layers in cross-section: a top layer, or surface tangential zone (superficial layer), a middle zone, and a deep zone. Beneath these three zones is a layer of calcified cartilage that forms a rigid attachment to the underlying subchondral bone.

The surface tangential zone is between 10-20% of the total thickness of cartilage, and has the highest content of collagen at 85% dry weight. Of the three zones, aggrecan concentration is the lowest in this zone. The collagen fibers are thin, densely packed and oriented parallel to the surface in this zone [14]. The articular surface is where cartilage is subject to the highest tensile forces, and the orientation of the fibers at the surface zone provides the tissue's strongest resistance to these forces. The fiber orientation also helps the tissue to resist shear strains when subjected to shearing forces. The fibers in these zones are highly oriented to minimize friction and damage under normal loading, and their orientation can be determined using the method developed by Hultkrantz [15]. With this method, a pin dipped in India ink is used to prick the cartilage surface and is removed with some ink remaining in the fibers. The pin separates the layers of fibers during insertion and the resulting ink pattern shows the fiber orientation (Figure 2.1) [16].

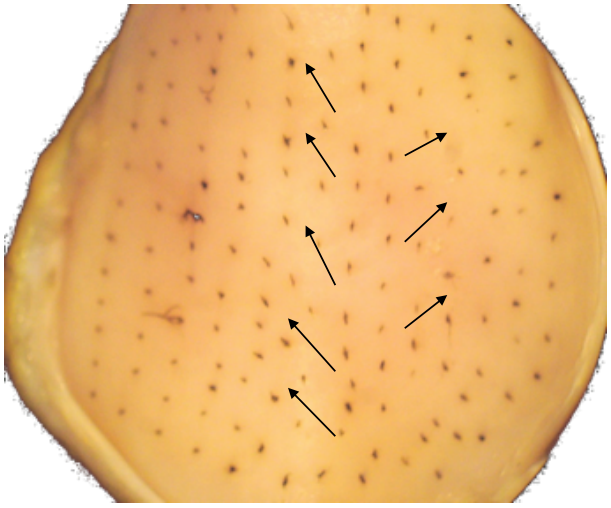

Figure 2.1. India ink pinprick of articular cartilage. A porcine patella articular surface was pricked with india ink to reveal fiber orientation in the surface layer. Overlying arrows are drawn to show the predominant orientation of the fibers.

The middle zone is directly beneath the surface tangential zone and occupies 40-60% of the thickness of the articular cartilage. Collagen content in this zone is lower than the superficial zone, and the fibers are thicker [12]. The fibers possess a random orientation and are homogenously distributed [14]. The aggrecan content is highest in this zone.

The deep zone occupies the bottom 30% of the cartilage layer thickness and contains a higher proteoglycan content than the mid zone (but not as high as the surface tangential zone). The collagen content is lowest in this zone, and the fibers form bundles that are oriented perpendicular to the surface and cross the tidemark region to insert into the calcified layer. The bundles then subdivide to form an interlocking network that anchor the tissue to the bone [14].

Water is the largest component of articular cartilage and accounts for between 70-85% of the wet weight of cartilage. Water is pulled into the matrix from the surrounding tissue by the negative charge of the proteoglycans. The mechanical properties of cartilage are very dependent upon both the internal movement of water within the cartilage and the efflux of water from the matrix during loading.

The articular joint is encased in a synovial capsule, with synovial fluid filling the void spaces of the joint. Because cartilage is an avascular tissue, it relies upon the synovial fluid for delivery of nutrients and removal of wastes. The attractive properties of aggrecan pull water from the synovial fluid in the interarticular spaces into the cartilage

matrix. The aggrecan continues to draw water and swell the tissue until restrained by the collagen network. A pre-stress of the tissue is developed by the balancing of the proteoglycan swelling forces and the collagen restraining forces. As the joint is loaded, the smooth surface of the cartilage resists shearing due to the orientation of the fibers and the low friction coefficient from the synovial fluid. Also, as the joint is loaded, the layer deforms slightly to increase the bearing surface between opposing joint surfaces and allows for a reduction in peak stresses. This deformation is created when the loading overcomes the attractive forces of the aggrecan for water, and water is forced out of the tissue to allow deformation and compression of the matrix components. The water exuded from the surface of the tissue helps to further lubricate the bearing surface. This same ability of cartilage to deform under load provides the joint with some shock absorption capability. The low friction surface also minimizes wear to the joint.

2.2 Osteoarthritis

Articular cartilage has limited ability for self-repair [17] due in large part to its lack of a vascular system and subsequent dependence upon synovial fluid for all nutrient supply and waste removal. Correspondingly, the development of lesions to the cartilage surface, perhaps related to a disease state such as OA, have severe lifelong ramifications for the patient. The implications of cartilage surface degradation are staggering. An epidemiological study of lesions in the knee found that in over 25,000 patients studied, 9% of patients under 50 years old were found to be potential candidates for a surgical repair to their cartilage [18]. This is a significant problem in a group of people that still

expects to be active and pain free. The number of people who will suffer from osteoarthritis is expected to rise to 59 million, or 18% of the population, by 2020 [2]. According to the National Institute of Arthritis and Musculoskeletal and Skin Diseases (NIAMS) OA effects 27 million Americans age 25 and older [1]. Additionally they estimate that by 2030, 72 million Americans (20% of the population) will be at high risk for developing OA. This is clearly a tremendous number of individuals who could stand to benefit from a greater understanding of how the disease process is initiated and progresses.

Little is known about the development of OA. Many factors are known to contribute: obesity, occupation, race, athletic endeavors, age, and genetics [3, 19, 20]. A prior joint injury is a known predisposing factor for the development of OA. In young adults, the presence of OA is most commonly due to a sustained joint injury [21]. A greater understanding of the functions, properties and damage process of articular cartilage is a crucial building block to develop treatments that one day may be able to slow, reverse or prevent damage to the cartilage surface.

Osteoarthritis is a disease of the entire joint which leads to painful joint movements, limited range of motion, and eventually, disability [22]. It causes changes to both the cartilage and the bone surfaces in the joint. As the disease progresses, the surface of the cartilage becomes fibrillated, demonstrating a surface characterized by a rough fibrous texture from the collagen fibers. The matrix wears away and leaves a surface that is not

smooth as in a normal articular joint and can eventually develop cracks or fissures, and full-thickness lesions (Figure 2.2).

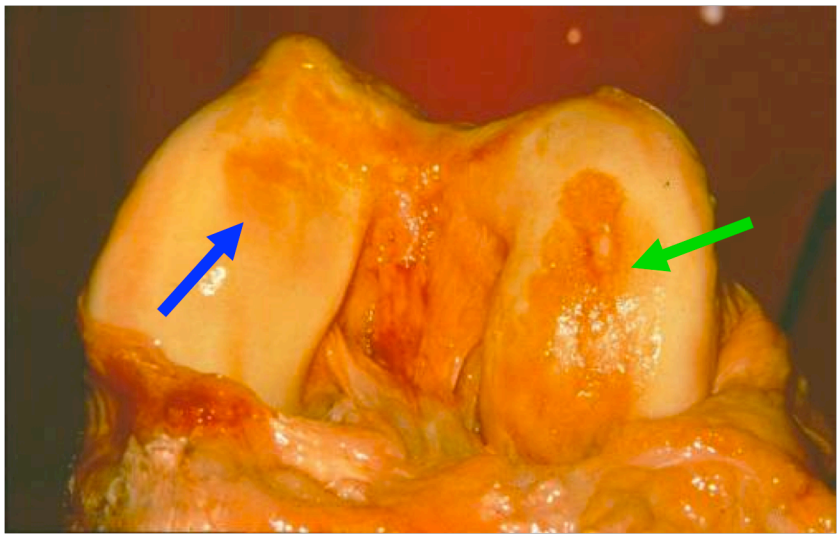

Figure 2.2. OA present on human condyles. OA can progress to full thickness lesions with exposed subchondral bone. The condyle on the left shows some loss of cartilage and a roughened surface (blue arrow), whereas the condyle on the right shows significantly more advanced OA with a large full-thickness lesion (green arrow).

Examples of different grades of cartilage surface degeneration in porcine femoral heads are shown in Figure 2.3. A grading method was used to measure the degree of OA by examining the cartilage surface for fibrillation and degradation. In this grading method the cartilage layer is stained with India ink, rinsed with saline, allowed to dry, and graded on the scale developed by Yamada *et al.* [23]. Grade 1 is an intact healthy surface; Grade 2 has a small amount of fibrillation; Grade 3 is cartilage with more developed fibrillation and black patches; and in Grade 4 there is erosion and loss of cartilage and exposed bone. A range of femoral heads was evaluated and allows a view of the progression of OA from mild to severe (Figure 2.3).

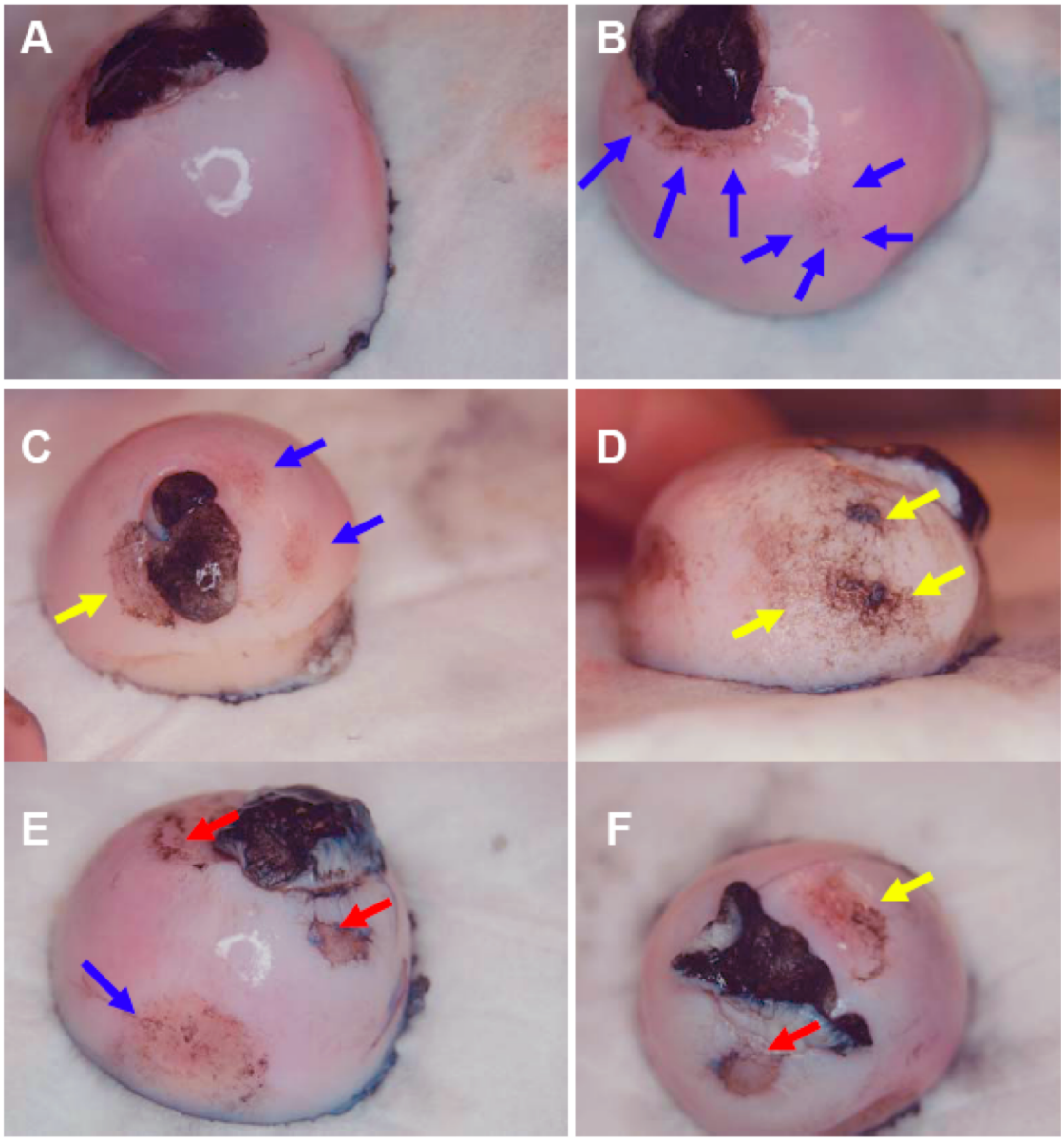

Figure 2.3. OA progression in porcine femoral heads. The degree of OA progresses sequentially from image A through image F. A: Grade 1 healthy, normal cartilage. B: Some fibrillation present in areas of light staining, grade 2. C: Blue arrows indicate a grade 2 area with some fibrillation, and deeper fibrillation (grade 3) area is indicated with a yellow arrow. D: More advanced grade 3 OA with areas of deep fibrillation. E: Grade 4 degradation with exposed subchondral bone (red arrows) and fibrillation (blue arrows – grade 2). F: Grade 4 fibrillation with exposed underlying bone (red arrow) and grade 3 deep fibrillation (yellow arrow).

An additional sign of OA progression is the loss of proteoglycans from the cartilage matrix. With proteoglycan loss, there is a reduction in attractive forces drawing water

into the matrix, and thus the matrix is less able to support compressive loading. With a reduction in the resistive forces, the matrix deforms and begins to break down more under load. This allows cartilage lesions to grow and spread, and eventually progressing through the full thickness of the layer down to the underlying bone [24]. Other signs of OA are increased fluid (water content) volume in the cartilage layers due to breakdown of the collagen structure, subchondral bone changes, narrowing joint space, and osteophyte formation [25]. These OA induced changes lead to a progression of changes in the mechanical properties of cartilage [25].

Treatments for OA are very limited and are focused mostly on minimizing pain and swelling. Physical therapy, stretching, and weight loss are often used to alleviate early OA symptoms. Pharmacological treatment generally focuses on pain management. As the disease progresses and becomes debilitating, many sufferers undertake surgery, usually in the form of joint replacement, to eliminate pain and restore mobility [26]. Popular over-the-counter treatments for OA, such as glucosamine and chondroitin, have shown inconclusive results, and in the best case only slightly alleviate disease progression [27].

2.3 Osteoarthritis Models

OA models allow research to be conducted in both *in vivo* and *in vitro* settings to observe and understand the progression of OA. Many different models with a wide range of approaches have been used. These models include: transgenic "knockout" mice that are

deficient in particular gene sequences that result in symptoms resembling OA [28]; disuse models that immobilize limbs to generate OA-like symptoms [29, 30]; and even pharmacological models, where a delivered drug generates OA symptoms [31]. A widely used means of modeling OA is a trauma, or injury model.

In the clinical setting, a prior joint injury has been shown to lead to OA. These joint injuries include ligament tears, miniscal tears, bone fractures, and trauma from such causes as a vehicular accident [3, 21, 32, 33]. These injuries often lead to a slow progression of OA that may not manifest until up to 50 years later [32]. The studies of humans are epidemiological in nature, or retrospective clinical studies, and don't have the controls associated with a laboratory study.

Replicating biological processes in a laboratory setting can be very challenging. A scientific study requires that as many variables as possible be controlled. Also, the time duration of the study can be a limiting factor. Recreating a joint injury as a model of OA (as opposed to other causes of OA) is therefore well suited to a laboratory endeavor. These models allow a control over the induced injury, precise sampling at specified times, and are prospective in nature.

2.4 ACL Transection OA Model

A prior anterior cruciate ligament (ACL) injury or tear is known to increase the chances of the development of OA [3, 21, 34]. The ACL is the ligament that connects the anterior

proximal aspect of the tibia to the posterior distal aspect of the femur. The ACL prevents anterior motion of the lower leg (tibia) in relation to the upper leg (femur). A tear of the ACL results in knee-joint instability, and abnormal transfer of mechanical loading through the articular cartilage. This abnormal, and multi-axis loading is believed to contribute to the development of OA. Researchers have endeavored to recreate joint instability induced OA in an animal model with a transected ACL.

In a bilateral ACL transection model, Marshall *et al.* showed with a histological analysis that symptoms similar to OA could be developed over a period of 2 to 12 months and duplicated in both hind legs of a canine when the ACL was transected in each leg's knee joint [35]. Therefore both knees responded similarly to the method of OA induction. One interesting finding of this study was that a single canine could act as its own control, with OA induced in one knee, and the other knee left normal. A study of New Zealand white rabbits with ACL transection showed progressive erosion of the cartilage layer along with developing ulceration over a 12 week follow-up [36]. The results also showed thinning of the entire cartilage layer on the medial condyle during the follow-up. OA progression also affects the range of motion of the joint and the forces generated during movement. In a feline ACL transection OA model, Suter *et al.* evaluated gait, loading distribution, and cartilage changes over a 12 month period [37]. They found significant gait changes beginning as early as one-week following transection, and peak forces and range of motion were all reduced. Radiographs over the 12-month follow-up showed progressive cartilage degeneration and osteophyte formation.

A mouse model was used to assess the relationship between degree of instability and progression of OA [38]. Eight-week old mice were used as the animal model and were randomized to 4 levels of instability. A mild model incorporated the transection of the ACL, a moderate model transected the medial meniscus and the ACL, a medial model cut the medial collateral ligament and the medial meniscus, and finally the severe model included transection of both cruciate and both lateral ligaments along with both menisci. The model showed that OA progression was directly related to joint instability, with the severe model showing development of OA at 2 weeks and the mild model showing beginning stage OA at 8 weeks.

To ensure that the ACL transection model was not a self-limiting injury that reached a certain level of damage and remained unchanged, Brandt *et al*. did a long-term follow-up study on a canine model [39]. Dog models underwent ACL transection and were evaluated over a 5-year follow-up period. The cartilage lesions that developed from the transections continued to progress during the time course until full thickness ulcerations developed on the femoral medial condyles and the tibial plateau. In other work, Brandt *et al.* found that after an ACL transection in canines, the gait pattern changed significantly, although the timing of the gait did not [40]. Also, after an ACL transection the joint instability induces degenerative changes in the cartilage and in the underlying subchondral bone, similar to changes observed in OA [41].

An ACL transection model is a very useful *in vivo* model for studying OA. The model creates an unstable joint, which disrupts the normal mechanical transfer of load from the upper leg to the lower leg, and results in degradation of the cartilage surface. However, one of the challenges of these models is that it is very difficult, if not impossible, to isolate the particular loads which lead to the development of OA. This model is not well suited to controlling the loading scenario to study the progression of OA.

2.5 Joint Impact OA Model

Impact injuries to the articular cartilage have also been shown to lead to OA progression via damage to chondrocytes and the cartilage matrix [4, 5, 34, 42-46]. Many of these models have used intact joints in an attempt to simulate the natural forces generated in a joint during an impact. The impacts are most often delivered by either a drop-tower set-up or a servo-hydraulic load frame. A drop tower uses gravity to cause a mechanical impactor to fall to the cartilage surface and a hydraulic load frame uses hydraulic power to move an impactor to cause the injury. The *in vivo* impact injuries have been delivered either as single impacts [6, 8, 9, 47-53] or as multiple impactions [7, 54-56]. For example, Donohue *et al*. utilized canine cadaver knees to measure forces generated with a drop tower, and then utilized live mongrel dogs for the actual testing [9]. His testing involved anesthetizing the canines and then securing their knee in a drop-tower loading device to generate an impact to the patella with a stress of approximately 0.30 N/mm^2. The forces were picked to not cause fractures, but were found to generate significant decrease in proteoglycan content. Newberry *et al*. used live rabbits as subjects for impact

injuries, where again, the patello-femoral joint was secured in a drop tower for delivery of the impact [53]. A load of approximately 560 N was delivered to the cartilage surface, and caused fissures in the surface, and thickening of the calcified cartilage layers. Thompson *et al.* also evaluated impact injuries to canine articular cartilage. Using a load of approximately 2170 N in a drop tower, cracks were generated in the subchondral bone and by 6 months generated osteoarthritic ulcerations [8]. There are advantages to an *in vivo* impact model: maintenance of joint integrity, normal joint alignment, and physiological transfer of forces between articulating surfaces. The difficulties of using an *in vivo* model arise in the quantification of forces: both applied and generated. In most cases it is impossible, or at a minimum, very difficult, to account for forces generated in ligaments, tendons, musculature, and other tissues. Attempting to quantify the complex delivery of forces to the articular cartilage surface is extremely difficult. Additionally, due to the natural variance in biological specimens, it is very difficult to generate similar forces in each test. This is compounded by the individual variance of all the tissues present in an *in vivo* model. Another challenge is that the level of activity is dependent upon the individual animal and can vary even if they are given identical treatments. This variance in activity could contribute to making the results harder to interpret.

To overcome the difficulties and lack of control or repeatability associated with *in vivo* testing, *in vitro* explant impact injuries are often used [4, 42, 57-73]. This testing method allows for much more accurate quantification of the mechanical forces delivered to the articular surface. Multiple methods may be used for preparing the explant: the cartilage

may remain attached to the surface of the subchondral bone, it may be removed from the bone surface, or a plug of cartilage and bone may be cut from the joint. Cutting the cartilage from the bone or cutting a plug may provide an easier experimental set-up, however it raises the question of what changes were introduced by the removal process. Most explant impact studies have utilized axial impactions [7-9, 42, 46, 50-52, 54, 55, 57-61, 65-68]. The axial load is generally delivered normal to the cartilage surface to generate the impact injury. Repo *et al*. used a drop tower with human cartilage explants and showed that forces experienced in an auto accident, enough to cause a femoral fracture, could result in chondrocyte death and fissuring leading to OA [4]. A 9mm diameter explant was removed from a human cadaver knee and impacted to generate strains of 10 to 40 percent. They found that at a critical strain of 25% delivered at a rate of 500 s^{-1} to 1000 s^{-1}, a critical threshold is crossed that results in both chondrocyte death and fissuring of the cartilage. Newberry *et al.* impacted rabbit cartilage with a drop tower using a 1.33kg mass dropped from 0.46 m [53]. After the impact, the modulus was measured and it was found that the subchondral bone thickness increased, and the cartilage modulus decreased. In a cyclic loading method, Clements *et al.* used a compressive load of 1-70% of the load shown to cause damage in a single loading cycle (35MPa) for 3600 cycles [66]. It was found that chondrocyte viability decreased when a threshold of 6MPa was crossed, and continued to decrease inversely proportional to the increase in delivered stress. The duration of the damaging loading event has been shown to generate significantly higher chondrocyte apoptosis than the speed of the load delivery[54]. In this study Jefferey *et al.* subjected human femoral head explants to either

a fast impact of 21.7 MPa for 1.5 sec, or a slow loading of 0.8 MPa for 0.42 sec [54]. After 72hr, the slower loading resulted in 70% of the chondrocytes being apoptotic, whereas in the faster loading event, only 10% were apoptotic. These impact loads can result in permanent damage to the cartilage matrix, proteoglycan loss and rupturing of the collagen fibers [55]. In this analysis, Torzilli *et al.* used 7mm diameter bovine explants and subjected them to cyclical loading of either 0.2 MPa or 0.5 MPa at 0.5 Hz for 3 days. Wilson *et al.* used full thickness 8.5mm cartilage plugs from bovine tibial plateaus, and subjected them to a mechanical axial load of 25N [61]. The authors evaluated fibril damage, and found that thinner cartilage was more prone to collagen damage than thicker cartilage.

2.6 Shear Forces In OA Models

The loading associated with delivering a primarily axial load is straightforward to measure, and can be carefully controlled. A normal load can also be readily generated in most testing set-ups involving a drop-tower or servo-hydraulic load frame. A real impact injury to a joint would realistically result in a very complex transfer of loads from the exterior impact site to the articular cartilage within. The physiologic loads would in most cases involve loading along multiple axes, not only loads normal to the surface. Shear forces along the articular surface are likely to be present along with normal (compressive) loading. Simulating these more complex loads in a controlled experiment can be difficult and, by omission, most axial-only impact studies ignore shear forces. Part of the justification for neglecting shear forces is that the union, or contact, between two articular

cartilage surfaces with synovial fluid present has a very low coefficient of friction that reduces shear forces to a minimum [7]. However, during an impact injury, the normal or compressive forces deform the cartilage and make shear forces much more traumatic for the tissue. The difficulty in developing and measuring shear forces also likely accounts for the much higher prevalence of axial impact studies.

While work in this area is not extensive, there has been some. Flachsmann *et al.* developed a shear model using explants of cartilage with subchondral bone in a pendulum testing apparatus to evaluate shear forces in ox and bovine specimens [56]. The study found that fractures developed in the cartilage surface from the induced shear forces and that, in mature cartilage specimens, there was some separation of layers in the tidemark area (between calcified and uncalcified cartilage). These osteochondral fractures (separation between cartilage and bone layers) were also found in a shear loading experiment with porcine condyles [7]. The condylar cartilage was positioned with custom molds and loaded in shear with both a drop-tower and a load-frame. They loaded the cartilage at different speeds and found that at low speeds the cartilage deforms and then eventually develops lesions at the cartilage-bone interface. With high velocity shear impactions, however, the viscoelastic properties of cartilage cause stiffening, as the fluid cannot move as quickly as the impact. This results in tears or fractures at the cartilage surface. Buckley *et al*. also found viscoelastic stiffening of cartilage in shear experiments and found the exact response depended upon the cartilage layer that was

being evaluated [74]. Higher stiffness was found on the surface, and this decreased to a minimum at 200 μm below the surface, and the stiffness then increased with depth.

Other methods of evaluating shear forces in cartilage have been used. Ficklin *et al.* developed a method to test cartilage explants with rotational shear between two porous platens in a load frame [57]. Hashimoto *et al*. seeded chondrocytes in a Flexcell system to generate shear forces [58]. The chondrocytes showed increased apoptosis under shear stresses. In another approach, bovine chondrocytes were seeded onto a three dimensional polyurethane scaffold and tested in a bioreactor [59]. Shear forces were induced on the scaffold by repetitively cycling a ceramic hip ball back and forth and showed that low-level shear forces improved chondrogenesis. Small shear forces have been used extensively with tissue engineered cartilage [60]. The low-level shear forces used for tissue engineering are generally not intended to simulate an injury, but more commonly to generate a simulated normal physiological loading environment to promote the development and growth of chondrocytes. These dynamic shear strains are usually less than 5%. Shear forces larger than this range have not been extensively studied.

Impact injuries have been studied extensively but have largely included only forces normal to the articular surface. A physiological joint impact injury, such as a sports or vehicular injury, is likely to develop complex multi-axial loads with significant shear forces in the articular cartilage. There is a need for more work to study the more intricate force generation in an impact injury. The effects of shear forces and the associated

cartilage deformation and fluid movement is likely more detrimental than that of axial loads alone. Tearing of the cartilage matrix may occur during the injury and the hydrostatic forces generated by fluid movement may cause excessive local stresses resulting in damage and chondrocyte death.

2.7 Cartilage Changes from OA Disease Process

The progression and pathology of OA following an injury is still not completely understood, but the ramifications of this disease make it important for continued study. Following an injury, or joint trauma, mechanical damage may take place in the form of fissures in the cartilage surface or osteochondral fractures where the cartilage separates from the bone [7-9, 44, 48, 53, 54, 74-76]. After an injury, cartilage undergoes swelling, which is due to damage in the matrix of collagen fibers. This may be due to a combination of mechanical damage to the collagen fibers and cleavage of the fibers by matrix metalloproteinases (MMPs) [61]. The damage to the collagen framework reduces its ability to restrain the swelling pressure of the proteoglycan attraction for water and excessive swelling results. The chondrocytes may generate the MMPs, or other degenerative enzymes, in an attempt to rebuild the damaged collagen matrix by eliminating the damaged sections of tissue. This weakening of the collagen matrix also leads to an increase in permeability of the cartilage allowing more water movement [44]. There is also proteoglycan loss from the matrix following an injury [8, 53, 62]. It has been proposed that chondrocytes may attempt to repair the damage by initiating cell cloning of chondrocytes to either replace the damaged cells or to create additional cells to

assist with matrix repairs [8, 63]. Necrosis (cell death from an acute injury), or apoptosis (programmed cell death) may result from a joint trauma as the chondrocytes respond to the injury [64-66]. Following an injury, chondrocytes may not differentiate correctly due to either the mechanical stimulus or signaling molecules. Type I collagen may be more highly expressed, with type II collagen expression reduced [65, 67-69]. Type II collagen is more prevalent in articular cartilage, whereas type I collagen is more associated with fibro-cartilage, a dense connective tissue found in many locations, including the menisci and intervertebral discs. Therefore, the higher expression of type I collagen may indicate that the chondrocytes are reverting to a more fibroblastic-phenotype. These changes in the articular cartilage following an injury seem to point to attempts for self-repair. However, it has been shown that impact injuries lead to OA, indicating that the repair efforts are not successful in the face of large acute loading scenarios.

2.8 Functional Genomics in OA

OA is a multi-factorial disease, and its causes are not well understood. Functional genomics is one method of attempting to discern the basis for morphological changes in OA. Functional genomics attempts to understand the role and function of genes in the body. This approach can identify differences in gene transcript levels between normal and OA cartilage. Using a functional genomics approach, it may be possible to identify potential therapeutic targets for early intervention in the progression of OA.

This task holds challenge, though, as the cartilage transcriptome has between 13,200 and 15,800 unique genes [70]. While this provides a wealth of potential genes associated with the progression of OA, an understanding of what genes are expressed differently in OA cartilage is needed. Microarrays specific to cartilage have been utilized to study the OA process, and have identified numerous differences in gene levels in OA cartilage and normal cartilage. OA may affect signaling pathways in cartilage [71], apoptosis [72], chondrocyte metabolism [73]. The findings of microarray studies have opened the door for the evaluation of genes potentially related to OA. Microarrays have the ability to identify differences or changes in expression of large groups of genes. However, the findings of some of these studies of OA have differed. While some studies have found collagen types I and II to be upregulated [77, 78] another study found their levels to be unchanged [79]. As another example, expression of sex determining region Y-box 9 (*sox-9*), which stimulates the expression and maintenance of the chondrocyte phenotype [13] and has been shown to be correlated with collagen II expression [80], has been found to be both downregulated in OA cartilage [72] and unchanged [81]. Some have identified changes in numerous genes never before associated with OA progression [82].

Our own lab has constructed and sequenced two Serial Analysis of Gene Expression (SAGE) libraries of impacted cartilage and normal (or control) cartilage from porcine patellae [65]. SAGE analysis provides a comprehensive list of sequence tags representing the entire mRNA population in a sample. The tags are then referenced with a sequence database to determine the represented genes. In this previous study axial

impactions (to 2000N) were delivered to porcine patellae as an impact trauma model for OA. The impacted and non-impacted controls were kept in culture for 14 days to evaluate temporal changes in articular cartilage as a result of the impactions. SAGE analysis was performed on pooled RNA from the impacted specimens and compared to the control. The results showed many differentially expressed genes between the impacted and control at two weeks, including genes associated with matrix remodeling, iron and phosphate transport, protein synthesis, skeletal development, cell proliferation, and inflammatory response.

2.9 Gene Expression Measurement

Microarray or SAGE analyses provide broad-based approaches to identifying individual genes, which may be associated with OA development. A microarray uses probes, or templates, to bind segments of cDNA representing target genes, by measuring fluorescence levels of each probe, an indication of the relative amount of gene expression can be determined. Additionally, an oligonucleotide based microarray uses short segments of cDNA or PCR product that correspond to particular mRNA sequences. SAGE on the other hand, provides a snapshot of all the mRNA present in a particular sample that is then compared to a database. Both of these methods are high throughput and allow for potentially examining thousands of genes at a time. However, they present a broad picture of what is occurring and lack precision in measuring the changes in expression of an individual gene. Additionally, they are costly and therefore may not be practical for evaluating a large number of specimens, as multiple specimens generally

have to be pooled. They can, however, provide the target genes for further research and investigation.

Quantitative real time reverse transcriptase PCR (qRT-PCR) is an analytical method that allows for a focused, and more sensitive, analysis of individual genes across multiple samples and/or time points. With this method an individual gene is targeted and precisely evaluated for differences in gene expression levels. Taqman probes are one method of detection. The Taqman probe is designed to target a particular segment of DNA and binds. There are two fluorophores associated with the probe. A quencher fluorophore on the 3' end of the probe reduces (or quenches) the fluorescence from the reporter fluorophore on the 5' end of the probe. If the probe binds to the targeted segment, then during amplification the polymerase frees the reporter. This allows the reporter's fluorescence to be measured (it is now unquenched), and it therefore, indicates expression levels of the targeted segment. Therefore Taqman probes provide a very accurate method of quantifying the expression of a particular gene. SYBR on the other hand is a fluorescent marker that binds to double stranded DNA. It is dependent upon the development of accurate primers to ensure that the segments of double stranded DNA it binds to are the target of interest. SYBR can be significantly more economical to use than Taqman depending on the number of samples to be evaluated.

When measuring gene expression levels, both absolute and relative quantification may be used to measure levels of expression. In absolute quantification, the amplified cDNA is

compared to a standard of known quantity. The amount of cDNA in the sample is thus measured by comparison to the standard. The difficulties with this method are that their must be a reliable template for comparison, and that template must be amplified in conjunction with the samples of interest every time the experiment is performed. Relative quantification, however, uses an internal control (reference gene) to normalize the expression results for comparison across samples. The internal control accounts for quantity and quality of RNA and pipetting errors to allow for accurate comparisons. This study used a qRT-PCR analysis with SYBR and relative expression quantification.

2.10 Loading Models and Differential Gene Expression

Evaluating gene expression changes after an impact injury to articular cartilage may be important to understanding the progression of OA. A wide range of studies have evaluated impact trauma or mechanical loading as an initiator of OA. These studies vary in the animal model used, the joints evaluated, the type of loading applied, duration of loading, and the time period of monitoring. These differences may prove difficult in making comparisons between findings from different studies, however, all of the work contributes to a body of knowledge that aids the scientific community in identifying the changes in early stage OA. Fehrenbacher *et al.* cyclically loaded porcine bone-cartilage plugs in compression with loads of 10-12MPa, simulating *in vivo* loading, and maintained the explants in culture for up to 16 hours [83]. The findings showed that *collagen I* and *II* (*col1a1* and *col2a1*) levels significantly decreased while *aggrecan* (*agc)* and *mmp* levels remained unchanged. In another explant study, Fitzgerald *et al.* loaded bovine mid-zone

cartilage explants with a compressive strain of 25 or 50% which was maintained constant for periods from 1 to 24 hours [84]. Their findings showed that *aggrecan*, *collagen* type *II* and *link protein* rose during the first 8 hours, and subsequently dropped below the levels of the control specimens. Also, *mmp*-3, *9* and *13* and ADAM metallopeptidase with thrombospondin type 1 motif 4 (*adamts-4*) increased over 24 hours. These results point to matrix remodeling with large compressive strains. In 2006, Fitzgerald *et al.* conducted a similar study where explants were loaded with dynamic compressive and shear strains over 1-24 hours [75]. The findings showed that most *mmps* were upregulated by 24 hours in both shear and compressive loading.

A rat model was used to study OA progression in temporomandibular joint (TMJ) cartilage, with a surgical resection model used to generate OA in the experimental group [76]. The rats were kept for time periods up to 12 weeks, and differences between control and experimental groups were measured via microarray. No external loading was applied; only normal TMJ function generated the loading in the joint cartilage. A total of 138 genes were identified as having either up- or down-regulation differing by greater than 2 fold. These included genes associated with matrix degradation, apoptosis, and remodeling.

Natoli *et al*. evaluated temporal changes in cartilage-bone explants from bovine elbow joints [85]. The explants were axially loaded with either a low (1.1 J) or high (2.8 J) impact. The low level corresponded to an impact that would not cause visible damage,

whereas the high load was chosen to cause immediate identifiable damage. The explants were cultured for 24 hrs, 1-week, or 4 weeks. *Aggrecan* was elevated at 24 h and 1-week, but decreased by 4-weeks. *Collagen type II* was decreased at all time points. Superficial zone protein (*szp*) was increased at 24 h and decreased at both 1- and 4-weeks. *Collagen type I* was decreased at 24 h, and then was up 35 fold at 1-week and then 378 fold at 4-weeks in the injured tissue. *Mmp-1* and *timp-1* were elevated in the high impact specimens at 24 h, and then decreased at 1- and 4-weeks.

The different types of impact and trauma used in these studies can generate differences in gene expression levels measured. There are many loading scenarios to consider and many different time points for evaluation, however all of these studies help contribute to information needed for an understanding of the progression of OA. The aim of this study is to use an *in vitro* model, to deliver accurate discrete loading events and carefully monitor changes in gene expression over the days following the impact.

2.11 Genes Selected for Analysis

Understanding how gene expression levels change and develop over the days and weeks following an impact injury may provide a clearer picture of the processes that occur within the cartilage which may lead to OA. In order to study these changes, a panel of genes was selected from literature for qRT-PCR analysis with this impact model. A total of 18 genes were selected for analysis from the following functional categories: cartilage

matrix constituents, degradative enzymes and their inhibitors, inflammatory response, and cell proliferation and apoptosis.

Cartilage Matrix:

Collagen type 2 alpha-1 was chosen for analysis as it encodes for type II collagen, a critical building block of the cartilage matrix [86]. Of the many types of collagen, type 2 is the most prevalent collagen found in cartilage and has been found to be upregulated in some OA related studies of articular cartilage [87-89]. Collagen type I alpha-1 was also chosen for analysis, as it is more prevalent in fibrocartilage and may be an indicator of a reversion of the chondrocytes to a more fibroblastic phenotype in response to matrix damage. It has been shown to be unchanged [79, 81], or upregulated [65, 80] in OA.

Aggrecan is one of the main building blocks of cartilage and is made up of proteoglycans to provide the osmotic properties of cartilage, which allow it to resist compressive loads. During OA there is generally a loss of aggrecan from the matrix [80, 90] though its transcript has been reported to be upregulated in some cases [71]. Sex determining region Y-box 9 (*Sox-9)* was selected as it encodes for a transcription factor of both aggrecan and type 2 collagen [81, 91-93]. *Sox-9* has been reported to be downregulated in several OA studies [80, 84] while it has also been reported to be mildly upregulated at early time points following loading [75]. Osteopontin was also selected, as it codes for an extracellular structural protein and its expression has been linked to a critical stage of chondrocyte maturation as it transitions to bone [94]. It has been found to be upregulated

in OA [78, 95-99] and during cyclical joint loading [60]. There may be little to no osteopontin expression in healthy cartilage [97]. The final cartilage matrix gene selected was cartilage oligomeric matrix protein (*comp*). This gene encodes for an abundant extracellular matrix protein, however its function is not fully known [88]. It has been found to be upregulated in cyclic tension and compression [77, 100] and in OA [101-103], however its downregulation may signal matrix degradation [20, 59].

Degradative Enzymes and Inhibitors:

A crucial category of genes to evaluate in an analysis of OA is those genes that are associated with the breakdown of the cartilage matrix. These include matrix metalloproteinases (*mmps*), which encode enzymes that breakdown the components of the cartilage matrix. An understanding of the expression changes for these genes may help to understand the repair efforts after the damaging effects of an impact model of OA. *Mmp-1, 3,* and *13* were selected for analysis and have been shown to be upregulated [78, 89] in some studies of OA, though other studies have found *mmp*-3 to be downregulated [65, 96, 104]. *Mmp-1* and *13* are both collagenases that break down type II collagen fibers in the cartilage matrix. Mmp-3, however, is a stromelysin that can breakdown other matrix proteins, including proteoglycans, type III and IX collagen, but not type II collagen. Tissue inhibitors of matrix metalloproteinases 1 and 2 (*timp-1 and 2*) were also evaluated. These are general inhibitors that block or inhibit the degradative action of mmps, they are not specific to an individual mmp. They were unchanged in our earlier work [65], but have been found to be altered in multiple studies [67, 81, 104].

Adamts-4 is an aggrecanase, which contributes to the breakdown of aggrecan in the matrix. It has been shown to be upregulated in OA studies [78, 88, 105].

Inflammatory Response and signaling:

Genes related to an inflammatory response or biological stress signaling were also selected for analysis. These are genes whose expression changes in response to an injury to either initiate a reparative process or signal other cellular actions. Transforming growth factor beta (*tgfb*) encodes an inflammatory mediator and its expression sets in motion many events critical to inflammation and repair efforts including: white blood cell recruitment, vascular growth, and limiting inflammation and aiding in repair efforts [106]. As an inflammatory mediator, one of the ways it assists repairs is by stimulating the production of extracellular matrix components and it has been linked to cell proliferation and growth and is upregulated in OA cartilage [76, 92, 107] and in mechanically stimulated cartilage [77]. Its early upregulation may abate to be followed in OA cartilage by lower later expression [108]. Indian hedgehog homolog (*ihh*) encodes a signaling molecule that binds to a membrane bound receptor, Patched1 (Ptc1), as an integral part of the chondrocyte maturation process. Increases in its signaling have also been associated with chondrocyte proliferation, and a negative influence on chondrocyte maturation and subsequent ossification [109]. *Ihh* has been found to be more highly expressed in very early stage OA cartilage [87, 93] and downregulated in later stage OA [110]. Chitinase 3-like 1 (*Chi3l1* or *gp38k*) is an inflammatory marker, or gene that indicates inflammatory processes are underway, and is also associated with a cartilage

remodeling and may be downregulated at 2 weeks following an injury [65]. It has also been found to be upregulated during OA [111] and more highly upregulated in areas of higher biomechanical load [112]. It may be upregulated initially after cartilage is placed in culture and diminishes over time, however its levels may rise upon new injury or damage [113]. Inducible nitric oxide synthase (*inos* or *nos2*) encodes an enzyme responsible for the production of nitric oxide, a signaling molecule. It plays a role in both inflammation and possibly apoptosis [114] and plays a role in the progression of OA [73, 115-117]. In fact, it was shown that inhibiting *inos* production in a dog model of OA slowed cartilage degradation [118] and *inos* knockout mice are resistant to the development of OA [117].

Cell Proliferation and Apoptosis:

Caspases (*casp*) are genes that are associated with cell apoptosis [119, 120] and have been shown to be upregulated in OA cartilage [73, 87]. A mechanical injury model of OA may induce apoptosis via a caspase pathway [120]. The activation of caspase induced apoptosis may be induced by nitrous oxide [117]. Inhibition of caspase-3 and 8 in a rabbit ACL transection model of OA showed reduced cartilage degradation [121]. Caspase-8, an initiator in the caspase pathway, activates downstream effector caspases in the apoptotic pathway and has been found to be upregulated in naturally occurring human OA [87], induced rabbit OA [122], and in a canine OA model [123]. Another apoptosis related gene, TNF receptor superfamily, member 6 (*fas*), encodes a protein with a death domain and is crucial in the sequence of an apoptosis pathway. Expression of *fas* by

chondrocytes may be responsible for part of the cartilage degradation during OA [122, 124] and has been shown to be upregulated in the early stages of a rabbit OA model [125]. Chondrocytes produce *fas* in early stage OA, and may produce their own fas ligand that binds to the death receptor, or the receptor responsible for initiating apoptosis, and catastrophically amplifies the apoptosis signal [125]. *Fas* has been found to be more highly expressed in the region of OA lesions in cartilage [126].

2.12 Housekeeping Genes

With qRT-PCR, multiple genes across many specimens may be evaluated to measure changes in expression. However, to accurately determine the relative expression levels, and the corresponding fold changes for up- or down-regulation, a normalization gene is necessary. Reference genes, frequently termed "housekeeping genes," are used to normalize the expression results for differences in cDNA quantity of different specimens. This enables comparisons between the genes of interest across treatments. Because the housekeeping gene is used as a reference, it is important that it be stable with its expression unchanged regardless of treatment. These are genes whose expression is generally unchanged with treatment conditions, and are most often associated with basic cellular processes such as metabolism.

For our work with impact injury models in the study of differential gene expression, it was necessary to identify an adequate reference gene for cartilage. A variety of genes have been used in the past as housekeeping genes in cartilage studies. *Gapdh*

(Glyceraldehyde-3-phosphate dehydrogenase) has been used as a housekeeping gene in studies of human, bovine, porcine, and caprine articular cartilage [127, 128]. *Gapdh* has also been used as a reference gene for both human normal and OA cartilage [99, 129]. Swingler *et al*. selected succinate dehydrogenase complex, subunit A, flavoprotein (*sdha)* as a reference gene for human OA cartilage [87]. Pombo-Suarez *et al.* evaluated reference genes for human cartilage with advanced OA and found TATA box binding protein (*tbp)*, ribosomal protein L13a (*rpl13a)* and beta-2-microglobulin (*b2m)* to be the most stably expressed genes [130]. *Rpl13a* and *sdha* were identified as the most stable reference genes for canine normal and OA cartilage [131]. Fitzgerald *et al.* used *gapdh* and 18S ribosomal RNA (*18s)* for normalization of bovine cartilage explants in a mechanical compression study [84]. *Gapdh* was again used for normalization in a sheep OA cartilage model [132]. However, an analysis has not previously been conducted to determine the ideal reference gene(s) for porcine articular cartilage.

Two methods have been developed to identify the best housekeeping gene(s) from an initial panel of multiple genes. Vandesompele *et al.*, developed a method of using a panel of ten genes and ranking those genes in order of stability across samples and treatments [133]. In this method, pairwise comparisons are made between each combination of samples for each gene. The two genes that demonstrate the least variance in comparison with all other genes are ranked as the best genes to be used as reference genes. The subsequent genes in the panel are ranked in order of their stability. The authors developed a free Visual Basic Application (VBA) for Microsoft Excel (geNorm) for this study.

A second method for finding a suitable reference gene is BestKeeper. This method also uses an Excel based application to determine the best housekeeping gene from a panel. Developed by Pfaffl *et al*., the method can evaluate up to ten potential genes for use as housekeeping genes [134]. The geometric mean of the cycle threshold values (Ct values) for each sample across all housekeeping genes are combined together to form the BestKeeper index. Subsequently, each individual gene is compared in a pair-wise fashion with Pearson correlation coefficients to the index. The outcome is a ranked order of the ten potential housekeeping genes in terms of their stability. The highest ranked gene is the most stable, and the authors recommended the use of the top 3 genes as that provides a realistic number of housekeeping genes to evaluate that provide enough accuracy of results.

The geNorm approach was used by Nygard *et al*. to evaluate a panel of nine genes in porcine tissue [98]. The genes evaluated were genes commonly used in porcine tissue studies, including: skin, muscle, lung and liver. Seventeen different porcine tissues were evaluated and the geNorm software identified beta-actin (*actb)*, ribosomal protein L4 (*rpl4)*, TATA box binding protein (*tpb)*, and hypoxanthine phosphoribosyltransferase 1 (*hprt1)* as the most stably expressed housekeeping genes across all tissues. Although 17 different tissues were evaluated, articular cartilage was not included. The genes included in Nygard *et al.* included all of the genes previously discussed as commonly used in cartilage with the exception of *rpl13a* and *18s*. However, Nygard *et al.* did include *rpl4*

which, like *rpl13a,* encodes for a protein of the 60S subunit of ribosomes. Additionally, *18s* has been shown to vary in proportion to total RNA and is not a useful housekeeper [134]. Therefore, our study evaluated the nine genes used in the Nygard study to determine the best housekeeping genes to be used specifically in porcine articular cartilage. One additional gene, peptidylprolyl isomerase A (cyclophilin A) (*ppia),* was also evaluated as a potential housekeeping gene. *Ppia* was chosen because it has been used as a normalizing gene for other OA related studies [135-138]; and it exhibited no differential expression in impacted and control specimens in our previous work [65].

There is a challenge in identifying housekeeping genes. The reason for using a reference gene is to control for differences in the amount of starting material, efficiency of amplification enzymes, and differences in expression from cells and the overall level of transcription [133]. Selecting a stable housekeeping gene is therefore inherently challenging. If expression of a particular gene is measured, then its variation in expression may be due to any or all of the afore-mentioned factors. This presents a circular problem: determining a stable gene when that gene is expressed differently across samples/tissues. Therefore, both of these programs attempt to provide a measure of stability by evaluating a panel of genes by comparing their individual stability in relation to that of the entire panel.

2.13 Purpose and Overview of Experiment

OA is a progressive and debilitating disease that affects a significant portion of our population. Joint trauma and impact injuries have been shown to cause the changes seen in OA and numerous studies have evaluated impact injuries to articular cartilage. The majority of these studies, however, have included only axial loads delivered normal to the cartilage surface. Most of this body of work neglects shear or tangential forces on the surface of the cartilage, even though the addition of shear forces likely more closely resemble what happens during a physiologic loading in a joint injury.

This study evaluated impact trauma to porcine patellae in an *in vitro* experiment. A hydraulic load frame was used to deliver either an axial load normal to the surface or a shear load (with a small axial load) across the surface. The patellae were maintained in culture and full thickness cartilage samples from the loading site and sites adjacent to the loading area were obtained at 0, 3, 7 and 14 days. These samples were used for qRT-PCR analysis of gene expression in impacted samples as compared to control specimens. A panel of genes for analysis was selected based upon literature and previous work in this lab. The aim of this analysis was to identify key gene expression changes in early stage OA. A greater understanding of these early-stage changes may aid the future identification of therapeutic intervention strategies.

3. METHODS

3.1 Overview of Methods

The aim of this study was to study gene expression changes following impact injuries to articular cartilage. Patellae were removed from porcine knee joints and were given one of three treatments: a primarily normal impaction, an impaction with elevated shear forces, or a non-impacted control. The patellae were rigidly mounted and the impacts were delivered with a servo-hydraulic loadframe. Following the impaction, the intact patellae were kept in culture for up to two weeks. One of the important considerations was to maintain the cartilage attached to the bony surface. This eliminated the risk of measuring undesired side effects of cutting the cartilage from the underlying bone. Gene expression changes for a panel of 18 genes were evaluated at day 0 (approximately 2 hours post-impaction), day 3, day 7 or day 14 following the impact event. These changes were measured in full thickness tissue directly below the impact site and in tissue adjacent to the impact location. The differential gene expression over time and across treatments was evaluated.

3.2 Tissue Acquisition and Preparation

A local slaughterhouse provides fresh intact porcine knee joints, which are obtained fresh within two hours of slaughter. Paired right and left joints were from retired sows weighing at least 180kg, and the age of the animals was unknown. Right and left legs from each animal were assigned the same culture time period and randomized to a

combination of the treatment groups (axial/shear, axial/control, shear/control; Table 3.1). Each group of treatment combinations was repeated three times at each time point for a total of 18 patellae at each time point (6 axial, 6 shear, and 6 control). 72 patellae were used over all time points and the 36 pairs were randomly assigned at the outset of the experiment. A total of 75 patellae were collected, with three lost due to infection in culture.

Table 3.1. Treatment assignments by animal and leg. A total of 36 animals were included in this analysis (3 samples were removed from analysis due to infection during culture and were repeated as additional samples for animals 37 and 38 – highlighted in red). Treatment assignment for each leg are designated as a one letter description of treatment type (A – axial, S – shear, and C – Control) and a culture time point (00 – 0 day, 03 – 3 day, 07 – 7 day, and 14 – 14 day).

Treatment assignments by animal number and leg		
Animal Number	**Left Legs Treatment/Culture Time**	**Right Legs Treatment/Culture Time**
01	S00	A00
02	S07	C07
03	S00	C00
04	S14	C14
05	C14	S14
06	A00	C00
07	C00	S00
08	A03	S03
09	C03	A03
10	S14	C14
11	A14	C14
12	A03	S03
13	C00	A00
14	C14	A14
15	S03	C03
16	C03	A03
17	A14	S14
18	C07	A07
19	C00	A00
20	S07	A07
21	S03	C03
22	A03	C03
23	A07	S07
24	A00	S00
25	S00	C00
26	S03	A03
27	A14	S14
28	S14	A14
29	C07	S07
30	C14	A14
31	S07	C07
32	C03	S03
33	A00	S00
34	C07	A07
35	A07	C07
36	A07	S07
37	C14	A14
38		C07

Upon arrival in the lab, the knee joints were swabbed with betadine and sprayed down with 70% ethanol to sterilize the exterior of the joints. The knees were then dissected under sterile conditions to remove the patellae from the joint capsule, and all soft tissue was removed from the anterior (bony) portion of the patellae. The articular surfaces were inspected for irregularities (fibrillation, lesions, or other damage) and only healthy specimens were included in this analysis (Figure 3.1). Once removed from the joint the patellae were kept immersed in PBS with antibiotics to minimize chances of infection or drying of the cartilage. All equipment and tools used during the procedure (and subsequent culture) that contacted the patellae were pre-sterilized by autoclaving for 60 minutes at 121°C.

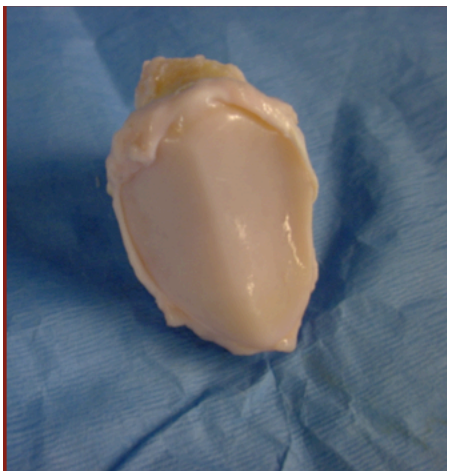

Figure 3.1. Healthy Patella. Image shows a healthy patella that has been removed from the joint capsule. Most of the soft tissue has been removed in preparation for testing. The cartilage surface is in good condition and shows no signs of fibrillation or lesions.

During the impactions, it was important to position the patellae accurately and then hold them securely for delivery of the loads. Therefore, the anterior bony portion of the patellae was pressed into a partially set polymethyl methacrylate (PMMA – "bone cement;" Osteobond, Zimmer, Warsaw, IN) hemi-spherical mold to create a custom matched individual holder for each patella (Figure 3.2). The patellae were removed immediately after creating the impression and returned to the PBS solution to avoid the chance of thermal damage from the curing exothermic PMMA.

Figure 3.2. PMMA patella molds. Image shows two PMMA patella molds. The mold on the right is being custom fit for an individual patella by pressing the patella into a partially cured bed of PMMA. The molds are then positioned in the custom x-y jig for testing.

3.3 Testing

Patellae were placed into the cooled, finished, and cured PMMA hemi-spherical mold. The mold was then positioned in a custom x-y positioning jig on the base of a servo-hydraulic load frame (MTS Mini Bionix 858, MTS Systems Inc., Minneapolis, MN)

(Figure 3.3). Previous work in our lab has shown that this set-up provided a rigid testing platform that minimizes unintended movement during the impaction. The x-y positioning jig allowed for movement in any direction in the x-y plane. The hemi-spherical mold, with the hemi-spherical receptacle in the x-y jig, allowed the patellae to be rotated for positioning to ensure that the plane of either facet was perpendicular to the loading direction. Once the mold was positioned in the correct orientation, bolts were used to secure the x-y jig to the load frame. Also, three bolts were used to secure the mold within the x-y jig to prevent any undesired movement.

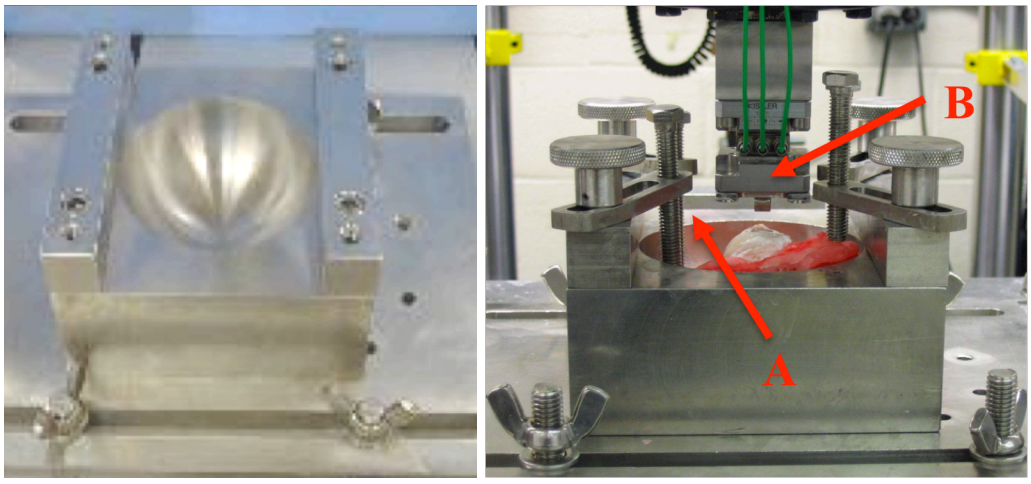

Figure 3.3. Custom x-y Jig. The image on the left shows the hemi-spherical receptacle for the PMMA mold. This shape allows the patellae to be oriented such that a facet is perpendicular to the axial loading direction. The image on the right shows the x-y jig with a patella PMMA mold in place. The mold is at an angle and secured with the 3 securing bolts (red arrow A). The impactor tip is attached to the Kistler piezoelectric load cell (red arrow B). In this image the hydraulic load frame is configured to conduct an axial impaction with a load normal to the cartilage surface.

The actuator of the MTS machine was fitted with a 3-axis piezoelectric load cell (Kistler 3 component force sensor model 9347, Kistler Instrument Corp., Winterhur,

Switzerland). A custom impactor was then fitted to the end (bottom) of the load cell. The impactor was a 10mm long, 10mm diameter stainless steel cylinder. The central axis of the cylindrical impactor was oriented perpendicular to the direction of loading and in-line with the medial-lateral axis of the patella. The medial and lateral facets of the patella are approximately flat in the area of the impaction, but some variance exists. Therefore, the impactor was designed to accommodate unevenness of the surface (Figure 3.4). To achieve this, the impactor was pinned to its base with the pin running along the radial axis. This allowed the impactor to rotate around the radial axis to accommodate deviations of the patellar surface.

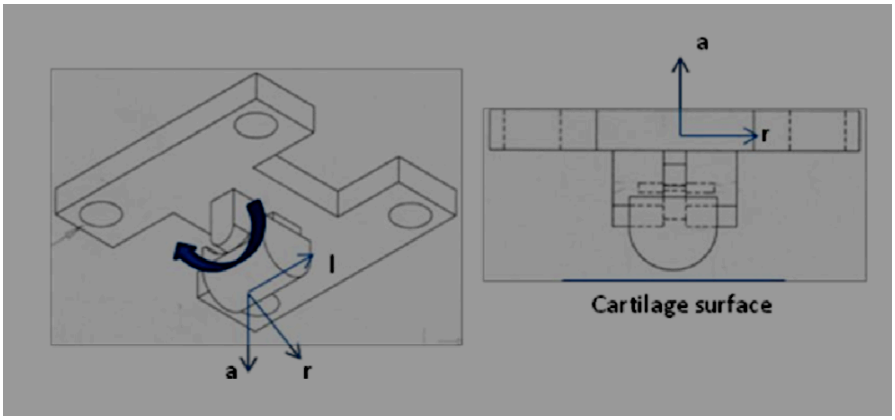

Figure 3.4. Impactor diagram. The impactor is a 10mm by 10mm cylinder which contacts the patellar surface during the impaction. The left image shows the three axes of the impactor. The axial axis (a) is the vertical axis along which the actuator of the load frame travels to deliver the normal load. Both the radial axis (r) and the longitudinal axis (l) are perpendicular to the axial axis. The longitudinal axis is aligned with the medial-lateral direction of the patellar surface and the pinned design of the impactor allows the impactor tip to rotate around the radial axis to allow it to accommodate any unevenness of the surface.

The 72 patellae included in this experiment were randomized to one of three treatments: axial impaction, shear impaction, or non-impacted control. Axial impactions were used

to deliver a load normal to the patellar facet (Figure 3.3). A targeted peak load of 2000N was applied at a displacement rate of 25mm/s. The piezoelectric load cell captured the axial loads and any loads in the radial and longitudinal directions. The longitudinal axis was oriented in the direction of the medial-lateral patellar axis, and the impactor radial axis was oriented along the proximal-distal axis of the patella. Each patella was impacted with identical impactions at the middle of the medial and lateral facets. The force and displacement data from each trial were collected with a custom LabVIEW program (National Instruments Corporation, Austin, TX). The location of the impaction was marked with tissue marking dye (india ink) adjacent to the impacted area. The dye remained on the cartilage surface throughout the culture period.

The shear impaction method utilized a more complex testing configuration. The same x-y jig was used to rigidly hold the patella mold, however the jig was not rigidly secured to the load frame base. Instead, the x-y jig was bolted to a platform that allowed uni-axial translation. A pulley arrangement attached the x-y jig to a second hydraulic load frame (Instron 8501, Instron Corporation, Canton, MA) (Figure 3.5). The first load frame slowly delivered a smaller axial load of 500 N at 0.5 mm/sec normal to the cartilage surface. Once the axial load reached 500 N, the MTS actuator maintained a constant position as the patella was displaced 10 mm tangentially in the anterior-posterior direction at 200 mm/sec via the pulley system. This generated the shearing impaction on the cartilage surface. The loading was again recorded with LabVIEW software.

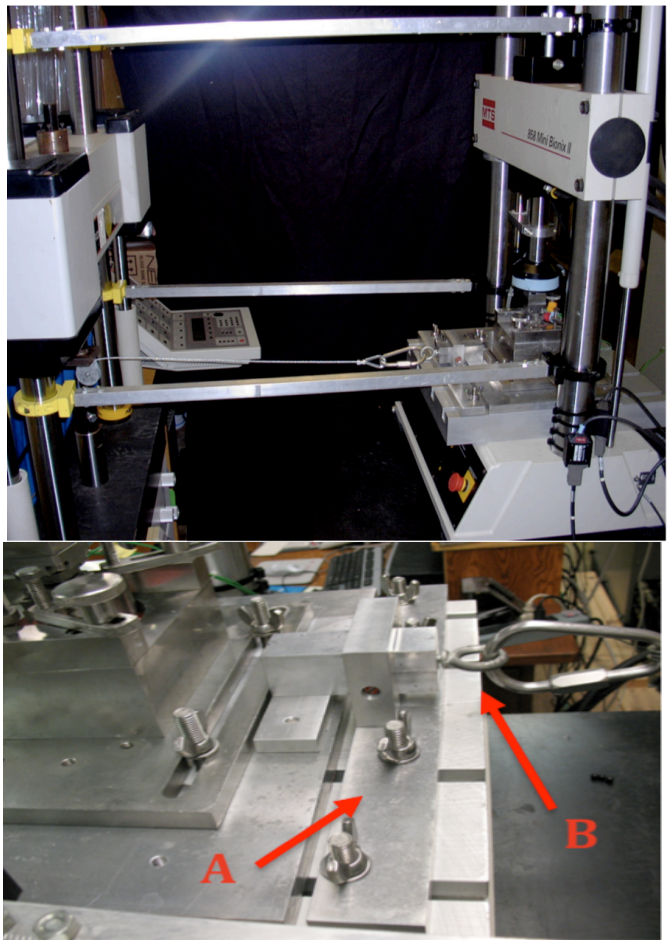

Figure 3.5. Shear impaction. The top image shows the testing configuration for conducting shear impactions of patellae. The patella is positioned in the x-y jig in the hydraulic load frame at the right of the picture. The x-y jig is on a moveable platform attached via a cable and pulley to a second load frame at the left of the picture. The bottom picture shows a close-up of the platform for the x-y jig for shear impactions. The platform is allowed to translate from left to right in the image and is stopped by the stop bar (red arrow A) as it is pulled by the cable (red arrow B).

The surface of the patella is approximately flat, but not perfectly so. The unevenness of the surface can generate some off-axis loading as the impactor makes contact with the surface. This results in axial impactions generating some forces in the radial and longitudinal directions (shear forces). Thus, axial impactions consist of both axial and shear forces, and similarly, by design, the shear impactions include both axial and shear

forces. The aim of the two types of loading scenarios was to generate axial impactions with primarily compressive loads and minimal shear forces, and shear impactions with significantly larger radial shear forces.

3.4 Organ Culture

Upon completion of the impaction, the patellae were placed into culture for 3, 7, or 14 days. The patellae were first washed three times with a PBS solution containing antibiotics. They were then transferred to culture dishes sufficiently large enough to allow complete immersion of the patella. The culture media consisted of: Delbecco's MEM/Ham's F12 with 10% fetal calf serum, ascorbic acid (25 μg/ml), and antibiotics (penn. 100units/ml, strep. 100μg/ml, and amphotericin B 25 μg/ml). The patella were then placed in a humidified incubator at 37°C with 5% CO_2. Culture media was changed daily to ensure health of the patellae and to minimize chance of infection. A rocking shaker was used to agitate the culture dishes.

3.5 Tissue Collection

At the scheduled time point (0, 3, 7, or 14 days) cartilage specimens were collected from the patellae for gene expression analysis. For the day 0 specimens, cartilage specimens were collected approximately 2 hours following the impaction. The patellae were removed from culture and the tissue dye was used to identify the location of the impaction site. Full thickness cartilage slices (down to the level of the subchondral bone) were removed from the impaction area with a scalpel. A sample was taken from the area

of the impaction (area of interest sample – AOI) and two samples from areas directly adjacent to the impacted area along the proximal-distal axis (Figure 3.6).

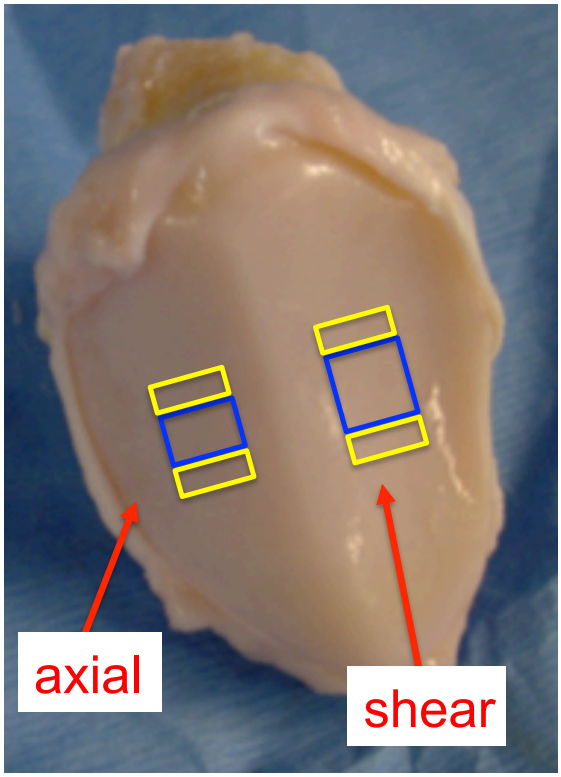

Figure 3.6. Specimen locations. Full-thickness cartilage specimens were harvested from the location directly below the impact site (AOI sample in blue), and in the tissue adjacent to the impaction site (ADJ sample in yellow). The relative size of the axial specimens is shown on the left, and the shear on the right. This figure is for demonstration only, actual patellae were given identical treatments on each facet.

For the axial impaction, an AOI specimen of dimensions 10 mm by 5 mm was removed from the impaction site. Also, two specimens from the adjacent areas (ADJ) were removed at the proximal and distal ends of the AOI of approximately 3 mm by 10 mm, and were pooled for analysis. A longer AOI specimen (10mm by 10mm) was removed from the shear-impacted patellae to accommodate the tangential displacement during the

impact event. Two different ADJ samples were obtained from the shear specimens; one in the direction of the shear event (ADJ forward – ADJF) and one behind the direction of the shearing event (ADJ behind – ADJB) (each approximately 3 x 10 mm). After the specimens were removed they were immediately flash frozen in liquid nitrogen (approximately -200°C) and transferred to a freezer at -80°C until later RNA extraction. Tissue was also collected from identical areas of non-impacted controls.

After eliminating 3 patellae infected in culture, a total of 72 patellae were included in this analysis (Table 3.2). This consisted of 36 right and 36 left patellae. Thus there were 6 patellae for each impaction type at each culture time. Both facets of each patella were given identical treatments.

Table 3.2. Distribution of sample numbers by treatment and culture days.

Tissue numbers			
	Impaction Treatment		
Culture time (days)	Axial	Shear	Control
0	6	6	6
3	6	6	6
7	6	6	6
14	6	6	6
Total Specimens	72		

3.6 Overview of Gene Expression Methods

Gene expression refers to the process whereby the genetic information recorded on DNA is used to produce a product such as RNA. The interim "messenger" in the process of

gene expression is messenger-RNA (mRNA). mRNA consists of a nucleotide sequence that is a copy of specific segments of DNA code that is used to pass the information to the ribosomes to create proteins. mRNA types and quantities are measured to determine the relative expression of genes in the cells.

Total RNA, which is composed of mRNA, tRNA (transfer RNA) and rRNA (ribosomal RNA), was extracted from the cartilage samples. This involved grinding the tissue in a mortar and pestle cooled by liquid nitrogen, and then homogenization (agitating, or mixing), to break down the cellular membranes and the cartilage matrix. A DNase digestion was used to remove genomic DNA contamination. In this process, RNA is bound to the substrate in the column while DNA passes through. The RNA is then released in a later step, resulting in a purified sample. Genomic contamination is raw DNA from the nuclei present in the extracted RNA. This can generate inaccuracies in the subsequent measurements if DNA is measured instead of RNA.

The mRNA, however, is relatively unstable due to the ubiquitous presence of RNAses (enzymes that degrade RNA) and because mRNA is single stranded. Therefore, RNA was reverse-transcribed to complementary-DNA (cDNA) which is much more stable and less prone to degradation by enzymes. cDNA is essentially a copy of the information contained in mRNA, but in a much more highly stable double stranded form.

Specific genes are then chosen for analysis, based upon our previous work, and those reported in literature. Once a particular gene is targeted, primer pairs are designed that correspond to that DNA representing that gene. A primer pair consists of a forward primer that starts at one end of the specific targeted section of cDNA segment, and the reverse primer that starts at the opposite end. The primer pairs are designed so that they target a unique segment of genetic code, to ensure that they are specific to only that one gene.

The primer pairs are then placed in a reaction well of a 96-well plate in a qRT-PCR instrument. The reaction wells also contain a DNA polymerase; an enzyme that copies the nucleotide information on a strand of cDNA. The machine cycles through multiple amplification cycles. During these cycles the temperature first rises to a denaturation temperature where the double stranded cDNA "melts" open into single stranded cDNA segments. The temperature is then lowered to allow the primer pair to anneal (or bind) to the single stranded cDNA. The temperature then rises for the extension phase, where the polymerase generates complementary copies of the single stranded cDNA segments using random primers. Once the copy is completed, the cDNA is again double stranded (until the next denaturation phase).

A fluorescent marker is added at the beginning of the reaction (SYBR Green) that binds to double stranded cDNA and fluoresces; it doesn't fluoresce on single stranded cDNA. During each amplification cycle, the qRT-PCR instrument measures the amount of

fluorescence present and plots this value with each cycle. There is a certain level of background "noise" that is measured by the machine. A threshold level, or cycle threshold, is set above the level of the background noise. Once the amount of measured fluorescence crosses the threshold, the number of cycles (Ct) required to cross the threshold is recorded. In qRT-PCR, as opposed to just PCR, the fluorescence is measured during each amplification cycle, as a "real-time" measure of PCR product.

If a particular gene is highly expressed in a tissue, there will be a correspondingly high amount of mRNA for that gene in the cell. Therefore, after being reverse-transcribed, the initial cellular high level of the gene expression will result in a high quantity of cDNA. With a large initial amount, less qRT-PCR amplification cycles will be required to detect the fluorescence crossing the threshold (Ct value). Therefore a gene that is highly expressed will have a low Ct value, whereas a gene that has lower expression will have a higher Ct value (less starting cDNA present, therefore more cycles required for the fluorescence level to cross the threshold).

The differences in the gene expression can then be compared with standard statistical testing techniques to evaluate differences in gene expression. A fold change value, or ratio, is usually calculated to compare a gene expression level in one treatment group to another (i.e. ratio of expression, fold change, for axial impacted specimens at day 3 compared to control specimens at day 3 for a particular gene).

3.7 RNA Extraction

Total RNA from the lateral specimens for each patella was extracted first, and if the extraction failed to produce sufficient quantity or quality of RNA, then RNA was extracted from the medial specimens. RNA was extracted from the AOI tissue specimens for each patella, the ADJF for each shear impacted patella, and the two ADJ tissue samples were pooled for each facet of the axially impacted specimens.

Total RNA was extracted from the articular chondrocytes by first grinding the cartilage specimens in a mortar and pestle cooled by liquid nitrogen. The resulting fine powder was then dissolved in Tri Reagent (Molecular Research Center Inc., Cincinnati, OH) which is a combination of both phenol and guanidine thiocyanate in a mono-phase solution that inhibits RNase activity. The tissue was then homogenized in a BeadBeater® (Biospec Products model 3110x, Bartlesville, OK), a high energy cell disrupter that aggressively agitates a specimen vial, for 10 seconds at 4800 oscillations per minute. Following homogenization a chloroform precipitation step was used to remove contaminants (including genomic DNA and cellular debris). A subsequent phenol/chloroform/iso-amyl alcohol step was used to further precipitate out any contaminates. Following these steps, RNA was precipitated in the presence of acetic acid [116], followed with a second precipitation step in the presence of ammonium acetate [139] to yield a higher purity RNA pellet. Finally, on-column DNAse digestion was accomplished with an RNeasy kit (Qiagen, Valencia, CA) to remove genomic DNA contamination. After an ethanol precipitation and subsequent centrifugation, the RNA

pellet was re-suspended in Diethylpyrocarbonate (DEPC)-treated water (water treated to remove RNases). The purity of the RNA was measured and quantitated on a Nanodrop-1000 spectrophotometer (Thermo Scientific, Wilmington, DE). As a backup measurement, the extractions were also spot-checked for quality by visualizing on 1.2% agarose gel to verify the quality of the extracted RNA. The agarose gel is subjected to a 95V charge that creates an electric field that drives the RNA through the gel due to its charge. The varying segment lengths of the RNA generates distinct bands (by RNA size) in the gel. The gel is stained with ethidium bromide to allow for visualization of the bands. A bright 28S and 18S band correspond to rRNA and are indicative of intact RNA. This was not done for all specimens as it required using more of the available RNA and it is a very low throughput method.

3.8 qRT-PCR

Gene primer pairs for qRT-PCR were designed with Beacon Designer software (Premier Biosoft International, Palo Alto, CA). The ideal target length for the amplified product of a PCR reaction is 60-200 base pairs in length to insure accurate replication during the length of time of an amplification cycle. However, the product length may be slightly outside this range as long as accurate verification (sequence validation) of the product is confirmed. The primers were designed to target a product in this range. When possible, primers were designed from porcine gene sequences. If not available, they were designed from conserved regions (regions of DNA coding that have the same sequences across

species) of human, bovine, or canine sequences as these species generally have similar gene coding sequences.

A eukaryotic gene represented in a particular section of DNA usually contains both introns (non-coding sections) and exons (coding sections). The introns are spliced out during the mRNA processing (as it goes from pre-mRNA to mRNA) so that a mature mRNA only contains exonic sequence. A primer pair is designed to cross over these intron-exon boundaries to detect genomic contamination. Genomic contamination is residual DNA in the reaction wells from the cell nuclei. If genomic contamination is present, the primer pairs may amplify the DNA in addition to the mRNA and give a false indication of the amount of gene expression for that sample. If a primer pair crosses an intron-exon boundary, amplified segments of genomic contamination will be much larger than amplified segments of cDNA. The differences in sizes are then detected in a melt curve analysis or gel electrophoresis analysis. Additionally, the intron(s) section may be of sufficient length that amplification will not occur during the amplification cycle. The intron-exon boundaries were predicted by comparing the porcine cDNA sequence to the human genome using UCSC BLAT (http://genome.uscs.edu/cgi-bin/hgBlat). This is a database that includes the entire genomic sequence, finds the cDNA sequence in the genome, and where exons and introns are predicted to occur. The database also detects if there are other similar but unrelated sequences that will be amplified using the same primers (and therefore confound the results).

A High Capacity cDNA Reverse Transcription Kit (Applied Biosystems Inc., Foster City, CA) was used for reverse transcription of 250ng of total RNA. The kit included the necessary components for synthesizing cDNA from RNA. Included were random primers, dNTPs, and a reverse transcriptase. The random primers allow the kit to make copies of the RNA regardless of its actual sequence, the dNTPs are free nucleotides available for making the copies, and the reverse transcriptase is the enzyme that produces the cDNA from the RNA template. The contents of the kit were combined with the RNA solution and, and reverse transcription was performed in a thermal cycler. Reactions were diluted 1:10 for qRT-PCR to allow for more analyses to be conducted of each sample.

The qRT-PCR was performed in a 20μL reaction, consisting of 1 μL of diluted cDNA, 400nM of forward and reverse primers, 10nM fluorescein (as a reference dye), and 0.5μL of 1X Power SYBR Green I Master Mix [140]. A three-step amplification protocol was performed in an iCycler IQ (model 870-1740, Bio-Rad, Hercules, CA) with the following steps: denaturation with one cycle at 95°C for 7 minutes followed by 40 cycles of 30sec at 95°C for denaturation, 30sec at 56°-62°C for annealing, extension for 30sec at 72°C, and a product melting cycle of 5min at 72°C, 1min at 95°C, and 1min at 55°C. For this project 72 AOI samples (with 6 in each treatment/time point combination) and 72 ADJ samples (with 6 in each treatment/time point combination) were evaluated, for a total of 144 specimens. Reactions were performed in duplicate. This number of specimens

required the use of four 96-well plates for a qRT-PCR analysis, with room for a standard curve, for each gene on the full panel of specimens.

3.9 qRT-PCR Analysis

PCR amplification theoretically doubles the number of PCR product after each amplification cycle. The iCycler iQ Real-Time PCR Detection System Software v3.1 (Bio-Rad, Hercules CA) measured the fluorescence of the reactions. Because the fluorescent marker is incorporated into each double stranded PCR product, the measurement of fluorescence is a gauge of the total amount of product generated. The measured fluorescence is plotted against the number of cycles to generate amplification curves for the reactions (Figure 3.7).

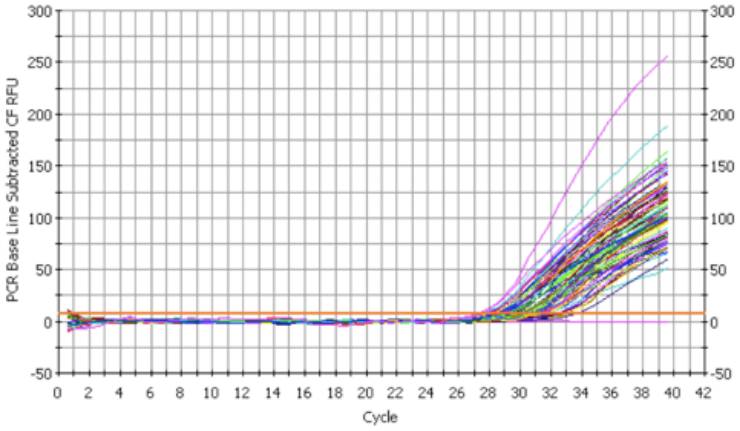

Figure 3.7. Typical Amplification Curve. This graph shows the amplifications curves for each well of a 96 well plate for the housekeeping gene *sdha*. Amplification cycles are represented along the x-axis and fluorescence is measured along the vertical y-axis. The threshold is the horizontal orange line.

The fluorescent trace rises with the number of amplification cycles as the total amount of double stranded product in the well increases. A threshold is set above baseline and

during the range when the amplifications are proceeding exponentially. When the amplifications are proceeding exponentially, there are sufficient reagents to efficiently create PCR products with each cycle. It is important that the threshold is set before the reactions plateau or rise linearly as this represents a point when the reagents may be limited or the primers are hampered by the concentration of the PCR products.

A cycle threshold (Ct) value is measured to determine the cycle number at which the fluorescent trace crosses a threshold. A trace that crosses the threshold at an earlier (lower value) cycle number indicates that there was more of the original cDNA template (transcript) available in the sample originally. For example: If specimen A has a lower Ct value than specimen B for a certain gene, then specimen A had more cDNA template for that gene in the sample which means that it had more mRNA for that gene, and therefore has higher expression of that gene.

In Figure 3.7, a single gene, *sdha*, is being amplified for multiple specimens. Each specimen has different concentrations of mRNA, therefore there are different quantities of cDNA produced for each specimen. The Ct values for each specimen differ because of these differences in starting amounts of cDNA. A lower Ct value for a particular specimen, therefore, indicates a higher expression of that gene.

In a qRT-PCR analysis, the efficiency of the amplification cycle is calculated to verify the amplification process. Dilutions of known concentrations of cDNA for the samples

(standards) are prepared and measured during the qRT-PCR amplification cycles. The different cDNA standards should amplify at different Ct values corresponding to their concentrations. Comparing the expected Ct values with the actual Ct values can be used to calculate the efficiency for the reaction. In theory, each cycle of qRT-PCR results in a doubling of cDNA. If the standard curve shows less than a doubling with each cycle, then the efficiency is less than 100%. Efficiency can be affected by the presence of nucleotides in solution (less are available the longer the reaction progresses), the amount of cDNA initially present, and the primer design. A low efficiency often indicates that the primers require redesign.

The PCR amplification efficiency of each qRT-PCR analysis for a gene (primer pair) was assessed with standard curves. The standard curves were evaluated for each primer by combining equal amounts of cDNA from each specimen into a pool. The pool was then diluted in separate dilutions of 1:3, 1:9, 1:27, 1:81, and 1:243. Because the amount of starting cDNA was known in each dilution, and the Ct value was measured for each dilution, the amount of cycles to reach the Ct threshold could be accurately measured. The number of cycles to the Ct threshold for each dilution was used to evaluate how effectively doubling occurred with each cycle for each dilution. A regression line is then fit to the Ct values of the dilution based upon their concentration. The efficiency is then calculated from the slope of the line (Equation 1).

$$E_x = 10^{(-1/\text{slope})} - 1$$

Equation 1.

slope = slope of regression line
E_x = Efficiency of reaction

The dilutions were evaluated in triplicate by iCycler iQ Real-Time PCR Detection System Software v3.1 (Bio-Rad, Hercules CA) to calculate amplification efficiency.

3.10 Melt Curve Analysis

The gene target specificity of the reactions was evaluated with a melt curve generated at the end of the PCR amplification cycle. The amount of energy (heat) required to separate the double stranded DNA increases with the length of the strand. SYBR green is a fluorescent marker that binds to double stranded DNA, but not single stranded. As the temperature increases, the strands separate, and the fluorescence rapidly decreases. If all of the amplified products are the same sequence and length then the temperature at which separation (melt temperature) occurs will be the same (i.e. there will be one peak). However, if the primers were not specific in what they amplified during the reaction, and produced multiple products, then the melt temperatures will differ (i.e. multiple peaks), indicating poor primer specificity (Figure 3.8 and 3.9). Therefore, the gene targeted may not necessarily be the only gene amplified. Additionally, one cDNA product from each primer pair was sequenced to verify that the PCR product corresponded to the intended gene. ABI Big Dye Terminator Version 1.1 and an ABI3100 Genetic Analyzer (Foster City, CA) were used for sequence validation. For sequence validation, the cDNA to be sequenced is put in solution with fluorescent dideoxynucleotides (complementary nucleotides to the cDNA sequence). A polymerase initiates copying of the cDNA segment and inserts the fluorescent nucleotides in the copy. The genetic analyzer can

precisely measure the sequence of the fluorescent markers attached to the nucleotides, and therefore determine the sequence of the original cDNA.

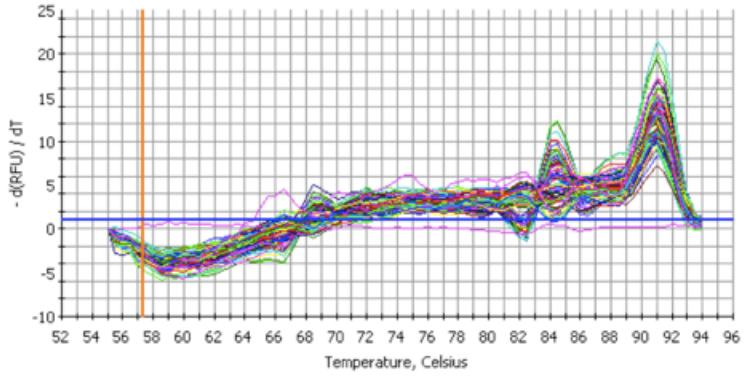

Figure 3.8. Melt curve results for initial *sox-9* primer pair. The two peaks in the melt curve suggest that there are two different products in the reaction wells. The peak with the lower melt temperature is likely from a PCR product of a shorter length and therefore requires less energy to break the bonds of the double stranded DNA. This primer pair was deemed of poor quality and another set had to de designed to assay the *sox-9* gene. Temperature is shown along the x-axis and the y-axis shows the amount of fluorescence (d(RFU)/dT) measured in the iCycler qRT-PCR unit.

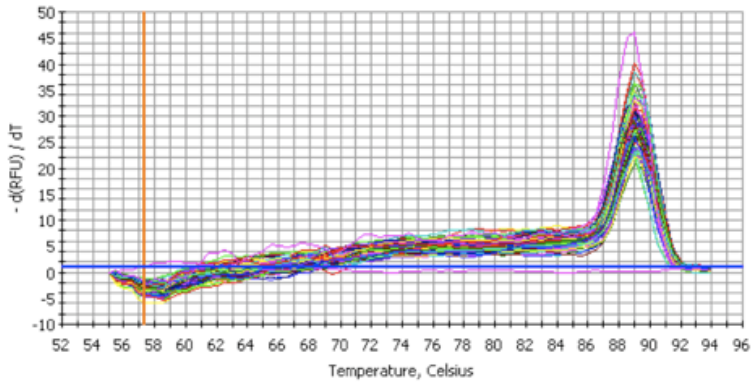

Figure 3.9. Melt curve results for *col2a1* primer pair. There is one central peak indicating that all products required the same energy to break their double stranded DNA bonds. This is considered a good primer pair. Note: there is a single trace that stays below the x-axis and demonstrates no melt curve. This is the negative control which had no cDNA in the reaction well. It was used to assess the chances of any contamination of the reagents. In this case there was no contamination.

3.11 Housekeeping Genes

The most stable reference genes for articular cartilage were evaluated from a panel of 10 genes (Table 3.3). The most stable genes were used to normalize the results of the genes of interest. The panel consisted of the panel of 9 genes used in porcine tissue from Nygard *et al*. [98]: beta-actin (*actb*), beta-2-microglobulin (*b2m1*), glyceraldehyde-3-phosphate dehydrogenase (*gapdh*), hydroxymethylbilane synthase (*hmbs*), hypoxanthine phosphoribosyltransferase I (*hprt1*), ribosomal protein L4 (*rpl4*), succinate dehydrogenase complex, subunit A (*sdha*), TATA box binding protein (*tbp*), and tyrosine 3-monooxygenase/tryptophan 5-monooxygenase activation protein, zeta polypeptide (*ywhaz*). These genes were selected for analysis as they are commonly used reference genes. One additional gene, peptidylprolyl isomerase A (cyclophilin A) (*ppia),* was also evaluated as a potential housekeeping gene. *Ppia* was chosen because it has been used as a normalizing gene for other studies [135-138]; and it exhibited no differential expression in impacted and control specimens in our previous work [65].

Table 3.3. Housekeeping Genes. Houskeeping gene abbreviations, names, primer pair sequences, and efficiency.

Housekeeping Genes Evaluated			
Gene Abbreviation	***Gene Name***	***Sequence (5' -> 3')***	***Efficiency (%)***
*actb**	Beta-actin	F: CACGCCATCCTGCGTCTGGA R: AGCACCGTGTTGGCGTAGAG	93.5
*b2m1**	Beta-2-microglobulin	F: CAAGATAGTTAAGTGGGATCGAGAC R: TGGTAACATCAATACGATTTCTGA	87.6
*gapdh**	Glyceraldehyde-3-phosphate dehydrogenase	F: ACACTCACTCTTCTACCTTTG R: CAAATTCATTGTCGTACCAG	93.4
*hmbs**	Hydroxymethylbilane synthase	F: AGGATGGGCAACTCTACCTG R: GATGGTGGCCTGCATAGTCT	109.1
*hprt1**	Hypoxanthine phosphoribosyltransferase 1	F: GGACTTGAATCATGTTTGTG R: CAGATGTTTCCAAACTCAAC	82.8
*rpl4**	Ribosomal protein L4	F: CAAGAGTAACTACAACCTTC R: GAACTCTACGATGAATCTTC	90.9
*sdha**	Succinate dehydrogenase complex, subunit A	F: CTACAAGGGGCAGGTTCTGA R: AAGACAACGAGGTCCAGGAG	107.8
*tbp**	TATA box binding protein	F: AACAGTTCAGTAGTTATGAGCCAGA R: AGATGTTCTCAAACGCTTCG	70.7
*ywhaz**	Tyrosine 3-monooxygenase/tryptophan 5-monooxygenase activation protein, zeta polypeptide	F: TGATGATAAGAAAGGGATTGTGG R: GTTCAGCAATGGCTTCATCA	101.8
ppia	peptidylprolyl isomerase A (cyclophilin A)	F: GCAGACAAAGTTCCAAAGACAG R: AGATGCCAGGACCCGTATG	84.4
** Primer pairs from Nygard et al.[98]*			

Both BestKeeper and geNorm were used to select the most stable housekeeping genes (Table 3.3). For the BestKeeper program, the raw Ct values were entered. The program calculates a BestKeeper index as the geometric mean of all housekeeping gene Ct values. Pearson correlations between each candidate gene and the index are calculated and reported as the BestKeeper correlation coefficient. The genes with the highest BestKeeper correlation coefficient are the most stably expressed. While there is no specific threshold for the BestKeeper correlation coefficient, it is recommended to use multiple genes that are geometrically averaged to control for outliers. Pfaffl *et al*. found 3 housekeeping genes to be a realistic number of housekeeping genes to manage for most laboratory studies that would ensure accurate normalization[134].

The input for the geNorm program is relative Ct values, where the Ct values for a particular gene are all normalized to the specimen with the highest expression for that gene (minimum Ct value). The normalized Ct values (Q) are calculated via the delta-Ct formula (Equation 2).

$$Q = E^{(\min Ct - \text{sample } Ct)}$$

Equation 2.

Q = normalized Ct values
E = efficiency (where 100% = 2)
minCt = minimum Ct value for a gene
sampleCt = the Ct value of the current sample

The program does pairwise comparisons of each reference gene with every other gene and then develops an index of the average pairwise variation of a particular gene with all others. Vandesompele *et al.* defined a gene stability measure M, as the mean of all pairwise variations V (Equation 3), where j and k are two reference genes, and n is the number of reference genes [133].

$$M_j = \frac{\sum_{k=1}^{n} V_{jk}}{n-1}$$

Equation 3.

M = gene stability measure
V = pairwise variation
j,k = pair of control genes
n = number of control genes

An ideal reference gene that does not vary across samples or treatments is unlikely to exist. The M value provides a measure of stability in comparison to other potential reference genes. Use of the top 3 or 4 most stable housekeeping genes is usually appropriate for accurate normalization [133].

As proposed by Vandesompele *et al*., the best reference genes for a particular tissue can be used for evaluating the expression levels of genes of interest [133]. This can be accomplished by taking the geometric mean (as compared to the arithmetic mean) of the selected reference genes. The arithmetic mean is the sum of the individual n values

divided by the n (the total number of values), whereas the geometric mean is the n-th root of the product of n numbers (Equation 4). The geometric mean is able to better control for outliers and abundance differences between genes than the arithmetic mean. The most accurate normalization strategy is to use the geometric mean of the top 3 or 4 most stable genes for normalization [133, 134].

$$Geometric\ mean = \sqrt[n]{a_1 a_2 \ldots a_n} \qquad \textbf{Equation 4.}$$

n = total number of specimens
a = individual Ct value for a specimen

3.12 OA Related Genes

A set of 18 genes potentially related to the progression of OA were selected for evaluation using qRT-PCR. The genes were selected from four categories: genes related to the cartilage matrix, degradative enzymes and inhibitors, inflammatory response and signaling, and cell proliferation and apoptosis. Some genes could have been appropriately listed in multiple categories, however for this work they were grouped based upon what is believed to be their primary function during early stage OA. From the cartilage matrix category, 6 genes were selected: Collagen, Type I, Alpha 1 (*col1a1*), Collagen, Type II, Alpha 1 (*col2a1*), Aggrecan (*agc*), SRY (sex determining gene region Y) box-9 (*sox-9*), Osteopontin (*opn*), and Cartilage oligometric matrix protein (*comp*). From the second category, degradative enzymes and inhibitors, 6 genes were selected for analysis: Matrix metalloprotease-1 (*mmp-1*), Matrix metalloprotease-3 (*mmp-3*), Matrix

metalloprotease-13 (*mmp-13*), TIMP Metallopeptidase Inhibitor-1 (*timp-1*), TIMP Metallopeptidase Inhibitor-2 (*timp-2*), and ADAM Metallopeptidase with Thrombospondin Type 1 Motif 5 (*adamts-5*). From the third category, inflammatory response and signaling, 4 genes were selected for analysis: Indian Hedgehog (*ihh*), Transforming growth factor β (*tgfb*), nitric oxide synthase 2, inducible (*inos*), and Chitinase-3-like protein 1 (*chi3l1*). And from the final category, cell proliferation and apoptosis, 2 genes were selected for analysis: Caspase-8 (*casp-8*), and Fas (TNF receptor superfamily, member 6) (*fas*). Table 3.4 provides the gene information along with the primer sequences used for amplification, the associated amplicon length for the mRNA segment amplified, and the National Center for Biotechnology Information (NCBI) accession number for the targeted gene. The accession number is a unique identifier assigned to a specific section of DNA sequence corresponding to a gene. Additionally, the length of the amplicon (amplified segment of cDNA) is provided.

Table 3.4. OA Related Genes. Full gene names, abbreviations, forward and reverse primer sequences, amplicon lengths, and NCBI numbers.

OA Related Genes				
Gene Name	***Gene Abbreviation***	***Sequence (5' -> 3')***	***Amplicon length***	***NCBI Number***
Cartilage Matrix				
Collagen, Type I, Alpha 1	*col1a1*	F: CAACCGCTTCACCTACAGC		
		R: TTTTGTATTCGATCACTGTCTTGCC	101	AK236626
Collagen, Type II, Alpha 1	*col2a1*	F: GAGAGGTCTTCCTGGCAAAG		
		R: AAGTCCCTGGAAGCCAGAT	118	AF201724.1
Aggrecan	*agc*	F: TGCAGGTGACCATGGCC		
		R: CGGTAATGGAACACAACCCCT	79	AF201722b
SRY (sex determining gene region Y) box-9	*sox-9*	F: CAGGGCTCTGTGCTCTACTCC		
		R: GGGTTACGGTCTTTCTTCGGT	230	NM_213843.1
Osteopontin	*opn*	F: CCGCAGCCAGGAGCAGTC		
		R: GTTGATCTCAGAAGACGCACTCTC	214	NM_214023.1
Cartilage oligometric matrix protein	*comp*	F: GGCTGGAAGGACAAGACATC		
		R: CCTCATAGAACCGCACTCTG	82	XM_003123529.1
Degradative Enzymes & Inhibitors				
Matrix metalloprotease-1	*mmp-1*	F: TGATGGACCTGGAGGAAACC		
		R: GAGCAGCCACACGATACAAG	131	NM_001166229
Matrix metalloprotease-3	*mmp-3*	F: GATGTTGGTTACTTCAGCAC		
		R: ATCATTATGTCAGCCTCTCC	197	NM_001166308.1
Matrix metalloprotease-13	*mmp-13*	F: CCAAAGGCTACAACTTGTTTCTTG		
		R: TGGGTCCTTGGAGTGGTCAA	77	AF069643
TIMP Metallopeptidase Inhibitor-1	*timp-1*	F: CCTCGTACCAGCGTTATG		
		R: CGTTCCACAGTTGTCCAG	177	NM_213857.1
TIMP Metallopeptidase Inhibitor-2	*timp-2*	F: ATATACGAGAACACCAGACC		
		R: GGAATGATTACAACGGATGC	152	AK237154.1
ADAM Metallopeptidase with Thrombospondin Type 1 Motif 5	*adamts-5*	F: CGCTGCCACCACACTCAA		
		R: CGTAGTGCTCCTCATGGTCATCT	80	NM_007038.3

Table 3.4. Continued.

Gene Name	*Gene Abbreviation*	*Sequence (5' -> 3')*	*Amplicon length*	*NCBI Number*
Inflammatory Response				
Indian Hedgehog	*ihh*	F: CAGCGGGCGCTATGAAGGCA		
		R: GGTCCTTGCAGCGCTGGGTC	140	XM_001925486.1
Transforming growth factor β	*tgfb*	F: GGAGTGGCTGTCCTTTGATGT		
		R: AGTGTGTTATCTTTGCTGTCA	117	NM_214015.1
nitric oxide synthase 2, inducible	*inos*	F: TGAATTTGTCAACCTGTATTAC		
		R: CTTTGTTACCGCTTCCAC	82	NM_001143690.1
Chitinase-3-like protein 1	*chi3l1*	F: TGACGCTCTATGACACAC		
		R: GGCTAGGTCCAGTCCATC	194	NM_001001540
Cell Proliferation and Apoptosis				
Caspase-8	*casp-8*	F: TGGGCAAACAGATGCCACAACCT		
		R: CCCCTTCAATCTAGCCCACCCCC	153	NM_001031779.2
Fas (TNF receptor superfamily, member 6)	*fas*	F: TAGAGTTTGTGATGGAGAA		
		R: ATTGAGAAGTGTGACAGA	107	NM_213839.1

3.13 Analysis of OA Related Genes

The qRT-PCR data for the 18 OA related genes were evaluated by comparing the relative gene expression levels (Ct values) across treatments and across time. A linear mixed model was used for analysis following the methods proposed by Steibel et al. [141]. A mixed model takes into account both fixed and random effects. The model used was:

$$y_{ijklmnopq} = \mu + pig_i + rep_{j(i)} + leg_k + T_{lmn} + date_o + plate_p + well_{q(p)} + e_{ijklmnopq}$$

Equation 5.

Where $y_{ijklmnopq}$ = gene expression levels (Ct); μ = factor common to all observations; pig_i = random effect of pig (37 individual pigs); $rep_{j(i)}$ = random effect of replicate sample within each pig (samples run in duplicate); leg_k = fixed effect of leg (right or left); T_{lmn} = fixed effect of the combination of gene (l), treatment (m) and culture time (n); $date_n$ = fixed effect of date (13 different testing dates); $plate_p$ = random effect of plate due to which of the 4 real-time plates (p) the particular sample was evaluated on; $well_{q(p)}$ = random effect of well within plate due to which well of the 96 well plate the sample was evaluated in; $e_{ijklmnop}$ = random residual error. Standard distributional assumptions for all random effects were employed.

Using the model from Equation 5, differences for comparisons of interest were evaluated for statistical significance using PROC MIXED in SAS 9.2 statistical software (SAS Institute Inc., Cary, NC). The raw p-values were adjusted for multiple comparisons using

the false discovery rate method (FDR) [142]. A standard Bonferroni correction of the family wise error rate (FWER) controls the possibility of making even one type I error to below the alpha value (threshold). The FWER is the probability of making a type I error in any one test out of all the pairwise comparisons, where a type I error is when the null hypothesis is incorrectly rejected, or a "false positive." This method often results in reduced sensitivity and can be overly restrictive in evaluating results. The FDR method, however, controls the possibility of making a type I error within those results evaluated as significant [143]. Due to the relatively small number of samples in each combination of treatment and time in this experiment, the threshold for a significant FDR adjusted p-value (q-value) was set at $q < 0.2$. This threshold allows for an appropriate sensitivity for the analyses being conducted and insures that the interpretation of the data is not overly restrictive in eliminating potentially valuable findings that may not achieve a higher level of significance. Due to the fundamental difference in how FDR controls for a type I error rate within results already deemed significant, a higher threshold may be acceptable, up to even 0.5 [144].

For each comparison of groups (example: comparing day 0 shear AOI specimens to day 0 control specimens) the fold changes were calculated. Fold change calculations are a method of relating the expression levels in one sample of interest to another (or comparative) sample; they are, therefore, a ratio comparison between groups. Fold changes were calculated by first using Equation 6 [141] for the gene of interest (GOI) and

the geometric mean of the housekeeping genes (HKM). Where GOI represents one of the 18 OA related target genes (eg. *col1a1*).

$$diff_{group\,2-group\,1} = \left(Ct^{GOI}_{group\,2} - Ct^{GOI}_{group\,1}\right) - \left(Ct^{HKM}_{group\,2} - Ct^{HKM}_{group\,1}\right)$$

Equation 6.

The Ct values for a particular GOI for two groups are compared (i.e. day 0 shear specimens for *col1a1* compared to day 0 control specimens for *col1a1*). The comparison is normalized to the difference of the geometric mean of the housekeeping genes (HKM) for the same comparison. Equation 6 was then substituted into Equation 7 to complete the fold change (FC) calculation [141].

$$FC_{group\,2-group\,1} = 2^{-diff_{group\,2-group\,1}}$$

Equation 7.

A fold change greater than 1 indicates a particular gene is more highly expressed in the sample of interest as compared to the control. A fold change less than 1 indicates a lower level expression than control. Differential gene expression was first evaluated by comparing each treatment (axial vs. control, shear vs. control, and shear vs. axial) at each time point. Differential gene expression was next evaluated within each treatment (control, axial and shear) by comparing each time point (day 0, 3, 7 and 14) to day 0

control specimens. Day 0 control specimens were used as the reference for temporal changes as they most closely represent an un-impacted cartilage surface in its natural state.

4. RESULTS

4.1 Overview of Results

Impactions were completed on all patellae and total RNA was extracted from 144 specimens from 72 patellae and was reverse transcribed to cDNA. A panel of housekeeping genes were evaluated in a subset of specimens representing all treatments and time points to identify the most stable housekeeping genes for this treatment regimen. A panel of 18 genes was selected from previous work, both in our lab and from literature. All specimens were evaluated for the full panel of housekeeping and OA related genes.

4.2 Impaction Results

Seventy-five patellae total were removed from the knee joints and impacted, but 3 patellae developed what was likely infection in culture and were not included. Therefore, a total of 72 patellae were included in this analysis, 36 from the right leg, and 36 from the left leg. The patellae were randomized to treatment and time in culture with 6 patellae in each of the 12 treatment/time groups represented (e.g. 0 day axial impaction; Table 3.2).

Typical force traces (recorded force vs. time) from the piezoelectric load cell recordings are shown in Figures 4.1-4.3. The axial impaction event was characterized by application of a compressive load at 25 mm/sec (Figure 4.1). The load ramped to a target load of 2000 N, at which point the impactor was retracted from the cartilage surface at 200 mm/sec. Inability to align the patellae perfectly perpendicular to the loading direction

and unevenness of the surface generated some forces in the longitudinal and radial shear directions.

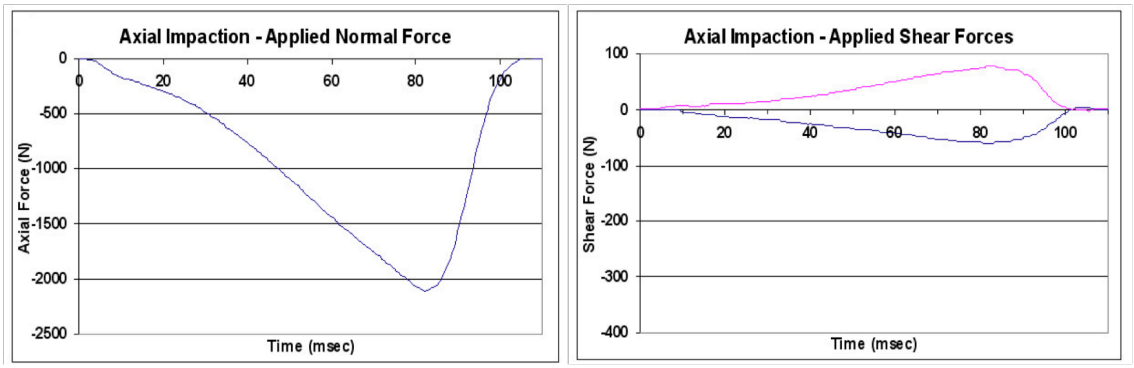

Figure 4.1. Axial impaction loading event. These images show typical force recordings of the normal and shear forces (recorded by the piezoelectric load cell) during the axial impactions. The image on the left shows the rise in the compressive (normal) forces as the impactor loads the cartilage surface at 25mm/sec up to a targeted load of 2000N. The image on the right shows the shear forces recorded during the axial loading event with the longitudinal forces in blue and the radial forces in red.

The shear impactions were conducted by slowly applying a compressive normal load to the cartilage surface at 0.05 mm/sec, and the load ramped to an axial load of 500 N (Figures 4.2 and 4.3). Once the 500 N targeted compressive force was reached, the second hydraulic load frame was triggered to displace the patella 10 mm tangentially in the radial shear direction. The initial 500 N load created a depression in the tissue as the impactor pushed below the level of the surrounding tissue. When the tangential displacement was generated, a spike in the normal force occurred as the impactor had to overcome the tissue at the side of the depression created by the 500 N load. The displacement also resulted in a rise in both longitudinal and radial shear forces.

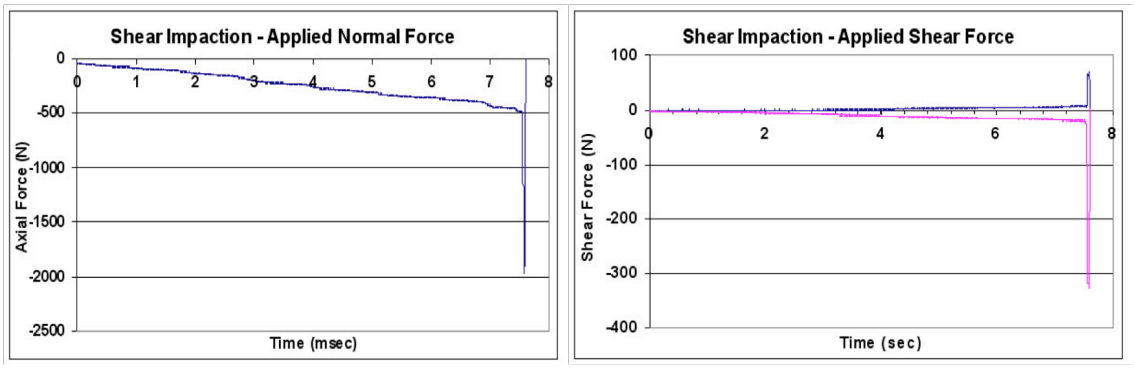

Figure 4.2. Shear impaction entire time history. These images depict the loading of a typical shear impacted patella. The forces (as recorded by the piezoelectric load cell) are shown along the vertical axis, and the time history is shown along the x-axis. The graph on the left shows the slow loading of the normal force at 0.05mm/sec up to 500 N. Once the 500N compressive load is reached, the load frame maintained the displacement level and the second load frame displaced the patella 10mm tangentially and generated the spike in the graph. The graph on the right shows the entire time history of the loading for the longitudinal (blue trace) and the radial (red trace) shear forces.

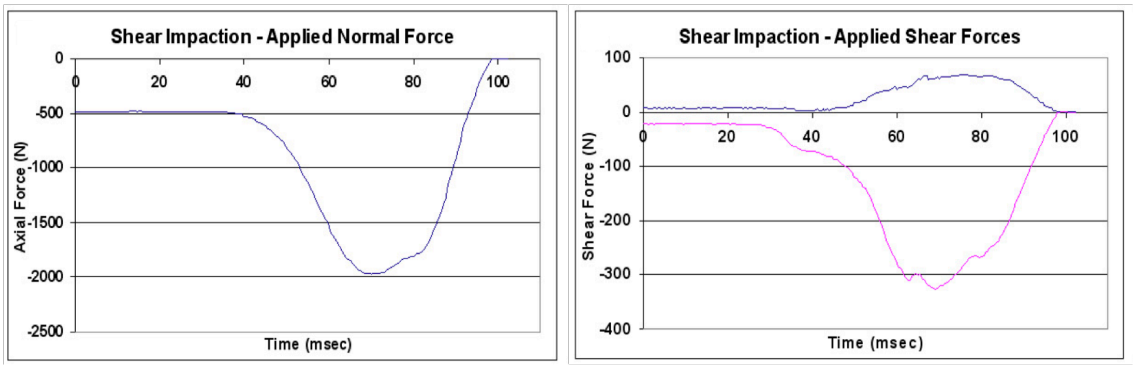

Figure 4.3. Shear loading event. The images show the final 110 ms (approximately) of the shear loading event. The image on the right shows the larger radial shear forces (red trace) generated in the shear impaction.

The axial impactions resulted in significantly higher normal forces imparted to the cartilage with a mean of -1965.9N ± 237.1, versus a mean of -1092.7N ± 205.4 ($p = <0.0001$) for the shear impactions (Figure 4.4). The shear impactions generated a significantly higher radial shear force (the direction of shearing displacement) with a

mean of 198.3N ± 59.2, as compared to the radial shear for the axial treatment, which had a mean of 79.0 N ± 73.4 (p = <0.0001). The longitudinal shear forces were not significantly different between shear (mean 59.7N ± 35.9) and axial impactions (mean 74.1N ± 55.3, p = 0.134).

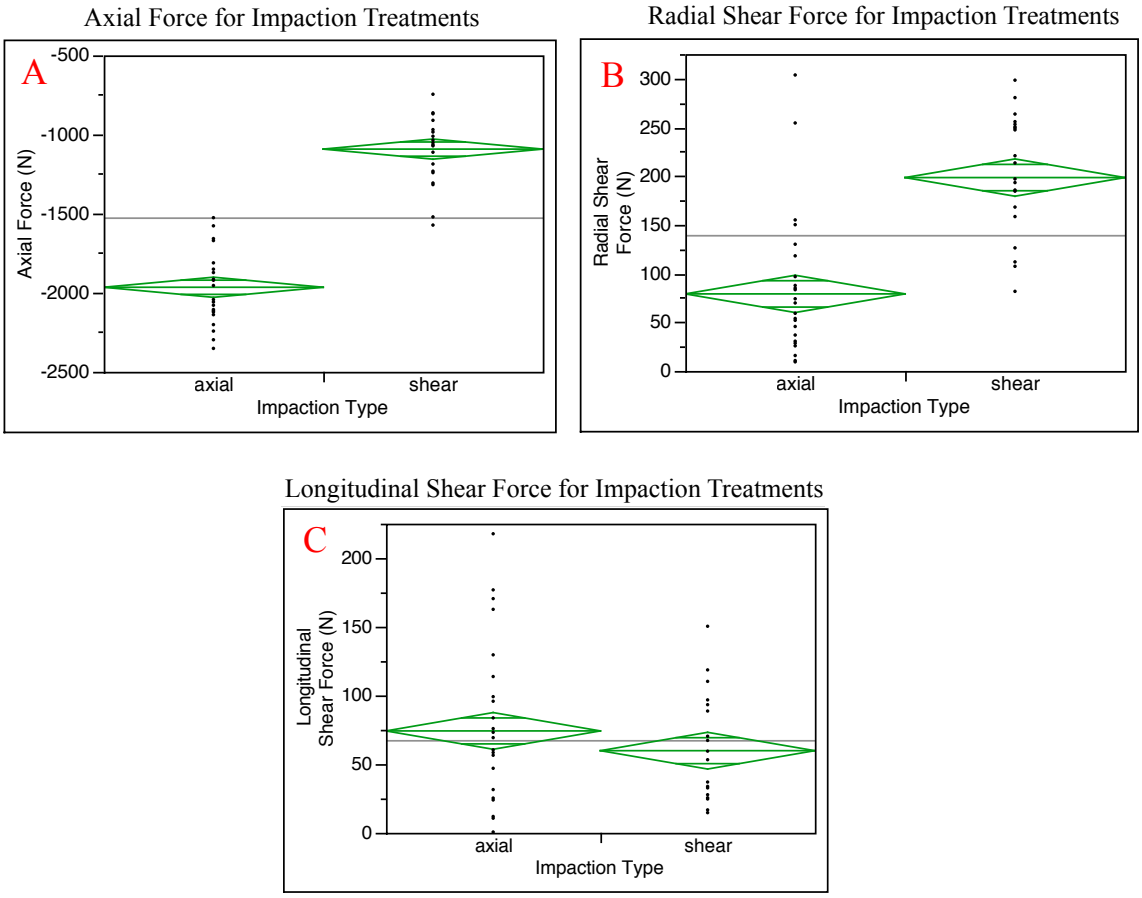

Figure 4.4. Axial forces and radial shear forces. Image A shows a diamond scatter plot (JMP 7) of the axial forces for each of the axial and shear impaction treatments. The horizontal center line of the diamond indicates the mean value, and the top and bottom of the diamond indicate the 95% confidence interval. Diamond scatter plots for the radial shear forces (B) and longitudinal shear forces (C) in each impaction treatment are shown.

4.3 Culture and RNA Extraction

Of the 72 patellae included in this experiment, 3 patellae became infected (due to bacterial growth) in culture. The culture media was changed daily to minimize the chances of infection. However, even with the best laboratory technique it is difficult to keep a biological specimen as large as a patella, with its multiple tissues, free of bacterial growth (identified by cloudiness in the normally clear, red culture media). The 3 patellae which were infected were discarded with no tissue collected, and their treatments were repeated with replacement patellae from other animals. The discarded patellae included: one 7-day control right, one 14-day axial impaction right, and one 14-day control left patella.

RNA was extracted from AOI and ADJ tissue specimens for the lateral facet of each patellae. Each patellae facet was given identical treatments and the lateral was used for this analysis. This side was not chosen for any reason other than to attempt to have some consistency across specimens. However, in the instances where the extraction failed on the lateral specimen, the medial facet specimen was used. A total of 144 specimens were evaluated. Extraction failed to produce RNA of high enough quality in 9 of the 144 extractions as determined by spectrophotometer. In these 9 cases where an extraction failed on either the AOI or ADJ specimen, RNA was extracted from the cartilage specimen from the medial facet.

4.4 Housekeeping Genes

Ten housekeeping genes were evaluated in cartilage for the treatment conditions. Two or more specimens at each impaction treatment/time point combination were evaluated for a total of 40 patellae (Table 4.1). The housekeeping analysis was conducted early in the study progression, therefore it was conducted on a subset of the specimens (only AOI specimens) that had been generated at that point.

Table 4.1. Distribution of sample numbers by treatment and culture days.

Tissue numbers			
	Impaction Treatment		
Culture time (days)	Axial	Shear	Control
0	4	3	3
3	4	4	3
7	3	3	2
14	4	4	3
Total Specimens	40		

The genes evaluated were: *actb, b2m1, gapdh, hmbs, hprt1, rpl4, sdha, tbp, ywhaz,* and *ppia*. One of the housekeeping genes, *hprt*, was excluded from further analysis as it displayed consistently high cycle threshold (Ct) values (greater than 35) and failed to amplify for five wells. The high Ct values indicate very little initial presence of the transcript, thus indicating that this gene is not useful as an internal reference. The 40 cycle threshold values from each of the candidate genes were used directly in the

BestKeeper software and were used to calculate the input values (Q values) for geNorm [145].

BestKeeper results showed the stability ranking of the nine genes to be (in order of most stable to least stable): *gapdh*, *ppia*, *actb*, *sdha*, *ywaz*, *rpl4*, *b2m1*, *tbp*, and *hmbs2* (Figure 4.5). The geNorm results differed slightly and showed the stability order to be: *sdha*/*ppia (tied)*, *actb*, *gapdh*, *tbp*, *ywaz*, *hmbs-2*, *rpl4*, and *b2m1* (Figure 4.6).

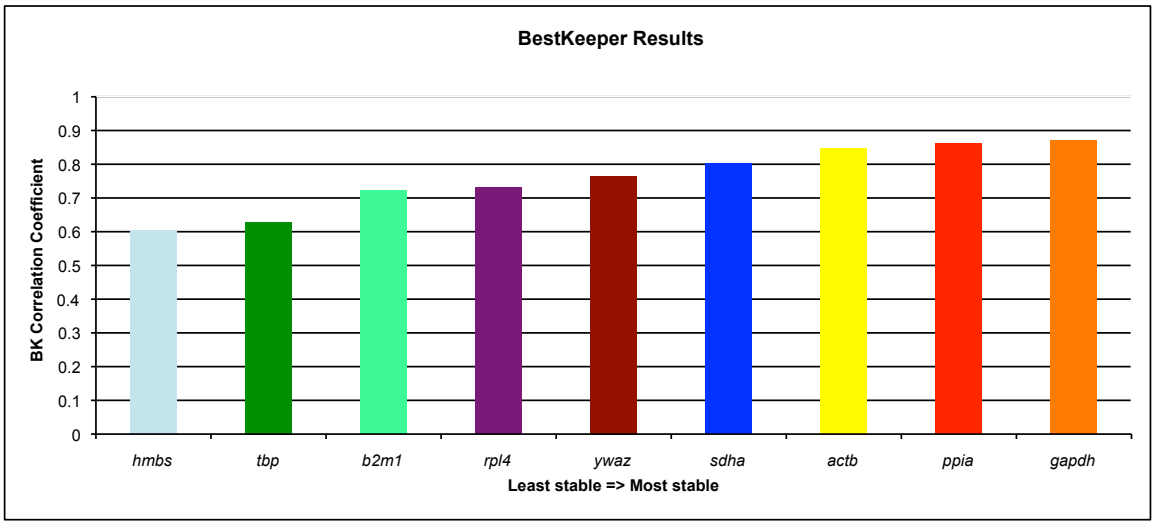

Figure 4.5. The BestKeeper results for candidate genes. BK correlation coefficients for each gene are given. A higher correlation coefficient corresponds to a more stably expressed gene.

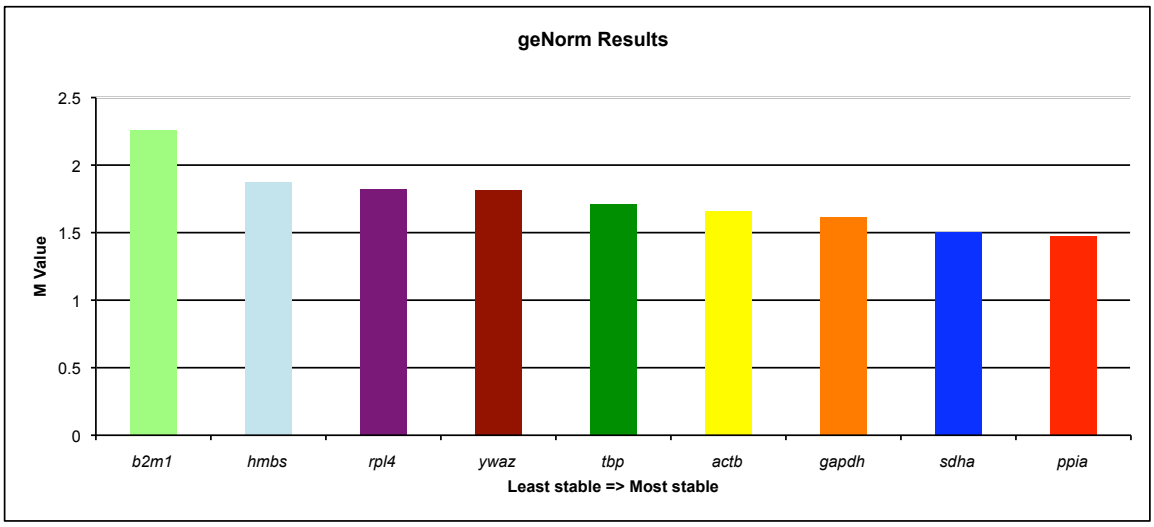

Figure 4.6. The geNorm results for candidate genes. The M-value calculated by geNorm is a measure of stability of the gene expression across specimens. Genes with lower M-values show increased stability.

Both programs found that the same four genes exhibit the highest stability in porcine cartilage (across our three treatment groups and four time points), with only the order differing between the two methods. The most stable genes were *gapdh*, *ppia*, *actb*, and *sdha.* The programs' authors recommend 3 or 4 housekeeping genes for an accurate normalization strategy [133, 134, 145]. Therefore, the geometric mean of *gapdh*, *ppia*, *actb*, and *sdha* was used for normalization of the OA related genes.

4.5 Results of OA Related Genes

As an assessment of early stage OA progression, a panel of 18 genes related to cartilage degeneration were evaluated in 144 specimens. The panel consisted of genes related to the cartilage matrix (*col1a1, col2a1, agc, sox-9, spp1, comp*), degradative enzymes and inhibitors (*mmp-1, mmp-3, mmp-13, timp-1, timp-2, adamts-5*), inflammatory response and signaling (*ihh, tgfb, inos, chi3l1*), and cell proliferation and apoptosis (*casp-8, fas*).

The genes were evaluated in both AOI and ADJ specimens at all time points (0, 3, 7, and 14 days) and treatments (control, axial and shear). Raw p-values were adjusted for multiple testing using the FDR method, and adjusted p-values (q-values) were considered significant for $q < 0.2$.

4.6 Comparison of Treatments at Each Time Point

Differential gene expression was first evaluated by comparing each treatment (axial vs. control, shear vs. control, and shear vs. axial) at each time point. Results are presented for Axial AOI vs. Control AOI (Table 4.2), Axial ADJ vs. Control ADJ (Table 4.3), Shear AOI vs. Control AOI (Table 4.4), Shear ADJ vs Control ADJ (Table 4.5), Shear AOI vs. Axial AOI (Table 4.6), and Shear vs. Axial ADJ (Table 4.7).

Table 4.2. Differential gene expression for Axial AOI compared to Control AOI specimens at each time point. Fold changes are shown on the left, and the corresponding q-values are shown on the right. Significant q-values ($q < 0.2$) and the associated fold changes are highlighted in blue.

Comparing Treatments within Time point

	Fold Changes **Axial AOI vs. Control AOI**				***q-Values (FDR)*** **Axial AOI vs. Control AOI**			
Gene	***Day 0***	***Day 3***	***Day 7***	***Day 14***	***Day 0***	***Day 3***	***Day 7***	***Day 14***
Cartilage Matrix								
col1a1	0.26	1.09	0.32	2.43	0.29	0.92	0.29	0.34
col2a1	2.57	0.39	2.73	1.83	0.07	0.07	0.07	0.20
agc	1.25	1.12	0.94	0.74	0.87	0.87	0.87	0.87
sox-9	1.12	0.57	0.60	0.45	0.76	0.20	0.20	0.09
opn	1.05	1.66	0.62	0.22	0.92	0.43	0.43	0.01
comp	1.45	0.93	1.25	0.56	0.52	0.83	0.67	0.32
Degradative Enzymes & Inhibitors								
mmp-1	0.55	0.59	0.80	0.46	0.69	0.69	0.71	0.69
mmp-3	1.56	0.38	1.12	0.47	0.71	0.56	0.87	0.56
mmp-13	3.09	0.65	2.08	0.27	0.18	0.51	0.36	0.18
timp-1	0.94	0.97	1.20	0.68	0.93	0.93	0.93	0.93
timp-2	0.37	0.57	0.68	0.65	0.05	0.30	0.34	0.34
adamts-5	0.26	0.58	0.45	1.50	0.12	0.48	0.35	0.51
Inflammatory Response & Signaling								
ihh	1.16	0.30	0.91	0.76	0.87	0.16	0.87	0.87
tgfb	1.41	1.93	0.97	0.39	0.35	0.06	0.91	0.01
inos	2.22	0.55	1.51	0.15	0.29	0.36	0.45	< 0.01
chi3l1	1.86	0.84	1.15	0.32	0.33	0.76	0.76	0.04
Cell Proliferation & Apoptosis								
casp-8	1.10	0.61	0.60	0.44	0.80	0.21	0.21	0.08
fas	0.83	1.30	0.44	0.80	0.66	0.66	0.24	0.66

Table 4.3. Differential gene expression for Axial ADJ compared to Control ADJ specimens at each time point. Fold changes are shown on the left, and the corresponding q-values are shown on the right. Significant q-values (q < 0.2) and the associated fold changes are highlighted in blue.

Comparing Treatments within Time point

	Fold Changes **Axial ADJ vs. Control ADJ**				***q-Values (FDR)*** **Axial ADJ vs. Control ADJ**			
Gene	***Day 0***	***Day 3***	***Day 7***	***Day 14***	***Day 0***	***Day 3***	***Day 7***	***Day 14***
Cartilage Matrix								
col1a1	2.32	1.16	1.08	0.20	0.62	0.92	0.92	0.17
col2a1	1.87	0.56	1.47	2.63	0.29	0.29	0.42	0.17
agc	1.70	1.14	1.18	0.69	0.48	0.70	0.70	0.55
sox-9	1.42	0.56	0.57	1.84	0.31	0.15	0.15	0.15
opn	2.02	0.70	0.51	0.39	0.24	0.47	0.24	0.23
comp	1.27	0.61	1.04	0.83	0.77	0.56	0.90	0.77
Degradative Enzymes & Inhibitors								
mmp-1	0.66	0.33	0.27	0.32	0.69	0.09	0.09	0.09
mmp-3	0.39	0.40	0.61	0.48	0.40	0.40	0.49	0.40
mmp-13	7.68	0.77	1.68	0.88	0.01	0.85	0.85	0.85
timp-1	1.33	0.67	0.90	0.46	0.50	0.45	0.76	0.07
timp-2	0.84	0.65	1.05	1.34	0.88	0.88	0.91	0.88
adamts-5	1.45	1.12	1.60	1.02	0.97	0.97	0.97	0.97
Inflammatory Response & Signaling								
ihh	1.61	0.84	0.61	1.12	0.81	0.84	0.81	0.84
tgfb	1.81	0.77	1.31	0.80	0.21	0.46	0.46	0.46
inos	1.85	0.71	2.18	0.91	0.51	0.71	0.51	0.86
chi3l1	2.67	0.83	1.22	0.47	0.11	0.67	0.67	0.18
Cell Proliferation & Apoptosis								
casp-8	1.48	0.68	0.60	1.86	0.28	0.28	0.28	0.28
fas	0.50	1.38	0.90	0.62	0.43	0.61	0.81	0.56

Table 4.4. Differential gene expression for Shear AOI compared to Control AOI specimens at each time point. Fold changes are shown on the left, and the corresponding q-values are shown on the right. Significant q-values ($q < 0.2$) and the associated fold changes are highlighted in blue.

Comparing Treatments within Time point

	Fold Changes **Shear AOI vs. Control AOI**					***q-Values (FDR)*** **Shear AOI vs. Control AOI**			
Gene	***Day 0***	***Day 3***	***Day 7***	***Day 14***		***Day 0***	***Day 3***	***Day 7***	***Day 14***
Cartilage Matrix									
col1a1	1.37	5.36	0.17	0.35		0.70	0.09	0.09	0.24
col2a1	1.41	0.97	1.13	1.96		0.94	0.94	0.94	0.62
agc	0.82	1.29	1.14	1.53		0.70	0.70	0.70	0.70
sox-9	1.00	0.71	0.62	1.33		0.99	0.56	0.56	0.56
opn	1.02	2.26	0.78	0.58		0.97	0.40	0.83	0.53
comp	0.60	0.87	0.93	0.81		0.47	0.83	0.83	0.83
Degradative Enzymes & Inhibitors									
mmp-1	1.55	0.67	0.39	0.17		0.60	0.60	0.25	0.01
mmp-3	3.69	0.61	3.58	0.26		0.10	0.49	0.10	0.10
mmp-13	1.05	3.56	0.54	0.19		0.94	0.12	0.47	0.05
timp-1	1.24	0.85	0.96	0.84		0.84	0.84	0.90	0.84
timp-2	0.96	1.34	0.49	1.03		0.93	0.93	0.28	0.93
adamts-5	0.52	0.87	0.37	0.22		0.39	0.81	0.18	0.04
Inflammatory Response & Signaling									
ihh	2.33	0.83	2.05	1.27		0.42	0.74	0.42	0.74
tgfb	0.72	1.22	0.86	0.68		0.57	0.63	0.63	0.57
inos	0.77	0.92	0.94	0.31		0.91	0.91	0.91	0.13
chi3l1	2.00	0.46	1.20	0.51		0.17	0.17	0.69	0.17
Cell Proliferation & Apoptosis									
casp-8	0.98	0.70	0.63	1.31		0.95	0.58	0.58	0.58
fas	0.35	1.20	0.84	1.45		0.06	0.69	0.69	0.69

Table 4.5. Differential gene expression for Shear ADJ compared to Control ADJ specimens at each time point. Fold changes are shown on the left, and the corresponding q-values are shown on the right. Significant q-values ($q < 0.2$) and the associated fold changes are highlighted in blue.

Comparing Treatments within Time point

	Fold Changes **Shear ADJ vs. Control ADJ**				***q-Values (FDR)*** **Shear ADJ vs. Control ADJ**			
Gene	***Day 0***	***Day 3***	***Day 7***	***Day 14***	***Day 0***	***Day 3***	***Day 7***	***Day 14***
Cartilage Matrix								
col1a1	9.14	0.97	0.35	0.07	0.02	0.97	0.25	< 0.01
col2a1	0.75	0.55	0.28	2.15	0.54	0.27	0.03	0.21
agc	1.09	0.82	1.04	2.04	0.91	0.91	0.91	0.15
sox-9	1.01	1.37	0.74	1.60	0.98	0.53	0.53	0.53
opn	2.03	0.70	0.41	0.55	0.29	0.47	0.28	0.29
comp	0.89	0.59	0.78	1.09	0.80	0.43	0.80	0.80
Degradative Enzymes & Inhibitors								
mmp-1	2.18	0.32	0.38	0.38	0.45	0.16	0.16	0.16
mmp-3	1.59	0.47	0.46	0.69	0.60	0.57	0.57	0.60
mmp-13	4.54	1.59	0.59	2.09	0.10	0.49	0.49	0.49
timp-1	1.12	0.52	0.90	0.92	0.81	0.18	0.81	0.81
timp-2	0.70	0.53	0.80	1.58	0.50	0.45	0.56	0.49
adamts-5	3.45	0.99	1.13	0.89	0.15	0.98	0.98	0.98
Inflammatory Response & Signaling								
ihh	1.22	1.10	0.30	0.87	0.87	0.87	0.15	0.87
tgfb	1.12	0.59	0.72	1.04	0.90	0.36	0.55	0.90
inos	1.98	1.59	1.50	2.15	0.41	0.45	0.45	0.41
chi3l1	1.48	0.31	1.52	0.79	0.50	0.03	0.50	0.60
Cell Proliferation & Apoptosis								
casp-8	1.04	1.40	0.78	1.59	0.90	0.64	0.64	0.64
fas	1.11	1.15	0.58	1.35	0.81	0.81	0.81	0.81

Table 4.6. Differential gene expression for Shear AOI compared to Axial AOI specimens at each time point. Fold changes are shown on the left, and the corresponding q-values are shown on the right. Significant q-values (q < 0.2) and the associated fold changes are highlighted in blue.

Comparing Treatments within Time point

	Fold Changes **Shear AOI vs. Axial AOI**					***q-Values (FDR)*** **Shear AOI vs. Axial AOI**			
Gene	***Day 0***	***Day 3***	***Day 7***	***Day 14***		***Day 0***	***Day 3***	***Day 7***	***Day 14***
Cartilage Matrix									
col1a1	5.29	4.93	0.54	0.14		0.09	0.09	0.43	0.05
col2a1	0.55	2.46	0.41	1.07		0.27	0.12	0.12	0.88
agc	0.66	1.15	1.21	2.07		0.43	0.68	0.68	0.13
sox-9	0.89	1.26	1.02	2.95		0.95	0.95	0.95	0.01
opn	0.97	1.36	1.27	2.63		0.95	0.83	0.83	0.20
comp	0.41	0.94	0.75	1.44		0.03	0.84	0.51	0.51
Degradative Enzymes & Inhibitors									
mmp-1	2.84	1.13	0.49	0.37		0.32	0.84	0.32	0.32
mmp-3	2.36	1.62	3.19	0.56		0.45	0.50	0.41	0.50
mmp-13	0.34	5.51	0.26	0.71		0.14	0.05	0.08	0.60
timp-1	1.33	0.88	0.80	1.23		0.69	0.69	0.69	0.69
timp-2	2.63	2.36	0.71	1.58		0.06	0.06	0.39	0.33
adamts-5	2.02	1.49	0.82	0.14		0.52	0.66	0.74	0.01
Inflammatory Response & Signaling									
ihh	2.00	2.73	2.25	1.68		0.30	0.30	0.30	0.36
tgfb	0.51	0.63	0.89	1.72		0.11	0.18	0.72	0.15
inos	0.35	1.67	0.62	2.06		0.21	0.38	0.38	0.36
chi3l1	1.08	0.54	1.05	1.61		0.92	0.57	0.92	0.57
Cell Proliferation & Apoptosis									
casp-8	0.89	1.15	1.04	2.95		0.91	0.91	0.91	0.01
fas	0.43	0.92	1.90	1.81		0.19	0.85	0.22	0.22

Table 4.7. Differential gene expression for Shear ADJ compared to Axial ADJ specimens at each time point. Fold changes are shown on the left, and the corresponding q-values are shown on the right. Significant q-values ($q < 0.2$) and the associated fold changes are highlighted in blue.

Comparing Treatments within Time point	***Fold Changes*** **Shear ADJ vs. Axial ADJ**				***q-Values (FDR)*** **Shear ADJ vs. Axial ADJ**			
Gene	***Day 0***	***Day 3***	***Day 7***	***Day 14***	***Day 0***	***Day 3***	***Day 7***	***Day 14***
Cartilage Matrix								
col1a1	3.93	0.84	0.33	0.36	0.25	0.83	0.25	0.25
col2a1	0.40	0.98	0.19	0.82	0.11	0.97	< 0.01	0.89
agc	0.64	0.72	0.88	2.96	0.38	0.44	0.71	0.01
sox-9	0.71	2.46	1.29	0.87	0.65	0.06	0.65	0.68
opn	1.00	1.00	0.79	1.40	1.00	1.00	1.00	1.00
comp	0.70	0.96	0.75	1.30	0.56	0.89	0.56	0.56
Degradative Enzymes & Inhibitors								
mmp-1	3.31	0.98	1.37	1.19	0.53	0.98	0.98	0.98
mmp-3	4.05	1.16	0.75	1.44	0.20	0.84	0.84	0.84
mmp-13	0.59	2.05	0.35	2.37	0.43	0.37	0.37	0.37
timp-1	0.84	0.77	0.99	2.01	0.80	0.80	0.98	0.13
timp-2	0.84	0.81	0.76	1.18	0.68	0.68	0.68	0.68
adamts-5	2.38	0.88	0.71	0.88	0.57	0.83	0.83	0.83
Inflammatory Response & Signaling								
ihh	0.76	1.31	0.50	0.77	0.65	0.65	0.65	0.65
tgfb	0.62	0.77	0.55	1.30	0.24	0.40	0.20	0.40
inos	1.07	2.22	0.69	2.37	0.90	0.28	0.66	0.28
chi3l1	0.56	0.37	1.25	1.69	0.32	0.10	0.63	0.32
Cell Proliferation & Apoptosis								
casp-8	0.70	2.06	1.29	0.86	0.63	0.23	0.63	0.65
fas	2.22	0.83	0.64	2.19	0.15	0.68	0.42	0.15

4.7 Comparison of Time Points Within Each Treatment

Differential gene expression was next evaluated within each treatment (control, axial and shear) by comparing each time point (day 0, 3, 7 and 14) to day 0 control specimens. Day 0 control specimens were used as the reference for temporal changes as they most closely represent an un-impacted cartilage surface in its natural state. Tabulated results are presented for Control AOI (Table 4.8), Control ADJ (Table 4.9), Axial AOI (Table 4.10), Axial ADJ (Table 4.11), Shear AOI (Table 4.12), and Shear ADJ (Table 4.13).

Table 4.8. Differential gene expression for Control AOI over time compared to day 0 Control AOI specimens. Fold changes are shown on the left, and the corresponding q-values are shown on the right. Significant q-values (q < 0.2) and the associated fold changes are highlighted in blue.

Compare time points within treatment (all compared to day 0 control)

	Fold Changes **Control AOI at time point vs. Day 0 control AOI**				***q-Values (FDR)*** **Control AOI at time point vs. Day 0 control AOI**			
Gene	***Day 0***	***Day 3***	***Day 7***	***Day 14***	***Day 0***	***Day 3***	***Day 7***	***Day 14***
Cartilage Matrix								
col1a1	1.00	0.43	4.18	26.44	1.00	0.31	0.12	< 0.01
col2a1	1.00	0.68	0.33	0.08	1.00	0.42	0.03	< 0.01
agc	1.00	0.49	0.36	0.31	1.00	0.04	< 0.01	< 0.01
sox-9	1.00	0.34	0.26	0.24	1.00	< 0.01	< 0.01	< 0.01
opn	1.00	2.98	4.29	4.69	1.00	0.03	0.01	0.01
comp	1.00	0.28	0.05	0.03	1.00	< 0.01	< 0.01	< 0.01
Degradative Enzymes & Inhibitors								
mmp-1	1.00	86.98	34.36	314.70	1.00	< 0.01	< 0.01	< 0.01
mmp-3	1.00	86.85	10.87	23.63	1.00	< 0.01	< 0.01	< 0.01
mmp-13	1.00	132.41	120.85	2239.62	1.00	< 0.01	< 0.01	< 0.01
timp-1	1.00	3.22	3.46	2.95	1.00	< 0.01	< 0.01	< 0.01
timp-2	1.00	0.30	0.89	0.42	1.00	0.01	0.77	0.04
adamts-5	1.00	2.61	2.37	1.71	1.00	0.24	0.24	0.38
Inflammatory Response & Signaling								
ihh	1.00	1.38	1.02	2.30	1.00	0.86	0.98	0.44
tgfb	1.00	0.32	0.37	0.47	1.00	< 0.01	< 0.01	0.01
inos	1.00	5.01	0.57	6.79	1.00	< 0.01	0.31	< 0.01
chi3l1	1.00	23.14	12.80	21.79	1.00	< 0.01	< 0.01	< 0.01
Cell Proliferation & Apoptosis								
casp-8	1.00	0.33	0.26	0.24	1.00	< 0.01	< 0.01	< 0.01
fas	1.00	0.60	0.67	0.50	1.00	0.35	0.35	0.35

Table 4.9. Differential gene expression for Control ADJ over time compared to day 0 Control ADJ specimens. Fold changes are shown on the left, and the corresponding q-values are shown on the right. Significant q-values (q < 0.2) and the associated fold changes are highlighted in blue.

Compare time points within treatment (all compared to day 0 control)								
	Fold Changes **Control ADJ at time point vs. Day 0 control ADJ**				***q-Values (FDR)*** **Control ADJ at time point vs. Day 0 control ADJ**			
Gene	***Day 0***	***Day 3***	***Day 7***	***Day 14***	***Day 0***	***Day 3***	***Day 7***	***Day 14***
Cartilage Matrix								
col1a1	1.00	0.64	1.24	45.39	1.00	0.79	0.79	< 0.01
col2a1	1.00	0.64	0.45	0.06	1.00	0.34	0.15	< 0.01
agc	1.00	0.78	0.35	0.31	1.00	0.47	< 0.01	< 0.01
sox-9	1.00	0.34	0.46	0.15	1.00	< 0.01	0.03	< 0.01
opn	1.00	5.57	3.62	4.82	1.00	< 0.01	0.01	< 0.01
comp	1.00	0.30	0.06	0.03	1.00	< 0.01	< 0.01	< 0.01
Degradative Enzymes & Inhibitors								
mmp-1	1.00	436.47	109.28	1062.87	1.00	< 0.01	< 0.01	< 0.01
mmp-3	1.00	88.11	6.71	21.04	1.00	< 0.01	0.01	< 0.01
mmp-13	1.00	321.34	342.94	1435.13	1.00	< 0.01	< 0.01	< 0.01
timp-1	1.00	3.87	3.47	3.72	1.00	< 0.01	< 0.01	< 0.01
timp-2	1.00	0.66	0.50	0.34	1.00	0.29	0.12	0.02
adamts-5	1.00	7.52	1.91	6.63	1.00	< 0.01	0.28	< 0.01
Inflammatory Response & Signaling								
ihh	1.00	2.34	3.75	1.54	1.00	0.21	0.07	0.45
tgfb	1.00	0.80	0.34	0.34	1.00	0.46	< 0.01	< 0.01
inos	1.00	7.79	1.28	3.09	1.00	< 0.01	0.65	0.06
chi3l1	1.00	31.70	16.62	15.95	1.00	< 0.01	< 0.01	< 0.01
Cell Proliferation & Apoptosis								
casp-8	1.00	0.35	0.47	0.16	1.00	< 0.01	0.03	< 0.01
fas	1.00	1.25	0.90	1.31	1.00	0.82	0.82	0.82

Table 4.10. Differential gene expression for Axial AOI over time compared to day 0 Control AOI specimens. Fold changes are shown on the left, and the corresponding q-values are shown on the right. Significant q-values (q < 0.2) and the associated fold changes are highlighted in blue.

Compare time points within treatment (all compared to day 0 control)	***Fold Changes*** **Axial AOI at time point vs. Day 0 control AOI**				***q-Values (FDR)*** **Axial AOI at time point vs. Day 0 control AOI**			
Gene	***Day 0***	***Day 3***	***Day 7***	***Day 14***	***Day 0***	***Day 3***	***Day 7***	***Day 14***
Cartilage Matrix								
col1a1	0.26	0.47	1.32	64.25	0.29	0.50	0.73	< 0.01
col2a1	2.57	0.27	0.89	0.15	0.07	0.01	0.81	< 0.01
agc	1.25	0.55	0.34	0.23	0.87	0.11	< 0.01	< 0.01
sox-9	1.12	0.19	0.16	0.11	0.76	< 0.01	< 0.01	< 0.01
opn	1.05	4.94	2.64	1.03	0.92	0.01	0.10	0.95
comp	1.45	0.26	0.07	0.02	0.52	< 0.01	< 0.01	< 0.01
Degradative Enzymes & Inhibitors								
mmp-1	0.55	51.57	27.45	145.70	0.69	< 0.01	< 0.01	< 0.01
mmp-3	1.56	32.82	12.21	11.00	0.71	< 0.01	< 0.01	< 0.01
mmp-13	3.09	85.61	251.88	605.94	0.18	< 0.01	< 0.01	< 0.01
timp-1	0.94	3.13	4.15	2.00	0.93	< 0.01	< 0.01	0.05
timp-2	0.37	0.17	0.61	0.28	0.05	< 0.01	0.21	< 0.01
adamts-5	0.26	1.51	1.06	2.57	0.12	0.66	0.93	0.27
Inflammatory Response & Signaling								
ihh	1.16	0.42	0.92	1.74	0.87	0.54	0.89	0.67
tgfb	1.41	0.62	0.36	0.19	0.35	0.16	< 0.01	< 0.01
inos	2.22	2.77	0.87	1.03	0.29	0.24	0.96	0.96
chi3l1	1.86	19.51	14.69	6.89	0.33	< 0.01	< 0.01	< 0.01
Cell Proliferation & Apoptosis								
casp-8	1.10	0.20	0.15	0.10	0.80	< 0.01	< 0.01	< 0.01
fas	0.83	0.78	0.30	0.40	0.66	0.66	0.02	0.07

Table 4.11. Differential gene expression for Axial ADJ over time compared to day 0 Control ADJ specimens. Fold changes are shown on the left, and the corresponding q-values are shown on the right. Significant q-values (q < 0.2) and the associated fold changes are highlighted in blue.

Compare timepoints within treatment
(all compared to day 0 control)

	Fold Changes **Axial ADJ at time point vs. Day 0 control ADJ**				***q-Values (FDR)*** **Axial ADJ at time point vs. Day 0 control ADJ**			
Gene	***Day 0***	***Day 3***	***Day 7***	***Day 14***	***Day 0***	***Day 3***	***Day 7***	***Day 14***
Cartilage Matrix								
col1a1	2.32	0.74	1.35	9.23	0.62	0.72	0.72	0.03
col2a1	1.87	0.36	0.67	0.15	0.29	0.06	0.39	< 0.01
agc	1.70	0.89	0.42	0.21	0.48	0.73	0.02	< 0.01
sox-9	1.42	0.19	0.27	0.29	0.31	< 0.01	< 0.01	< 0.01
opn	2.02	3.91	1.86	1.88	0.24	0.02	0.21	0.21
comp	1.27	0.18	0.06	0.02	0.77	< 0.01	< 0.01	< 0.01
Degradative Enzymes & Inhibitors								
mmp-1	0.66	143.62	29.90	337.29	0.69	< 0.01	< 0.01	< 0.01
mmp-3	0.39	35.49	4.12	10.12	0.40	< 0.01	0.06	< 0.01
mmp-13	7.68	248.61	575.54	1266.00	0.01	< 0.01	< 0.01	< 0.01
timp-1	1.33	2.61	3.14	1.71	0.50	0.01	< 0.01	0.14
timp-2	0.84	0.43	0.52	0.46	0.88	0.10	0.13	0.10
adamts-5	1.45	8.42	3.06	6.76	0.97	< 0.01	0.08	< 0.01
Inflammatory Response & Signaling								
ihh	1.61	1.98	2.29	1.73	0.81	0.40	0.40	0.40
tgfb	1.81	0.62	0.45	0.28	0.21	0.11	0.02	< 0.01
inos	1.85	5.56	2.78	2.81	0.51	0.01	0.08	0.08
chi3l1	2.67	26.28	20.29	7.45	0.11	< 0.01	< 0.01	< 0.01
Cell Proliferation & Apoptosis								
casp-8	1.48	0.24	0.28	0.30	0.28	< 0.01	< 0.01	< 0.01
fas	0.50	1.73	0.81	0.81	0.43	0.42	0.63	0.63

Table 4.12. Differential gene expression for Shear AOI over time compared to day 0 Control AOI specimens. Fold changes are shown on the left, and the corresponding q-values are shown on the right. Significant q-values (q < 0.2) and the associated fold changes are highlighted in blue.

Compare time points within treatment (all compared to day 0 control)								
	Fold Changes				***q-Values (FDR)***			
	Shear AOI at time point vs. Day 0 control AOI				**Shear AOI at time point vs. Day 0 control AOI**			
Gene	***Day 0***	***Day 3***	***Day 7***	***Day 14***	***Day 0***	***Day 3***	***Day 7***	***Day 14***
Cartilage Matrix								
col1a1	1.37	2.32	0.71	9.18	0.70	0.64	0.70	0.03
col2a1	1.41	0.66	0.37	0.17	0.94	0.47	0.07	< 0.01
agc	0.82	0.63	0.41	0.47	0.70	0.24	0.03	0.05
sox-9	1.00	0.24	0.16	0.31	0.99	< 0.01	< 0.01	< 0.01
opn	1.02	6.72	3.36	2.71	0.97	< 0.01	0.03	0.06
comp	0.60	0.25	0.05	0.03	0.47	< 0.01	< 0.01	< 0.01
Degradative Enzymes & Inhibitors								
mmp-1	1.55	58.41	13.55	54.01	0.60	< 0.01	< 0.01	< 0.01
mmp-3	3.69	53.18	38.93	6.15	0.10	< 0.01	< 0.01	0.01
mmp-13	1.05	471.31	65.09	428.95	0.94	< 0.01	< 0.01	< 0.01
timp-1	1.24	2.75	3.32	2.47	0.84	< 0.01	< 0.01	0.01
timp-2	0.96	0.39	0.44	0.44	0.93	0.05	0.05	0.05
adamts-5	0.52	2.26	0.87	0.37	0.39	0.36	0.82	0.36
Inflammatory Response & Signaling								
ihh	2.33	1.14	2.08	2.93	0.42	0.82	0.27	0.24
tgfb	0.72	0.39	0.32	0.32	0.57	< 0.01	< 0.01	< 0.01
inos	0.77	4.62	0.54	2.12	0.91	0.02	0.34	0.33
chi3l1	2.00	10.61	15.36	11.08	0.17	< 0.01	< 0.01	< 0.01
Cell Proliferation & Apoptosis								
casp-8	0.98	0.23	0.16	0.31	0.95	< 0.01	< 0.01	< 0.01
fas	0.35	0.72	0.56	0.73	0.06	0.46	0.36	0.46

Table 4.13. Differential gene expression for Shear ADJ over time compared to day 0 Control ADJ specimens. Fold changes are shown on the left, and the corresponding q-values are shown on the right. Significant q-values (q < 0.2) and the associated fold changes are highlighted in blue.

Compare time points within treatment (all compared to day 0 control)								
	Fold Changes				***q-Values (FDR)***			
	Shear ADJ at time point vs. Day 0 control ADJ				**Shear ADJ at time point vs. Day 0 control ADJ**			
Gene	***Day 0***	***Day 3***	***Day 7***	***Day 14***	***Day 0***	***Day 3***	***Day 7***	***Day 14***
Cartilage Matrix								
col1a1	9.14	0.62	0.44	3.30	0.02	0.56	0.42	0.30
col2a1	0.75	0.35	0.13	0.12	0.54	0.04	< 0.01	< 0.01
agc	1.09	0.64	0.37	0.63	0.91	0.25	0.01	0.25
sox-9	1.01	0.47	0.34	0.25	0.98	0.05	0.01	< 0.01
opn	2.03	3.89	1.47	2.64	0.29	0.02	0.43	0.10
comp	0.89	0.17	0.04	0.03	0.80	< 0.01	< 0.01	< 0.01
Degradative Enzymes & Inhibitors								
mmp-1	2.18	141.38	41.07	402.65	0.45	< 0.01	< 0.01	< 0.01
mmp-3	1.59	41.07	3.11	14.57	0.60	< 0.01	0.15	< 0.01
mmp-13	4.54	509.62	202.22	2994.44	0.10	< 0.01	< 0.01	< 0.01
timp-1	1.12	2.00	3.12	3.44	0.81	0.05	< 0.01	< 0.01
timp-2	0.70	0.35	0.40	0.54	0.50	0.03	0.04	0.16
adamts-5	3.45	7.43	2.17	5.93	0.15	< 0.01	0.20	0.01
Inflammatory Response & Signaling								
ihh	1.22	2.58	1.14	1.33	0.87	0.40	0.82	0.82
tgfb	1.12	0.48	0.25	0.36	0.90	0.02	< 0.01	< 0.01
inos	1.98	12.35	1.92	6.64	0.41	< 0.01	0.23	< 0.01
chi3l1	1.48	9.69	25.28	12.61	0.50	< 0.01	< 0.01	< 0.01
Cell Proliferation & Apoptosis								
casp-8	1.04	0.50	0.36	0.26	0.90	0.07	0.01	< 0.01
fas	1.11	1.44	0.52	1.76	0.81	0.53	0.39	0.39

4.8 Comparison of AOI and ADJ at Each Time Point

The final comparison was AOI expression vs. ADJ expression at each time point, within the three treatments. Results follow for Control (Table 4.14), Axial (Table 4.15), and Shear (Table 4.16).

Table 4.14. Differential gene expression for Control AOI compared to Control ADJ specimens at each time point. Fold changes are shown on the left, and the corresponding q-values are shown on the right. Significant q-values (q < 0.2) and the associated fold changes are highlighted in blue.

Compare AOI and ADJ at each time point

	Fold Changes **Control AOI vs. ADJ**					***q-Values (FDR)*** **Control AOI vs. ADJ**			
Gene	***Day 0***	***Day 3***	***Day 7***	***Day 14***		***Day 0***	***Day 3***	***Day 7***	***Day 14***
Cartilage Matrix									
col1a1	0.66	0.45	2.23	0.39		0.63	0.43	0.43	0.43
col2a1	0.93	0.99	0.67	1.39		0.99	0.99	0.97	0.97
agc	1.28	0.81	1.30	1.28		0.53	0.53	0.53	0.53
sox-9	2.04	2.01	1.15	3.12		0.06	0.06	0.68	0.01
opn	0.66	0.36	0.79	0.65		0.54	0.15	0.63	0.54
comp	1.01	0.95	0.93	1.39		0.98	0.98	0.98	0.98
Degradative Enzymes & Inhibitors									
mmp-1	2.21	0.44	0.69	0.65		0.54	0.54	0.54	0.54
mmp-3	0.48	0.48	0.78	0.54		0.52	0.52	0.73	0.52
mmp-13	2.58	1.06	0.91	4.03		0.31	0.92	0.92	0.14
timp-1	0.98	0.82	0.98	0.78		0.96	0.96	0.96	0.96
timp-2	0.94	0.42	1.68	1.16		0.88	0.12	0.38	0.88
adamts-5	3.07	1.06	3.80	0.79		0.14	0.92	0.11	0.92
Inflammatory Response & Signaling									
ihh	1.34	0.79	0.36	2.00		0.68	0.68	0.31	0.45
tgfb	1.01	0.41	1.10	1.39		0.96	0.01	0.96	0.56
inos	2.32	1.49	1.04	5.08		0.24	0.62	0.94	0.01
chi3l1	1.44	1.05	1.11	1.97		0.82	0.91	0.91	0.51
Cell Proliferation & Apoptosis									
casp-8	2.14	1.99	1.18	3.13		0.06	0.07	0.63	0.01
fas	1.62	0.78	1.19	0.62		0.61	0.68	0.68	0.61

Table 4.15. Differential gene expression for Axial AOI compared to Axial ADJ specimens at each time point. Fold changes are shown on the left, and the corresponding q-values are shown on the right. Significant q-values (q < 0.2) and the associated fold changes are highlighted in blue.

Compare AOI and ADJ at each time point

	Fold Changes **Axial AOI vs. ADJ**				***q-Values (FDR)*** **Axial AOI vs. ADJ**			
Gene	***Day 0***	***Day 3***	***Day 7***	***Day 14***	***Day 0***	***Day 3***	***Day 7***	***Day 14***
Cartilage Matrix								
col1a1	0.07	0.42	0.65	4.62	0.01	0.41	0.59	0.10
col2a1	1.28	0.70	1.24	0.97	0.86	0.86	0.86	0.95
agc	0.94	0.79	1.04	1.37	0.91	0.91	0.91	0.91
sox-9	1.60	2.04	1.21	0.76	0.39	0.19	0.58	0.58
opn	0.35	0.84	0.95	0.36	0.08	0.91	0.91	0.08
comp	1.15	1.45	1.11	0.93	0.83	0.83	0.83	0.83
Degradative Enzymes & Inhibitors								
mmp-1	1.83	0.79	2.03	0.95	0.93	0.93	0.93	0.94
mmp-3	1.93	0.45	1.43	0.53	0.49	0.49	0.61	0.49
mmp-13	1.04	0.89	1.13	1.24	0.95	0.95	0.95	0.95
timp-1	0.69	1.18	1.30	1.15	0.66	0.66	0.66	0.66
timp-2	0.41	0.37	1.10	0.57	0.05	0.05	0.81	0.20
adamts-5	0.54	0.55	1.06	1.16	0.63	0.63	0.92	0.92
Inflammatory Response & Signaling								
ihh	0.97	0.28	0.54	1.35	0.95	0.12	0.57	0.80
tgfb	0.79	1.02	0.81	0.69	0.65	0.94	0.65	0.65
inos	2.78	1.15	0.72	0.85	0.25	0.79	0.79	0.79
chi3l1	1.00	1.07	1.04	1.33	0.99	0.99	0.99	0.99
Cell Proliferation & Apoptosis								
casp-8	1.58	1.78	1.18	0.75	0.40	0.40	0.63	0.54
fas	2.68	0.73	0.59	0.81	0.09	0.62	0.44	0.62

Table 4.16. Differential gene expression for Shear AOI compared to Shear ADJ specimens at each time point. Fold changes are shown on the left, and the corresponding q-values are shown on the right. Significant q-values (q < 0.2) and the associated fold changes are highlighted in blue.

Compare AOI and ADJ at each time point

	Fold Changes **Shear AOI vs. ADJ**				***q-Values (FDR)*** **Shear AOI vs. ADJ**			
Gene	***Day 0***	***Day 3***	***Day 7***	***Day 14***	***Day 0***	***Day 3***	***Day 7***	***Day 14***
Cartilage Matrix								
col1a1	0.10	2.50	1.07	1.84	0.02	0.53	0.93	0.58
col2a1	1.75	1.75	2.69	1.27	0.31	0.31	0.15	0.61
agc	0.97	1.28	1.42	0.96	0.92	0.92	0.92	0.92
sox-9	2.02	1.05	0.96	2.59	0.09	0.92	0.92	0.03
opn	0.33	1.15	1.52	0.68	0.11	0.78	0.59	0.59
comp	0.68	1.42	1.11	1.03	0.59	0.59	0.93	0.93
Degradative Enzymes & Inhibitors								
mmp-1	1.57	0.91	0.73	0.30	0.80	0.88	0.80	0.21
mmp-3	1.12	0.63	6.07	0.20	0.87	0.68	0.05	0.05
mmp-13	0.60	2.39	0.83	0.37	0.59	0.39	0.78	0.39
timp-1	1.09	1.35	1.05	0.71	0.89	0.71	0.89	0.71
timp-2	1.28	1.06	1.03	0.76	0.94	0.94	0.94	0.94
adamts-5	0.46	0.93	1.23	0.19	0.41	0.91	0.91	0.03
Inflammatory Response & Signaling								
ihh	2.55	0.59	2.45	2.94	0.16	0.36	0.16	0.16
tgfb	0.65	0.84	1.32	0.91	0.63	0.74	0.73	0.76
inos	0.90	0.87	0.65	0.74	0.84	0.84	0.84	0.84
chi3l1	1.95	1.58	0.88	1.27	0.54	0.61	0.77	0.77
Cell Proliferation & Apoptosis								
casp-8	2.00	0.99	0.95	2.58	0.09	0.98	0.98	0.03
fas	0.51	0.81	1.74	0.67	0.42	0.62	0.42	0.48

4.9 Cartilage Matrix

Genes related to the cartilage matrix (*col1a1, col2a1, agc, sox-9, spp1, comp*) were evaluated for expression changes over time, differences between treatments, and differences between areas.

4.9.1 Results for *Col1a1*

Fold Change With Time:

Col1a1 AOI specimens showed generally increasing fold changes over time for all treatments compared to day 0 control specimens. These changes were significant at day 7 for control (FC = 4.18, q = 0.12) and day 14 for all treatments (control: FC = 26.44, q < 0.01; axial: FC = 64.25, q < 0.1; shear: FC = 9.18, q = 0.03). When evaluating the ADJ specimens over time, the treatments showed a generally decreasing trend from day 0 to day 3, with an increase from day 3 to 14. The changes in shear compared to day 0 control were significant at day 0 (FC = 9.14, q = 0.02), and control and axial changes were significant at day 14 (control: FC = 45.39, q < 0.01; axial: FC = 9.23, q = 0.03).

Fold Change With Treatment:

Expression of *col1a1* in shear AOI specimens showed generally higher fold changes than either control or axial at day 0 and 3, and the trend reversed at day 7 and 14 for the AOI specimens. Shear compared to control specimens was higher at day 3 (FC = 5.36, q = 0.09). Shear expression was significantly higher at day 0 compared to axial specimens (FC = 5.29, q = 0.09) and at day 3 (FC = 4.93, q = 0.09), however expression was lower than axial at day 14 (FC = 0.14, q = 0.05). When evaluating the ADJ specimens, *col1a1*

expression was higher in shear vs. control at day 0 (FC = 9.14, q = 0.02) and lower at day 14 (FC = 0.07, q < 0.01). Expression was also lower in the axial ADJ vs. control at day 14 (FC = 0.20, q = 0.17).

Fold Change With Area:

Trends were more difficult to discern when comparing areas, though, both axial and shear appeared to have lower expression in the AOI specimens at day 0, and higher expression at day 14 when compared to ADJ specimens. At day 0 the changes were significant for axial AOI vs. ADJ (FC = 0.07, q = 0.01) and at day 14 (FC = 4.62, q = 0.10). Shear AOI had lower expression than ADJ at day 0 (FC = 0.10, q = 0.02).

Figures 4.7 A-E. Graphs of *col1a1* by time point, treatment and area.

Figure 4.7 A. *Col1a1*: Fold change with time – area of interest. Fold change is shown on the vertical axis as a log scale. Fold changes less than one indicate lowered expression and fold changes greater than one indicate higher expression. Days in culture are shown on the horizontal axis. At each time point, day 0 control specimens are used as the reference or comparative value. Error bars (standard error) are shown for each fold change. Control specimens are plotted in blue, axial are plotted in red, and shear are plotted in green. Significant differences in expression relative to day 0 control are indicated at each time point with an asterisk (*) in the respective color of the plotted treatment.

Figure 4.7 B. *Col1a1*: Fold change with treatment – area of interest. Fold change is shown on the vertical axis as a log scale, and days in culture is shown on the horizontal axis. The treatments are compared to each other at each time point. Axial vs. Control is shown in red, Shear vs. Control is shown in green, and Shear vs. Axial is shown in orange. Error bars (standard error) for fold change are depicted, and significant differences for the respective comparison are indicated with an asterisk (*).

Figure 4.7 C. *Col1a1*: Fold change with time – adjacent area. Fold change is shown on the vertical axis as a log scale. Fold changes less than one indicate lowered expression and fold changes greater than one indicate higher expression. Days in culture are shown on the horizontal axis. At each time point, day 0 control specimens are used as the reference or comparative value. Error bars (standard error) are shown for each fold change. Control specimens are plotted in blue, axial are plotted in red, and shear are plotted in green. Significant differences in expression relative to day 0 control are indicated at each time point with an asterisk (*) in the respective color of the plotted treatment.

Figure 4.7 D. *Col1a1*: Fold change with treatment – adjacent area. Fold change is shown on the vertical axis as a log scale, and days in culture is shown on the horizontal axis. The treatments are compared to each other at each time point. Axial vs. Control is shown in red, Shear vs. Control is shown in green, and Shear vs. Axial is shown in orange. Error bars (standard error) for fold change are depicted, and significant differences for the respective comparison are indicated with an asterisk (*).

Figure 4.7 E. *Col1a1*: Fold change with area – area of interest vs. adjacent area. Fold change is shown on the vertical axis as a log scale, and days in culture is shown on the horizontal axis. The treatment areas are compared to each other within each treatment at each time point. Control is shown in blue, axial is shown in red, and shear is shown in green. Error bars (standard error) for fold change are depicted, and significant differences for the respective comparison are indicated with an asterisk (*).

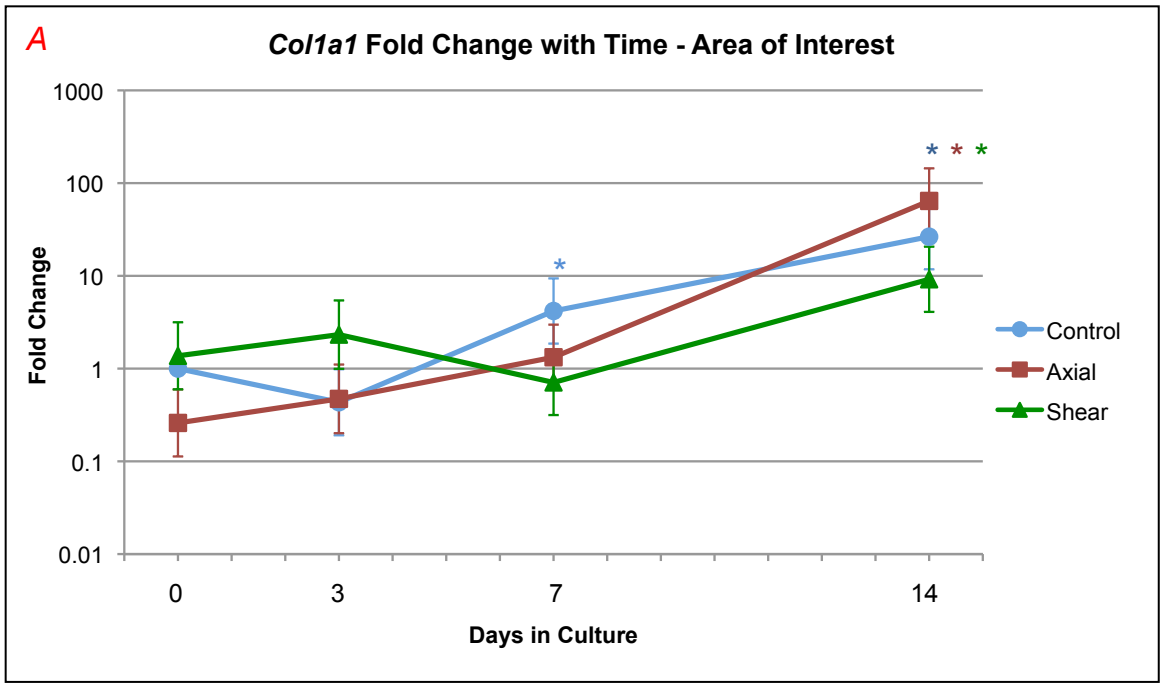
A
Col1a1 Fold Change with Time - Area of Interest
1000
100
10
1
0.1
0.01
Fold Change
0
3
7
14
Days in Culture
Control
Axial
Shear

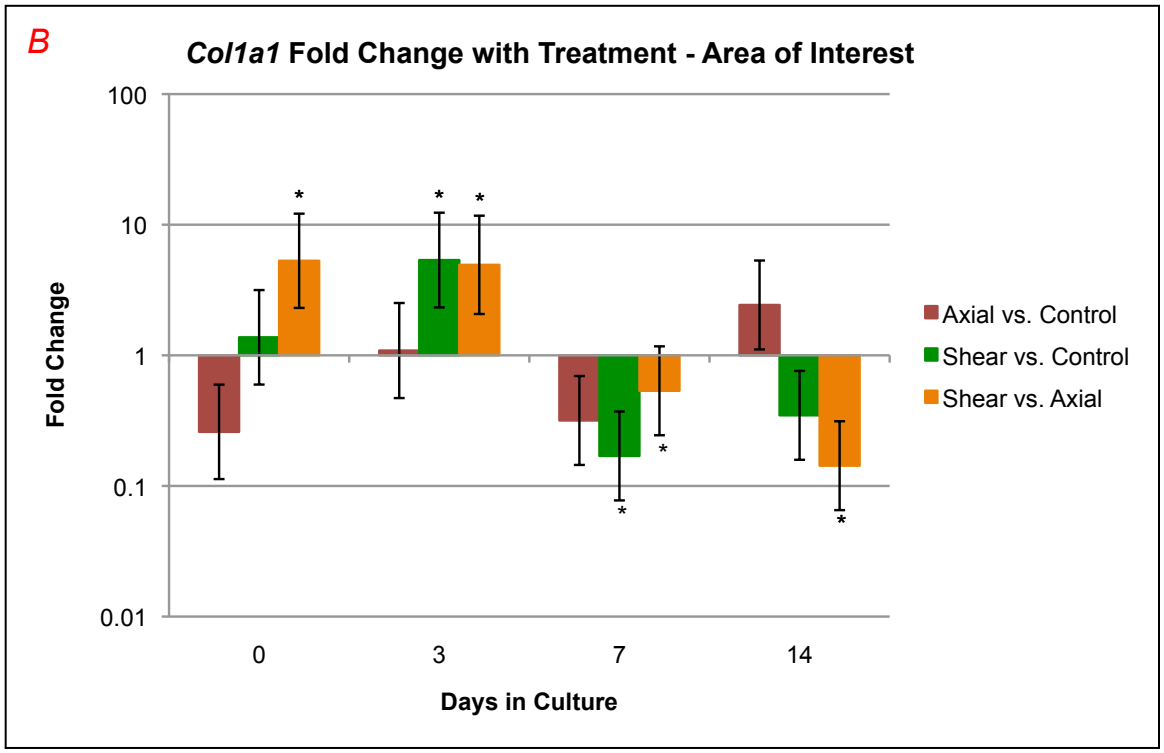
B
Col1a1 Fold Change with Treatment - Area of Interest
100
10
1
0.1
0.01
Fold Change
0
3
7
14
Days in Culture
Axial vs. Control
Shear vs. Control
Shear vs. Axial

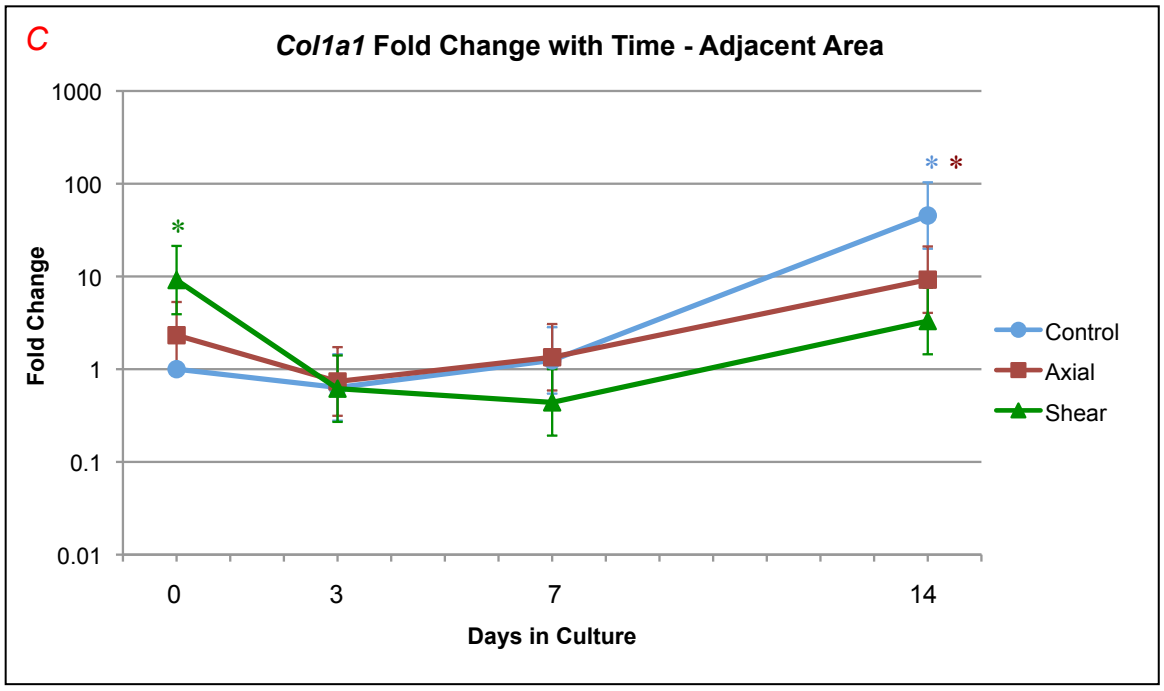
C
Col1a1 Fold Change with Time - Adjacent Area
1000
100
10
1
0.1
0.01
Fold Change
0
3
7
14
Days in Culture
Control
Axial
Shear

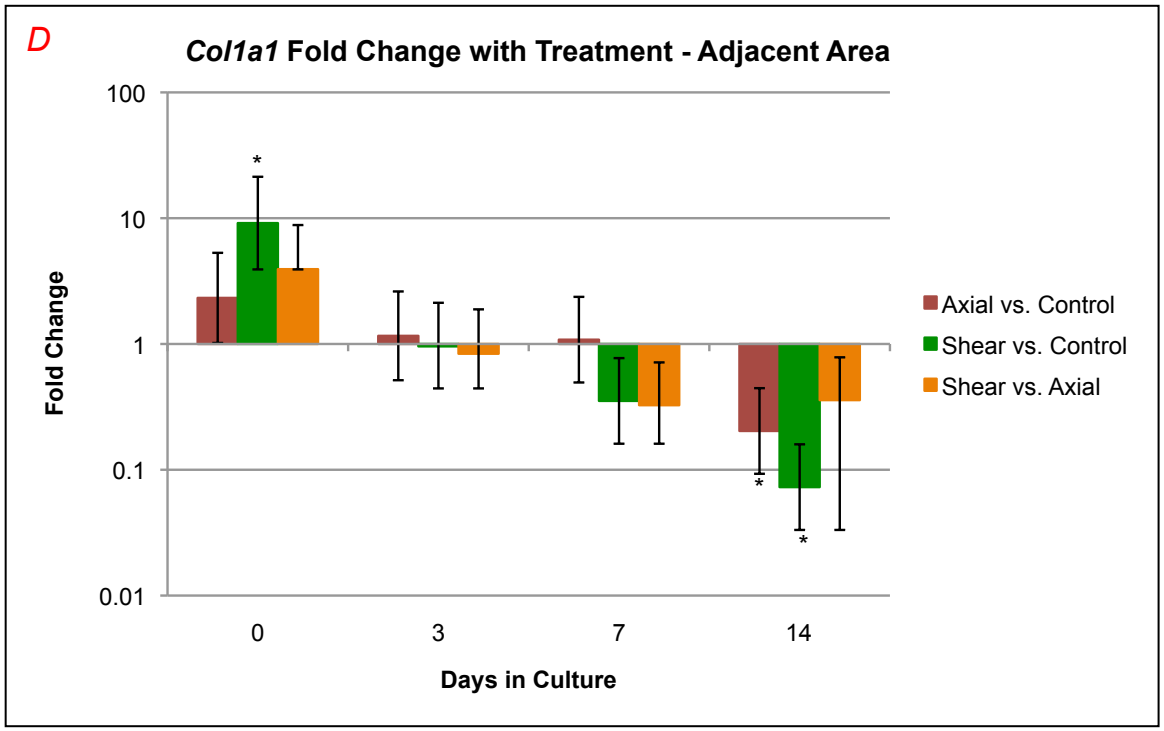
D
Col1a1 Fold Change with Treatment - Adjacent Area
100
10
1
0.1
0.01
Fold Change
0
3
7
14
Days in Culture
Axial vs. Control
Shear vs. Control
Shear vs. Axial

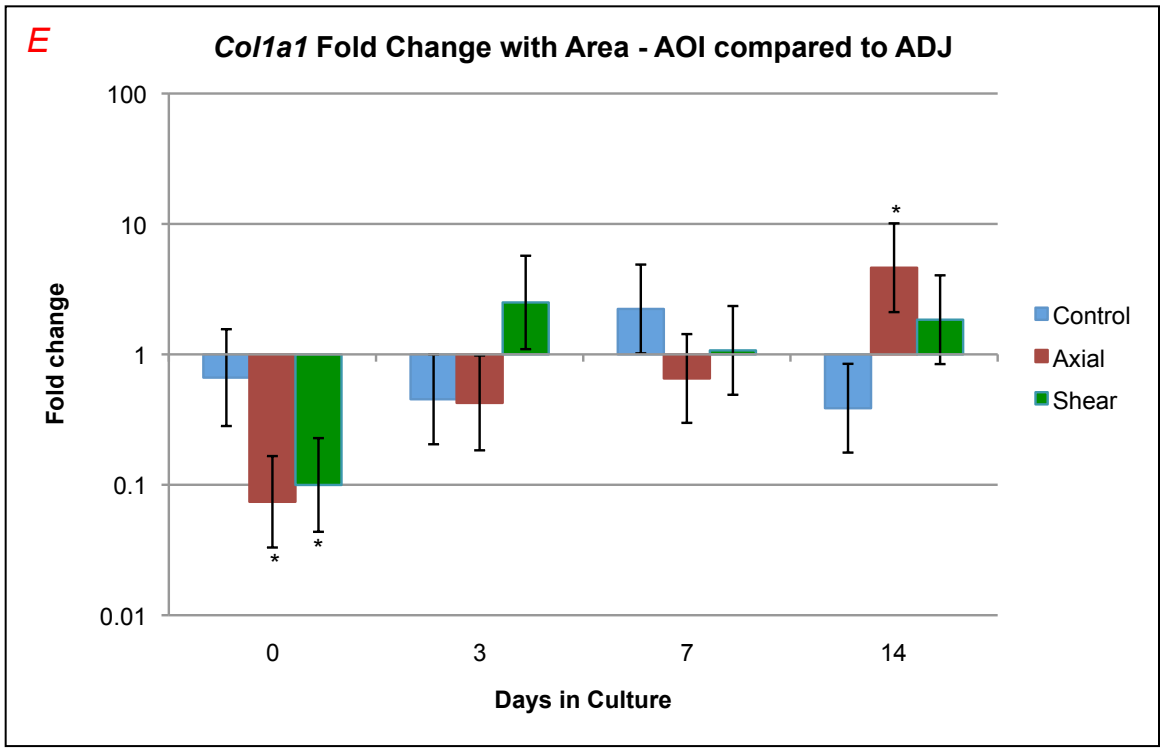
E
Col1a1 Fold Change with Area - AOI compared to ADJ
100
10
1
0.1
0.01
Fold change
0
3
7
14
Days in Culture
Control
Axial
Shear
*
*
*

4.9.2 Results for *Col2a1*

Fold Change With Time:

Col2a1 AOI specimens showed a generally decreasing trend of expression over time for all treatments compared to day 0 control specimens. At day 0 the axial specimens had higher expression (FC = 2.57, q = 0.07) but had lower expression at day 3 and 14 (FC = 0.27, q = 0.01; FC = 0.15, q < 0.01). Control AOI had lower expression at day 7 and 14 (FC = 0.33, q = 0.03; FC = 0.08, q < 0.01). Shear specimens had significantly lower expression at day 7 and 14 (FC = 0.37, q = 0.07; FC = 0.17, q < 0.01). The ADJ specimens also showed a decreasing trend over time, however it was much less pronounced than that of the AOI specimens. Axial ADJ specimens had significantly lower expression than day 0 control ADJ specimens at day 3 and 14 (FC = 0.36, q = 0.06; FC = 0.15, q < 0.01). Control showed lower expression at day 7 and 14 (FC = 0.45, q =0.15; FC = 0.06, q < 0.01). Shear ADJ specimens showed lower expression at day 3, 7 and 14 as well (FC = 0.35, q = 0.04; FC = 0.13, q < 0.01; FC = 0.12, q < 0.01).

Fold Change With Treatment:

The treatments were compared to each other for *col2a1*. No discernible trends were noted for either AOI or ADJ specimens. Axial AOI specimens were higher than control at day 0 (FC = 2.57, q = 0.07), lower at day 3 (FC = 0.39, q = 0.07), and higher again at day 7 (FC = 2.73, q = 0.07). Shear AOI specimens had higher expression than axial at day 3 (FC = 2.46, q = 0.12) and lower expression at day 7 (FC = 0.41, q = 0.12). The ADJ area appeared to have lower expression at the first three time points that rose by the

last time point. However, shear ADJ were significantly lower only at day 7 (FC = 0.28, q = 0.03). Shear ADJ specimens had lower expression than axial at day 0 and 7 (FC = 0.40, q = 0.11; FC = 0.19, q < 0.01). Axial ADJ were significantly higher than control at day 14 (FC = 2.63, q = 0.17).

Fold Change With Area:

AOI were compared to ADJ specimens, and shear AOI *col2a1* expression appeared consistently higher than that in the ADJ specimens. However, this difference was only significant at day 7 (FC = 2.69, q = 0.15).

Figures 4.8 A-E. Graphs of *col2a1* by time point, treatment and area.

Figure 4.8 A. *Col2a1*: Fold change with time – area of interest. Fold change is shown on the vertical axis as a log scale. Fold changes less than one indicate lowered expression and fold changes greater than one indicate higher expression. Days in culture are shown on the horizontal axis. At each time point, day 0 control specimens are used as the reference or comparative value. Error bars (standard error) are shown for each fold change. Control specimens are plotted in blue, axial are plotted in red, and shear are plotted in green. Significant differences in expression relative to day 0 control are indicated at each time point with an asterisk (*) in the respective color of the plotted treatment.

Figure 4.8 B. *Col2a1*: Fold change with treatment – area of interest. Fold change is shown on the vertical axis as a log scale, and days in culture is shown on the horizontal axis. The treatments are compared to each other at each time point. Axial vs. Control is shown in red, Shear vs. Control is shown in green, and Shear vs. Axial is shown in orange. Error bars (standard error) for fold change are depicted, and significant differences for the respective comparison are indicated with an asterisk (*).

Figure 4.8 C. *Col2a1*: Fold change with time – adjacent area. Fold change is shown on the vertical axis as a log scale. Fold changes less than one indicate lowered expression and fold changes greater than one indicate higher expression. Days in culture are shown on the horizontal axis. At each time point, day 0 control specimens are used as the reference or comparative value. Error bars (standard error) are shown for each fold change. Control specimens are plotted in blue, axial are plotted in red, and shear are plotted in green. Significant differences in expression relative to day 0 control are indicated at each time point with an asterisk (*) in the respective color of the plotted treatment.

Figure 4.8 D. *Col2a1*: Fold change with treatment – adjacent area. Fold change is shown on the vertical axis as a log scale, and days in culture is shown on the horizontal axis. The treatments are compared to each other at each time point. Axial vs. Control is shown in red, Shear vs. Control is shown in green, and Shear vs. Axial is shown in orange. Error bars (standard error) for fold change are depicted, and significant differences for the respective comparison are indicated with an asterisk (*).

Figure 4.8 E. *Col2a1*: Fold change with area – area of interest vs. adjacent area. Fold change is shown on the vertical axis as a log scale, and days in culture is shown on the horizontal axis. The treatment areas are compared to each other within each treatment at each time point. Control is shown in blue, axial is shown in red, and shear is shown in green. Error bars (standard error) for fold change are depicted, and significant differences for the respective comparison are indicated with an asterisk (*).

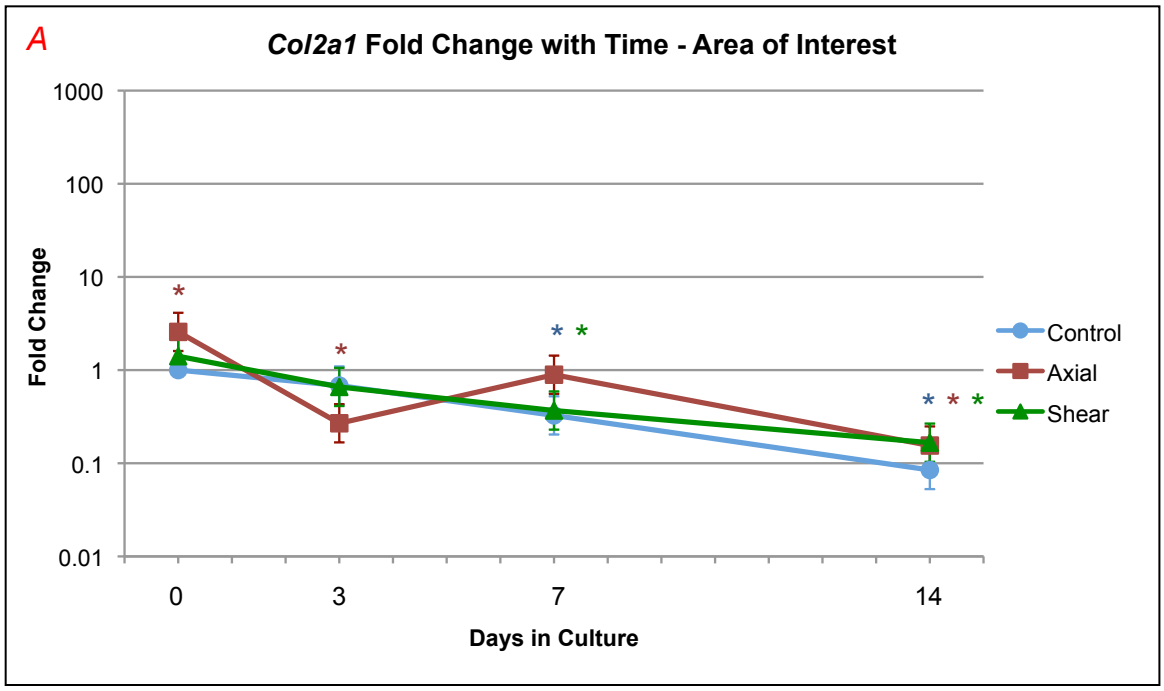
A
Col2a1 Fold Change with Time - Area of Interest
1000
100
10
1
0.1
0.01
Fold Change
0
3
7
14
Days in Culture
Control
Axial
Shear

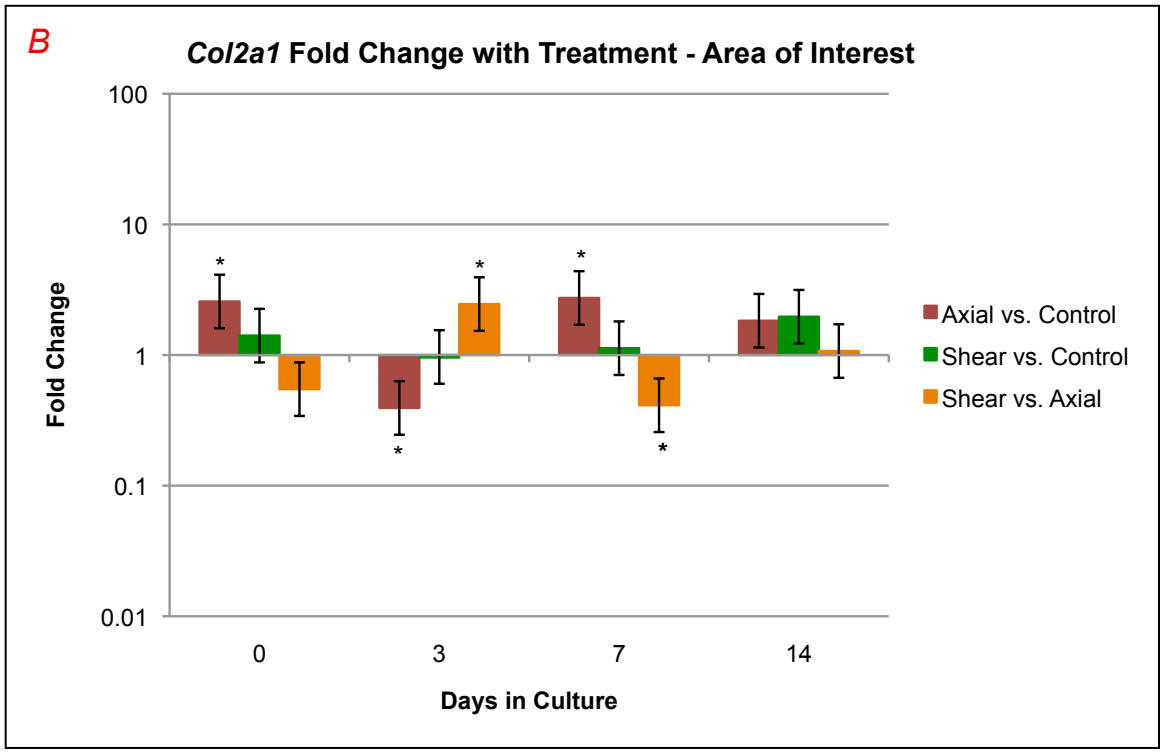
B
Col2a1 Fold Change with Treatment - Area of Interest
100
10
1
0.1
0.01
Fold Change
0
3
7
14
Days in Culture
Axial vs. Control
Shear vs. Control
Shear vs. Axial

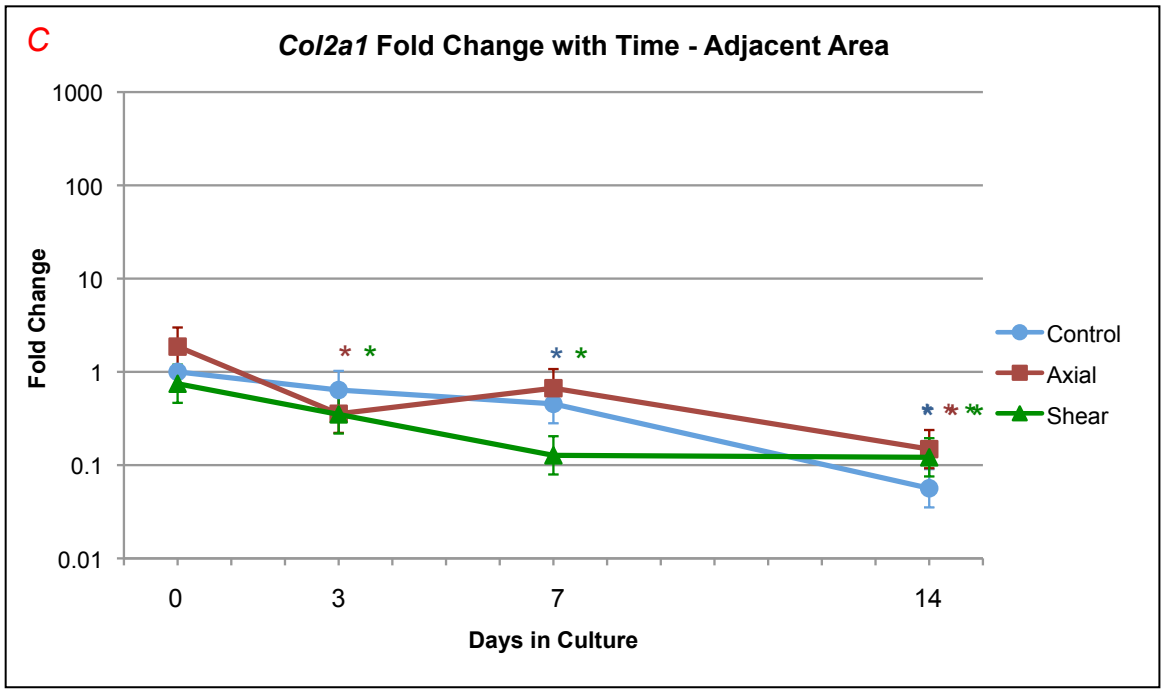
C
Col2a1 Fold Change with Time - Adjacent Area
1000
100
10
1
0.1
0.01
Fold Change
0
3
7
14
Days in Culture
Control
Axial
Shear

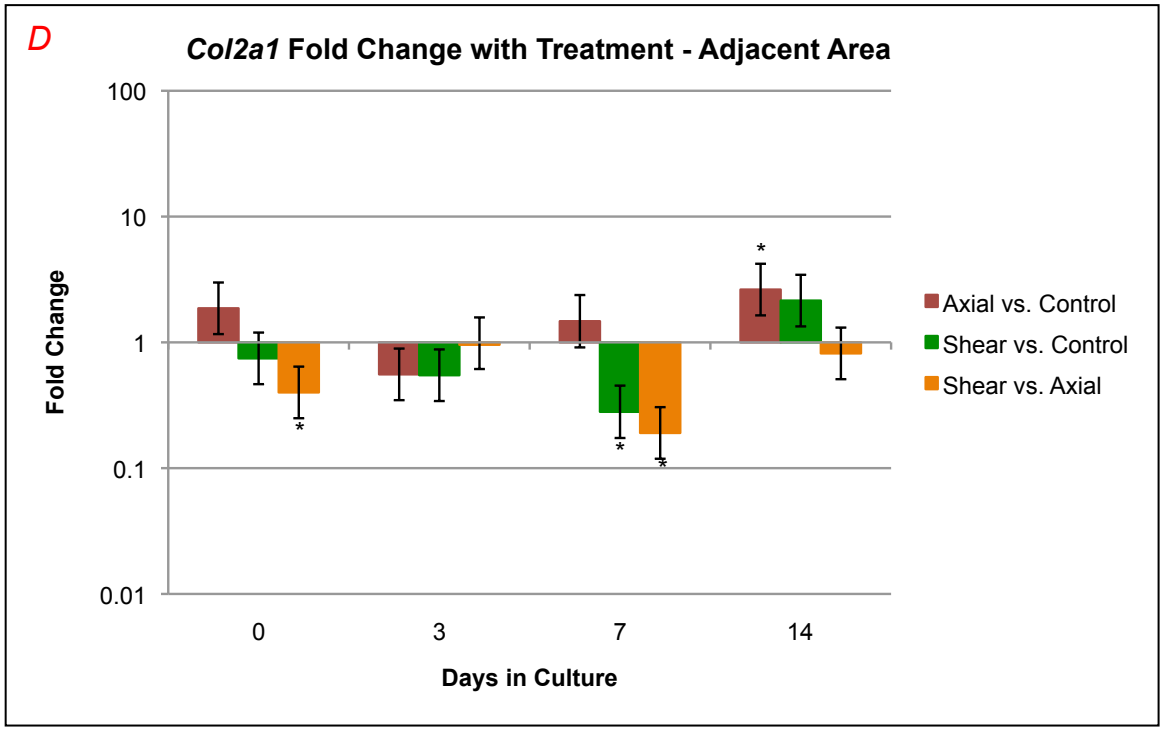
D
Col2a1 Fold Change with Treatment - Adjacent Area
100
10
1
0.1
0.01
Fold Change
0
3
7
14
Days in Culture
Axial vs. Control
Shear vs. Control
Shear vs. Axial

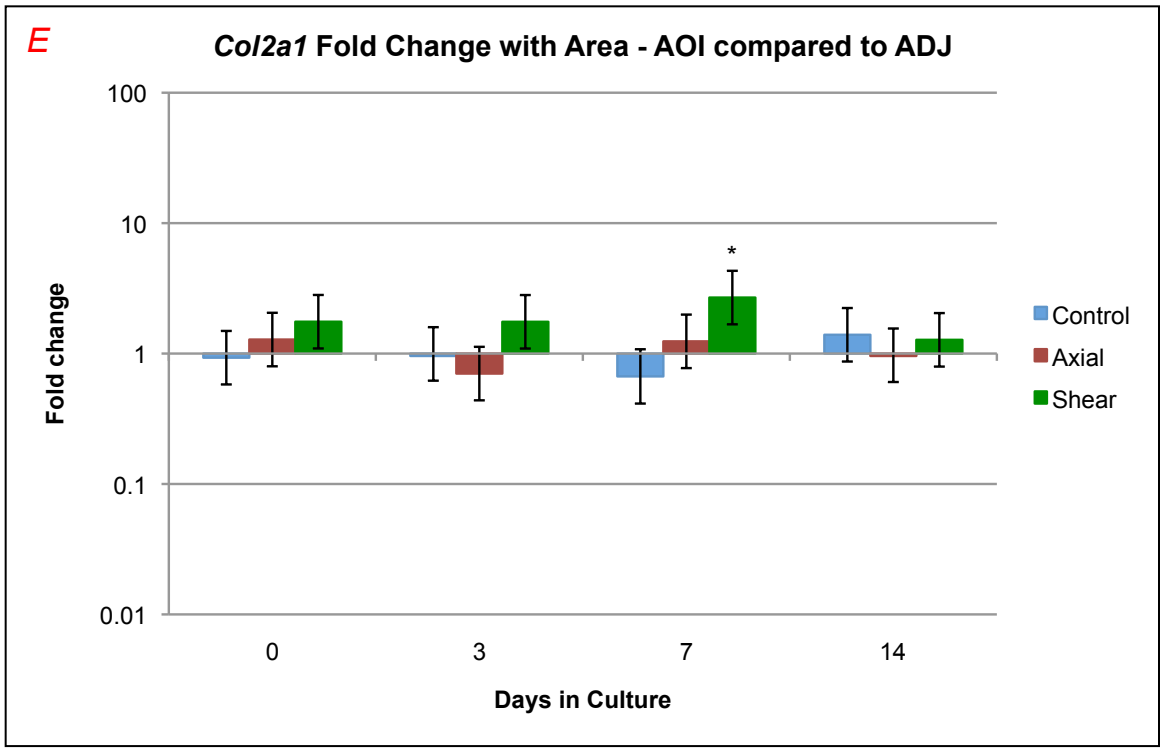
E
Col2a1 Fold Change with Area - AOI compared to ADJ
100
10
1
0.1
0.01
Fold change
*
0
3
7
14
Days in Culture
Control
Axial
Shear

4.9.3 Results for *Agc*

Fold Change With Time:

For *agc*, all three treatments showed a drop in AOI expression over time compared to day 0 control. The change was significant for control at day 3, 7, and 14 (FC = 0.49, q = 0.04; FC = 0.36, q < 0.01; FC = 0.31, q < 0.01). Axial also had significantly lower expression at day 3, 7 and 14 (FC = 0.55, q = 0.11; FC = 0.34, q < 0.01; FC = 0.23, q < 0.01). The shear AOI specimens had lower expression than day 0 control at day 7 and 14 (FC = 0.41, q = 0.03; FC = 0.47, q = 0.05). For ADJ specimens compared to day 0 control, there was a steady drop for all treatments up to day 7 and then the changes seemed to plateau at a lower expression level. Control ADJ specimens had significantly lower expression at day 7 and 14 (FC = 0.35, q < 0.01; FC = 0.31, q < 0.01). Axial ADJ specimens had lower expression at day 7 and 14 as well (FC = 0.42, q = 0.02; FC = 0.21, q < 0.01). Finally, shear specimens were lower at day 7 only (FC = 0.37, q = 0.01).

Fold Change With Treatment:

When treatments were compared, shear vs. control and shear vs. axial showed higher expression at the last time point for both AOI and ADJ comparisons. For the AOI specimens, shear was significantly higher than axial at day 14 (FC = 2.07, q = 0.13). For the ADJ specimens, shear was higher than control at day 14 (FC = 2.04, q = 0.15) and shear was higher than axial (FC = 2.96, q = 0.01).

Fold Change With Area:

For comparisons of AOI specimens vs. ADJ specimens at each time point, there were no consistent differences, and no comparisons were significantly different.

Figures 4.9 A-E. Graphs of *agc* by time point, treatment and area.

Figure 4.9 A. *Agc*: Fold change with time – area of interest. Fold change is shown on the vertical axis as a log scale. Fold changes less than one indicate lowered expression and fold changes greater than one indicate higher expression. Days in culture are shown on the horizontal axis. At each time point, day 0 control specimens are used as the reference or comparative value. Error bars (standard error) are shown for each fold change. Control specimens are plotted in blue, axial are plotted in red, and shear are plotted in green. Significant differences in expression relative to day 0 control are indicated at each time point with an asterisk (*) in the respective color of the plotted treatment.

Figure 4.9 B. *Agc*: Fold change with treatment – area of interest. Fold change is shown on the vertical axis as a log scale, and days in culture is shown on the horizontal axis. The treatments are compared to each other at each time point. Axial vs. Control is shown in red, Shear vs. Control is shown in green, and Shear vs. Axial is shown in orange. Error bars (standard error) for fold change are depicted, and significant differences for the respective comparison are indicated with an asterisk (*).

Figure 4.9 C. *Agc*: Fold change with time – adjacent area. Fold change is shown on the vertical axis as a log scale. Fold changes less than one indicate lowered expression and fold changes greater than one indicate higher expression. Days in culture are shown on the horizontal axis. At each time point, day 0 control specimens are used as the reference or comparative value. Error bars (standard error) are shown for each fold change. Control specimens are plotted in blue, axial are plotted in red, and shear are plotted in green. Significant differences in expression relative to day 0 control are indicated at each time point with an asterisk (*) in the respective color of the plotted treatment.

Figure 4.9 D. *Agc*: Fold change with treatment – adjacent area. Fold change is shown on the vertical axis as a log scale, and days in culture is shown on the horizontal axis. The treatments are compared to each other at each time point. Axial vs. Control is shown in red, Shear vs. Control is shown in green, and Shear vs. Axial is shown in orange. Error bars (standard error) for fold change are depicted, and significant differences for the respective comparison are indicated with an asterisk (*).

Figure 4.9 E. *Agc*: Fold change with area – area of interest vs. adjacent area. Fold change is shown on the vertical axis as a log scale, and days in culture is shown on the horizontal axis. The treatment areas are compared to each other within each treatment at each time point. Control is shown in blue, axial is shown in red, and shear is shown in green. Error bars (standard error) for fold change are depicted, and significant differences for the respective comparison are indicated with an asterisk (*).

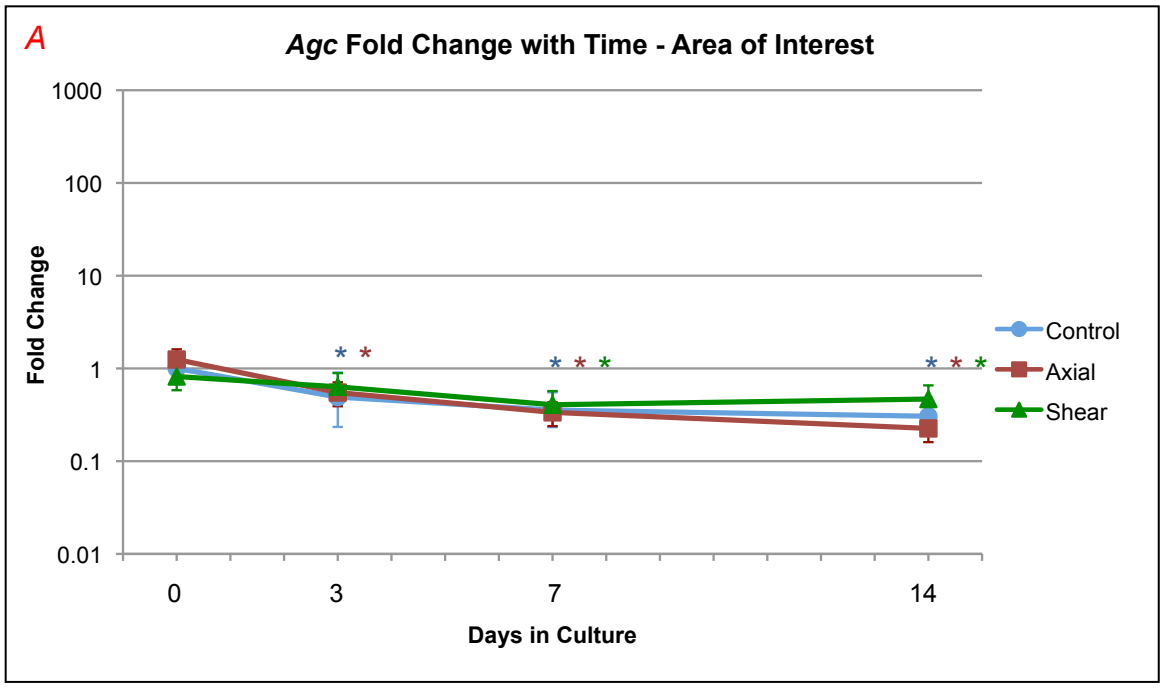
A
Agc Fold Change with Time - Area of Interest
1000
100
10
1
0.1
0.01
Fold Change
0
3
7
14
Days in Culture
Control
Axial
Shear

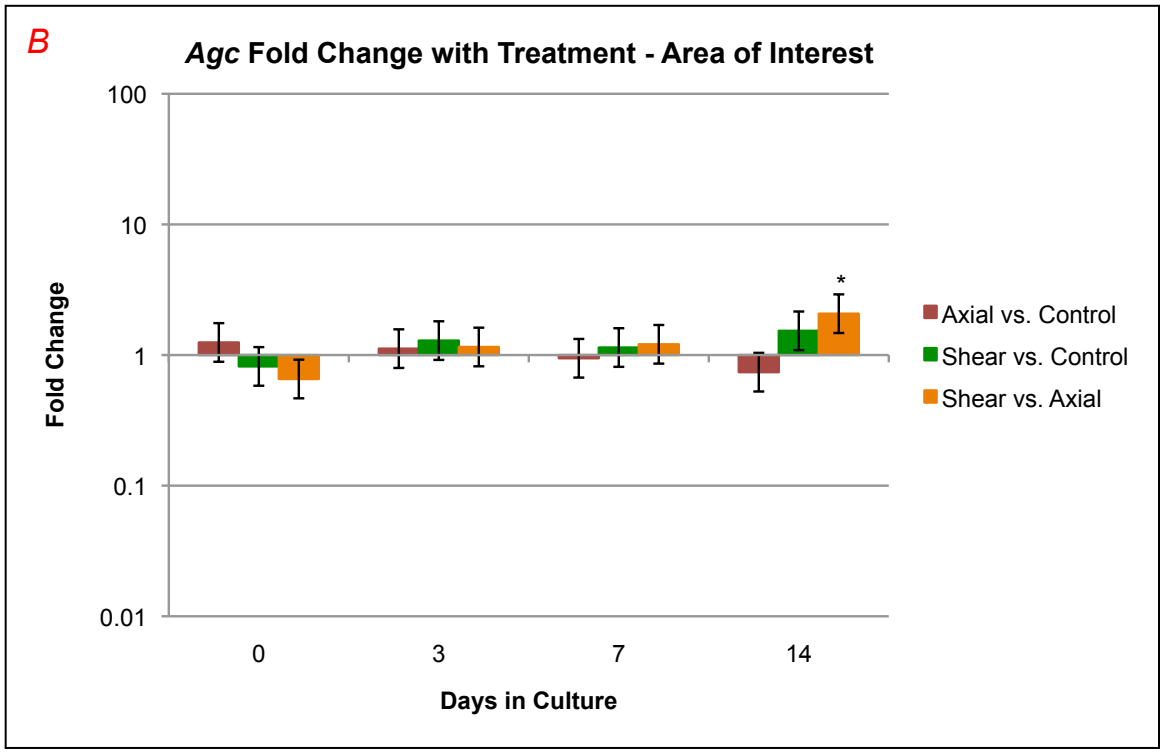
B
Agc Fold Change with Treatment - Area of Interest
100
10
1
0.1
0.01
Fold Change
0
3
7
14
Days in Culture
Axial vs. Control
Shear vs. Control
Shear vs. Axial

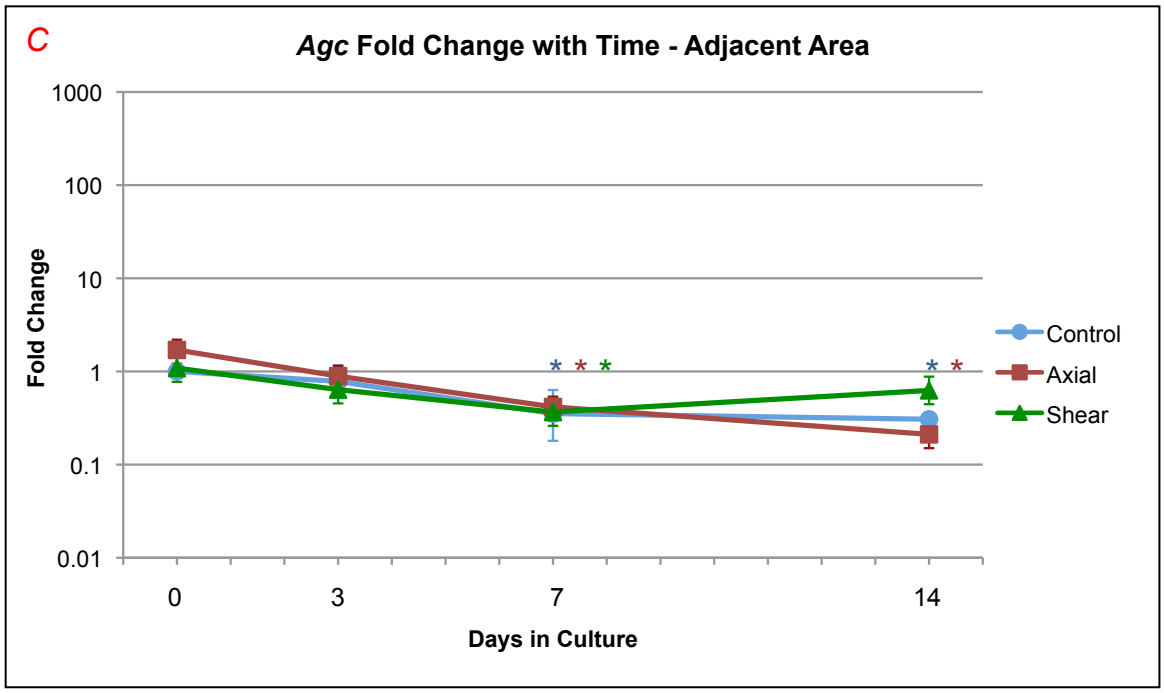
C
Agc Fold Change with Time - Adjacent Area
1000
100
10
1
0.1
0.01
Fold Change
0
3
7
14
Days in Culture
Control
Axial
Shear

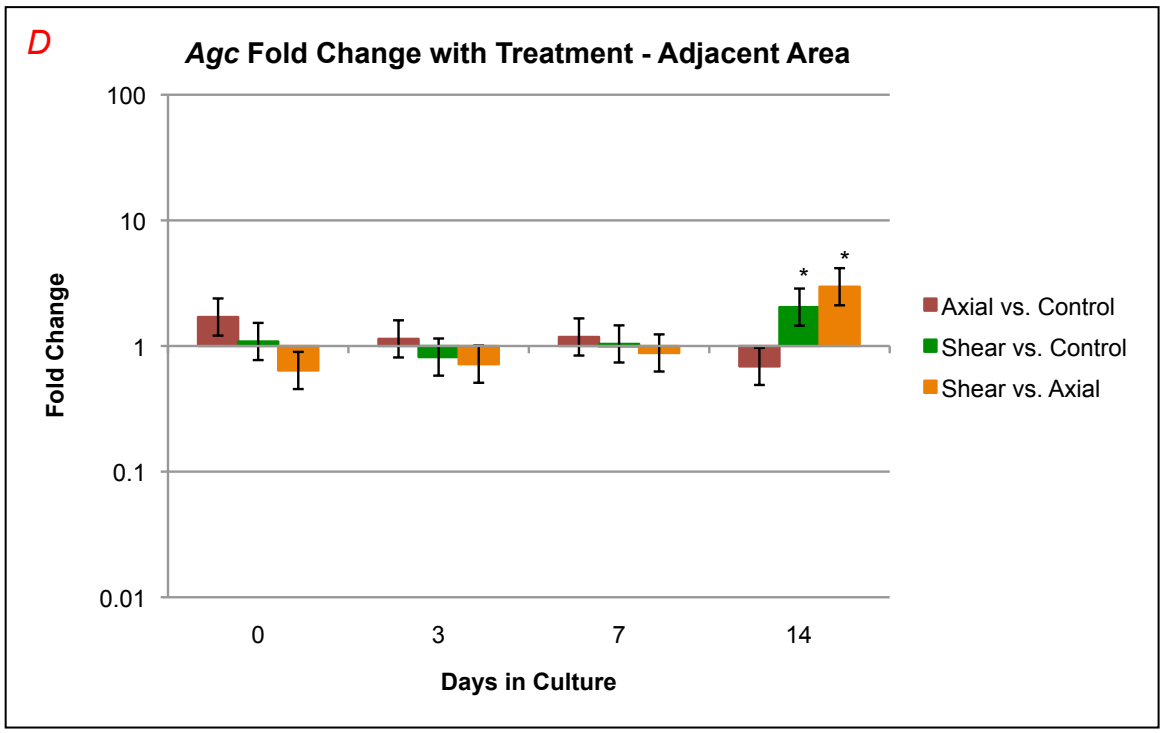
D
Agc Fold Change with Treatment - Adjacent Area
100
10
1
0.1
0.01
Fold Change
0
3
7
14
Days in Culture
Axial vs. Control
Shear vs. Control
Shear vs. Axial

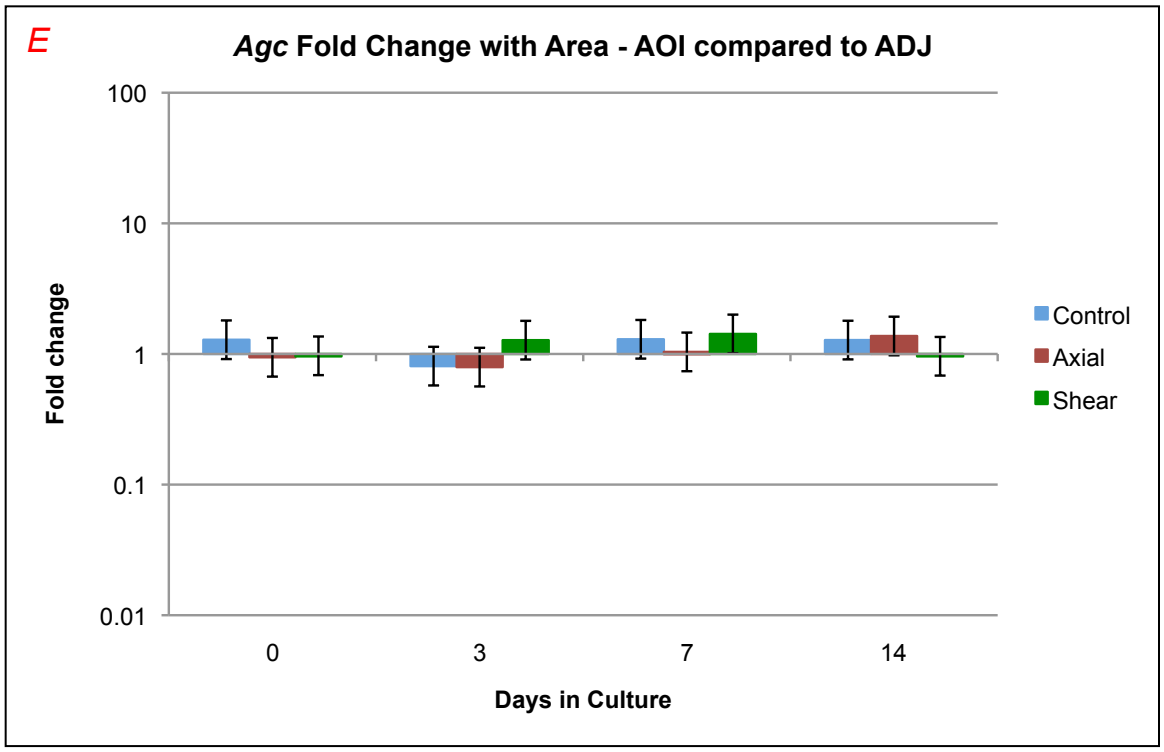
E
Agc Fold Change with Area - AOI compared to ADJ
100
10
1
0.1
0.01
Fold change
0
3
7
14
Days in Culture
Control
Axial
Shear

4.9.4 Results for *Sox-9*

Fold Change With Time:

For AOI specimens compared to day 0 control, *sox-9* showed an initial decreasing trend from day 0 to day 3 that then plateaued for the later time points, however, shear specimens showed a rise from day 7 to day 14. Control had significantly lower expression at day 3, 7 and 14 (FC = 0.34, $q < 0.01$; FC = 0.26, $q < 0.01$; FC = 0.24, $q < 0.01$). The axial specimens also showed lower expression at the same time points (FC = 0.19, $q < 0.01$; FC = 0.16, $q < 0.01$; FC = 0.11, $q < 0.01$). Finally, shear AOI showed lower expression than day 0 control at day 3, 7 and 14 as well (FC = 0.24, $q < 0.01$; FC = 0.16, $q < 0.01$; FC = 0.31, $q < 0.01$). For the ADJ specimens, there was a drop in expression from day 0 to day 3, but then all treatments stayed at relatively similar levels for the remaining time points. The changes for the control ADJ specimens were significant at day 3, 7 and 14 (FC = 0.34, $q < 0.01$; FC = 0.46, $q < 0.03$; FC = 0.15, $q < 0.01$). The axial ADJ specimens also had lower expression at day 3, 7 and 14 (FC = 0.19, $q < 0.01$; FC = 0.27, $q < 0.01$; FC = 0.29, $q < 0.01$). Finally the shear ADJ specimens had significantly lower expression at the same three time points (FC = 0.47, $q = 0.05$; FC = 0.34, $q = 0.01$; FC = 0.25, $q < 0.01$).

Fold Change With Treatment:

There were not many large changes in expression of AOI specimens between treatments until the day 14 time point, where shear was higher than axial. Axial expression was lower than control at day 3, 7 and 14 (FC = 0.57, $q = 0.20$; FC = 0.60, $q = 0.20$; FC =

0.45, q = 0.09). Shear was higher than axial at day 14 (FC = 2.07, q = 0.13). There were no consistent trends for the ADJ specimens when comparing treatments. Axial ADJ expression of *sox-9* was lower than control at day 3 and 7 (FC = 0.56, q = 0.15; FC = 0.57, q = 0.15; FC = 1.84, q = 0.15).

Fold Change With Area:

When AOI specimens were compared to ADJ at each time point, control AOI specimens had higher expression at day 0, 3, and 14 (FC = 2.04, q = 0.06; FC = 2.01, q = 0.06; FC = 3.12, q = 0.01). Axial AOI expression was higher than ADJ at day 3 (FC = 2.04, q = 0.19), and shear AOI expression was higher than ADJ at day 0 and 14 (FC 2.02, q = 0.09; FC = 2.59, q = 0.03).

Figures 4.10 A-E. Graphs of *sox-9* by time point, treatment and area.

Figure 4.10 A. *Sox-9*: Fold change with time – area of interest. Fold change is shown on the vertical axis as a log scale. Fold changes less than one indicate lowered expression and fold changes greater than one indicate higher expression. Days in culture are shown on the horizontal axis. At each time point, day 0 control specimens are used as the reference or comparative value. Error bars (standard error) are shown for each fold change. Control specimens are plotted in blue, axial are plotted in red, and shear are plotted in green. Significant differences in expression relative to day 0 control are indicated at each time point with an asterisk (*) in the respective color of the plotted treatment.

Figure 4.10 B. *Sox-9*: Fold change with treatment – area of interest. Fold change is shown on the vertical axis as a log scale, and days in culture is shown on the horizontal axis. The treatments are compared to each other at each time point. Axial vs. Control is shown in red, Shear vs. Control is shown in green, and Shear vs. Axial is shown in orange. Error bars (standard error) for fold change are depicted, and significant differences for the respective comparison are indicated with an asterisk (*).

Figure 4.10 C. *Sox-9*: Fold change with time – adjacent area. Fold change is shown on the vertical axis as a log scale. Fold changes less than one indicate lowered expression and fold changes greater than one indicate higher expression. Days in culture are shown on the horizontal axis. At each time point, day 0 control specimens are used as the reference or comparative value. Error bars (standard error) are shown for each fold change. Control specimens are plotted in blue, axial are plotted in red, and shear are plotted in green. Significant differences in expression relative to day 0 control are indicated at each time point with an asterisk (*) in the respective color of the plotted treatment.

Figure 4.10 D. *Sox-9*: Fold change with treatment – adjacent area. Fold change is shown on the vertical axis as a log scale, and days in culture is shown on the horizontal axis. The treatments are compared to each other at each time point. Axial vs. Control is shown in red, Shear vs. Control is shown in green, and Shear vs. Axial is shown in orange. Error bars (standard error) for fold change are depicted, and significant differences for the respective comparison are indicated with an asterisk (*).

Figure 4.10 E. *Sox-9*: Fold change with area – area of interest vs. adjacent area. Fold change is shown on the vertical axis as a log scale, and days in culture is shown on the horizontal axis. The treatment areas are compared to each other within each treatment at each time point. Control is shown in blue, axial is shown in red, and shear is shown in green. Error bars (standard error) for fold change are depicted, and significant differences for the respective comparison are indicated with an asterisk (*).

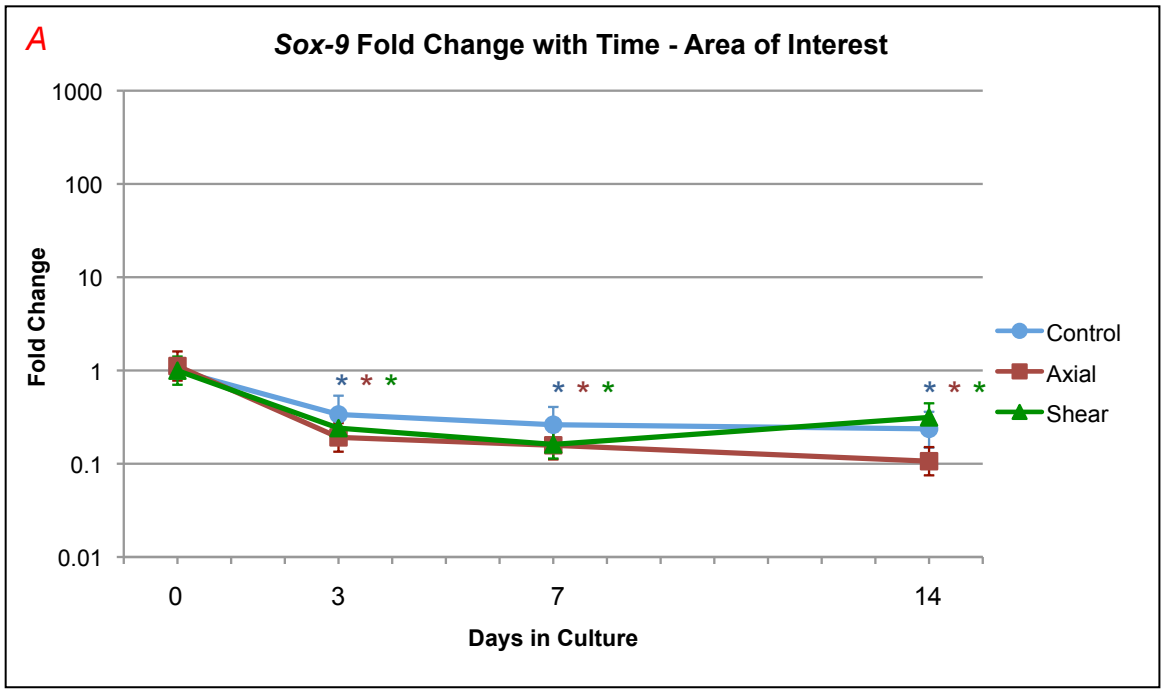
A
Sox-9 Fold Change with Time - Area of Interest
1000
100
10
1
0.1
0.01
Fold Change
0
3
7
14
Days in Culture
Control
Axial
Shear

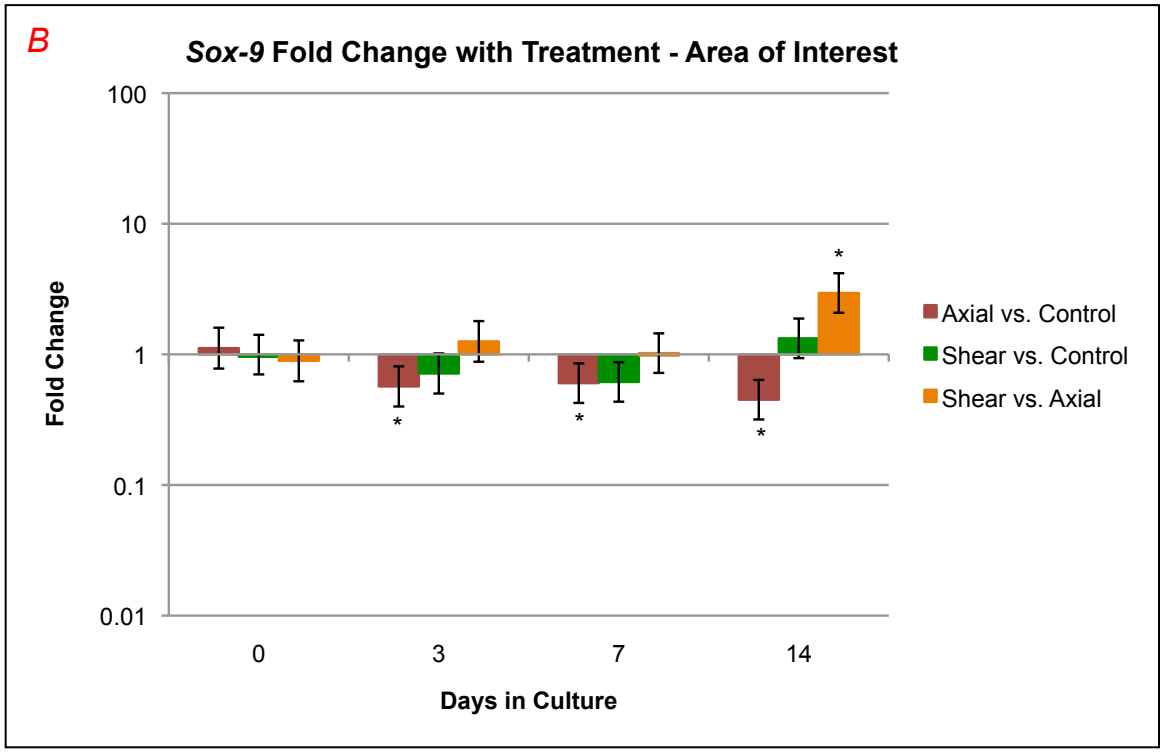
B
Sox-9 Fold Change with Treatment - Area of Interest
100
10
1
0.1
0.01
Fold Change
0
3
7
14
Days in Culture
Axial vs. Control
Shear vs. Control
Shear vs. Axial

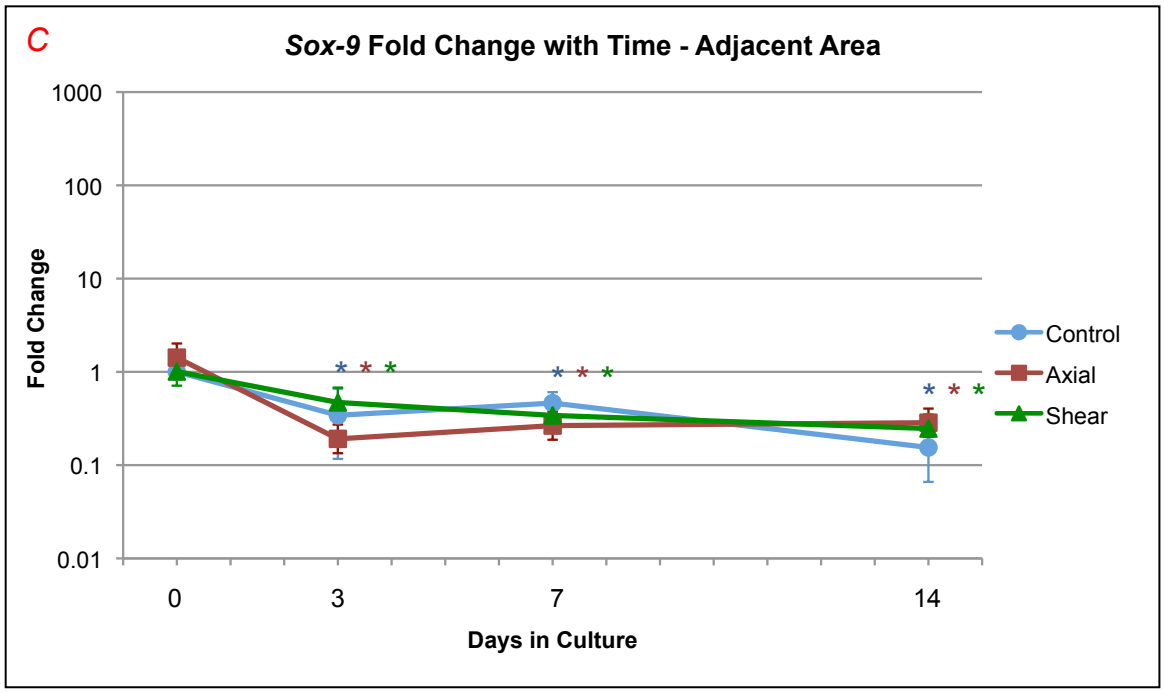
C
Sox-9 Fold Change with Time - Adjacent Area
1000
100
10
1
0.1
0.01
Fold Change
0
3
7
14
Days in Culture
Control
Axial
Shear

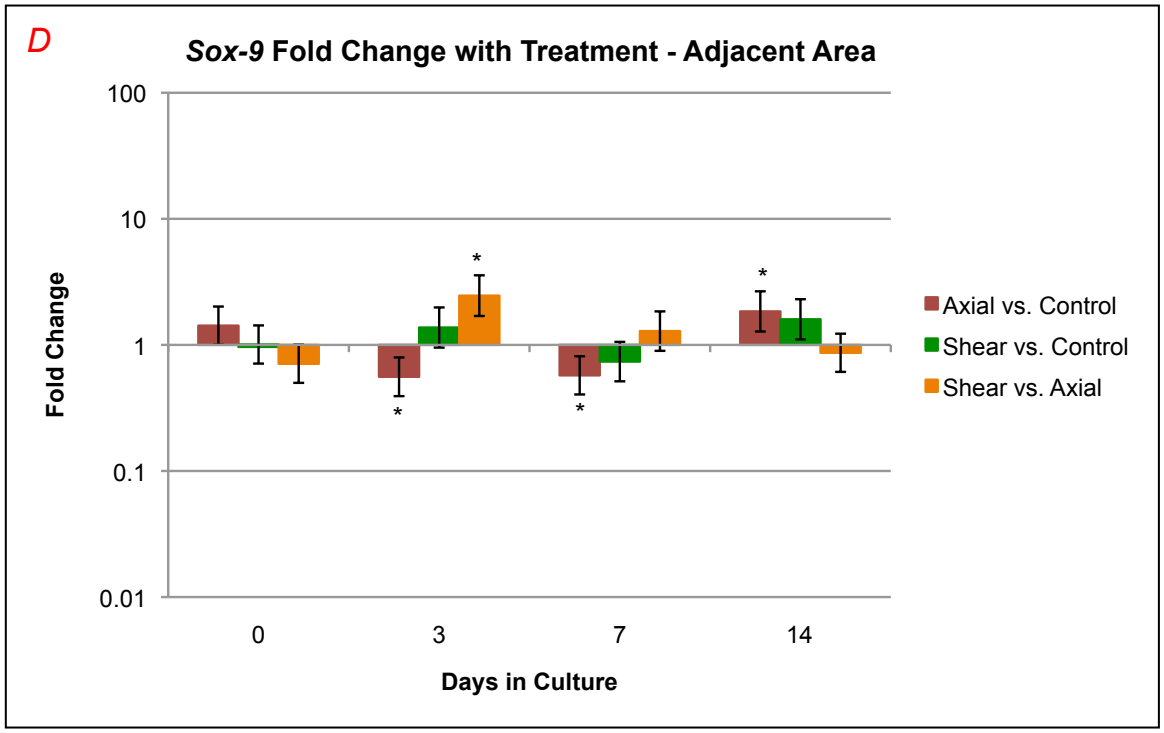
D
Sox-9 Fold Change with Treatment - Adjacent Area
100
10
1
0.1
0.01
Fold Change
0
3
7
14
Days in Culture
Axial vs. Control
Shear vs. Control
Shear vs. Axial

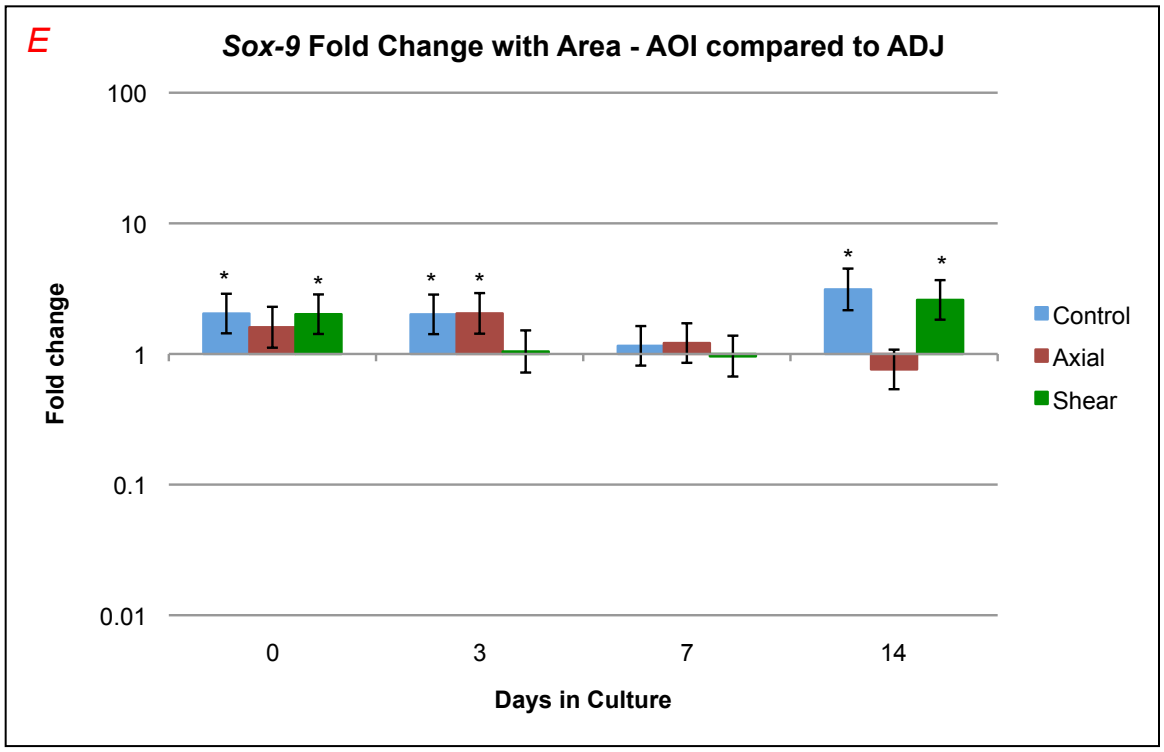
E
Sox-9 Fold Change with Area - AOI compared to ADJ
100
10
1
0.1
0.01
Fold change
0
3
7
14
Days in Culture
Control
Axial
Shear

4.9.5 Results for *Opn*

Fold Change With Time:

The expression of *opn* in the AOI specimens showed a rise for all treatments from day 0 to day 3, and then remained relatively constant for control and shear, but dropped in the shear specimens from that time point forward. The higher expression was significant for control at day 0, 7 and 14 (FC = 2.98, q = 0.03; FC = 4.29, q = 0.01; FC = 4.69, q = 0.01). The expression was higher in axial specimens at day 3 and 7 (FC = 4.94, q = 0.01; FC = 2.64, q = 0.10). Shear specimens showed higher expression at day 3, 7 and 14 (FC = 6.72, q <0.01; FC = 3.36, q = 0.03; FC = 2.71, q = 0.06). For the ADJ specimens there were no consistent expression changes. Control expression was higher at day 3, 7, and 14 in the ADJ specimens compared to day 0 control (FC = 5.57, q < 0.01; FC = 3.62, q = 0.01; FC = 4.82, q < 0.01). Shear expression was higher at day 3 and 14 (FC = 6.72, q < 0.01; FC = 3.36, q < 0.01; FC = 2.71, q < 0.01). Finally, axial ADJ specimens had higher expression only at day 3 (FC = 3.91, q = 0.02).

Fold Change With Treatment:

There were no discernible trends in a comparison of treatments for either AOI or ADJ specimens at any time point. Neither were there any significant differences.

Fold Change With Area:

When AOI specimens were compared to ADJ, the AOI specimens had noticeably lower expression in axial and shear at the day 0 time point and at the day 14 time point. Control

AOI expression was lower than ADJ at day 3 (FC = 0.36, q = 0.15). Axial AOI expression was lower at day 0 and 14 (FC = 0.35, q = 0.08; FC 0.36, q = 0.08). For shear, AOI expression was lower than ADJ at day 0 (FC = 0.33, q = 0.11).

Figures 4.11 A-E. Graphs of *opn* by time point, treatment and area.

Figure 4.11 A. *Opn*: Fold change with time – area of interest. Fold change is shown on the vertical axis as a log scale. Fold changes less than one indicate lowered expression and fold changes greater than one indicate higher expression. Days in culture are shown on the horizontal axis. At each time point, day 0 control specimens are used as the reference or comparative value. Error bars (standard error) are shown for each fold change. Control specimens are plotted in blue, axial are plotted in red, and shear are plotted in green. Significant differences in expression relative to day 0 control are indicated at each time point with an asterisk (*) in the respective color of the plotted treatment.

Figure 4.11 B. *Opn*: Fold change with treatment – area of interest. Fold change is shown on the vertical axis as a log scale, and days in culture is shown on the horizontal axis. The treatments are compared to each other at each time point. Axial vs. Control is shown in red, Shear vs. Control is shown in green, and Shear vs. Axial is shown in orange. Error bars (standard error) for fold change are depicted, and significant differences for the respective comparison are indicated with an asterisk (*).

Figure 4.11 C. *Opn*: Fold change with time – adjacent area. Fold change is shown on the vertical axis as a log scale. Fold changes less than one indicate lowered expression and fold changes greater than one indicate higher expression. Days in culture are shown on the horizontal axis. At each time point, day 0 control specimens are used as the reference or comparative value. Error bars (standard error) are shown for each fold change. Control specimens are plotted in blue, axial are plotted in red, and shear are plotted in green. Significant differences in expression relative to day 0 control are indicated at each time point with an asterisk (*) in the respective color of the plotted treatment.

Figure 4.11 D. *Opn*: Fold change with treatment – adjacent area. Fold change is shown on the vertical axis as a log scale, and days in culture is shown on the horizontal axis. The treatments are compared to each other at each time point. Axial vs. Control is shown in red, Shear vs. Control is shown in green, and Shear vs. Axial is shown in orange. Error bars (standard error) for fold change are depicted, and significant differences for the respective comparison are indicated with an asterisk (*).

Figure 4.11 E. *Opn*: Fold change with area – area of interest vs. adjacent area. Fold change is shown on the vertical axis as a log scale, and days in culture is shown on the horizontal axis. The treatment areas are compared to each other within each treatment at each time point. Control is shown in blue, axial is shown in red, and shear is shown in green. Error bars (standard error) for fold change are depicted, and significant differences for the respective comparison are indicated with an asterisk (*).

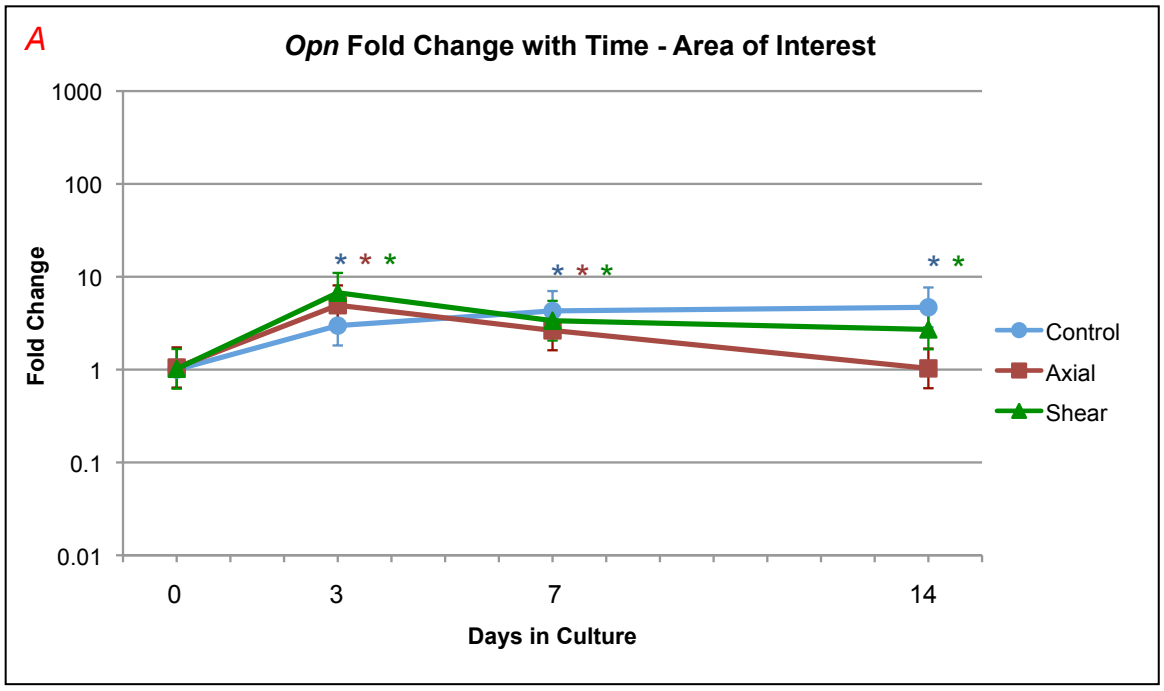
A
Opn Fold Change with Time - Area of Interest
1000
100
10
1
0.1
0.01
Fold Change
0
3
7
14
Days in Culture
Control
Axial
Shear

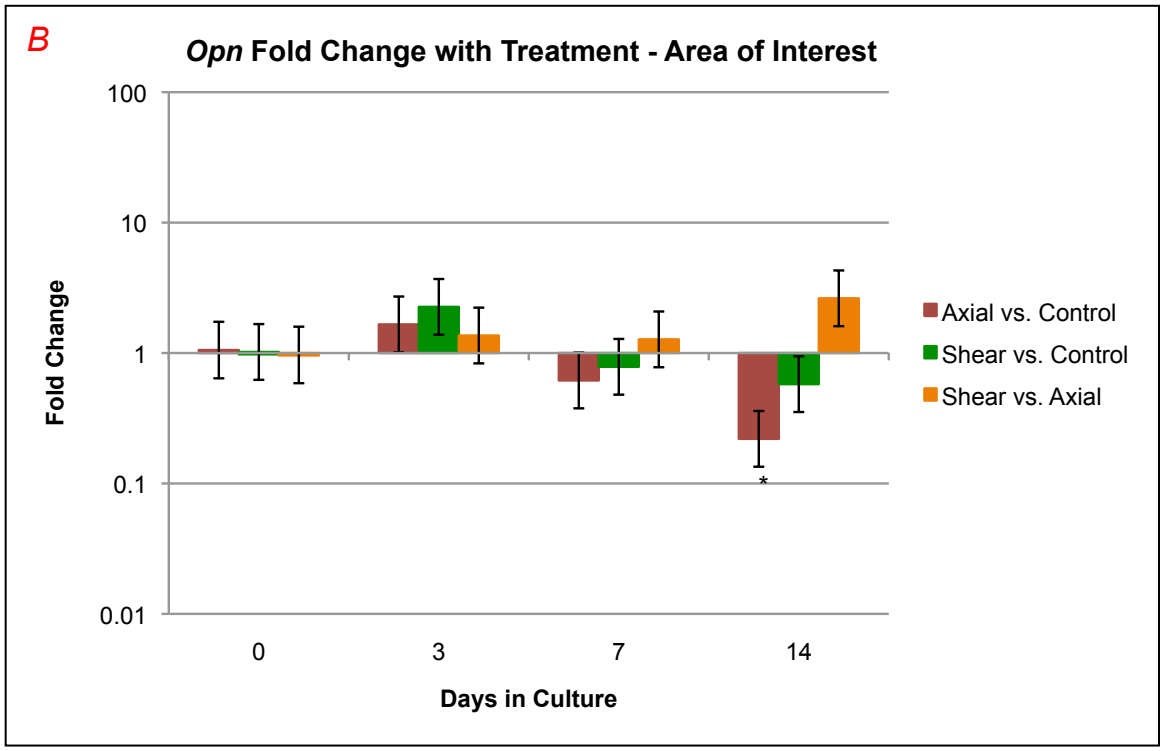
B
Opn Fold Change with Treatment - Area of Interest
100
10
1
0.1
0.01
Fold Change
0
3
7
14
Days in Culture
Axial vs. Control
Shear vs. Control
Shear vs. Axial

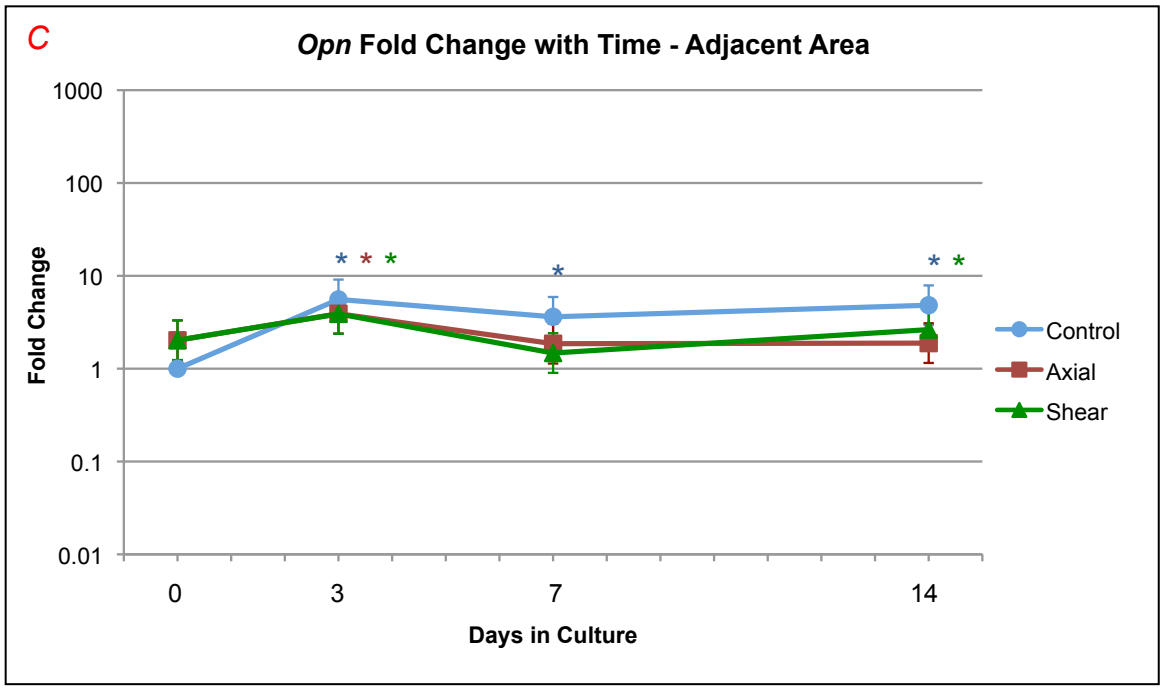
C
Opn Fold Change with Time - Adjacent Area
1000
100
10
1
0.1
0.01
Fold Change
* * *
*
* *
0
3
7
14
Days in Culture
Control
Axial
Shear

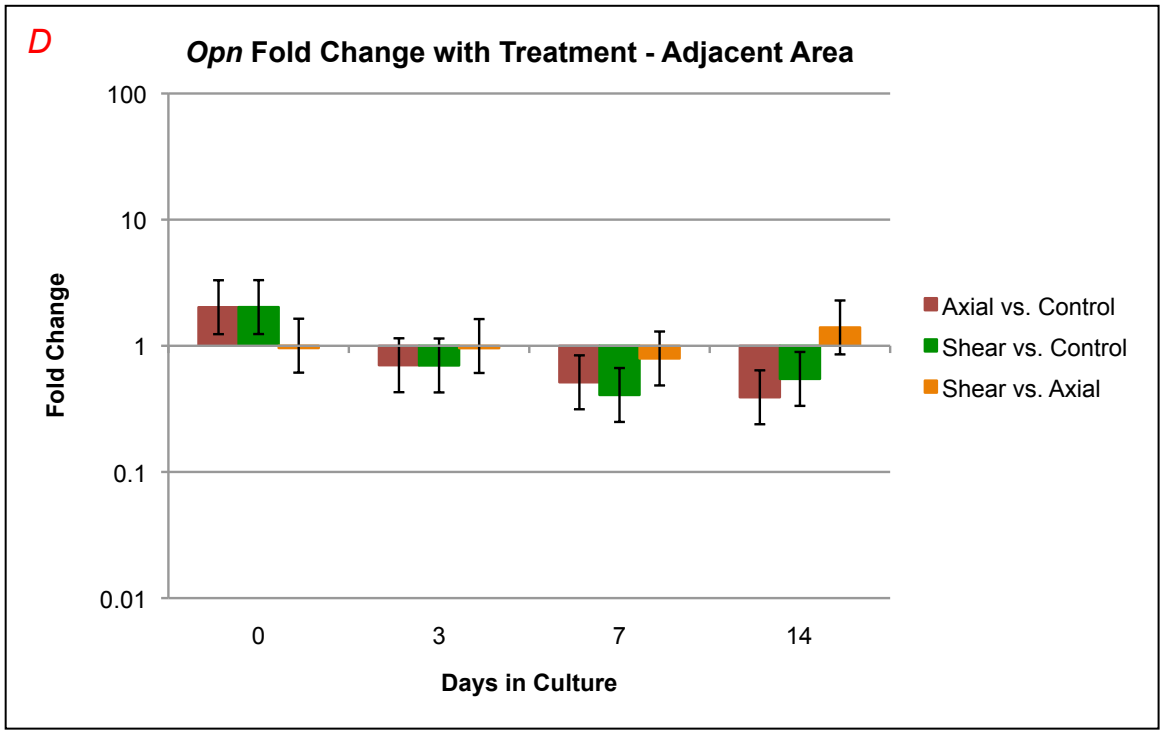
D
Opn Fold Change with Treatment - Adjacent Area
100
10
1
0.1
0.01
Fold Change
0
3
7
14
Days in Culture
Axial vs. Control
Shear vs. Control
Shear vs. Axial

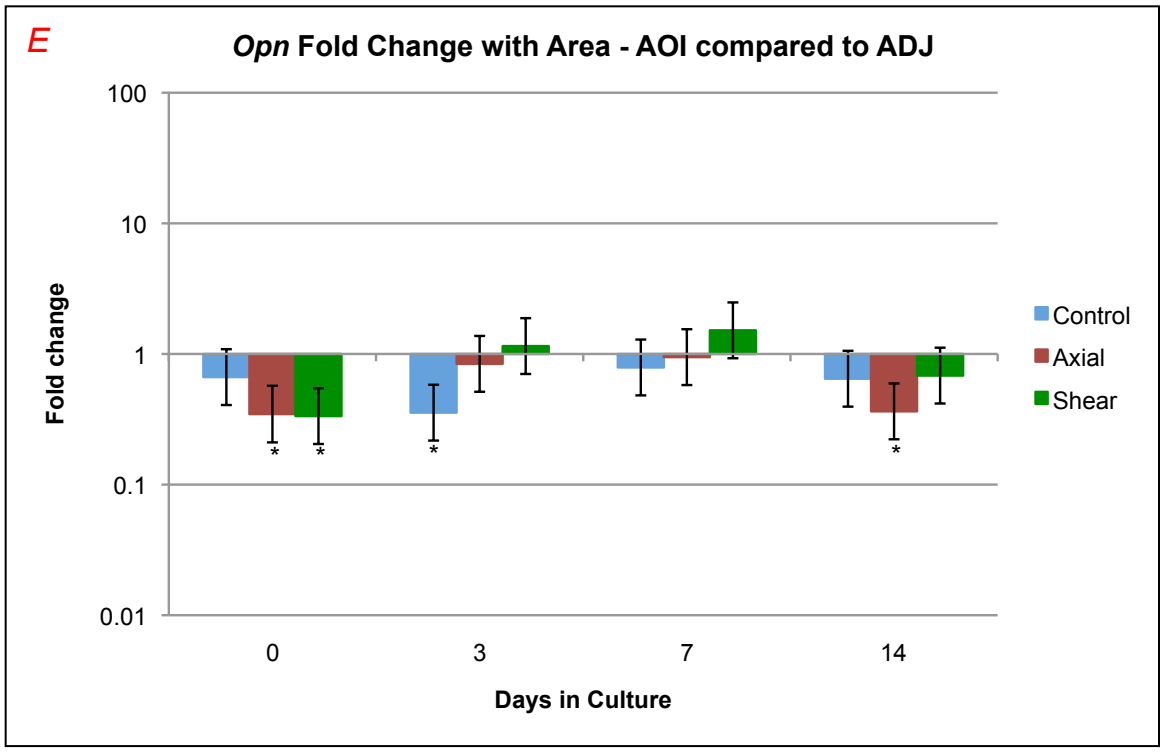
E
Opn Fold Change with Area - AOI compared to ADJ
100
10
1
0.1
0.01
Fold change
0
3
7
14
Days in Culture
Control
Axial
Shear
*
*
*
*

4.9.6 Results for *Comp*

Fold Change With Time:

Comp showed a decreasing trend of expression over time for all treatments in both AOI and ADJ. For control AOI the expression was significantly lower at day 3, 7 and 14 (FC = 0.28, $q < 0.01$; FC = 0.05, $q < 0.01$; FC = 0.03, $q < 0.01$). Axial had significantly lower expression at the same time points (FC = 0.26, $q < 0.01$; FC = 0.07, $q < 0.01$; FC = 0.02, $q < 0.01$). Shear also had lower expression in the AOI specimens compared to day 0 control at day 3, 7 and 14 (FC =0.25, $q < 0.01$; FC = 0.05, $q < 0.01$, FC = 0.03, $q < 0.01$). The ADJ specimens also showed lower expression at day 3, 7 and 14 for control (FC = 0.30, $q < 0.01$; FC = 0.06, $q < 0.01$; FC = 0.03, $q < 0.01$), axial (FC = 0.18, $q < 0.01$; FC = 0.06, $q < 0.01$; FC = 0.02, $q < 0.01$), and shear (FC = 0.17, $q < 0.01$; FC = 0.04, $q < 0.01$; FC = 0.03, $q < 0.01$).

Fold Change With Treatment:

There were no consistent trends when comparing treatments for either AOI or ADJ specimens. However, shear AOI expression was significantly lower than axial at day 0 (FC = 0.41, $q = 0.03$).

Fold Change With Area:

There were no trends or significant changes for *comp* when comparing AOI and ADJ specimens for each treatment at each time point.

Figures 4.12 A-E. Graphs of *comp* by time point, treatment and area.

Figure 4.12 A. *Comp*: Fold change with time – area of interest. Fold change is shown on the vertical axis as a log scale. Fold changes less than one indicate lowered expression and fold changes greater than one indicate higher expression. Days in culture are shown on the horizontal axis. At each time point, day 0 control specimens are used as the reference or comparative value. Error bars (standard error) are shown for each fold change. Control specimens are plotted in blue, axial are plotted in red, and shear are plotted in green. Significant differences in expression relative to day 0 control are indicated at each time point with an asterisk (*) in the respective color of the plotted treatment.

Figure 4.12 B. *Comp*: Fold change with treatment – area of interest. Fold change is shown on the vertical axis as a log scale, and days in culture is shown on the horizontal axis. The treatments are compared to each other at each time point. Axial vs. Control is shown in red, Shear vs. Control is shown in green, and Shear vs. Axial is shown in orange. Error bars (standard error) for fold change are depicted, and significant differences for the respective comparison are indicated with an asterisk (*).

Figure 4.12 C. *Comp*: Fold change with time – adjacent area. Fold change is shown on the vertical axis as a log scale. Fold changes less than one indicate lowered expression and fold changes greater than one indicate higher expression. Days in culture are shown on the horizontal axis. At each time point, day 0 control specimens are used as the reference or comparative value. Error bars (standard error) are shown for each fold change. Control specimens are plotted in blue, axial are plotted in red, and shear are plotted in green. Significant differences in expression relative to day 0 control are indicated at each time point with an asterisk (*) in the respective color of the plotted treatment.

Figure 4.12 D. *Comp*: Fold change with treatment – adjacent area. Fold change is shown on the vertical axis as a log scale, and days in culture is shown on the horizontal axis. The treatments are compared to each other at each time point. Axial vs. Control is shown in red, Shear vs. Control is shown in green, and Shear vs. Axial is shown in orange. Error bars (standard error) for fold change are depicted, and significant differences for the respective comparison are indicated with an asterisk (*).

Figure 4.12 E. *Comp*: Fold change with area – area of interest vs. adjacent area. Fold change is shown on the vertical axis as a log scale, and days in culture is shown on the horizontal axis. The treatment areas are compared to each other within each treatment at each time point. Control is shown in blue, axial is shown in red, and shear is shown in green. Error bars (standard error) for fold change are depicted, and significant differences for the respective comparison are indicated with an asterisk (*).

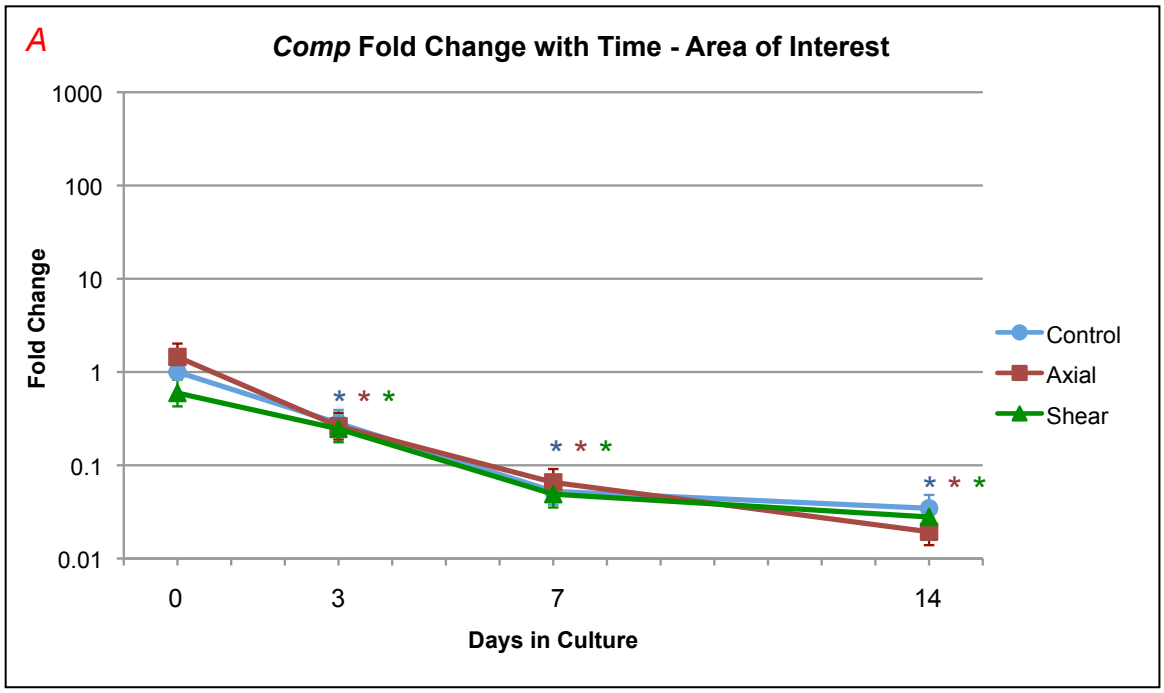
A
Comp Fold Change with Time - Area of Interest
1000
100
10
1
0.1
0.01
Fold Change
0
3
7
14
Days in Culture
Control
Axial
Shear

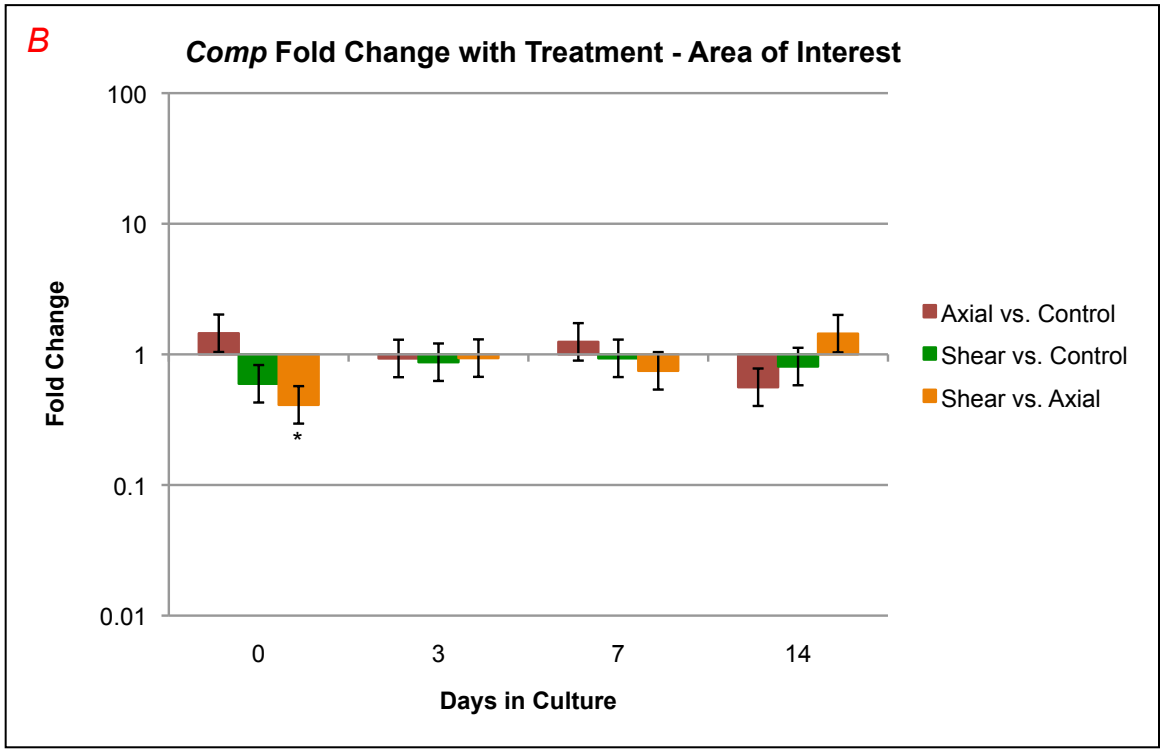
B
Comp Fold Change with Treatment - Area of Interest
100
10
1
0.1
0.01
Fold Change
0
3
7
14
Days in Culture
Axial vs. Control
Shear vs. Control
Shear vs. Axial

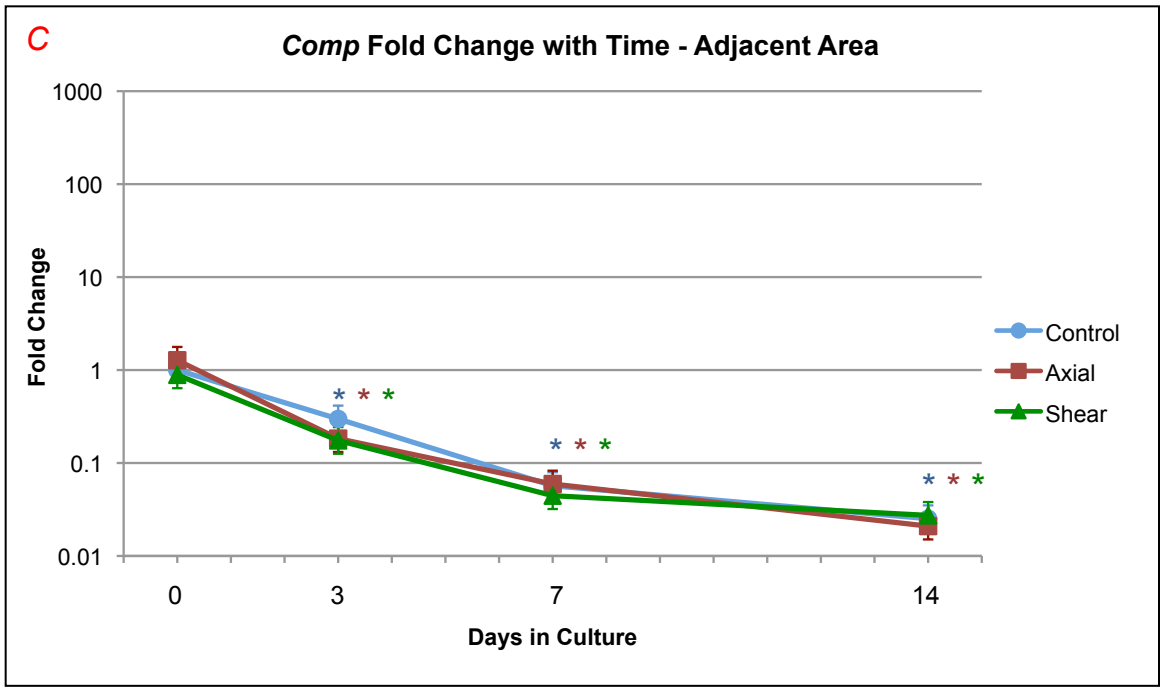
C
Comp Fold Change with Time - Adjacent Area
1000
100
10
1
0.1
0.01
Fold Change
* * *
* * *
* * *
0
3
7
14
Days in Culture
Control
Axial
Shear

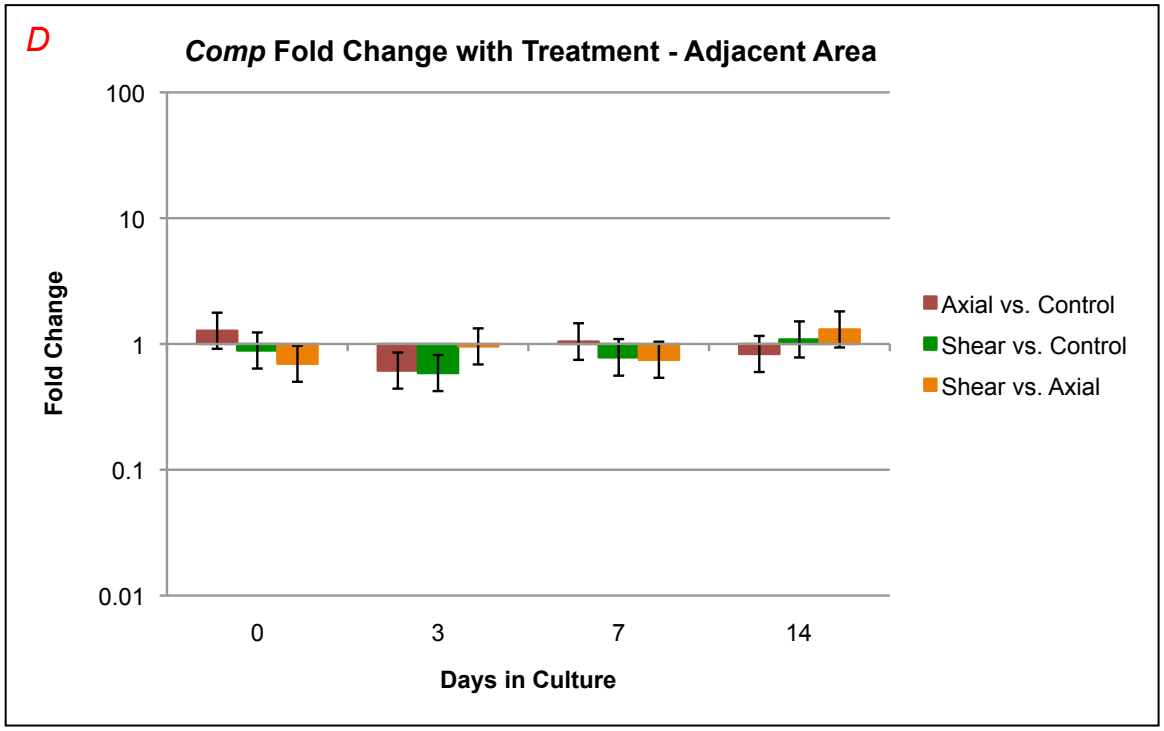
D
Comp Fold Change with Treatment - Adjacent Area
100
10
1
0.1
0.01
Fold Change
0
3
7
14
Days in Culture
Axial vs. Control
Shear vs. Control
Shear vs. Axial

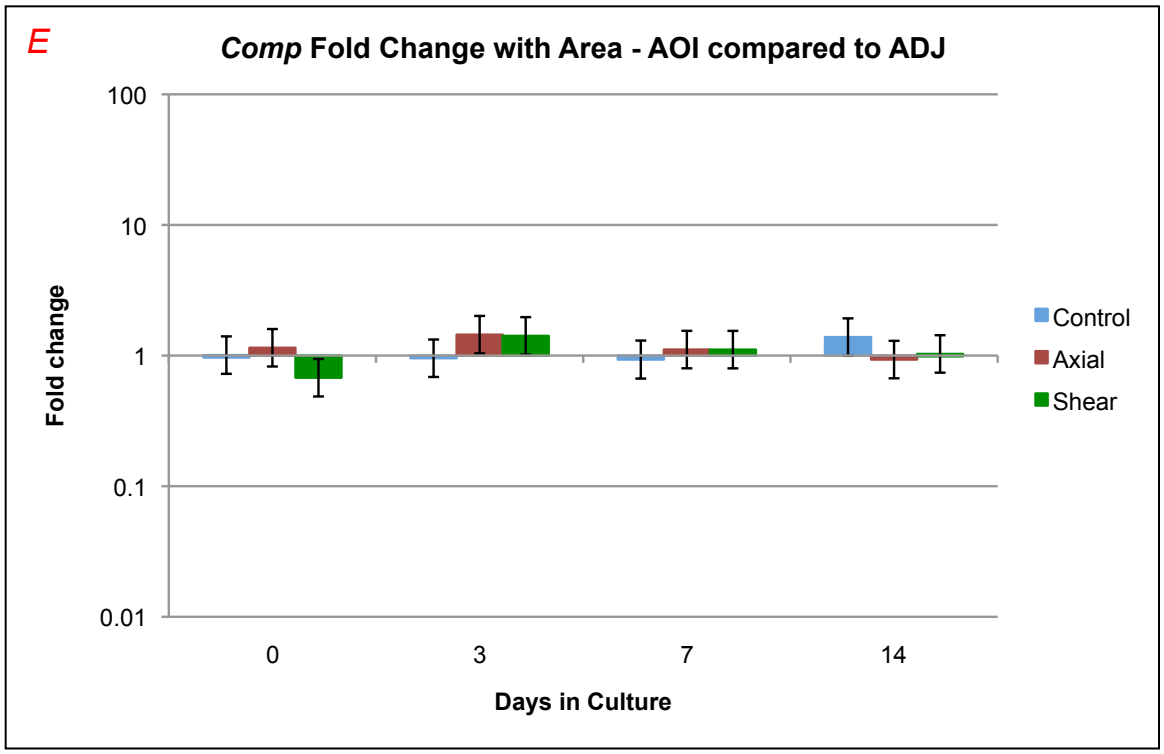
E
Comp Fold Change with Area - AOI compared to ADJ
100
10
1
0.1
0.01
Fold change
0
3
7
14
Days in Culture
Control
Axial
Shear

Summary of Cartilage Matrix:

Col1a1 expression increased over time in all treatments, whereas *col2a1* generally decreased in expression decreased. *Col1a1* had higher expression at day 3 in shear compared to control and at day 0 and 3 when shear were compared to axial. *Col2a1* was more highly expressed at day 3 in shear compared to axial specimens. In the AOI specimens, both *col1a1* and *col2a1* tapered in expression compared to control by day 7. *Agc*, *sox-9*, and *comp* all showed lowered expression over time in all treatments. *Sox-9* expression was higher in shear vs. axial at day 14. *Comp* expression was lower in the AOI shear specimens compared to axial at day 0.

Figures 4.13 A-F. Graphs of cartilage matrix genes by time point for AOI and ADJ. Fold change with time – area of interest. Fold change is shown on the vertical axis as a log scale. Fold changes less than one indicate lowered expression and fold changes greater than one indicate higher expression. Days in culture are shown on the horizontal axis. At each time point, day 0 control specimens are used as the reference or comparative value. Graph A and B show changes over time for the control specimens, graph C and D show changes over time for the axial specimens, and graph E and F show changes over time for the shear specimens.

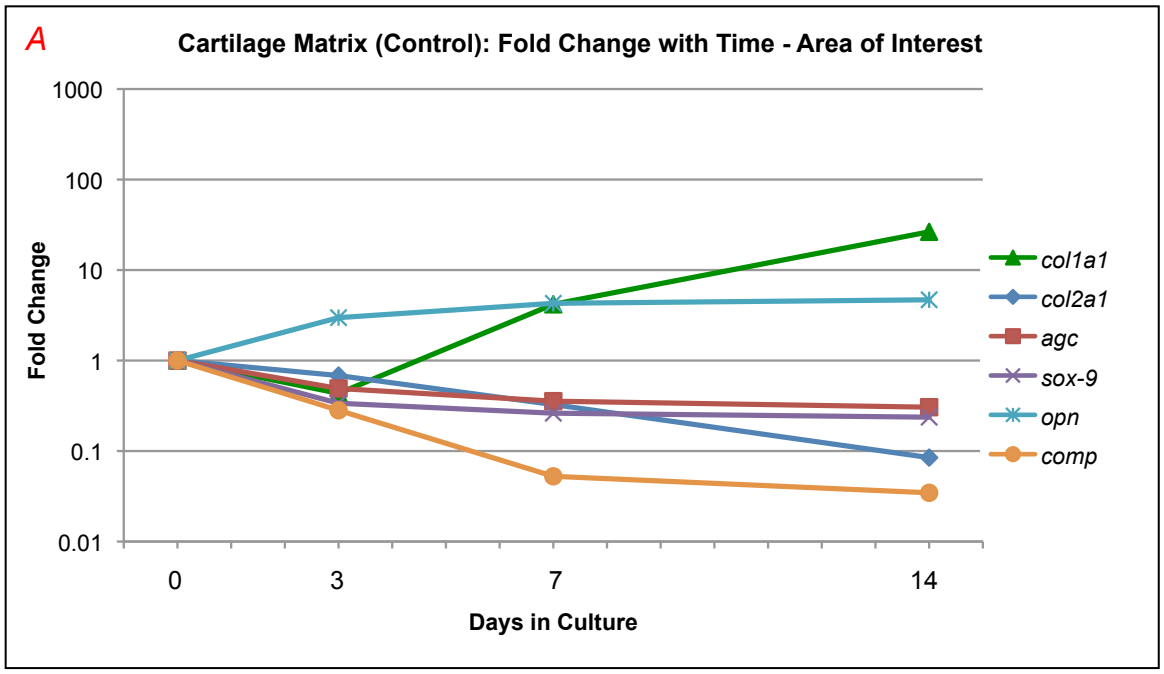
A
Cartilage Matrix (Control): Fold Change with Time - Area of Interest
1000
100
10
1
0.1
0.01
Fold Change
0
3
7
14
Days in Culture
col1a1
col2a1
agc
sox-9
opn
comp

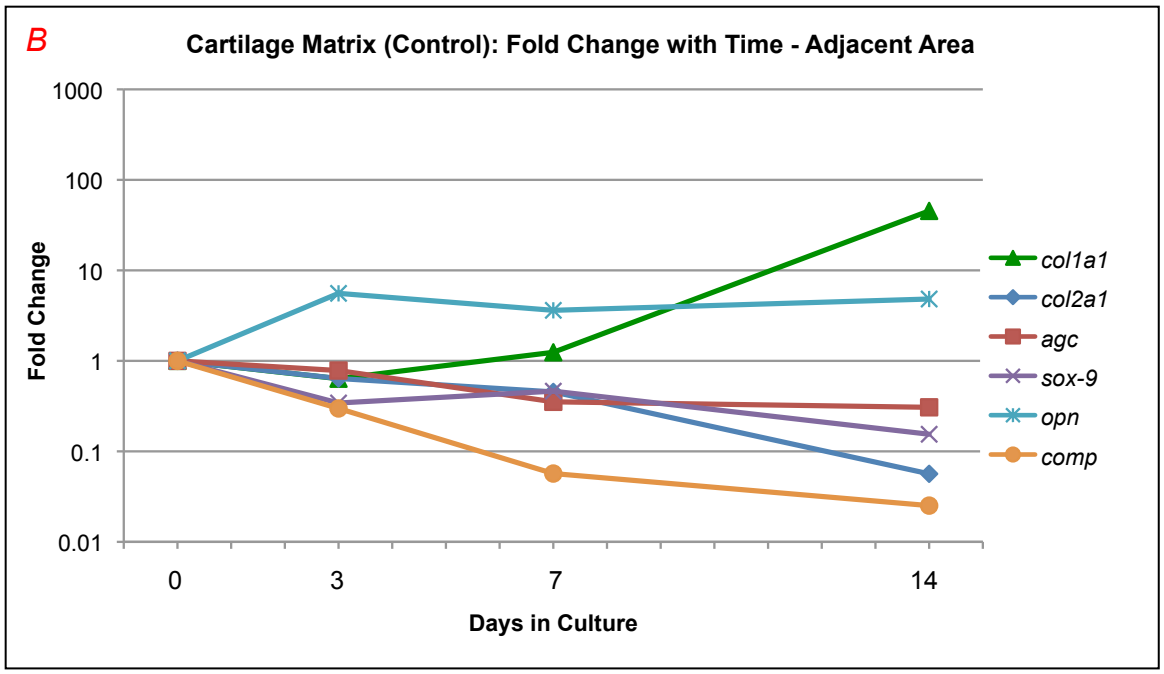
B
Cartilage Matrix (Control): Fold Change with Time - Adjacent Area
1000
100
10
1
0.1
0.01
Fold Change
0
3
7
14
Days in Culture
col1a1
col2a1
agc
sox-9
opn
comp

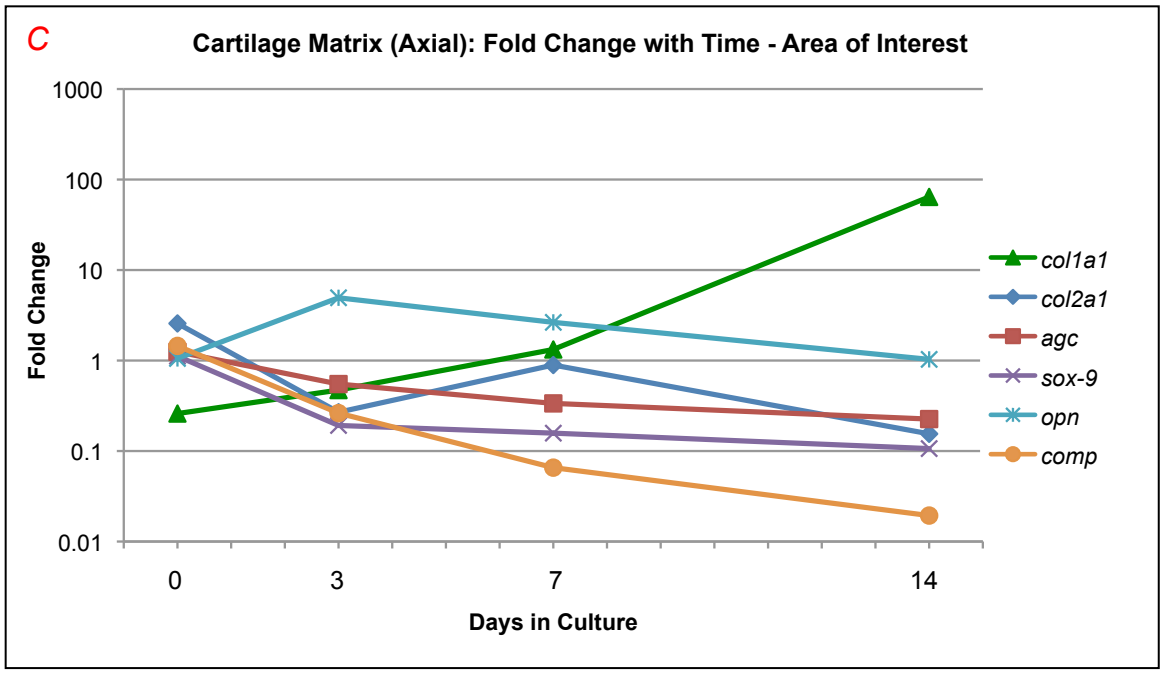
C
Cartilage Matrix (Axial): Fold Change with Time - Area of Interest
1000
100
10
1
0.1
0.01
Fold Change
0
3
7
14
Days in Culture
col1a1
col2a1
agc
sox-9
opn
comp

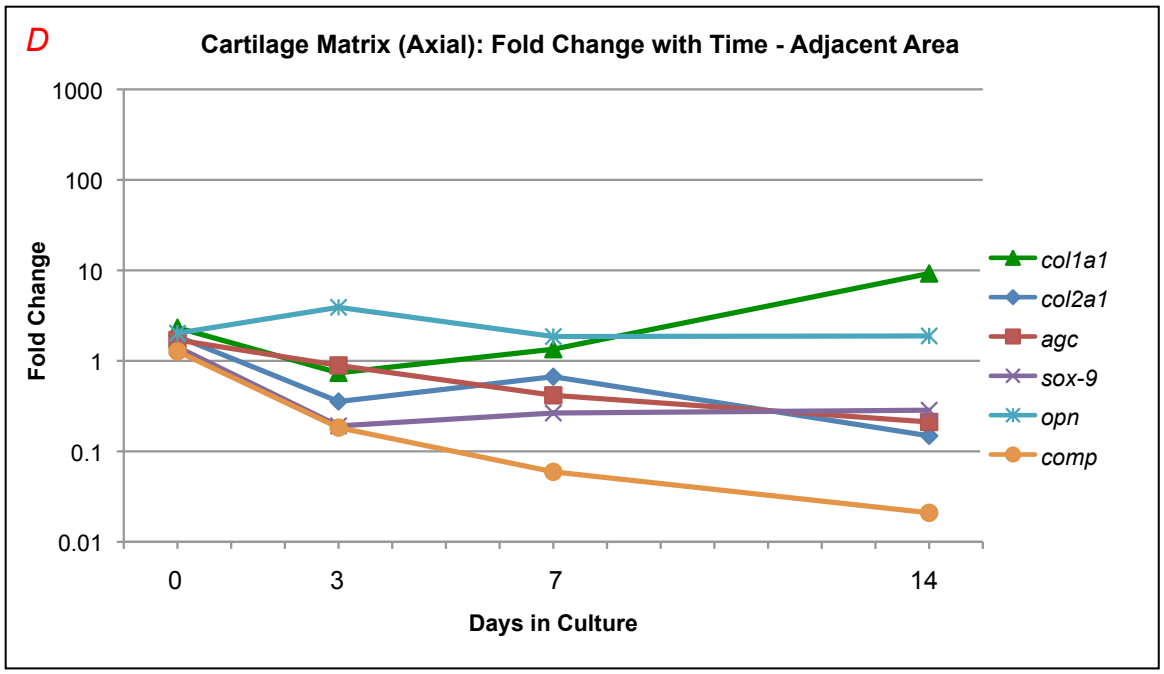
D
Cartilage Matrix (Axial): Fold Change with Time - Adjacent Area
1000
100
10
1
0.1
0.01
Fold Change
0
3
7
14
Days in Culture
col1a1
col2a1
agc
sox-9
opn
comp

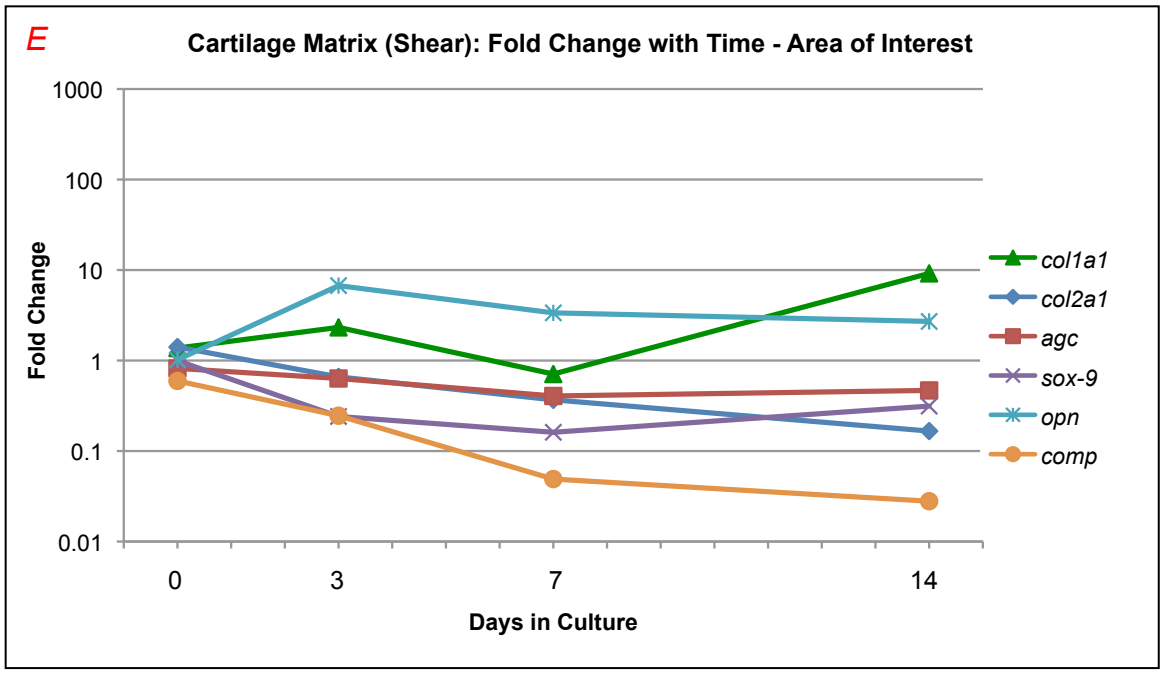
E
Cartilage Matrix (Shear): Fold Change with Time - Area of Interest
1000
100
10
1
0.1
0.01
Fold Change
0
3
7
14
Days in Culture
col1a1
col2a1
agc
sox-9
opn
comp

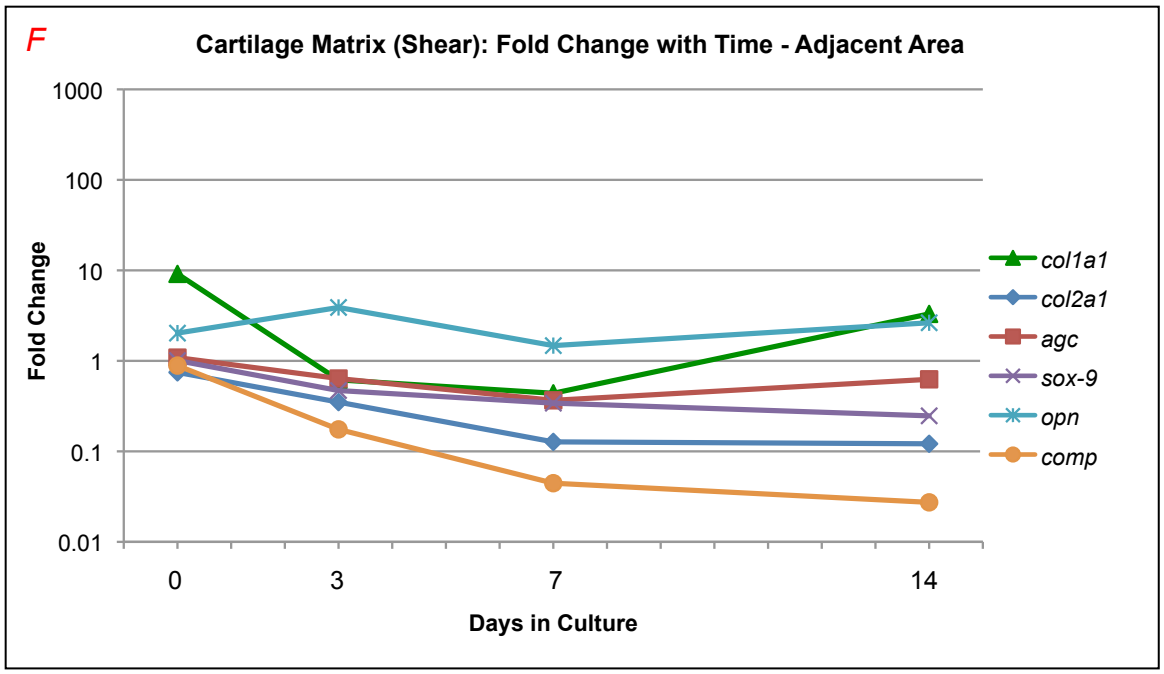
F
Cartilage Matrix (Shear): Fold Change with Time - Adjacent Area
1000
100
10
1
0.1
0.01
Fold Change
0
3
7
14
Days in Culture
col1a1
col2a1
agc
sox-9
opn
comp

4.10 Degradative Enzymes and Inhibitors

Genes related to the degradative enzymes and inhibitors (*mmp-1, mmp-3, mmp-13, timp-1, timp-2, adamts-5*) were evaluated for expression changes over time, differences between treatments, and differences between areas.

4.10.1 Results for *Mmp-1*

Fold Change With Time:

For both the AOI and ADJ specimens, *mmp-1* expression rose from day 0 to day 3, then dipped slightly at day 7 and rose again to day 14. The expression of AOI specimens was higher than day 0 control at day 3, 7 and 14 for control (FC = 86.98, $q < 0.01$; FC = 34.36, $q < 0.01$; FC = 314.70, $q < 0.01$), axial (FC = 51.57, $q < 0.01$; FC = 27.45, $q < 0.01$; FC = 145.70, $q < 0.01$) and shear (FC = 58.41, $q < 0.01$; FC = 13.55, $q < 0.01$; FC = 54.01, $q < 0.01$). ADJ specimens were also higher than day 0 control at day 3, 7 and 14 for control (FC = 436.47, $q < 0.01$; FC = 109.28, $q < 0.01$; FC = 1062.87, $q < 0.01$), axial (FC = 143.62, $q < 0.01$; FC = 29.90, $q < 0.01$; FC = 337.29, $q < 0.01$), and shear (FC = 141.38, $q < 0.01$; FC = 41.07, $q < 0.01$; FC = 402.65, $q < 0.01$).

Fold Change With Treatment:

Treatments were compared to each other for *mmp-1*, and for the AOI specimens the shear expression tended to be lower than control and axial at day 7 and 14, however the only significant difference was for shear vs. control at day 7 (FC = 0.17, $q = 0.01$). However for the ADJ specimens, both axial and shear had generally lower expression at day 3, 7 and 14. For axial ADJ compared to control these differences were significant at day 3, 7

and 14 (FC = 0.33, q = 0.09; FC = 0.27, q = 0.09; FC = 0.32, q = 0.09). For shear vs. control specimens the changes were significant at day 3, 7 and 14 as well (FC = 0.32, q = 0.16; FC = 0.38, q = 0.16; FC = 0.38, q = 0.16).

Fold Change With Area:

There were no discernible trends or significant differences for AOI compared to ADJ specimens.

Figures 4.14 A-E. Graphs of *mmp-1* by time point, treatment and area.

Figure 4.14 A. *Mmp-1*: Fold change with time – area of interest. Fold change is shown on the vertical axis as a log scale. Fold changes less than one indicate lowered expression and fold changes greater than one indicate higher expression. Days in culture are shown on the horizontal axis. At each time point, day 0 control specimens are used as the reference or comparative value. Error bars (standard error) are shown for each fold change. Control specimens are plotted in blue, axial are plotted in red, and shear are plotted in green. Significant differences in expression relative to day 0 control are indicated at each time point with an asterisk (*) in the respective color of the plotted treatment.

Figure 4.14 B. *Mmp-1*: Fold change with treatment – area of interest. Fold change is shown on the vertical axis as a log scale, and days in culture is shown on the horizontal axis. The treatments are compared to each other at each time point. Axial vs. Control is shown in red, Shear vs. Control is shown in green, and Shear vs. Axial is shown in orange. Error bars (standard error) for fold change are depicted, and significant differences for the respective comparison are indicated with an asterisk (*).

Figure 4.14 C. *Mmp-1*: Fold change with time – adjacent area. Fold change is shown on the vertical axis as a log scale. Fold changes less than one indicate lowered expression and fold changes greater than one indicate higher expression. Days in culture are shown on the horizontal axis. At each time point, day 0 control specimens are used as the reference or comparative value. Error bars (standard error) are shown for each fold change. Control specimens are plotted in blue, axial are plotted in red, and shear are plotted in green. Significant differences in expression relative to day 0 control are indicated at each time point with an asterisk (*) in the respective color of the plotted treatment.

Figure 4.14 D. *Mmp-1*: Fold change with treatment – adjacent area. Fold change is shown on the vertical axis as a log scale, and days in culture is shown on the horizontal axis. The treatments are compared to each other at each time point. Axial vs. Control is shown in red, Shear vs. Control is shown in green, and Shear vs. Axial is shown in orange. Error bars (standard error) for fold change are depicted, and significant differences for the respective comparison are indicated with an asterisk (*).

Figure 4.14 E. *Mmp-1*: Fold change with area – area of interest vs. adjacent area. Fold change is shown on the vertical axis as a log scale, and days in culture is shown on the horizontal axis. The treatment areas are compared to each other within each treatment at each time point. Control is shown in blue, axial is shown in red, and shear is shown in green. Error bars (standard error) for fold change are depicted, and significant differences for the respective comparison are indicated with an asterisk (*).

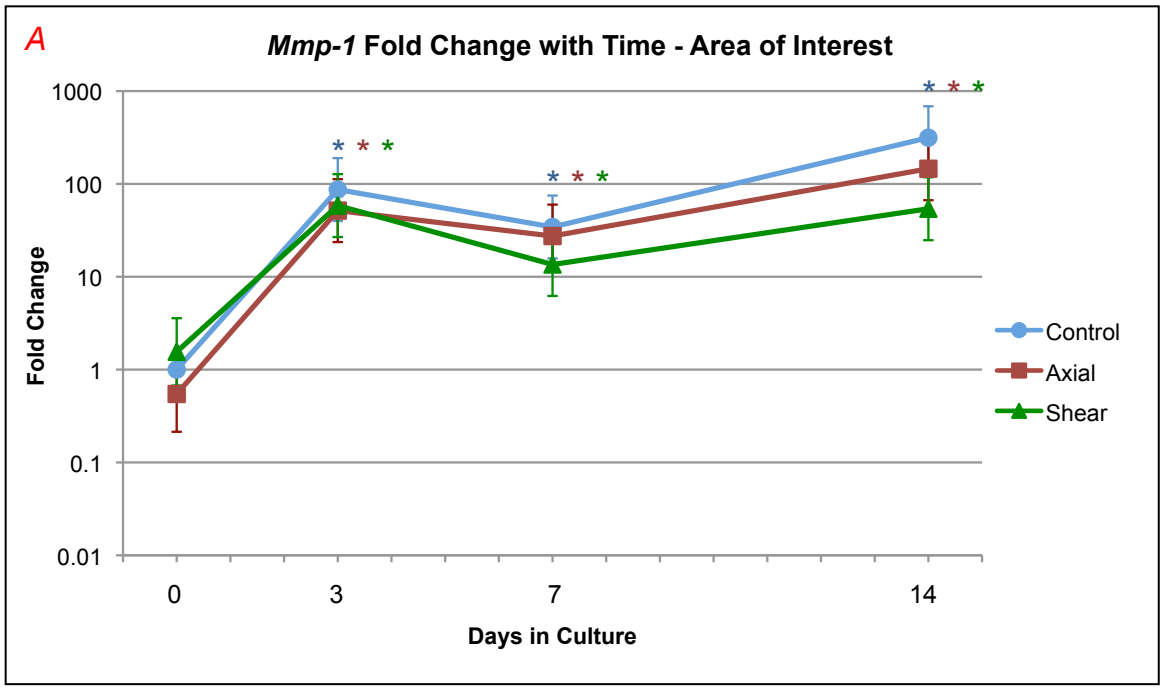
A
Mmp-1 Fold Change with Time - Area of Interest
1000
100
10
1
0.1
0.01
Fold Change
0
3
7
14
Days in Culture
Control
Axial
Shear

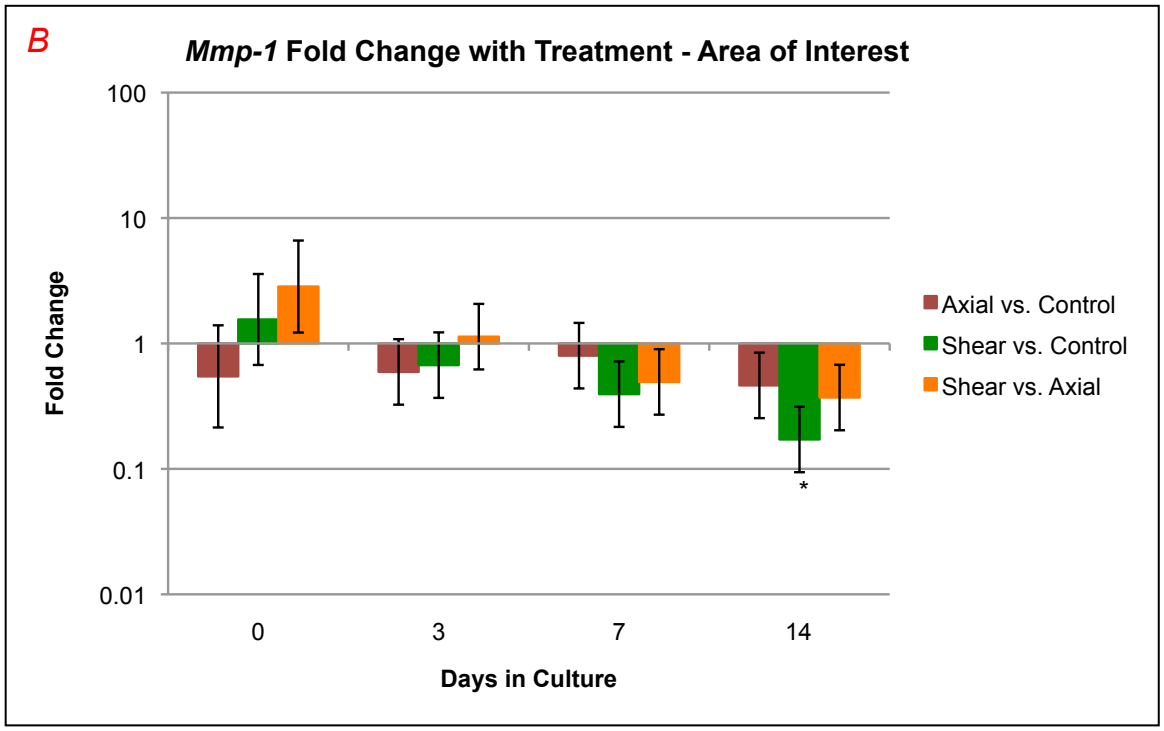
B
Mmp-1 Fold Change with Treatment - Area of Interest
100
10
1
0.1
0.01
Fold Change
0
3
7
14
Days in Culture
Axial vs. Control
Shear vs. Control
Shear vs. Axial

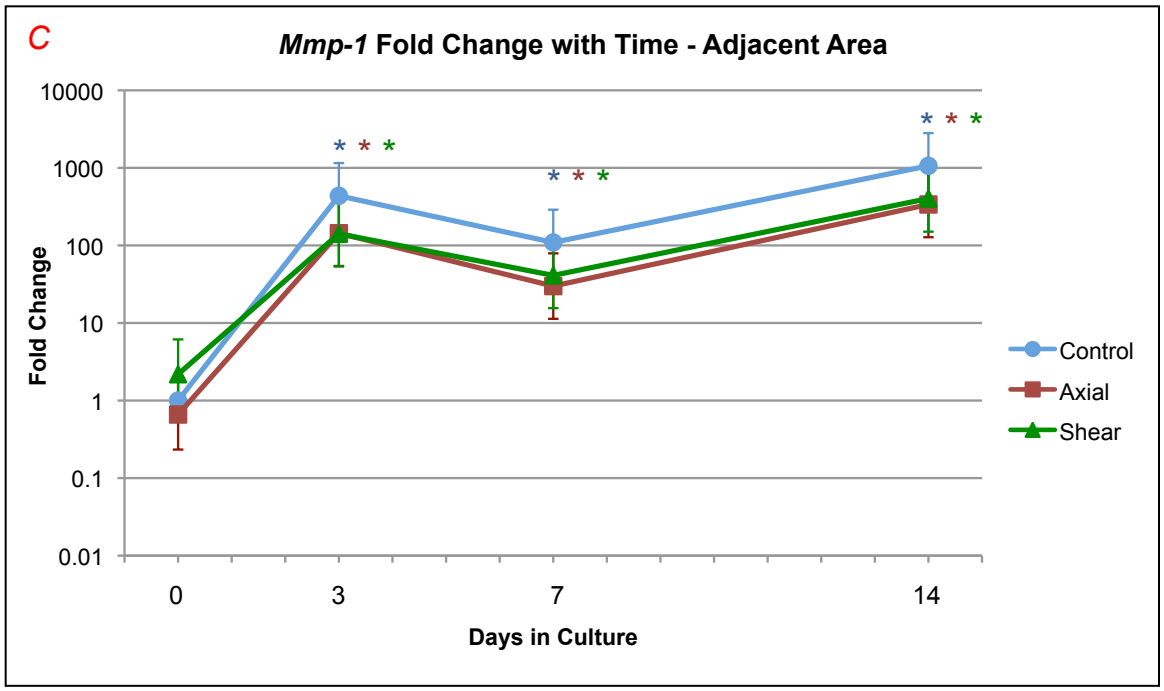
C
Mmp-1 Fold Change with Time - Adjacent Area
10000
1000
100
10
1
0.1
0.01
Fold Change
0
3
7
14
Days in Culture
Control
Axial
Shear

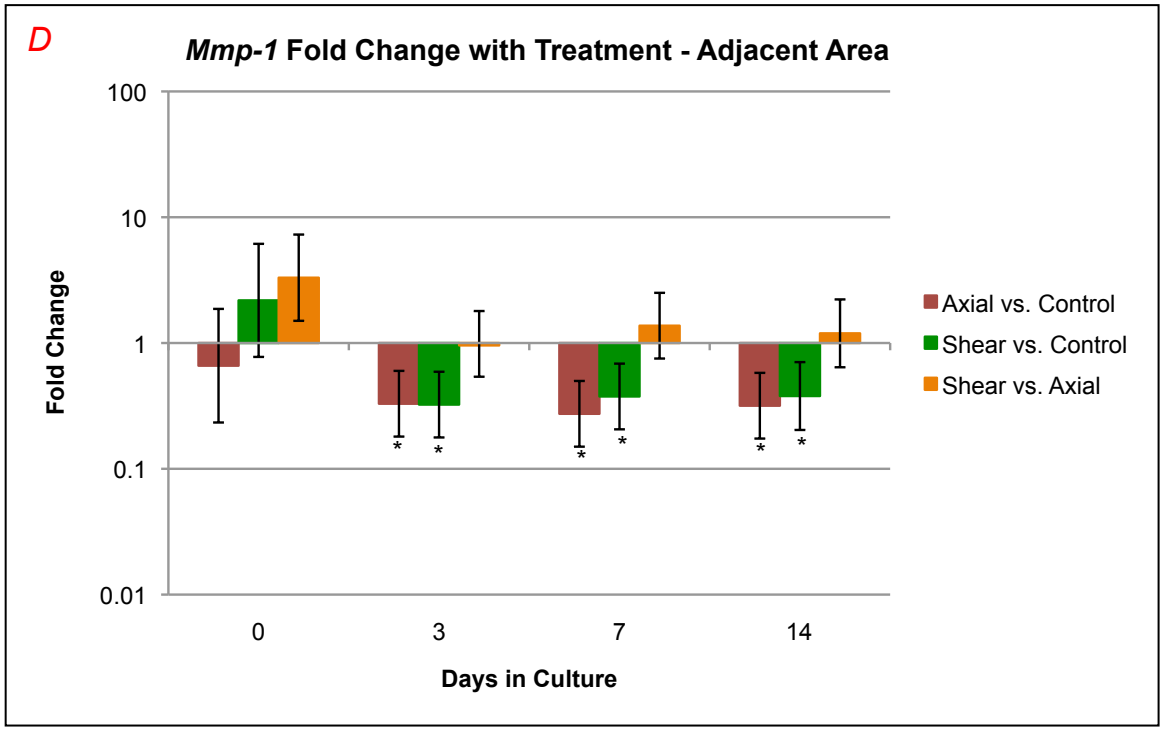
D
Mmp-1 Fold Change with Treatment - Adjacent Area
100
10
1
0.1
0.01
Fold Change
0
3
7
14
Days in Culture
Axial vs. Control
Shear vs. Control
Shear vs. Axial

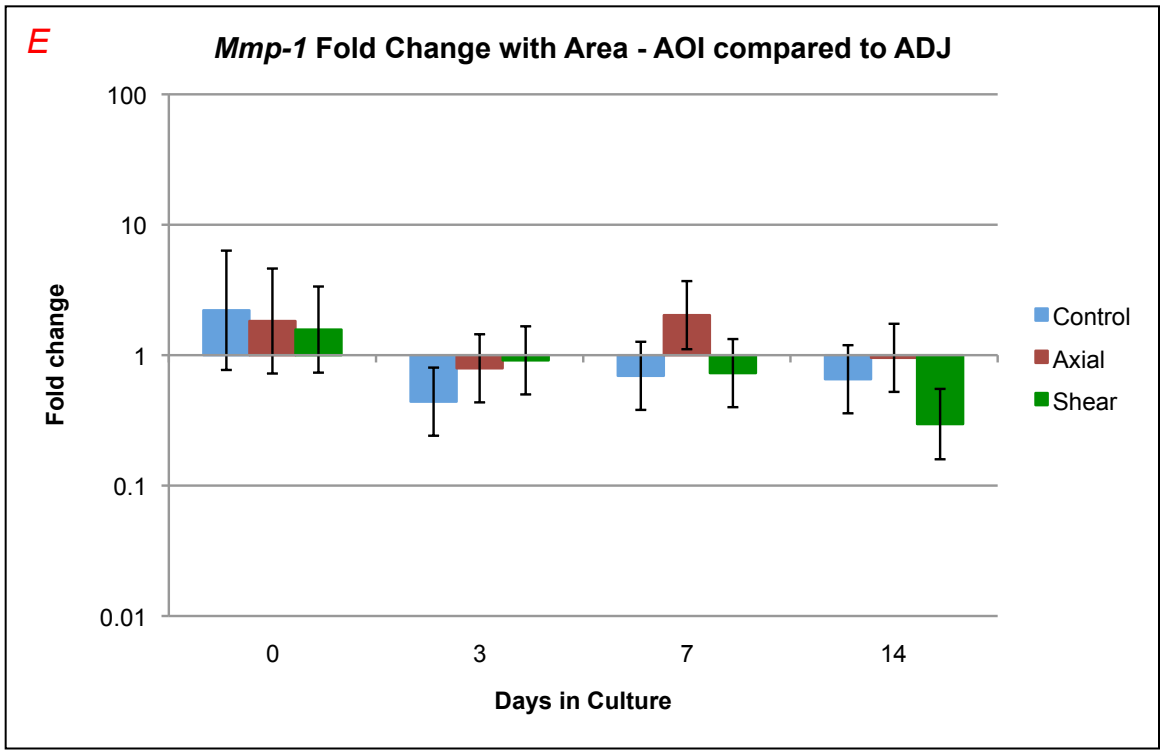
E
Mmp-1 Fold Change with Area - AOI compared to ADJ
100
10
1
0.1
0.01
Fold change
0
3
7
14
Days in Culture
Control
Axial
Shear

4.10.2 Results for *Mmp-3*

Fold Change With Time:

Mmp-3 expression was compared to day 0 control for each treatment. The expression rose from day 0 to 3 for all specimens and then dropped from day 3 to 7 through 14. The changes of control specimens were significant at day 3, 7 and 14 (FC = 86.85, $q < 0.01$; FC = 34.36, $q < 0.01$; FC = 314.70, $q < 0.01$). The changes for axial AOI specimens were also significant at day 3, 7 and 14 (FC = 32.82, $q < 0.01$; FC = 27.45, $q < 0.01$; FC = 145.70, $q < 0.01$). For the shear AOI specimens compared to control, the changes were significant at all time points, day 0, 3, 7 and 14 (FC = 3.69, $q = 0.10$; FC = 53.18, $q < 0.01$; FC = 38.93, $q < 0.01$; FC = 6.15, $q < 0.01$). For the ADJ specimens compared to day 0 control ADJ, the changes were significant at day 3, 7 and 14 for control (FC = 88.11, $q < 0.01$; FC = 6.71, $q = 0.01$; FC = 21.04, $q < 0.01$), axial (FC = 35.49, $q < 0.01$; FC = 4.12, $q = 0.06$; FC = 10.12, $q < 0.01$), and shear (FC = 41.07, $q < 0.01$; FC = 3.11, $q = 0.15$; FC = 14.57, $q < 0.01$).

Fold Change With Treatment:

AOI specimens were compared between treatments at all time points and shear was higher than control and axial expression at both day 0 and 7. Shear AOI compared to control was significantly higher at day 0 and 7 (FC = 3.69, $q = 0.10$; FC = 3.58, $q = 0.10$) and lower at day 14 (FC = 0.26, $q = 0.10$). For the ADJ specimens compared between treatments, axial expression was lower than control at all time points, and shear was significantly higher than axial at day 0 (FC = 4.05, $q = 0.20$).

Fold Change With Area:

AOI compared to ADJ for each treatment showed little discernible changes at day 0 or 3, however, at day 7 shear AOI expression was significantly higher than ADJ (FC = 6.07, q = 0.05), and at day 14 it was lower (FC = 0.20, q = 0.05).

Figures 4.15 A-E. Graphs of *mmp-3* by time point, treatment and area.

Figure 4.15 A. *Mmp-3*: Fold change with time – area of interest. Fold change is shown on the vertical axis as a log scale. Fold changes less than one indicate lowered expression and fold changes greater than one indicate higher expression. Days in culture are shown on the horizontal axis. At each time point, day 0 control specimens are used as the reference or comparative value. Error bars (standard error) are shown for each fold change. Control specimens are plotted in blue, axial are plotted in red, and shear are plotted in green. Significant differences in expression relative to day 0 control are indicated at each time point with an asterisk (*) in the respective color of the plotted treatment.

Figure 4.15 B. *Mmp-3*: Fold change with treatment – area of interest. Fold change is shown on the vertical axis as a log scale, and days in culture is shown on the horizontal axis. The treatments are compared to each other at each time point. Axial vs. Control is shown in red, Shear vs. Control is shown in green, and Shear vs. Axial is shown in orange. Error bars (standard error) for fold change are depicted, and significant differences for the respective comparison are indicated with an asterisk (*).

Figure 4.15 C. *Mmp-3*: Fold change with time – adjacent area. Fold change is shown on the vertical axis as a log scale. Fold changes less than one indicate lowered expression and fold changes greater than one indicate higher expression. Days in culture are shown on the horizontal axis. At each time point, day 0 control specimens are used as the reference or comparative value. Error bars (standard error) are shown for each fold change. Control specimens are plotted in blue, axial are plotted in red, and shear are plotted in green. Significant differences in expression relative to day 0 control are indicated at each time point with an asterisk (*) in the respective color of the plotted treatment.

Figure 4.15 D. *Mmp-3*: Fold change with treatment – adjacent area. Fold change is shown on the vertical axis as a log scale, and days in culture is shown on the horizontal axis. The treatments are compared to each other at each time point. Axial vs. Control is shown in red, Shear vs. Control is shown in green, and Shear vs. Axial is shown in orange. Error bars (standard error) for fold change are depicted, and significant differences for the respective comparison are indicated with an asterisk (*).

Figure 4.15 E. *Mmp-3*: Fold change with area – area of interest vs. adjacent area. Fold change is shown on the vertical axis as a log scale, and days in culture is shown on the horizontal axis. The treatment areas are compared to each other within each treatment at each time point. Control is shown in blue, axial is shown in red, and shear is shown in green. Error bars (standard error) for fold change are depicted, and significant differences for the respective comparison are indicated with an asterisk (*).

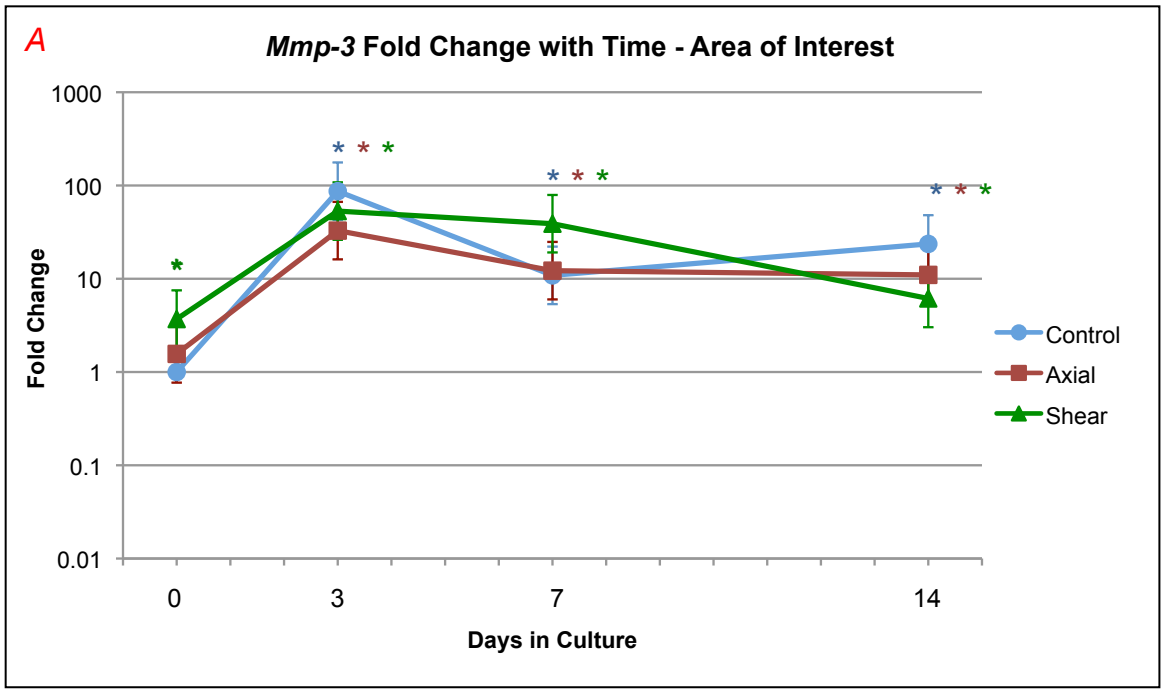
A
Mmp-3 Fold Change with Time - Area of Interest
1000
100
10
1
0.1
0.01
Fold Change
0
3
7
14
Days in Culture
Control
Axial
Shear

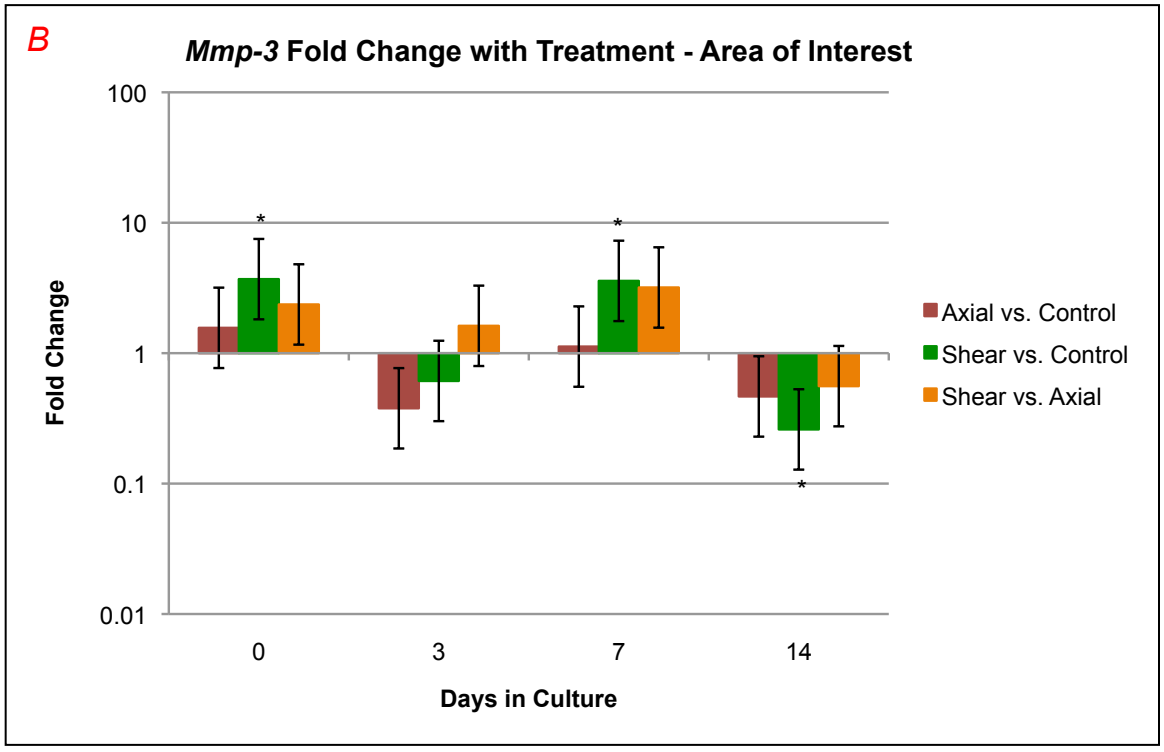
B
Mmp-3 Fold Change with Treatment - Area of Interest
100
10
1
0.1
0.01
Fold Change
0
3
7
14
Days in Culture
Axial vs. Control
Shear vs. Control
Shear vs. Axial

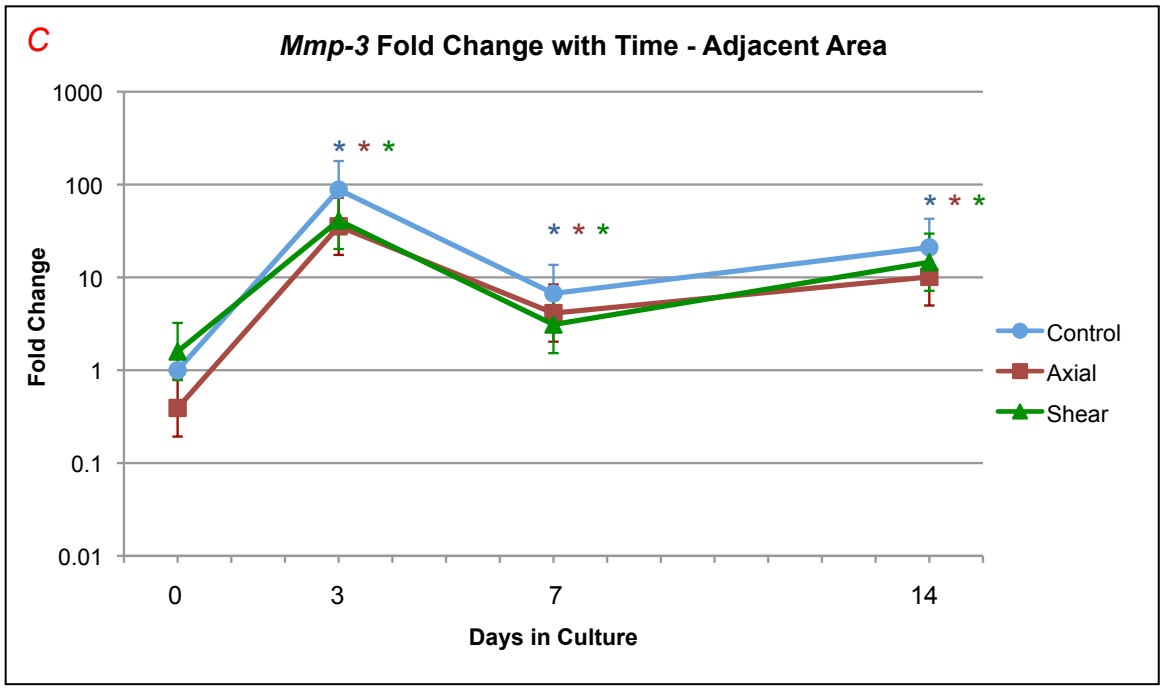
C
Mmp-3 Fold Change with Time - Adjacent Area
1000
100
10
1
0.1
0.01
Fold Change
* * *
* * *
* * *
0
3
7
14
Days in Culture
Control
Axial
Shear

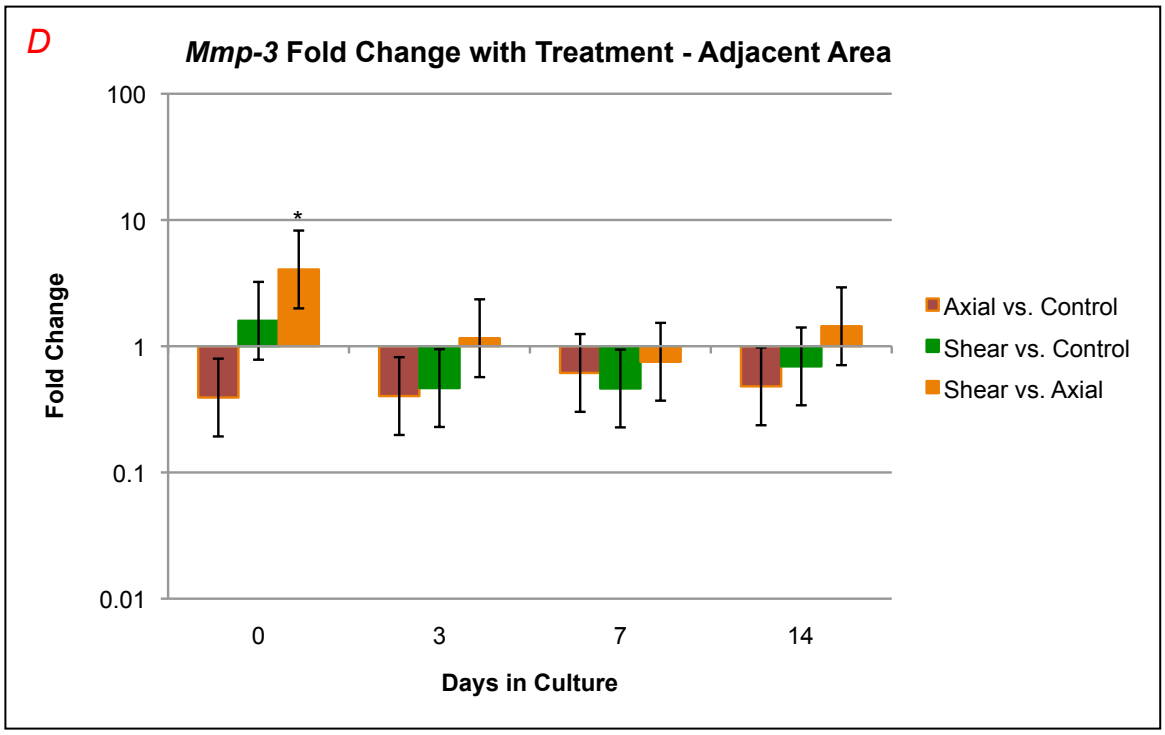
D
Mmp-3 Fold Change with Treatment - Adjacent Area
100
10
1
0.1
0.01
Fold Change
*
0
3
7
14
Days in Culture
Axial vs. Control
Shear vs. Control
Shear vs. Axial

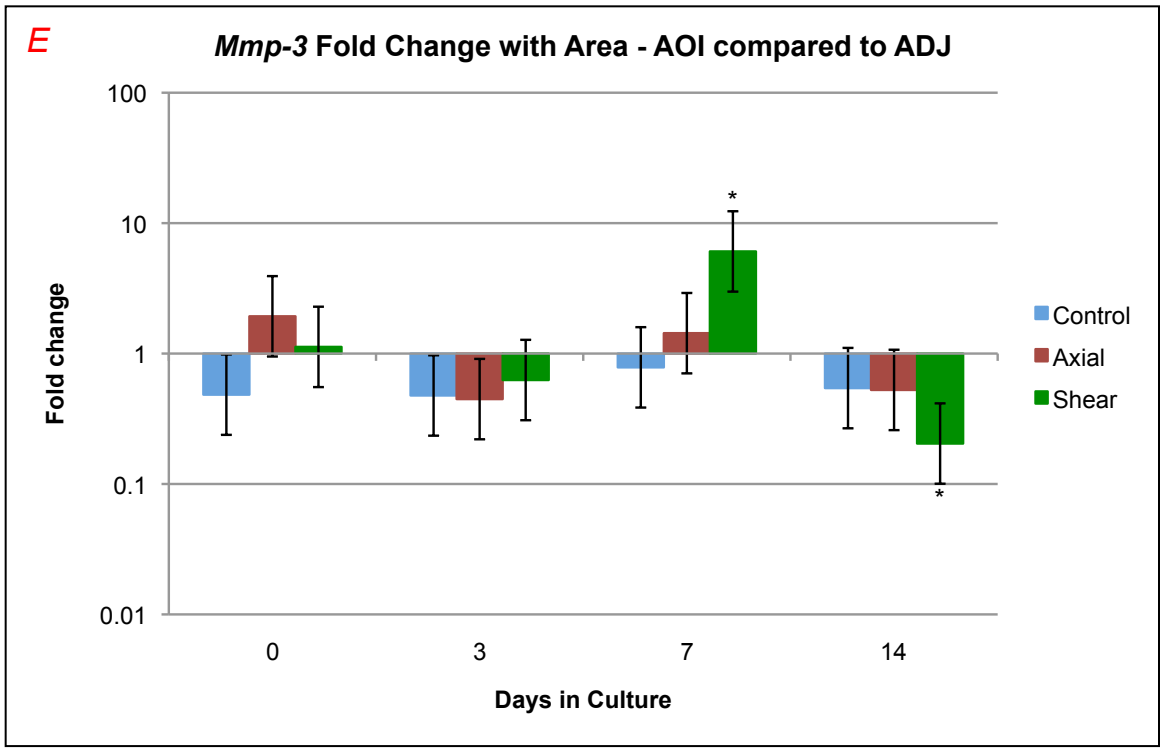
E
Mmp-3 Fold Change with Area - AOI compared to ADJ
100
10
1
0.1
0.01
Fold change
0
3
7
14
Days in Culture
Control
Axial
Shear
*
*

4.10.3 Results for *Mmp-13*

Fold Change With Time:

For both AOI and ADJ specimens compared to their respective day 0 control specimens, all treatments showed a rise in expression from day 0 to 3, and then a slow increase for the remaining time points. For the AOI specimens, the changes were significant at day 3, 7 and 14 for control (FC = 132.41, $q < 0.01$; FC = 120.85, $q < 0.01$; FC = 2239.62, $q < 0.01$) and shear (FC = 471.31, $q < 0.01$; FC = 65.09, $q < 0.01$; FC = 428.95, $q < 0.01$). For axial these changes were significant at day 0 as well as day 3, 7 and 14 (FC = 3.09, $q = 0.18$; FC = 85.61, $q < 0.01$; FC = 251.88, $q < 0.01$; FC = 605.94, $q < 0.01$). The ADJ specimens showed the same trends of higher expression over time with significantly higher expression at day 3, 7 and 14 in axial (FC = 7.68, $q = 0.01$; FC = 248.61, $q < 0.01$; FC = 575.54, $q < 0.01$; FC = 1266.00, $q < 0.01$) and shear (FC = 4.54, $q = 0.10$; FC = 509.62, $q < 0.01$; FC = 202.22, $q < 0.01$; FC = 2994.44, $q < 0.01$). Control ADJ specimens showed higher expression at day 3, 7 and 14 (FC = 321.34, $q < 0.01$; FC = 342.94, $q < 0.01$; FC = 1435.13, $q < 0.01$).

Fold Change With Treatment:

Treatments were compared at each time, and shear was higher than axial and control expression for AOI specimens at day 3, but lower at day 7 and 14. Axial AOI expression was higher than control at day 0 (FC = 3.09, $q = 0.18$) and lower at day 14 (FC = 0.27, $q = 0.18$). Shear was higher than control at day 3 for AOI specimens (FC = 3.56, $q = 0.12$) and lower at day 14 (FC = 0.19, $q = 0.05$). Shear was higher than axial at day 3 (FC =

5.51, q = 0.05) but lower at day 0 and 7 (FC = 0.34, q = 0.14; FC = 0.26, q = 0.08). When ADJ specimens were compared between treatments, there were no observable trends, and the only significant changes occurred at day 0 for axial vs. control (FC = 7.68, q = 0.10), and for shear vs. control (FC = 4.54, q = 0.10).

Fold Change With Area:

There were no consistent trends for AOI compared to ADJ specimens within the treatments, and the only significant difference was for control AOI vs. ADJ at day 14 (FC = 4.03, q = 0.14).

Figures 4.16 A-E. Graphs of *mmp-13* by time point, treatment and area.

Figure 4.16 A. *Mmp-13*: Fold change with time – area of interest. Fold change is shown on the vertical axis as a log scale. Fold changes less than one indicate lowered expression and fold changes greater than one indicate higher expression. Days in culture are shown on the horizontal axis. At each time point, day 0 control specimens are used as the reference or comparative value. Error bars (standard error) are shown for each fold change. Control specimens are plotted in blue, axial are plotted in red, and shear are plotted in green. Significant differences in expression relative to day 0 control are indicated at each time point with an asterisk (*) in the respective color of the plotted treatment.

Figure 4.16 B. *Mmp-13*: Fold change with treatment – area of interest. Fold change is shown on the vertical axis as a log scale, and days in culture is shown on the horizontal axis. The treatments are compared to each other at each time point. Axial vs. Control is shown in red, Shear vs. Control is shown in green, and Shear vs. Axial is shown in orange. Error bars (standard error) for fold change are depicted, and significant differences for the respective comparison are indicated with an asterisk (*).

Figure 4.16 C. *Mmp-13*: Fold change with time – adjacent area. Fold change is shown on the vertical axis as a log scale. Fold changes less than one indicate lowered expression and fold changes greater than one indicate higher expression. Days in culture are shown on the horizontal axis. At each time point, day 0 control specimens are used as the reference or comparative value. Error bars (standard error) are shown for each fold change. Control specimens are plotted in blue, axial are plotted in red, and shear are plotted in green. Significant differences in expression relative to day 0 control are indicated at each time point with an asterisk (*) in the respective color of the plotted treatment.

Figure 4.16 D. *Mmp-13*: Fold change with treatment – adjacent area. Fold change is shown on the vertical axis as a log scale, and days in culture is shown on the horizontal axis. The treatments are compared to each other at each time point. Axial vs. Control is shown in red, Shear vs. Control is shown in green, and Shear vs. Axial is shown in orange. Error bars (standard error) for fold change are depicted, and significant differences for the respective comparison are indicated with an asterisk (*).

Figure 4.16 E. *Mmp-13*: Fold change with area – area of interest vs. adjacent area. Fold change is shown on the vertical axis as a log scale, and days in culture is shown on the horizontal axis. The treatment areas are compared to each other within each treatment at each time point. Control is shown in blue, axial is shown in red, and shear is shown in green. Error bars (standard error) for fold change are depicted, and significant differences for the respective comparison are indicated with an asterisk (*).

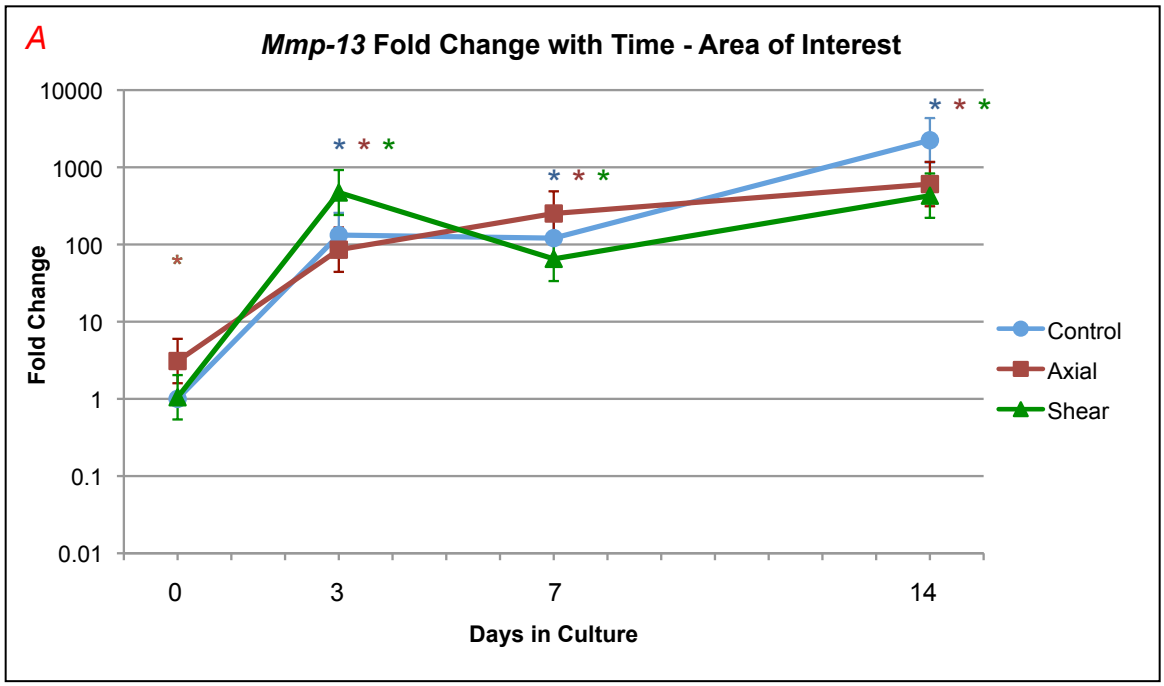
A
Mmp-13 Fold Change with Time - Area of Interest
10000
1000
100
10
1
0.1
0.01
Fold Change
0
3
7
14
Days in Culture
Control
Axial
Shear

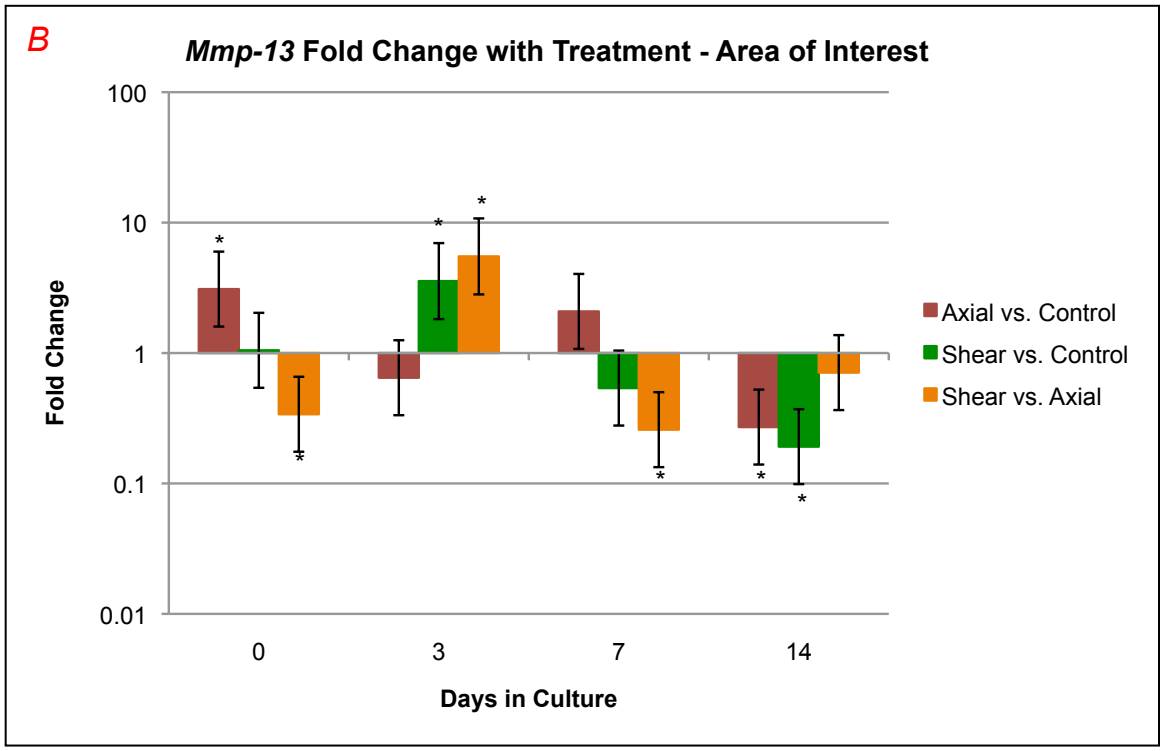
B
Mmp-13 Fold Change with Treatment - Area of Interest
100
10
1
0.1
0.01
Fold Change
0
3
7
14
Days in Culture
Axial vs. Control
Shear vs. Control
Shear vs. Axial

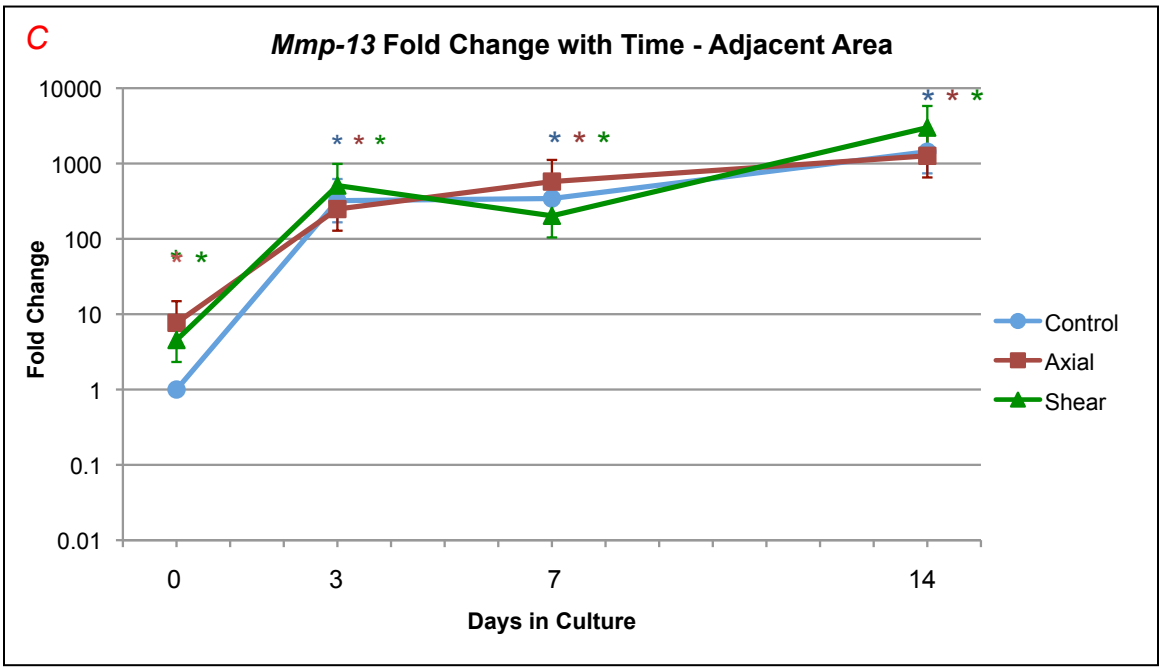
C
Mmp-13 Fold Change with Time - Adjacent Area
10000
1000
100
10
1
0.1
0.01
Fold Change
0
3
7
14
Days in Culture
Control
Axial
Shear

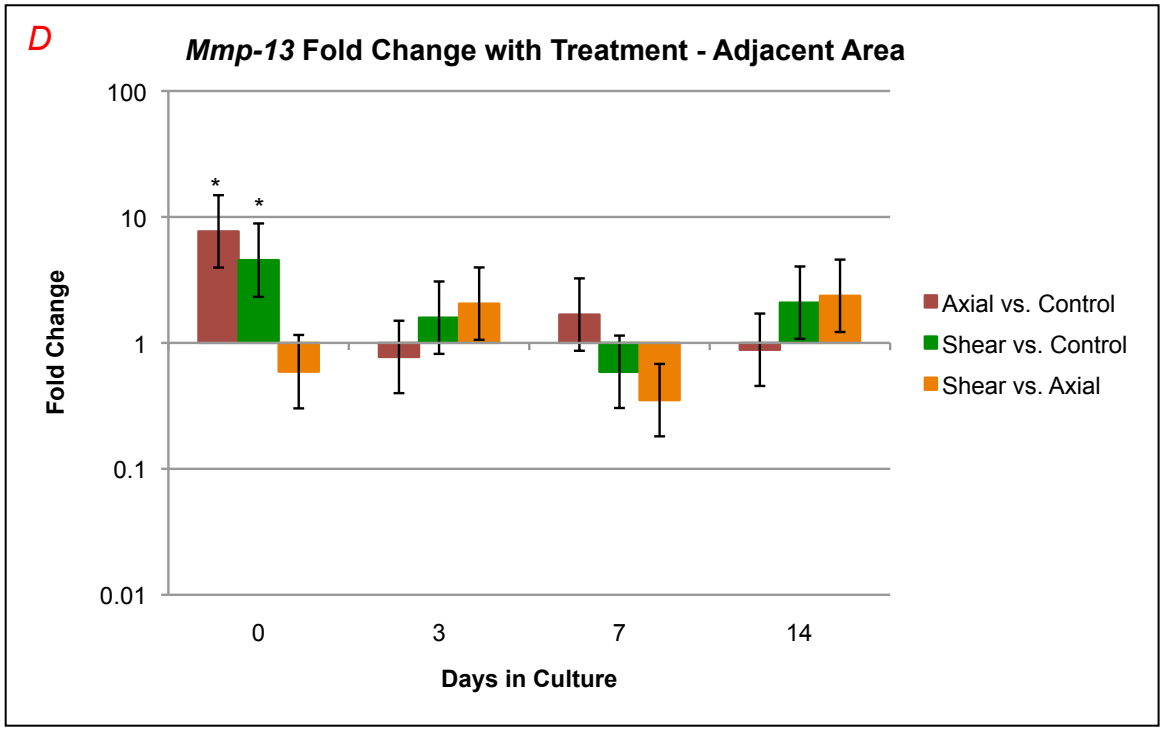
D
Mmp-13 Fold Change with Treatment - Adjacent Area
100
10
1
0.1
0.01
Fold Change
0
3
7
14
Days in Culture
Axial vs. Control
Shear vs. Control
Shear vs. Axial

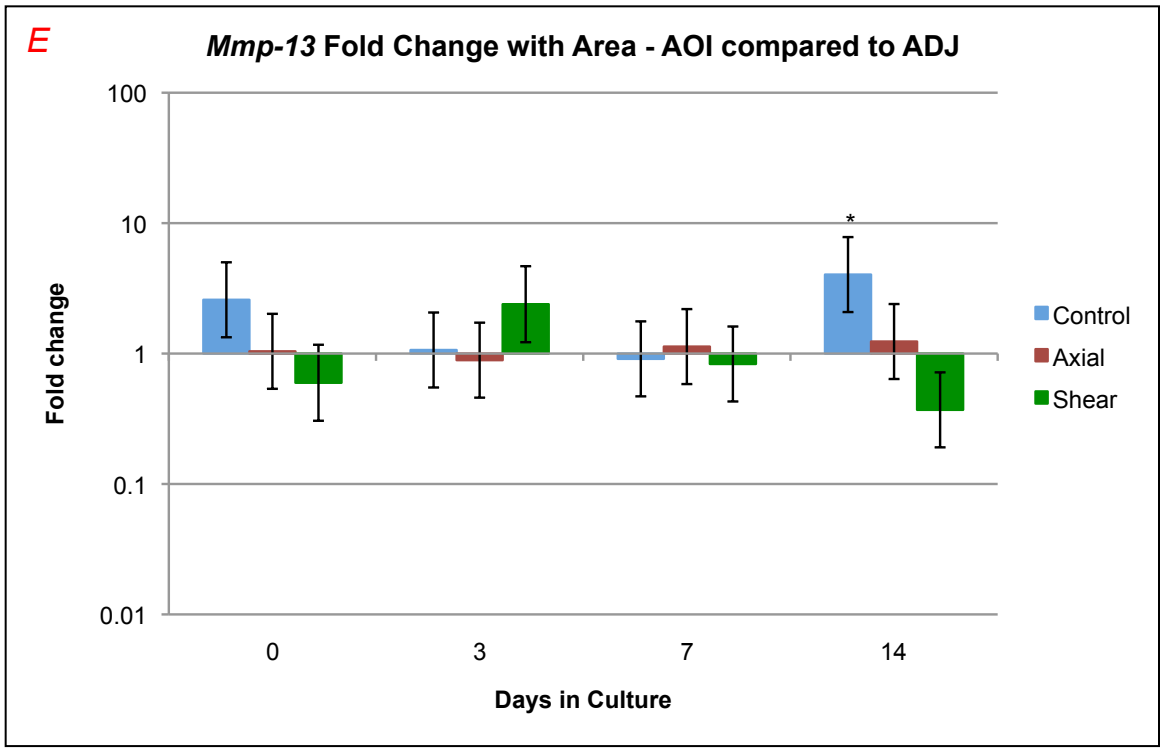
E
Mmp-13 Fold Change with Area - AOI compared to ADJ
100
10
1
0.1
0.01
Fold change
*
0
3
7
14
Days in Culture
Control
Axial
Shear

4.10.4 Results for *Timp-1*

Fold Change With Time:

For *timp-1* expression the AOI and ADJ specimens, when compared to day 0 control, showed a rise from day 0 to 3 and a relatively constant expression for the remaining time points. The higher expression of the AOI specimens was significant at day 3, 7 and 14 for control (FC = 3.22, $q < 0.01$; FC = 3.46, $q < 0.01$; FC = 2.95, $q < 0.01$), axial (FC = 3.13, $q < 0.01$; FC = 4.15, $q < 0.01$; FC = 2.00, $q = 0.05$), and shear (FC = 2.75, $q < 0.01$; FC = 3.32, $q < 0.01$; FC = 2.47, $q = 0.01$). The changes in ADJ specimens compared to day 0 control were also significant at day 3, 7 and 14 for control (FC = 3.87, $q < 0.01$; FC = 3.47, $q < 0.01$; FC = 3.72, $q < 0.01$), axial (FC = 2.61, $q = 0.01$; FC = 3.14, $q < 0.01$; FC = 1.71, $q < 0.14$), and shear (FC = 2.00, $q = 0.05$; FC = 3.12, $q < 0.01$; FC = 3.44; $q < 0.01$).

Fold Change With Treatment:

There were no consistent trends for a comparison of treatments at each time point for either AOI or ADJ specimens. There were no significant differences for AOI specimens. For ADJ specimens, shear was lower than control expression at day 3 (FC = 0.52, $q = 0.18$), axial was lower than control at day 14 (FC = 0.46, $q = 0.07$), and shear was higher than axial at day 14 (FC = 2.01, $q = 0.13$).

Fold Change With Area:

There were no significant differences or trends for a comparison of *timp-1* expression in AOI vs ADJ specimens.

Figures 4.17 A-E. Graphs of *timp-1* by time point, treatment and area.

Figure 4.17 A. *Timp-1*: Fold change with time – area of interest. Fold change is shown on the vertical axis as a log scale. Fold changes less than one indicate lowered expression and fold changes greater than one indicate higher expression. Days in culture are shown on the horizontal axis. At each time point, day 0 control specimens are used as the reference or comparative value. Error bars (standard error) are shown for each fold change. Control specimens are plotted in blue, axial are plotted in red, and shear are plotted in green. Significant differences in expression relative to day 0 control are indicated at each time point with an asterisk (*) in the respective color of the plotted treatment.

Figure 4.17 B. *Timp-1*: Fold change with treatment – area of interest. Fold change is shown on the vertical axis as a log scale, and days in culture is shown on the horizontal axis. The treatments are compared to each other at each time point. Axial vs. Control is shown in red, Shear vs. Control is shown in green, and Shear vs. Axial is shown in orange. Error bars (standard error) for fold change are depicted, and significant differences for the respective comparison are indicated with an asterisk (*).

Figure 4.17 C. *Timp-1*: Fold change with time – adjacent area. Fold change is shown on the vertical axis as a log scale. Fold changes less than one indicate lowered expression and fold changes greater than one indicate higher expression. Days in culture are shown on the horizontal axis. At each time point, day 0 control specimens are used as the reference or comparative value. Error bars (standard error) are shown for each fold change. Control specimens are plotted in blue, axial are plotted in red, and shear are plotted in green. Significant differences in expression relative to day 0 control are indicated at each time point with an asterisk (*) in the respective color of the plotted treatment.

Figure 4.17 D. *Timp-1*: Fold change with treatment – adjacent area. Fold change is shown on the vertical axis as a log scale, and days in culture is shown on the horizontal axis. The treatments are compared to each other at each time point. Axial vs. Control is shown in red, Shear vs. Control is shown in green, and Shear vs. Axial is shown in orange. Error bars (standard error) for fold change are depicted, and significant differences for the respective comparison are indicated with an asterisk (*).

Figure 4.17 E. *Timp-1*: Fold change with area – area of interest vs. adjacent area. Fold change is shown on the vertical axis as a log scale, and days in culture is shown on the horizontal axis. The treatment areas are compared to each other within each treatment at each time point. Control is shown in blue, axial is shown in red, and shear is shown in green. Error bars (standard error) for fold change are depicted, and significant differences for the respective comparison are indicated with an asterisk (*).

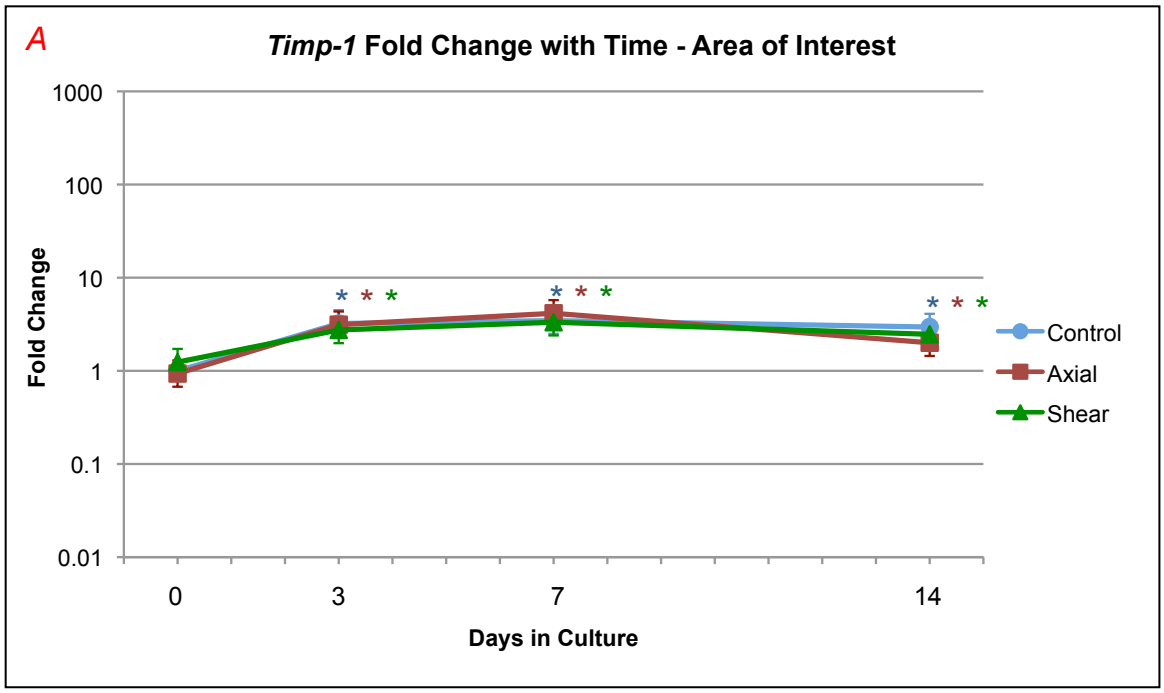
A
Timp-1 Fold Change with Time - Area of Interest
1000
100
10
1
0.1
0.01
Fold Change
0
3
7
14
Days in Culture
Control
Axial
Shear

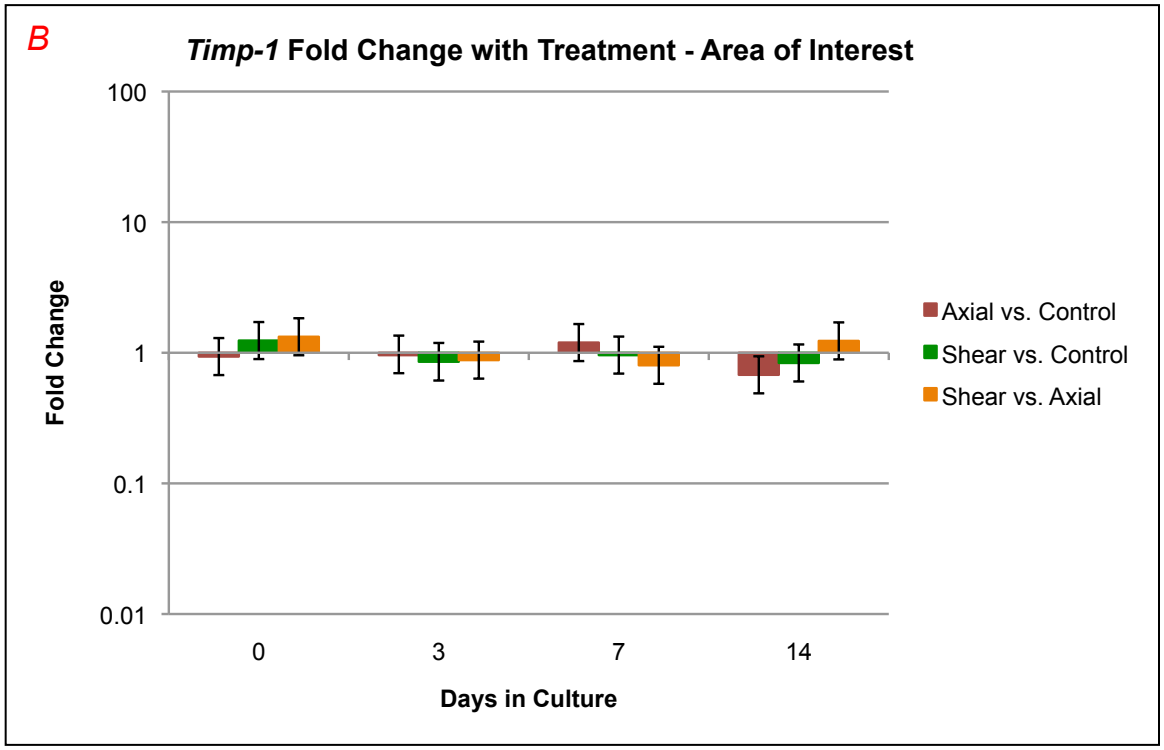
B
Timp-1 Fold Change with Treatment - Area of Interest
100
10
1
0.1
0.01
Fold Change
0
3
7
14
Days in Culture
Axial vs. Control
Shear vs. Control
Shear vs. Axial

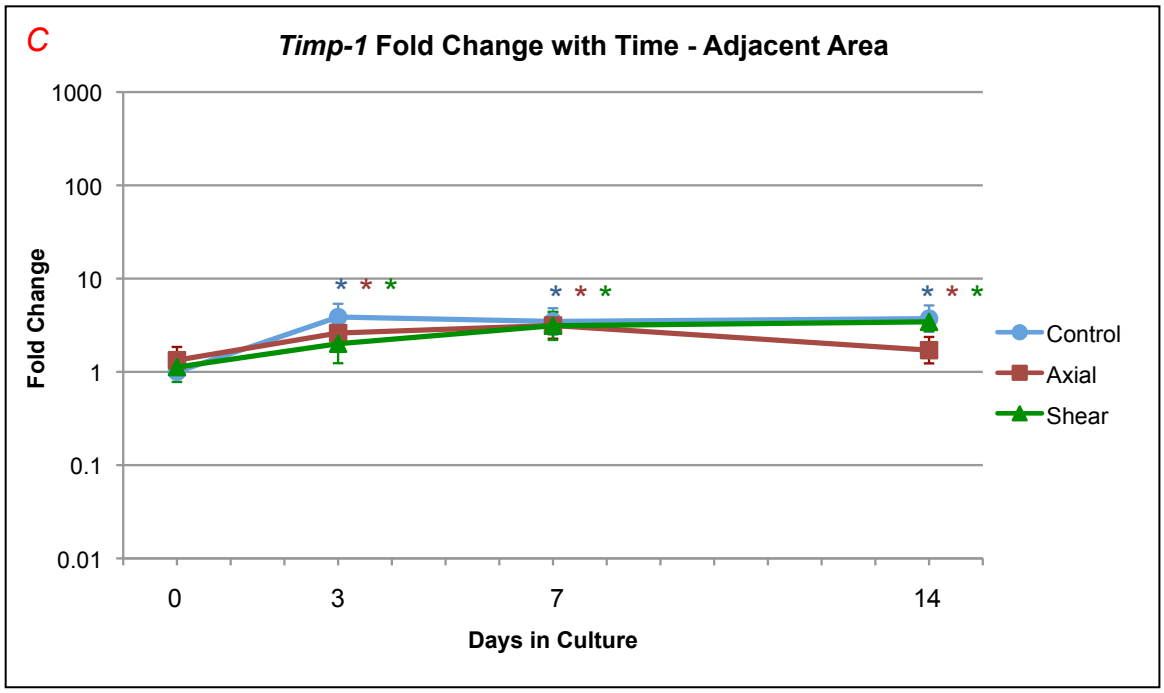
C
Timp-1 Fold Change with Time - Adjacent Area
1000
100
10
1
0.1
0.01
Fold Change
0
3
7
14
Days in Culture
Control
Axial
Shear

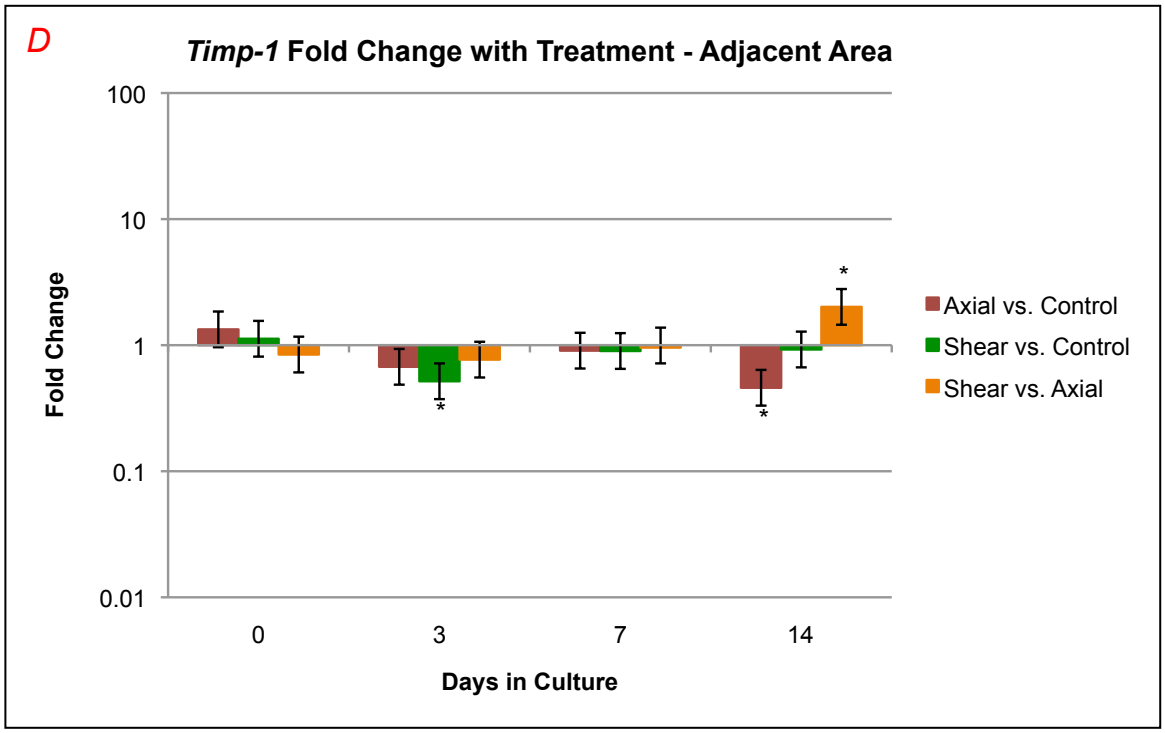
D
Timp-1 Fold Change with Treatment - Adjacent Area
100
10
1
0.1
0.01
Fold Change
0
3
7
14
Days in Culture
Axial vs. Control
Shear vs. Control
Shear vs. Axial

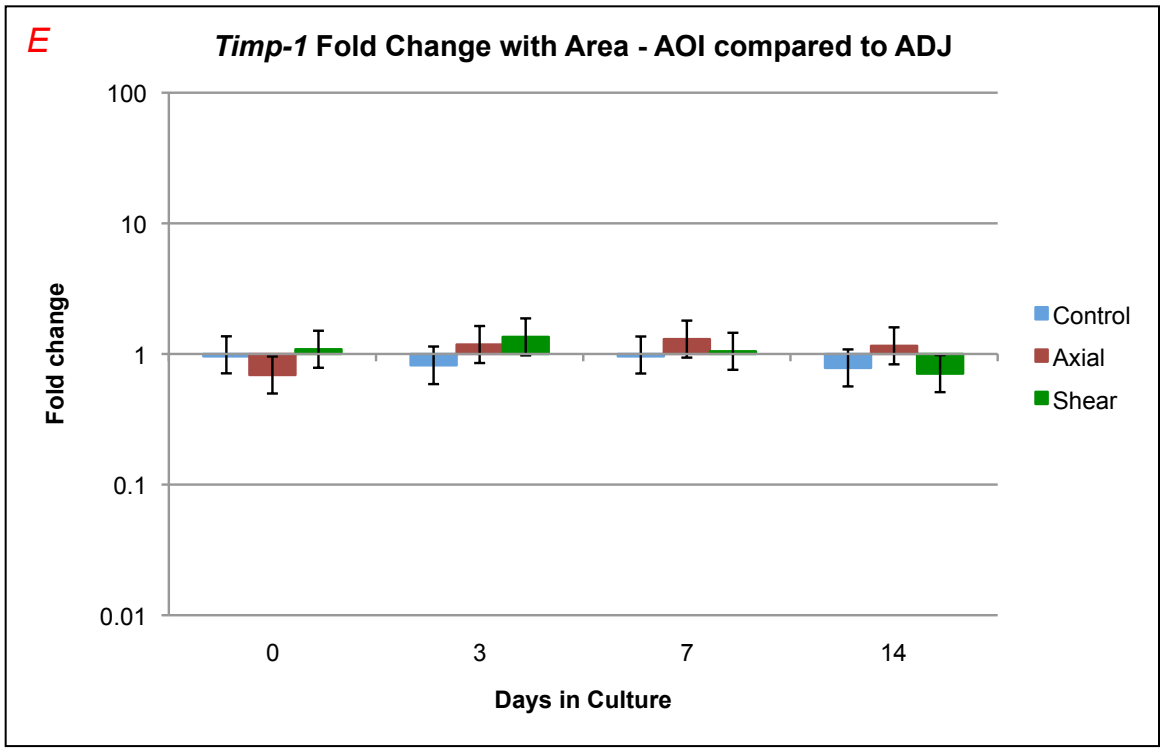
E
Timp-1 Fold Change with Area - AOI compared to ADJ
100
10
1
0.1
0.01
Fold change
0
3
7
14
Days in Culture
Control
Axial
Shear

4.10.5 Results for *Timp-2*

Fold Change With Time:

The AOI specimens for each treatment compared to control day 0 showed relatively little change in expression over time, though expression was lower. The changes were significant for control at day 3 and 14 (FC = 0.30, q = 0.01; FC = 0.42, q = 0.42); axial at day 0, 3 and 14 (FC = 0.37, q = 0.05; FC = 0.17, q < 0.01; FC = 0.28, q < 0.01); and shear at day 3, 7 and 14 (FC = 0.39, q = 0.05; FC = 0.44, q = 0.05; FC = 0.44; q = 0.05). The ADJ specimens also showed lower expression but was relatively constant compared to day 0 control. The changes were significant for control specimens at day 7 and 14 (FC = 0.50, q = 0.12; FC = 0.34, q = 0.02). The expression was significantly lower in ADJ specimens at day 3, 7 and 14 for both axial (FC = 0.43, q = 0.10; FC = 0.52, q = 0.30; FC = 0.46, q = 0.10) and shear (FC = 0.35, q = 0.03; FC = 0.40, q = 0.04; FC = 0.54, q = 0.16).

Fold Change With Treatment:

With a comparison of treatments, in the AOI specimens, axial had generally lower expression than control, and shear was generally higher than axial expression. Axial AOI expression was significantly lower than control at day 0 (FC = 0.37, q = 0.05), and shear expression was higher than axial at both day 0 and 3 (FC = 2.63, q = 0.06; FC = 2.36, q = 0.06). There were no noticeable trends or significant differences in a comparison of ADJ specimens between treatments.

Fold Change With Area:

When AOI were compared to ADJ specimens in each treatment, axial AOI specimens had significantly lower expression than ADJ at day 0 and 3 (FC = 0.41, q = 0.05; FC = 0.37, q = 0.05); and control ADJ was significantly lower than AOI at day 3 (FC = 0.42, q = 0.12).

Figures 4.18 A-E. Graphs of *timp-2* by time point, treatment and area.

Figure 4.18 A. *Timp-2*: Fold change with time – area of interest. Fold change is shown on the vertical axis as a log scale. Fold changes less than one indicate lowered expression and fold changes greater than one indicate higher expression. Days in culture are shown on the horizontal axis. At each time point, day 0 control specimens are used as the reference or comparative value. Error bars (standard error) are shown for each fold change. Control specimens are plotted in blue, axial are plotted in red, and shear are plotted in green. Significant differences in expression relative to day 0 control are indicated at each time point with an asterisk (*) in the respective color of the plotted treatment.

Figure 4.18 B. *Timp-2*: Fold change with treatment – area of interest. Fold change is shown on the vertical axis as a log scale, and days in culture is shown on the horizontal axis. The treatments are compared to each other at each time point. Axial vs. Control is shown in red, Shear vs. Control is shown in green, and Shear vs. Axial is shown in orange. Error bars (standard error) for fold change are depicted, and significant differences for the respective comparison are indicated with an asterisk (*).

Figure 4.18 C. *Timp-2*: Fold change with time – adjacent area. Fold change is shown on the vertical axis as a log scale. Fold changes less than one indicate lowered expression and fold changes greater than one indicate higher expression. Days in culture are shown on the horizontal axis. At each time point, day 0 control specimens are used as the reference or comparative value. Error bars (standard error) are shown for each fold change. Control specimens are plotted in blue, axial are plotted in red, and shear are plotted in green. Significant differences in expression relative to day 0 control are indicated at each time point with an asterisk (*) in the respective color of the plotted treatment.

Figure 4.18 D. *Timp-2*: Fold change with treatment – adjacent area. Fold change is shown on the vertical axis as a log scale, and days in culture is shown on the horizontal axis. The treatments are compared to each other at each time point. Axial vs. Control is shown in red, Shear vs. Control is shown in green, and Shear vs. Axial is shown in orange. Error bars (standard error) for fold change are depicted, and significant differences for the respective comparison are indicated with an asterisk (*).

Figure 4.18 E. *Timp-2*: Fold change with area – area of interest vs. adjacent area. Fold change is shown on the vertical axis as a log scale, and days in culture is shown on the horizontal axis. The treatment areas are compared to each other within each treatment at each time point. Control is shown in blue, axial is shown in red, and shear is shown in green. Error bars (standard error) for fold change are depicted, and significant differences for the respective comparison are indicated with an asterisk (*).

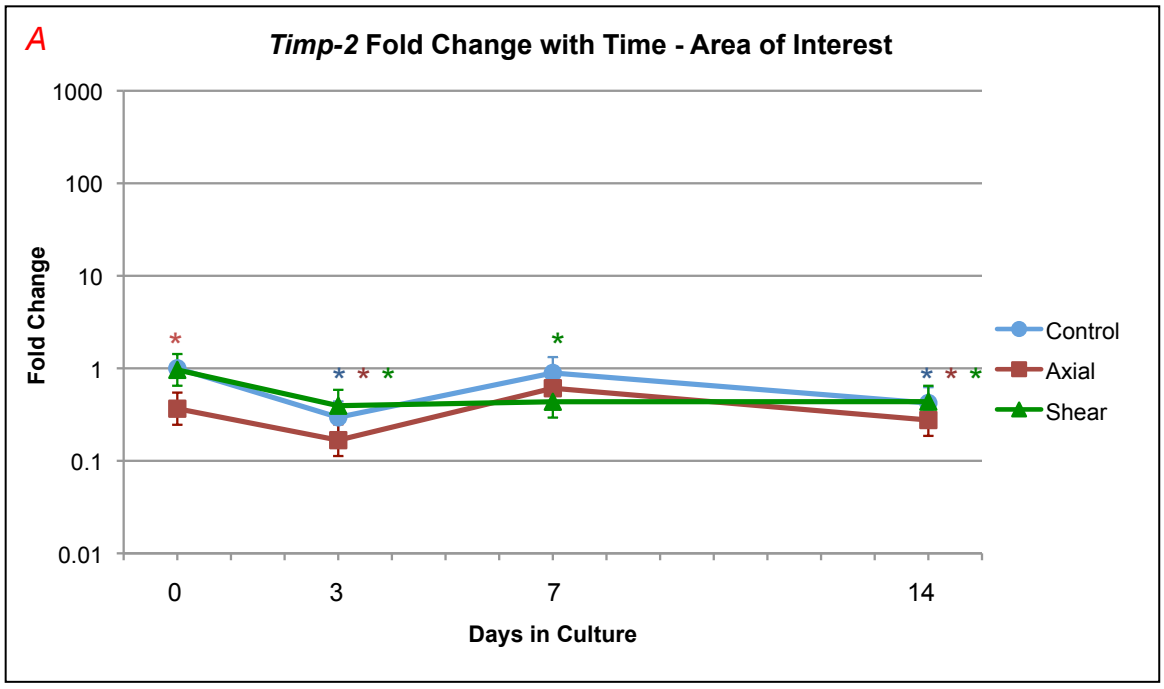
A
Timp-2 Fold Change with Time - Area of Interest
1000
100
10
1
0.1
0.01
Fold Change
0
3
7
14
Days in Culture
Control
Axial
Shear

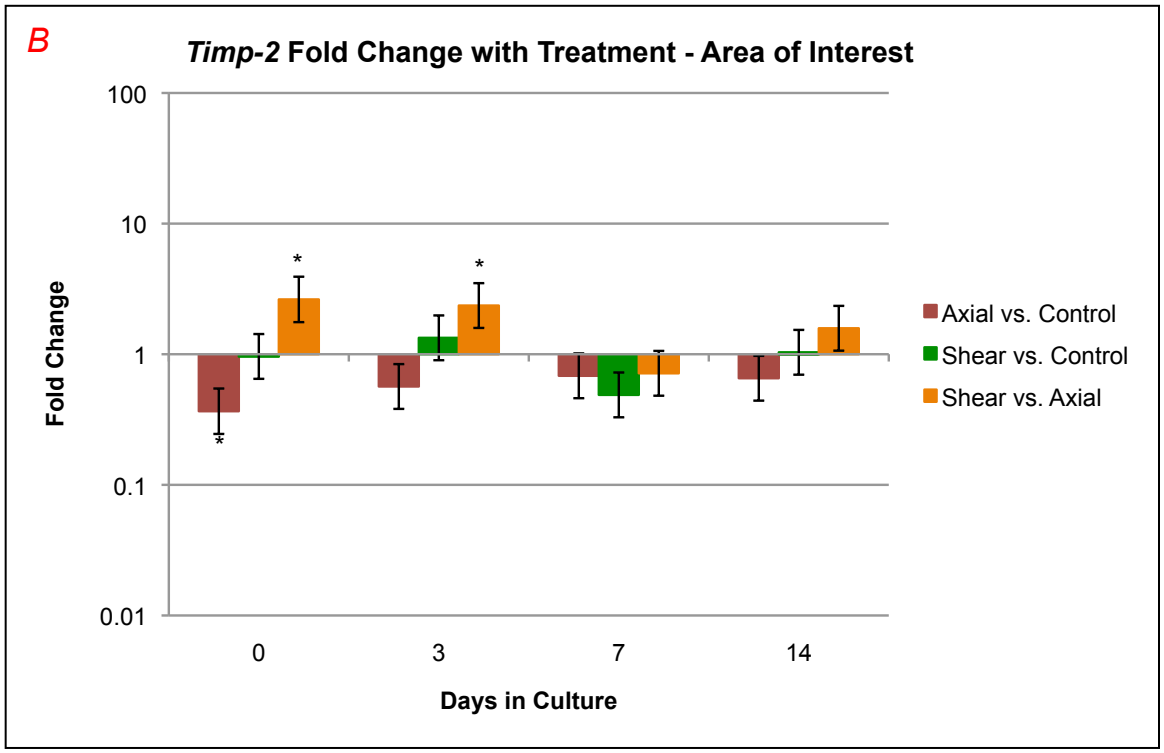
B
Timp-2 Fold Change with Treatment - Area of Interest
100
10
1
0.1
0.01
Fold Change
0
3
7
14
Days in Culture
Axial vs. Control
Shear vs. Control
Shear vs. Axial

C

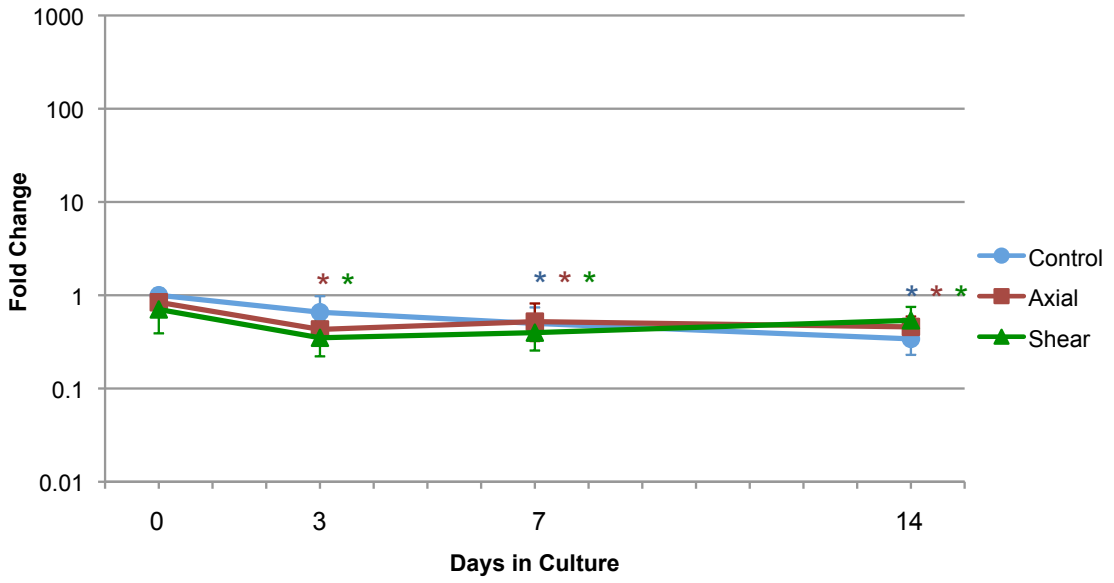
Timp-2 Fold Change with Time - Adjacent Area
1000
100
10
1
0.1
0.01
Fold Change
* *
* * *
* * *
0
3
7
14
Days in Culture
Control
Axial
Shear

D

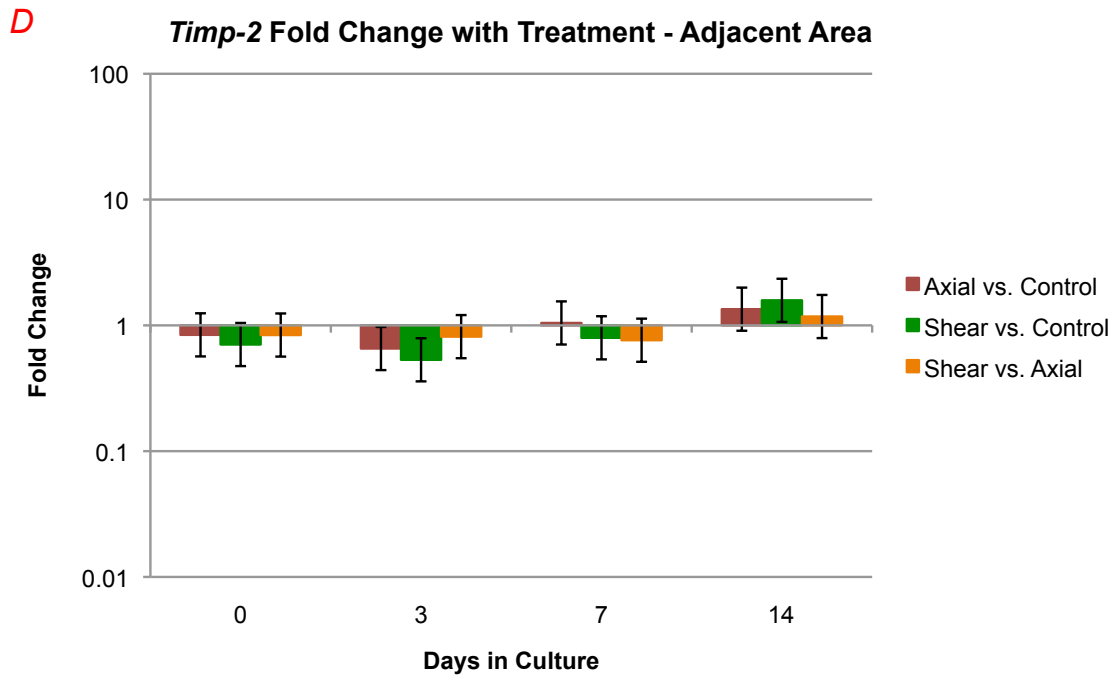
Timp-2 Fold Change with Treatment - Adjacent Area
100
10
1
0.1
0.01
Fold Change
0
3
7
14
Days in Culture
Axial vs. Control
Shear vs. Control
Shear vs. Axial

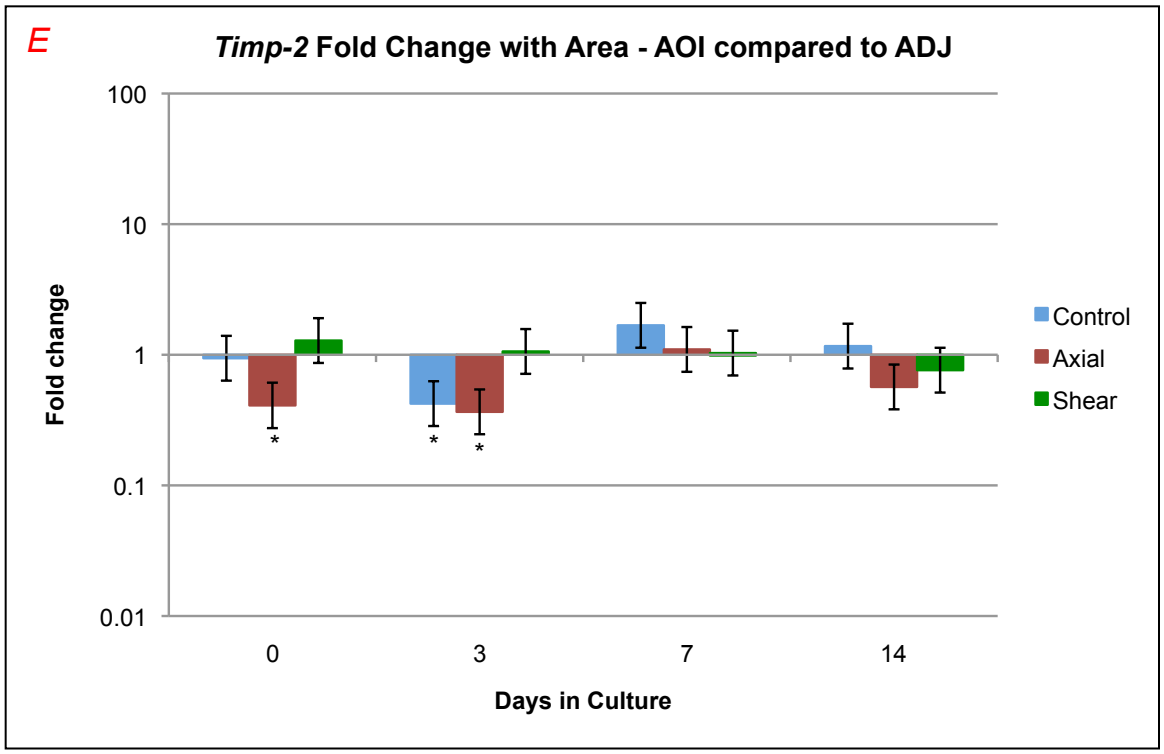
E
Timp-2 Fold Change with Area - AOI compared to ADJ
100
10
1
0.1
0.01
Fold change
0
3
7
14
Days in Culture
Control
Axial
Shear
*
*
*

4.10.6 Results for *Adamts-5*

Fold Change With Time:

For *adamts-5* changes over time, the AOI expression rose in all treatments for the day 3 time point, and then tapered in the control and shear, but rose in axial from day 7 to 14. The only significant change, however, was for axial AOI compared to day 0 control at day 0 (FC = 0.26, q = 0.12). The ADJ expression showed the same general rise to day 3, but then tapered to day 7 and rose again to day 14 for all treatments. Control changes were significantly higher than day 0 control at day 3 and 14 (FC = 7.52, $q < 0.01$; FC = 6.63, $q < 0.01$). Axial expression was significantly higher in ADJ specimens at day 3, 7 and 14 (FC = 8.42, $q < 0.01$; FC = 3.06, q = 0.08; FC = 6.76, $q < 0.01$). Finally, shear expression was higher in ADJ specimens compared to day 0 control at day 0, 3, 7 and 14 (FC = 3.45, q = 0.15; FC = 7.43, $q < 0.01$; FC = 2.17, q = 0.20; FC = 5.93, q = 0.01).

Fold Change With Treatment:

For comparison of treatments at each time point, axial AOI specimens had lower expression than control at day 0 (FC = 0.26, q = 0.12). Shear expression was lower than control at day 7 and 14 (FC = 0.37, q = 0.18; FC = 0.22, q = 0.04), and shear was lower than axial at day 14 (FC = 0.14, q = 0.01). In comparing ADJ specimens there were no noticeable trends, though shear expression was higher than control at day 0 (FC = 3.45, q = 0.15).

Fold Change With Area:

There were no trends across time points, but shear was significantly lower in AOI specimens compared to ADJ at day 14 (FC = 0.19, q = 0.03). In control specimens, AOI expression was higher than ADJ at day 0 and 7 (FC = 3.07, q = 0.14; FC = 3.80, q = 0.11).

Figures 4.19 A-E. Graphs of *adamts-5* by time point, treatment and area.

Figure 4.19 A. *Adamts-5*: Fold change with time – area of interest. Fold change is shown on the vertical axis as a log scale. Fold changes less than one indicate lowered expression and fold changes greater than one indicate higher expression. Days in culture are shown on the horizontal axis. At each time point, day 0 control specimens are used as the reference or comparative value. Error bars (standard error) are shown for each fold change. Control specimens are plotted in blue, axial are plotted in red, and shear are plotted in green. Significant differences in expression relative to day 0 control are indicated at each time point with an asterisk (*) in the respective color of the plotted treatment.

Figure 4.19 B. *Adamts-5*: Fold change with treatment – area of interest. Fold change is shown on the vertical axis as a log scale, and days in culture is shown on the horizontal axis. The treatments are compared to each other at each time point. Axial vs. Control is shown in red, Shear vs. Control is shown in green, and Shear vs. Axial is shown in orange. Error bars (standard error) for fold change are depicted, and significant differences for the respective comparison are indicated with an asterisk (*).

Figure 4.19 C. *Adamts-5*: Fold change with time – adjacent area. Fold change is shown on the vertical axis as a log scale. Fold changes less than one indicate lowered expression and fold changes greater than one indicate higher expression. Days in culture are shown on the horizontal axis. At each time point, day 0 control specimens are used as the reference or comparative value. Error bars (standard error) are shown for each fold change. Control specimens are plotted in blue, axial are plotted in red, and shear are plotted in green. Significant differences in expression relative to day 0 control are indicated at each time point with an asterisk (*) in the respective color of the plotted treatment.

Figure 4.19 D. *Adamts-5*: Fold change with treatment – adjacent area. Fold change is shown on the vertical axis as a log scale, and days in culture is shown on the horizontal axis. The treatments are compared to each other at each time point. Axial vs. Control is shown in red, Shear vs. Control is shown in green, and Shear vs. Axial is shown in orange. Error bars (standard error) for fold change are depicted, and significant differences for the respective comparison are indicated with an asterisk (*).

Figure 4.19 E. *Adamts-5*: Fold change with area – area of interest vs. adjacent area. Fold change is shown on the vertical axis as a log scale, and days in culture is shown on the horizontal axis. The treatment areas are compared to each other within each treatment at each time point. Control is shown in blue, axial is shown in red, and shear is shown in green. Error bars (standard error) for fold change are depicted, and significant differences for the respective comparison are indicated with an asterisk (*).

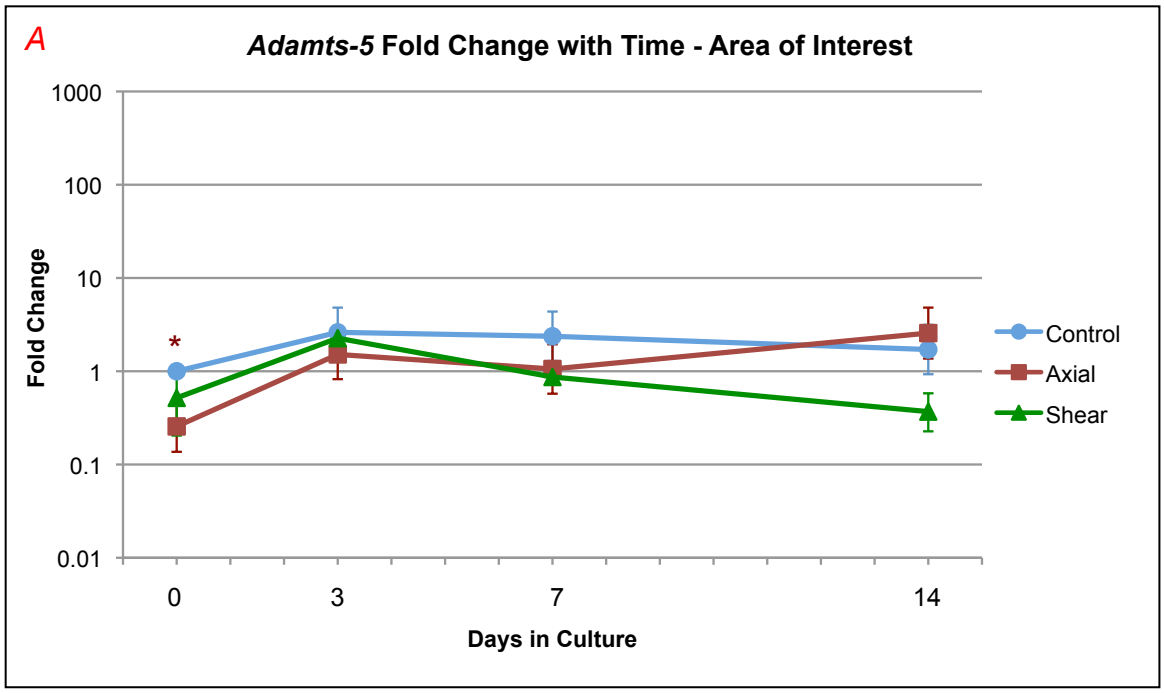
A
Adamts-5 Fold Change with Time - Area of Interest
1000
100
10
1
0.1
0.01
Fold Change
*
0
3
7
14
Days in Culture
Control
Axial
Shear

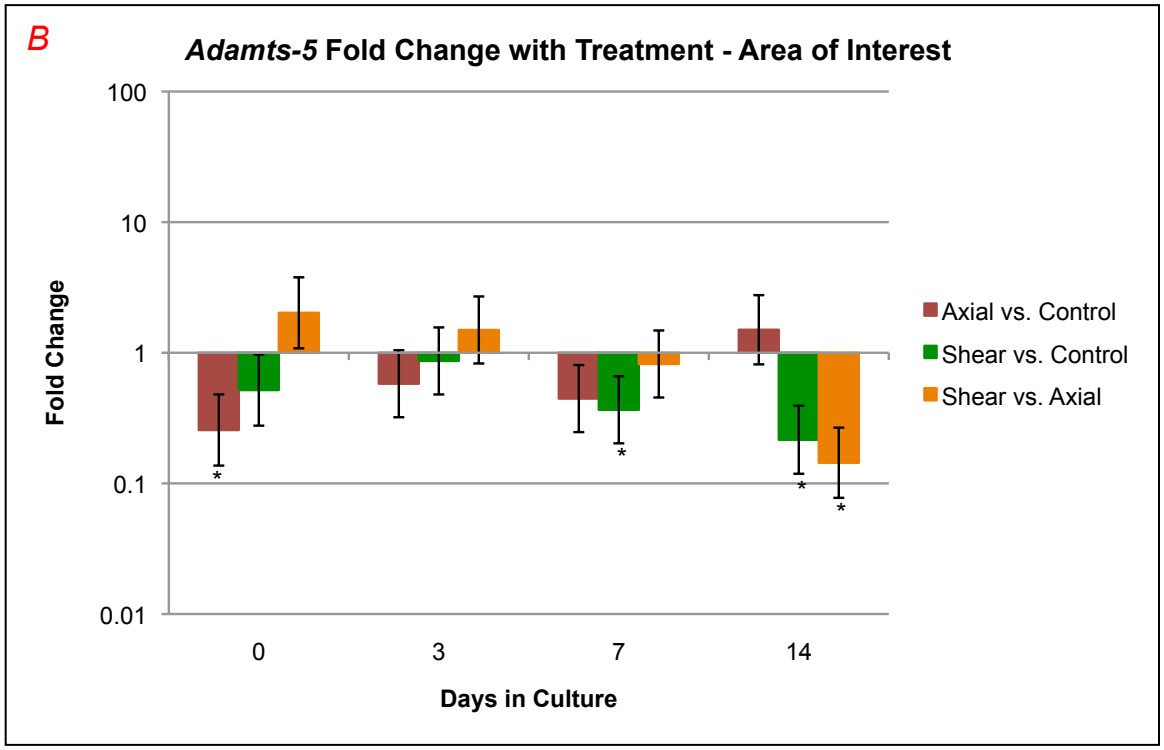
B
Adamts-5 Fold Change with Treatment - Area of Interest
100
10
1
0.1
0.01
Fold Change
*
*
*
*
0
3
7
14
Days in Culture
Axial vs. Control
Shear vs. Control
Shear vs. Axial

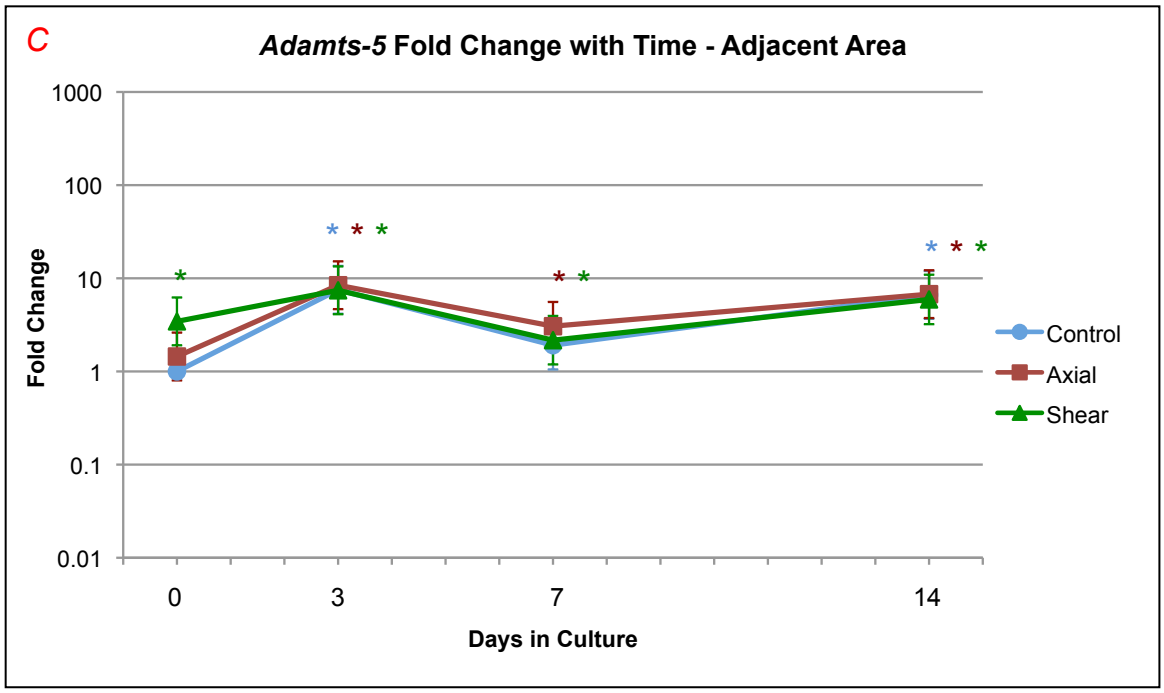
C
Adamts-5 Fold Change with Time - Adjacent Area
1000
100
10
1
0.1
0.01
Fold Change
0
3
7
14
Days in Culture
Control
Axial
Shear

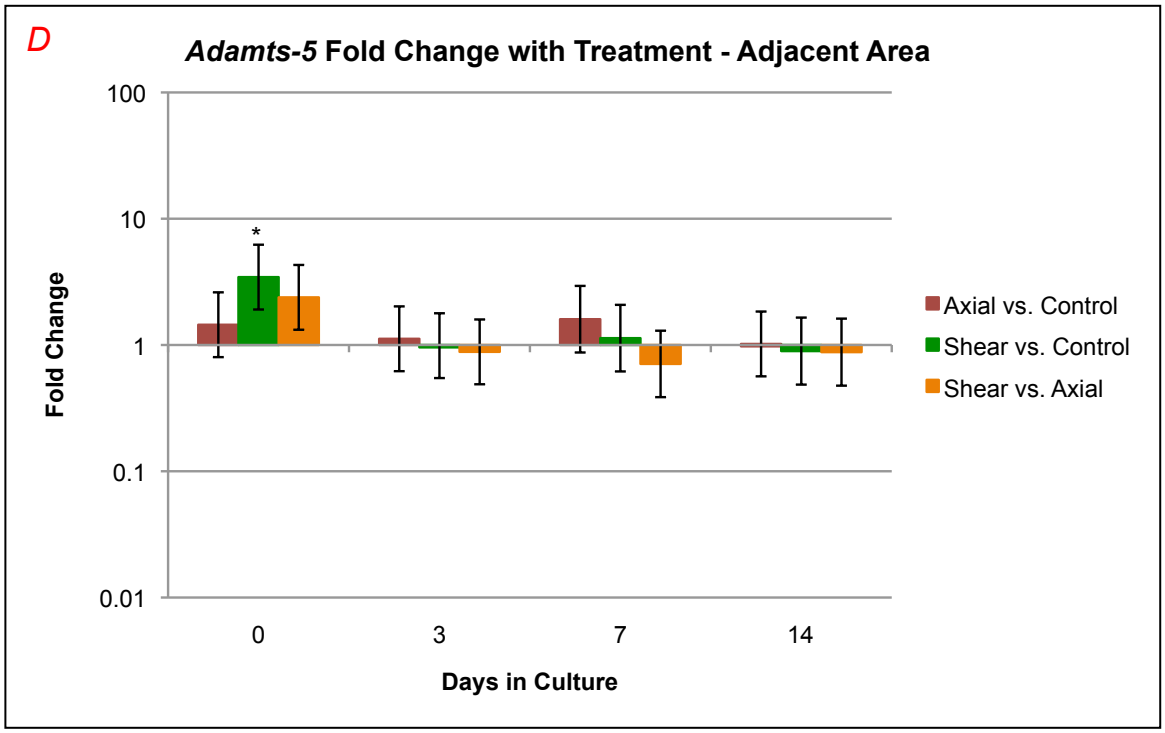
D
Adamts-5 Fold Change with Treatment - Adjacent Area
100
10
1
0.1
0.01
Fold Change
0
3
7
14
Days in Culture
Axial vs. Control
Shear vs. Control
Shear vs. Axial

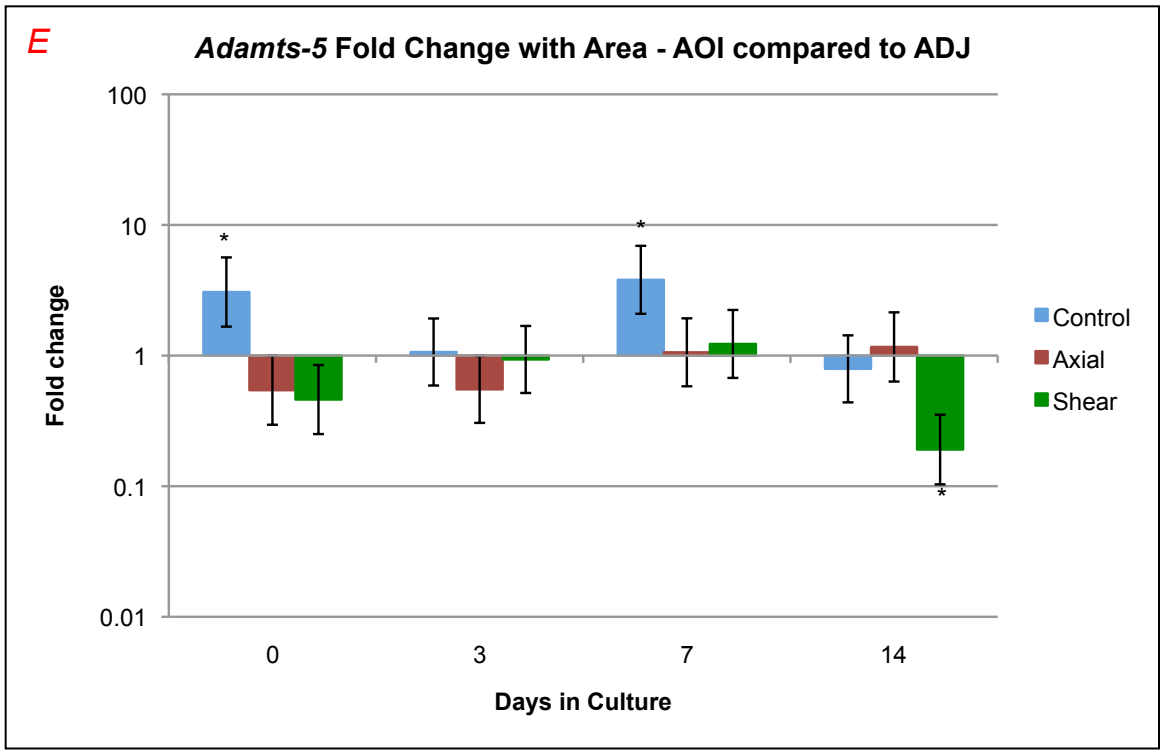
E
Adamts-5 Fold Change with Area - AOI compared to ADJ
100
10
1
0.1
0.01
Fold change
0
3
7
14
Days in Culture
Control
Axial
Shear
*
*
*

Summary of Degradative Enzymes and Inhibitors:

Mmp-1, *3*, and *13* all showed increased expression over time in all treatments. When treatments were compared at each time point, *mmp-1* was lower in shear AOI compared to axial at day 14 and in axial ADJ compared to control, and in shear ADJ compared to control. *Mmp-13* showed higher expression at day 0 in axial AOI compared to control, but by day 3, *mmp-13* was more highly expressed in shear AOI compared to both control and axial. *Timp-1* expression was higher across the time points, while *timp-2* had lower expression in axial AOI compared to control, but had higher expression in shear AOI compared to axial at day 0 and 3. *Adamts-5* was lower in axial AOI compared to control at day 0, and lower in both shear vs. control, and shear vs. axial at the later time points.

Figures 4.20 A-F. Graphs of degradative enzymes and inhibitor genes by time point for AOI and ADJ. Fold change with time – area of interest. Fold change is shown on the vertical axis as a log scale. Fold changes less than one indicate lowered expression and fold changes greater than one indicate higher expression. Days in culture are shown on the horizontal axis. At each time point, day 0 control specimens are used as the reference or comparative value. Graph A and B show changes over time for the control specimens, graph C and D show changes over time for the axial specimens, and graph E and F show changes over time for the shear specimens.

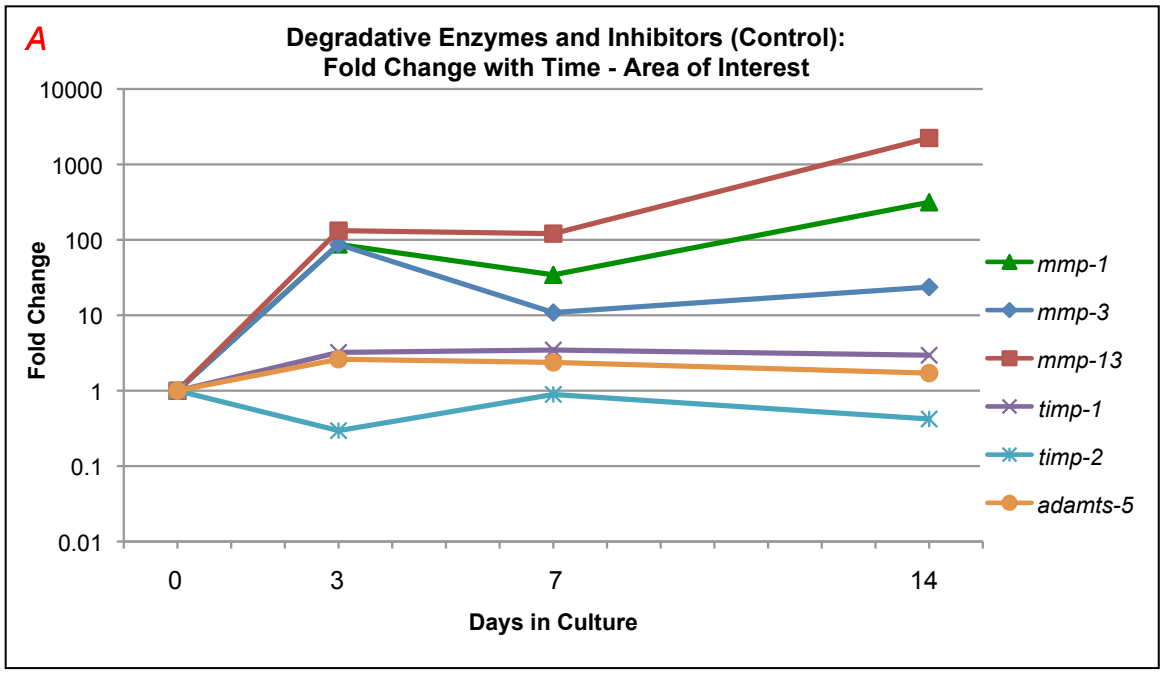
A
Degradative Enzymes and Inhibitors (Control):
Fold Change with Time - Area of Interest
10000
1000
100
10
1
0.1
0.01
Fold Change
0
3
7
14
Days in Culture
mmp-1
mmp-3
mmp-13
timp-1
timp-2
adamts-5

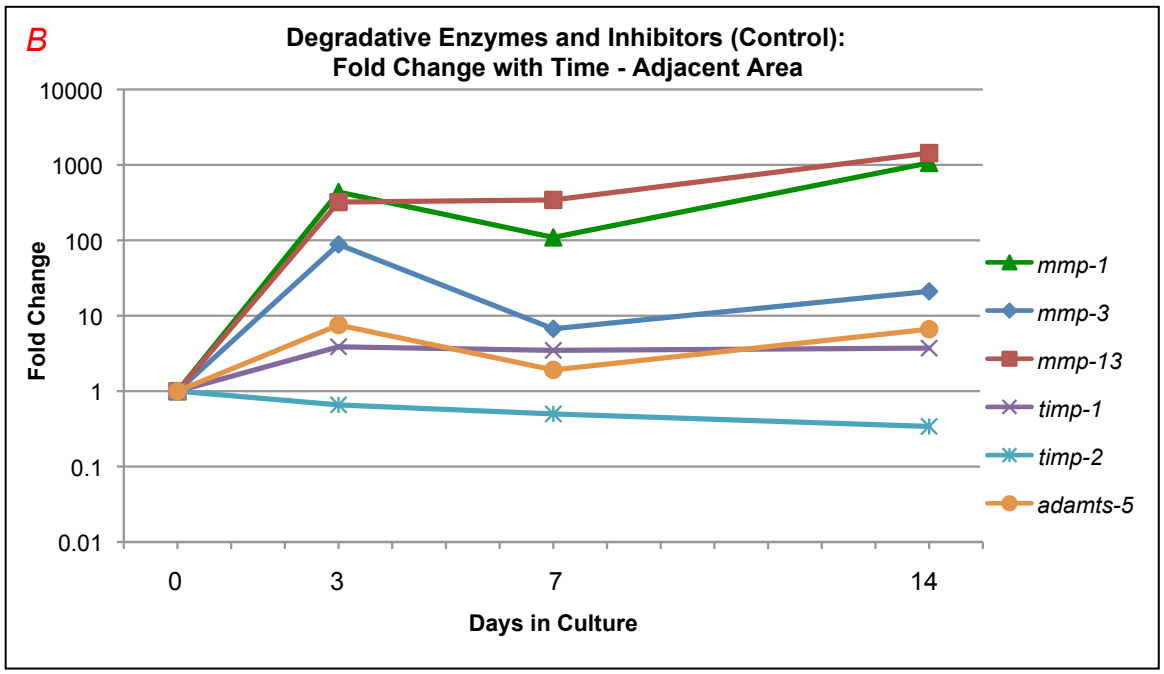
B
Degradative Enzymes and Inhibitors (Control):
Fold Change with Time - Adjacent Area
10000
1000
100
10
1
0.1
0.01
Fold Change
0
3
7
14
Days in Culture
mmp-1
mmp-3
mmp-13
timp-1
timp-2
adamts-5

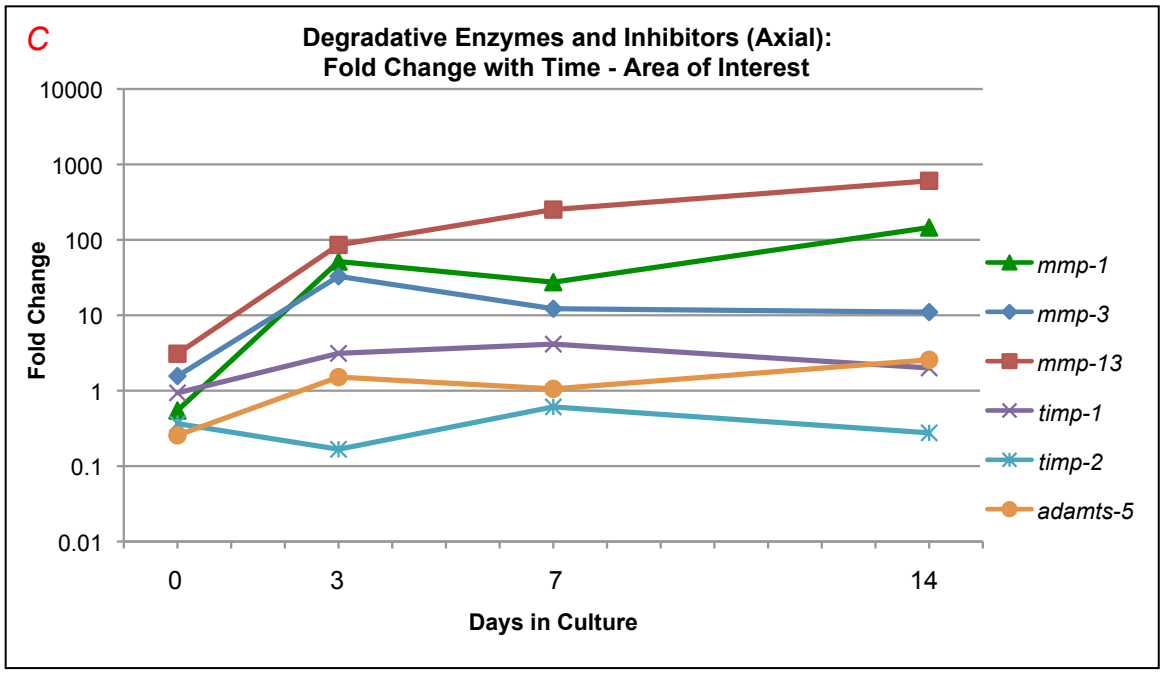
C
Degradative Enzymes and Inhibitors (Axial):
Fold Change with Time - Area of Interest
10000
1000
100
10
1
0.1
0.01
Fold Change
0
3
7
14
Days in Culture
mmp-1
mmp-3
mmp-13
timp-1
timp-2
adamts-5

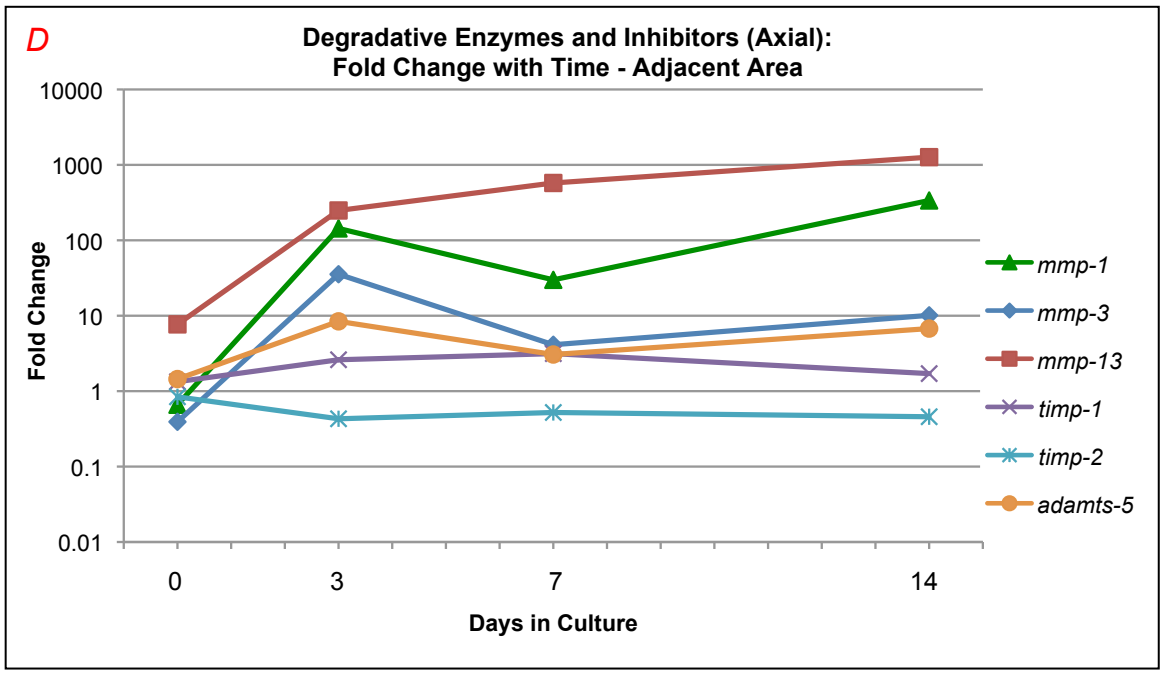
D
Degradative Enzymes and Inhibitors (Axial):
Fold Change with Time - Adjacent Area
10000
1000
100
10
1
0.1
0.01
Fold Change
0
3
7
14
Days in Culture
mmp-1
mmp-3
mmp-13
timp-1
timp-2
adamts-5

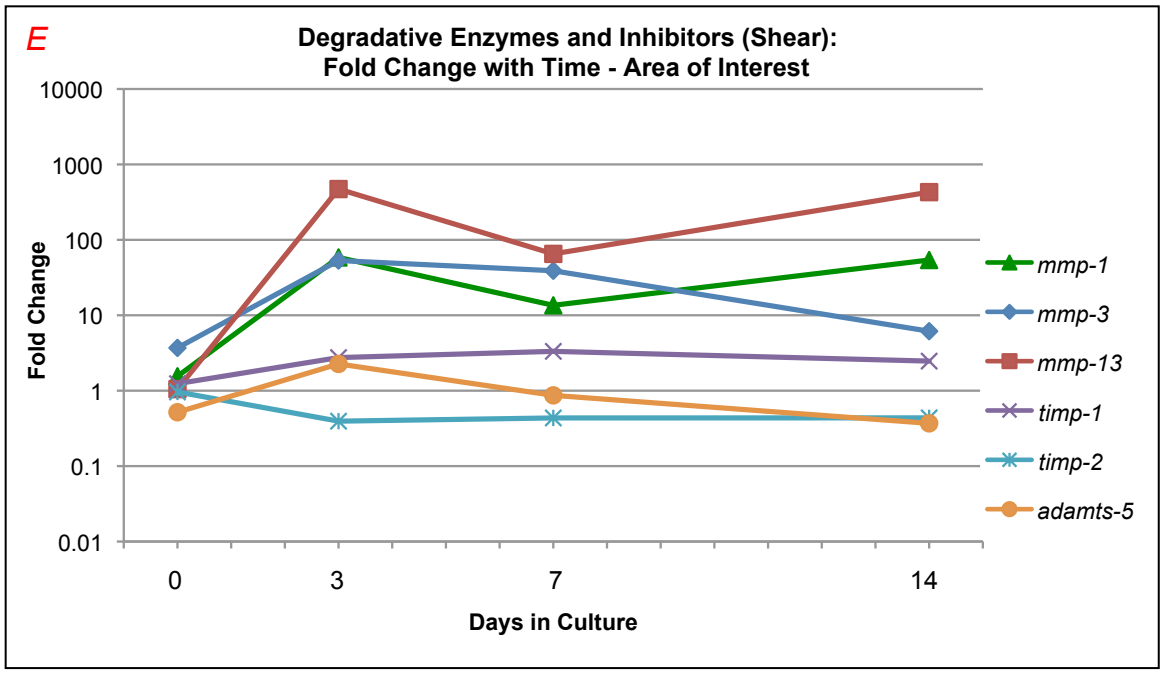
E
Degradative Enzymes and Inhibitors (Shear):
Fold Change with Time - Area of Interest
10000
1000
100
10
1
0.1
0.01
Fold Change
0
3
7
14
Days in Culture
mmp-1
mmp-3
mmp-13
timp-1
timp-2
adamts-5

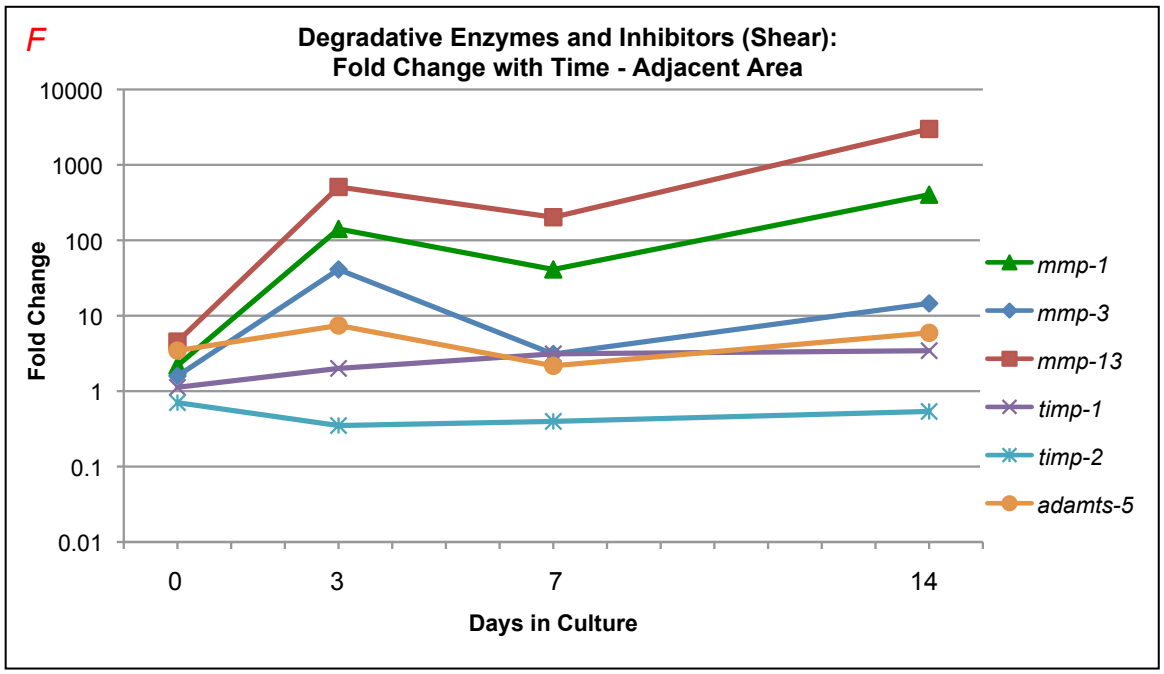
F
Degradative Enzymes and Inhibitors (Shear):
Fold Change with Time - Adjacent Area
10000
1000
100
10
1
0.1
0.01
Fold Change
0
3
7
14
Days in Culture
mmp-1
mmp-3
mmp-13
timp-1
timp-2
adamts-5

4.11 Inflammatory Response and Signaling

Genes related to the inflammatory response and signaling (*ihh, tgfb, inos, chi3l1*) were evaluated for expression changes over time, differences between treatments, and differences between areas.

4.11.1 Results for *Ihh*

Fold Change With Time:

Ihh showed a relatively constant expression for treatments compared to day 0 control in both AOI and ADJ specimens. In fact, the only significant difference was higher expression in the control ADJ specimens at day 7 compared to day 0 (FC = 3.75, q = 0.07).

Fold Change With Treatment:

In an evaluation of expression changes across treatments at each time point for AOI specimens, shear was generally higher than control and axial however these changes were not significant. The one significant difference for AOI specimens was axial had lower expression than control at day 3 (FC = 0.30, q = 0.16). The same evaluation for ADJ specimens revealed no consistent trends, however shear was significantly lower expression than control at day 7 (FC = 0.30, q = 0.15).

Fold Change With Area:

In a comparison of AOI to ADJ specimens, AOI expression was generally higher than ADJ for shear, and was significantly so at day 0, 7 and 14 (FC = 2.55, q = 0.16; FC = 2.45, q = 0.16; FC = 2.94, q = 0.16). Additionally, axial AOI expression was lower than control at day 3 (FC = 0.28, q =0.12).

Figures 4.21 A-E. Graphs of *ihh* by time point, treatment and area.

Figure 4.21 A. *Ihh*: Fold change with time – area of interest. Fold change is shown on the vertical axis as a log scale. Fold changes less than one indicate lowered expression and fold changes greater than one indicate higher expression. Days in culture are shown on the horizontal axis. At each time point, day 0 control specimens are used as the reference or comparative value. Error bars (standard error) are shown for each fold change. Control specimens are plotted in blue, axial are plotted in red, and shear are plotted in green. Significant differences in expression relative to day 0 control are indicated at each time point with an asterisk (*) in the respective color of the plotted treatment.

Figure 4.21 B. *Ihh*: Fold change with treatment – area of interest. Fold change is shown on the vertical axis as a log scale, and days in culture is shown on the horizontal axis. The treatments are compared to each other at each time point. Axial vs. Control is shown in red, Shear vs. Control is shown in green, and Shear vs. Axial is shown in orange. Error bars (standard error) for fold change are depicted, and significant differences for the respective comparison are indicated with an asterisk (*).

Figure 4.21 C. *Ihh*: Fold change with time – adjacent area. Fold change is shown on the vertical axis as a log scale. Fold changes less than one indicate lowered expression and fold changes greater than one indicate higher expression. Days in culture are shown on the horizontal axis. At each time point, day 0 control specimens are used as the reference or comparative value. Error bars (standard error) are shown for each fold change. Control specimens are plotted in blue, axial are plotted in red, and shear are plotted in green. Significant differences in expression relative to day 0 control are indicated at each time point with an asterisk (*) in the respective color of the plotted treatment.

Figure 4.21 D. *Ihh*: Fold change with treatment – adjacent area. Fold change is shown on the vertical axis as a log scale, and days in culture is shown on the horizontal axis. The treatments are compared to each other at each time point. Axial vs. Control is shown in red, Shear vs. Control is shown in green, and Shear vs. Axial is shown in orange. Error bars (standard error) for fold change are depicted, and significant differences for the respective comparison are indicated with an asterisk (*).

Figure 4.21 E. *Ihh*: Fold change with area – area of interest vs. adjacent area. Fold change is shown on the vertical axis as a log scale, and days in culture is shown on the horizontal axis. The treatment areas are compared to each other within each treatment at each time point. Control is shown in blue, axial is shown in red, and shear is shown in green. Error bars (standard error) for fold change are depicted, and significant differences for the respective comparison are indicated with an asterisk (*).

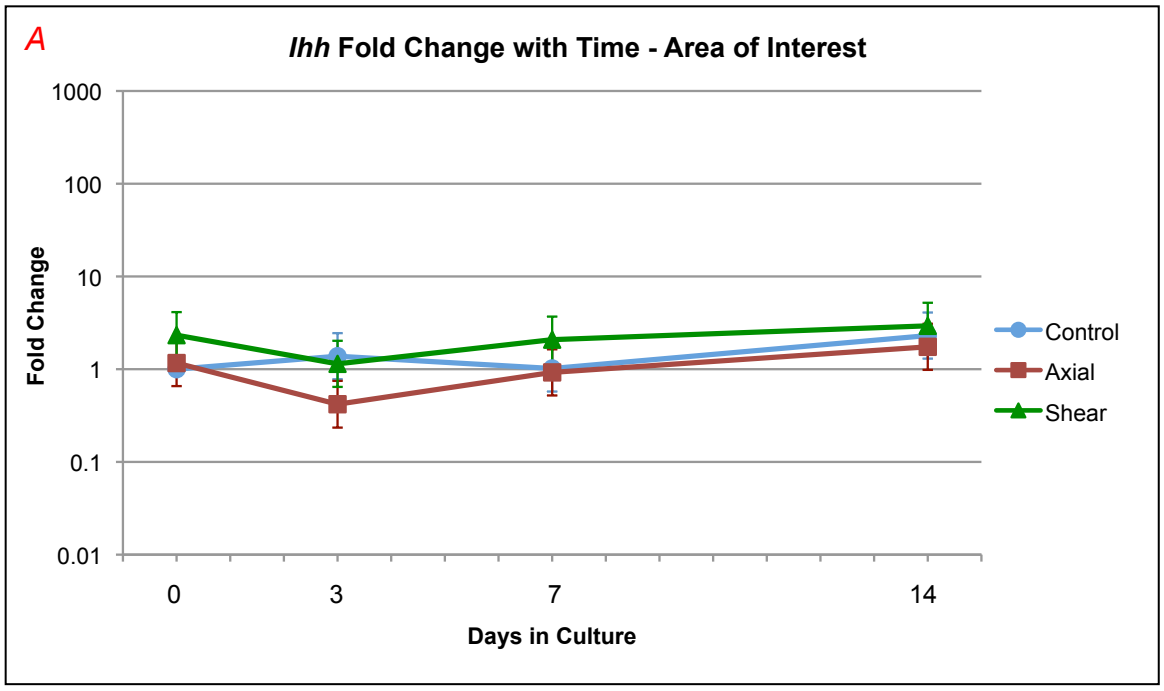
A
Ihh Fold Change with Time - Area of Interest
1000
100
10
1
0.1
0.01
Fold Change
0
3
7
14
Days in Culture
Control
Axial
Shear

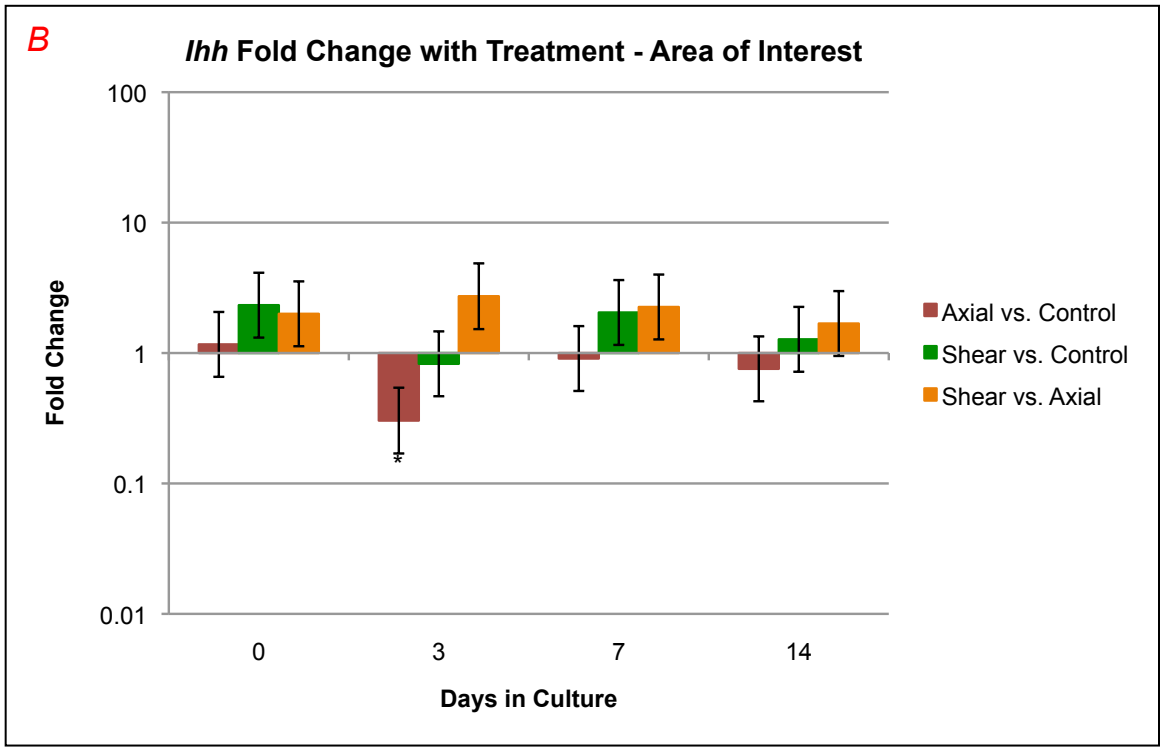
B
Ihh Fold Change with Treatment - Area of Interest
100
10
1
0.1
0.01
Fold Change
*
0
3
7
14
Days in Culture
Axial vs. Control
Shear vs. Control
Shear vs. Axial

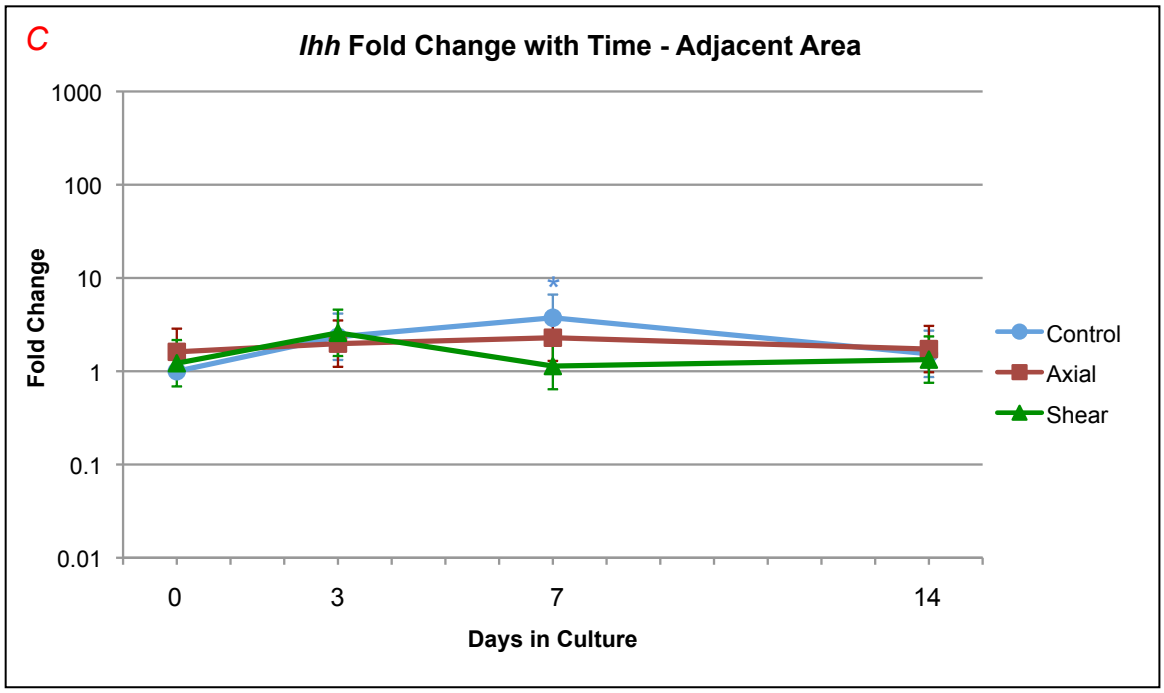
C
Ihh Fold Change with Time - Adjacent Area
1000
100
10
1
0.1
0.01
Fold Change
0
3
7
14
Days in Culture
*
Control
Axial
Shear

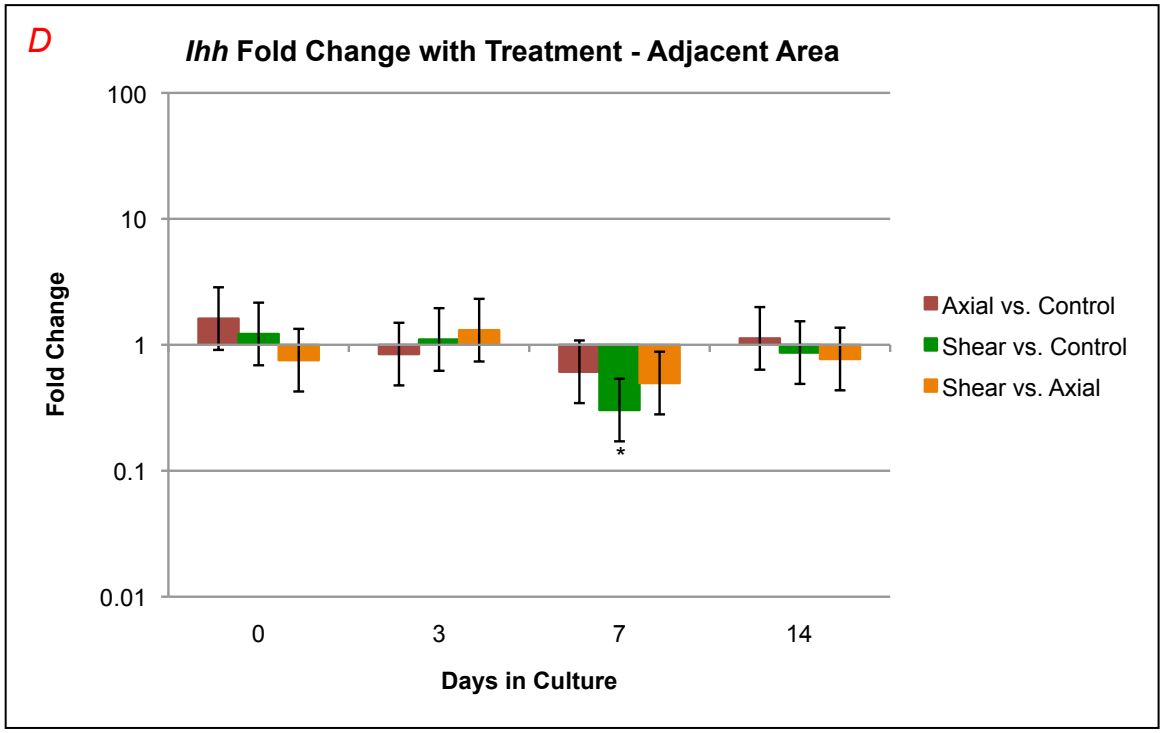
D
Ihh Fold Change with Treatment - Adjacent Area
100
10
1
0.1
0.01
Fold Change
0
3
7
14
Days in Culture
*
Axial vs. Control
Shear vs. Control
Shear vs. Axial

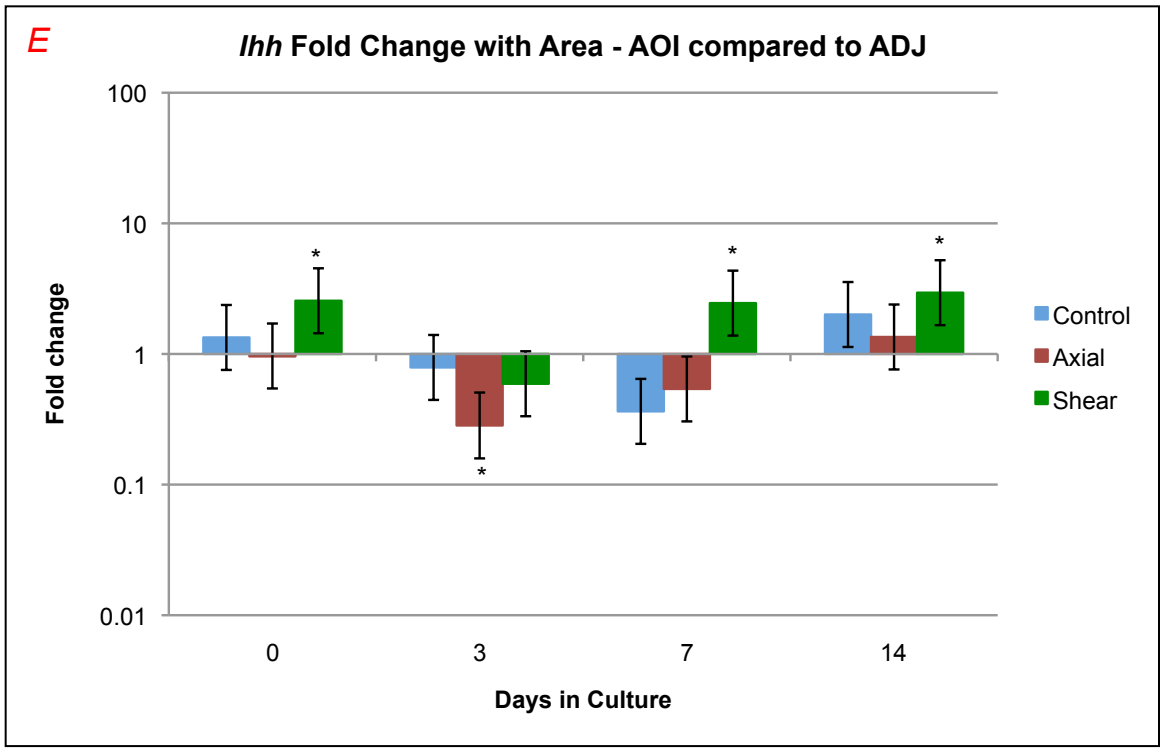
E
Ihh Fold Change with Area - AOI compared to ADJ
100
10
1
0.1
0.01
Fold change
0
3
7
14
Days in Culture
Control
Axial
Shear
*
*
*
*

4.11.2 Results for *Tgfb*

Fold Change With Time:

For both AOI and ADJ specimens, the expression of *tgfb* showed a general decrease in expression over time compared to day 0 control. The changes were significant in AOI specimens at day 3, 7 and 14 for control (FC = 0.32, $q < 0.01$; FC = 0.37, $q < 0.01$; FC = 0.47, $q = 0.01$), axial (FC = 0.62, $q = 0.16$; FC = 0.36, $q < 0.01$; FC = 0.19, $q < 0.01$), and shear (FC = 0.39, $q < 0.01$; FC = 0.32, $q < 0.01$; FC = 0.32; $q < 0.01$). For the ADJ specimens the differences were significant at day 3, 7 and 14 for axial (FC = 0.62, $q = 0.11$; FC = 0.45, $q = 0.02$; FC = 0.28, $q < 0.01$), and shear (FC = 0.48, $q = 0.02$; FC = 0.25, $q < 0.01$; FC = 0.36, $q < 0.01$). The changes were significant for control specimens at day 7 and 14 (FC = 0.34, $q < 0.01$; FC = 0.34, $q < 0.01$).

Fold Change With Treatment:

Expression of *tgfb* was lower in shear AOI specimens compared to axial at day 0 and 3 (FC = 0.51, $q = 0.11$; FC = 0.63, $q = 0.18$) and higher at day 14 (FC = 1.72, $q = 0.15$). Expression was higher in axial vs. control at day 3 (FC = 1.93, $q = 0.06$; FC = 0.39, $q = 0.01$). The only significant difference for the ADJ specimens was that shear expression was lower than axial at day 7 (FC = 0.55, $q = 0.20$).

Fold Change With Area:

A comparison of AOI to ADJ specimens in each treatment yielded no trends. Control AOI expression was significantly lower at day 3 compared to ADJ (FC = 0.41, $q = 0.01$).

Figures 4.22 A-E. Graphs of *tgfb* by time point, treatment and area.

Figure 4.22 A. *Tgfb*: Fold change with time – area of interest. Fold change is shown on the vertical axis as a log scale. Fold changes less than one indicate lowered expression and fold changes greater than one indicate higher expression. Days in culture are shown on the horizontal axis. At each time point, day 0 control specimens are used as the reference or comparative value. Error bars (standard error) are shown for each fold change. Control specimens are plotted in blue, axial are plotted in red, and shear are plotted in green. Significant differences in expression relative to day 0 control are indicated at each time point with an asterisk (*) in the respective color of the plotted treatment.

Figure 4.22 B. *Tgfb*: Fold change with treatment – area of interest. Fold change is shown on the vertical axis as a log scale, and days in culture is shown on the horizontal axis. The treatments are compared to each other at each time point. Axial vs. Control is shown in red, Shear vs. Control is shown in green, and Shear vs. Axial is shown in orange. Error bars (standard error) for fold change are depicted, and significant differences for the respective comparison are indicated with an asterisk (*).

Figure 4.22 C. *Tgfb*: Fold change with time – adjacent area. Fold change is shown on the vertical axis as a log scale. Fold changes less than one indicate lowered expression and fold changes greater than one indicate higher expression. Days in culture are shown on the horizontal axis. At each time point, day 0 control specimens are used as the reference or comparative value. Error bars (standard error) are shown for each fold change. Control specimens are plotted in blue, axial are plotted in red, and shear are plotted in green. Significant differences in expression relative to day 0 control are indicated at each time point with an asterisk (*) in the respective color of the plotted treatment.

Figure 4.22 D. *Tgfb*: Fold change with treatment – adjacent area. Fold change is shown on the vertical axis as a log scale, and days in culture is shown on the horizontal axis. The treatments are compared to each other at each time point. Axial vs. Control is shown in red, Shear vs. Control is shown in green, and Shear vs. Axial is shown in orange. Error bars (standard error) for fold change are depicted, and significant differences for the respective comparison are indicated with an asterisk (*).

Figure 4.22 E. *Tgfb*: Fold change with area – area of interest vs. adjacent area. Fold change is shown on the vertical axis as a log scale, and days in culture is shown on the horizontal axis. The treatment areas are compared to each other within each treatment at each time point. Control is shown in blue, axial is shown in red, and shear is shown in green. Error bars (standard error) for fold change are depicted, and significant differences for the respective comparison are indicated with an asterisk (*).

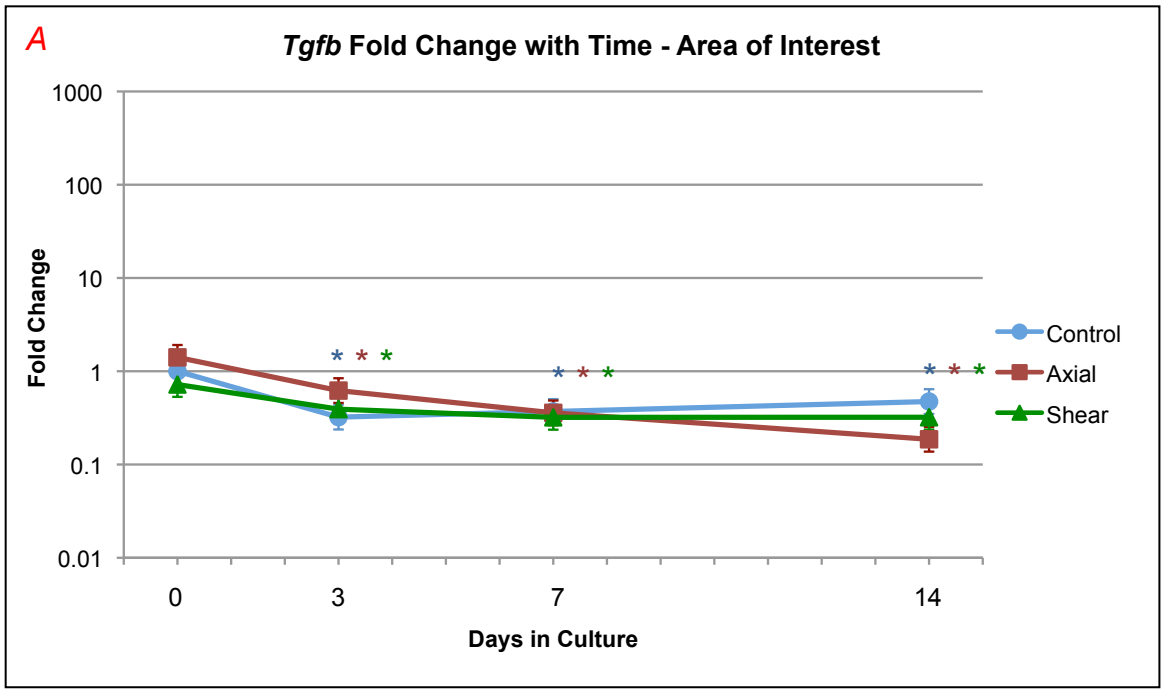
A
Tgfb Fold Change with Time - Area of Interest
1000
100
10
1
0.1
0.01
Fold Change
0
3
7
14
Days in Culture
Control
Axial
Shear

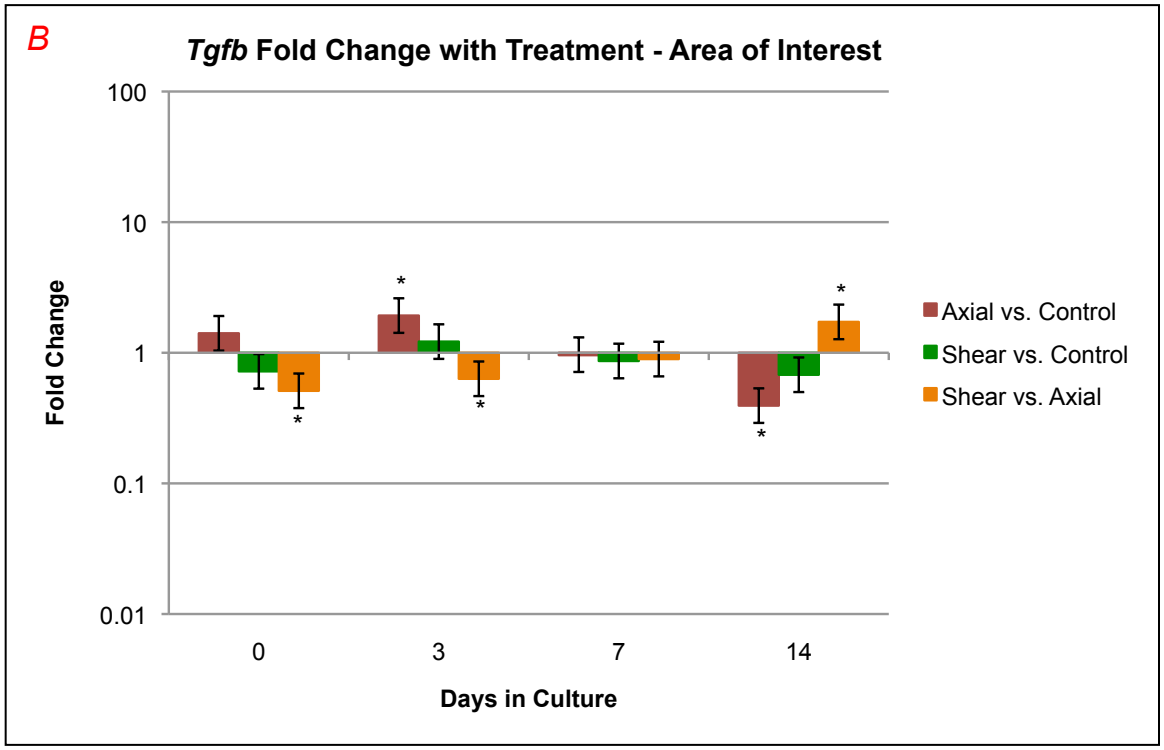
B
Tgfb Fold Change with Treatment - Area of Interest
100
10
1
0.1
0.01
Fold Change
0
3
7
14
Days in Culture
Axial vs. Control
Shear vs. Control
Shear vs. Axial

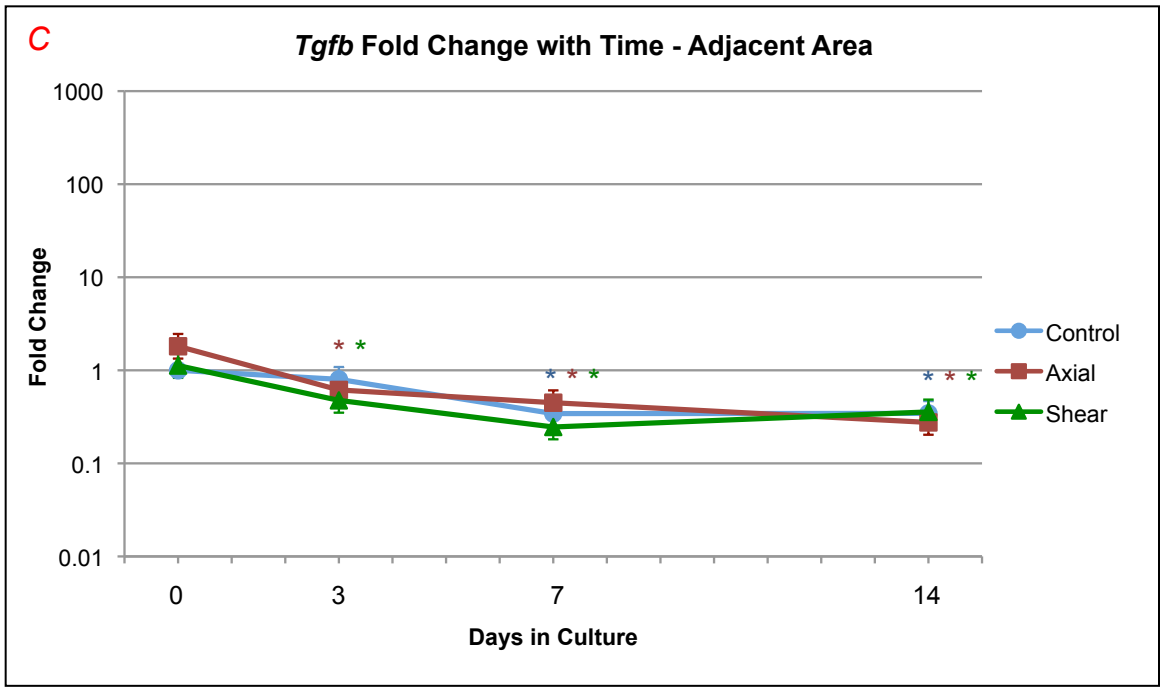
C
Tgfb Fold Change with Time - Adjacent Area
1000
100
10
1
0.1
0.01
Fold Change
0
3
7
14
Days in Culture
Control
Axial
Shear

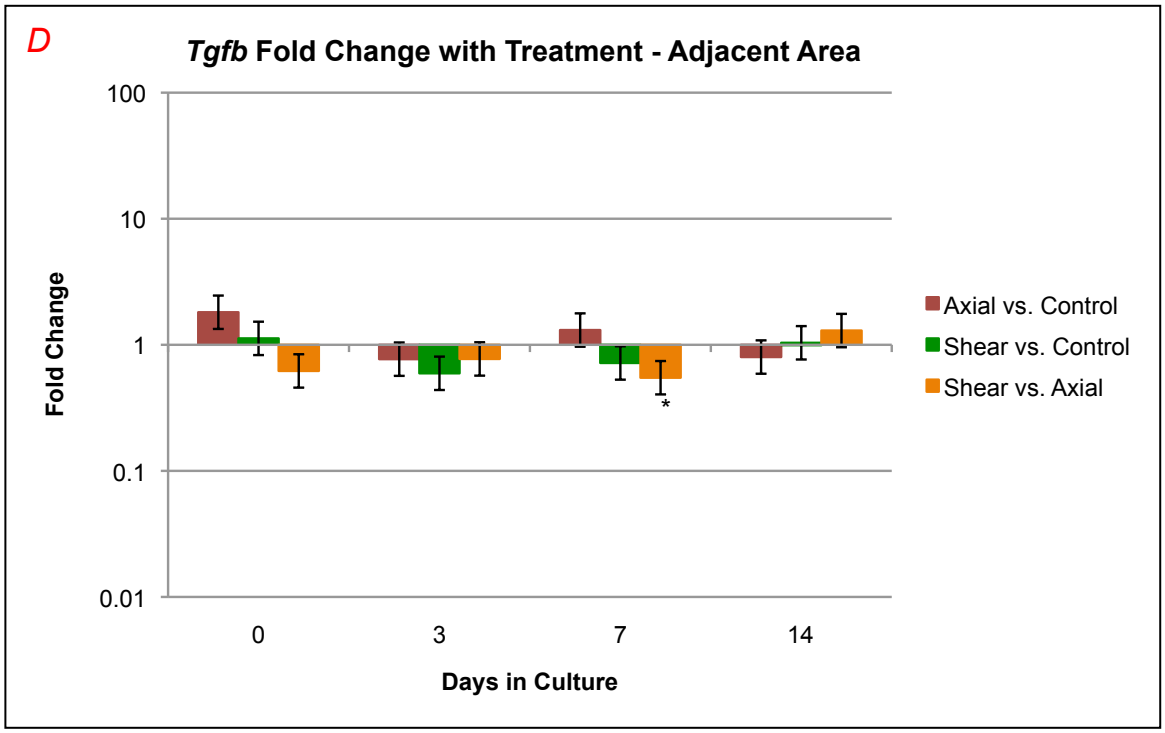
D
Tgfb Fold Change with Treatment - Adjacent Area
100
10
1
0.1
0.01
Fold Change
0
3
7
14
Days in Culture
Axial vs. Control
Shear vs. Control
Shear vs. Axial

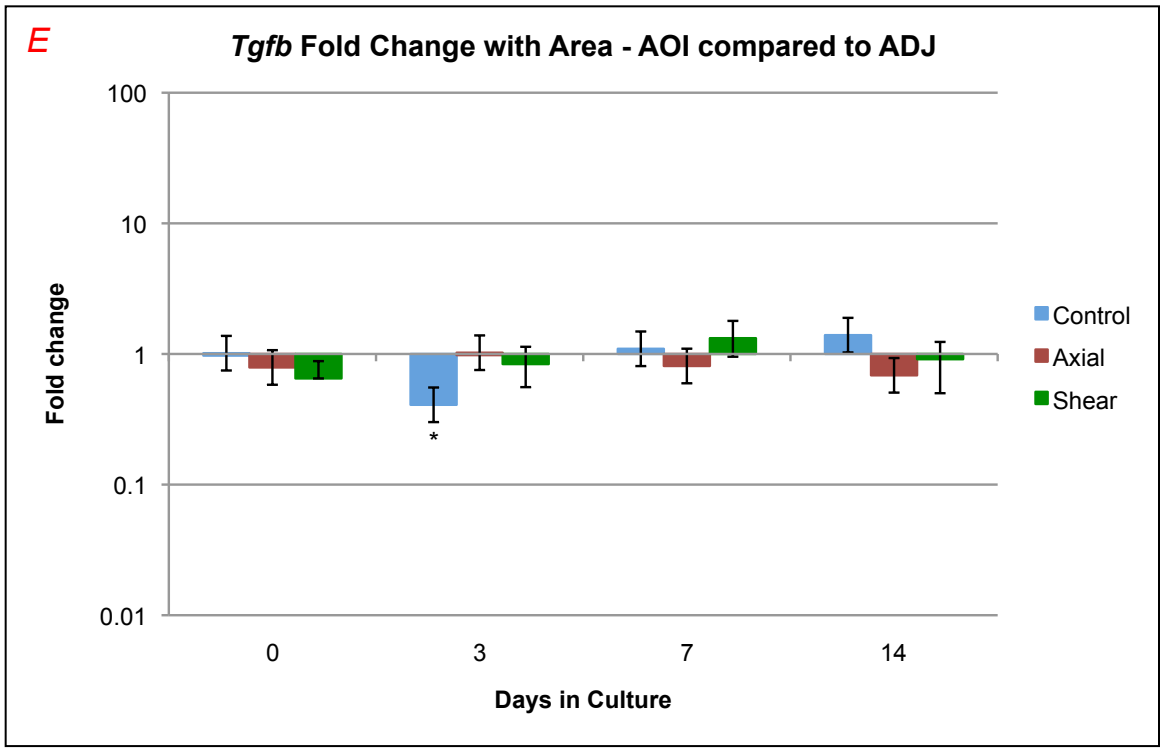
E
Tgfb Fold Change with Area - AOI compared to ADJ
100
10
1
0.1
0.01
Fold change
*
0
3
7
14
Days in Culture
Control
Axial
Shear

4.11.3 Results for *Inos*

Fold Change With Time:

For *inos* changes over time, in both AOI and ADJ specimens, expression rose in the control and shear treatments from day 0 to 3, then dropped off to day 7 and stayed relatively constant to day 14, however axial expression stayed relatively stable from day 0 to day 3, and then tapered off for the later time points. For AOI specimens control had higher expression at day 3 and 14 (FC = 5.01, $q < 0.01$; FC = 6.79, $q < 0.01$), and shear had higher expression at day 3 as well (FC = 4.62, $q = 0.02$). For the ADJ specimens, control had higher expression at day 3 and 14 (FC = 7.79, $q < 0.01$; FC = 3.09, $q = 0.06$), as did shear (FC = 12.35, $q < 0.01$; FC = 6.64, $q < 0.01$). Axial ADJ specimens had higher expression at day 3, 7 and 14 (FC = 5.56, $q = 0.01$; FC = 2.78, $q = 0.08$; FC = 2.81, $q = 0.08$).

Fold Change With Treatment:

In comparing treatments, there were no apparent trends, but axial AOI had lower expression than control at day 14 (FC = 0.15, $q < 0.01$) as did shear AOI (FC = 0.31, $q = 0.13$). There were no significant differences or trends in a comparison of ADJ specimens across treatments.

Fold Change With Area:

The only significant difference when comparing AOI to ADJ expression was in control specimens at day 14 (FC = 5.08, $q = 0.01$).

Figures 4.23 A-E. Graphs of *inos* by time point, treatment and area.

Figure 4.23 A. *Inos*: Fold change with time – area of interest. Fold change is shown on the vertical axis as a log scale. Fold changes less than one indicate lowered expression and fold changes greater than one indicate higher expression. Days in culture are shown on the horizontal axis. At each time point, day 0 control specimens are used as the reference or comparative value. Error bars (standard error) are shown for each fold change. Control specimens are plotted in blue, axial are plotted in red, and shear are plotted in green. Significant differences in expression relative to day 0 control are indicated at each time point with an asterisk (*) in the respective color of the plotted treatment.

Figure 4.23 B. *Inos*: Fold change with treatment – area of interest. Fold change is shown on the vertical axis as a log scale, and days in culture is shown on the horizontal axis. The treatments are compared to each other at each time point. Axial vs. Control is shown in red, Shear vs. Control is shown in green, and Shear vs. Axial is shown in orange. Error bars (standard error) for fold change are depicted, and significant differences for the respective comparison are indicated with an asterisk (*).

Figure 4.23 C. *Inos*: Fold change with time – adjacent area. Fold change is shown on the vertical axis as a log scale. Fold changes less than one indicate lowered expression and fold changes greater than one indicate higher expression. Days in culture are shown on the horizontal axis. At each time point, day 0 control specimens are used as the reference or comparative value. Error bars (standard error) are shown for each fold change. Control specimens are plotted in blue, axial are plotted in red, and shear are plotted in green. Significant differences in expression relative to day 0 control are indicated at each time point with an asterisk (*) in the respective color of the plotted treatment.

Figure 4.23 D. *Inos*: Fold change with treatment – adjacent area. Fold change is shown on the vertical axis as a log scale, and days in culture is shown on the horizontal axis. The treatments are compared to each other at each time point. Axial vs. Control is shown in red, Shear vs. Control is shown in green, and Shear vs. Axial is shown in orange. Error bars (standard error) for fold change are depicted, and significant differences for the respective comparison are indicated with an asterisk (*).

Figure 4.23 E. *Inos*: Fold change with area – area of interest vs. adjacent area. Fold change is shown on the vertical axis as a log scale, and days in culture is shown on the horizontal axis. The treatment areas are compared to each other within each treatment at each time point. Control is shown in blue, axial is shown in red, and shear is shown in green. Error bars (standard error) for fold change are depicted, and significant differences for the respective comparison are indicated with an asterisk (*).

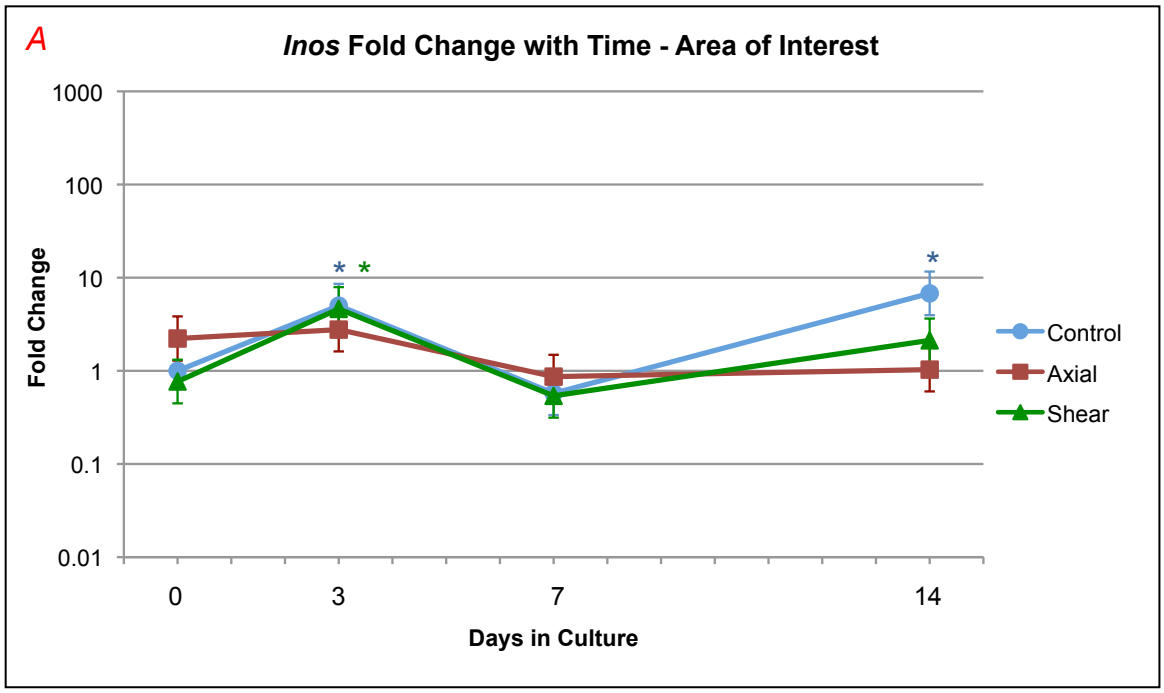
A
Inos Fold Change with Time - Area of Interest
1000
100
10
1
0.1
0.01
Fold Change
* *
*
0
3
7
14
Days in Culture
Control
Axial
Shear

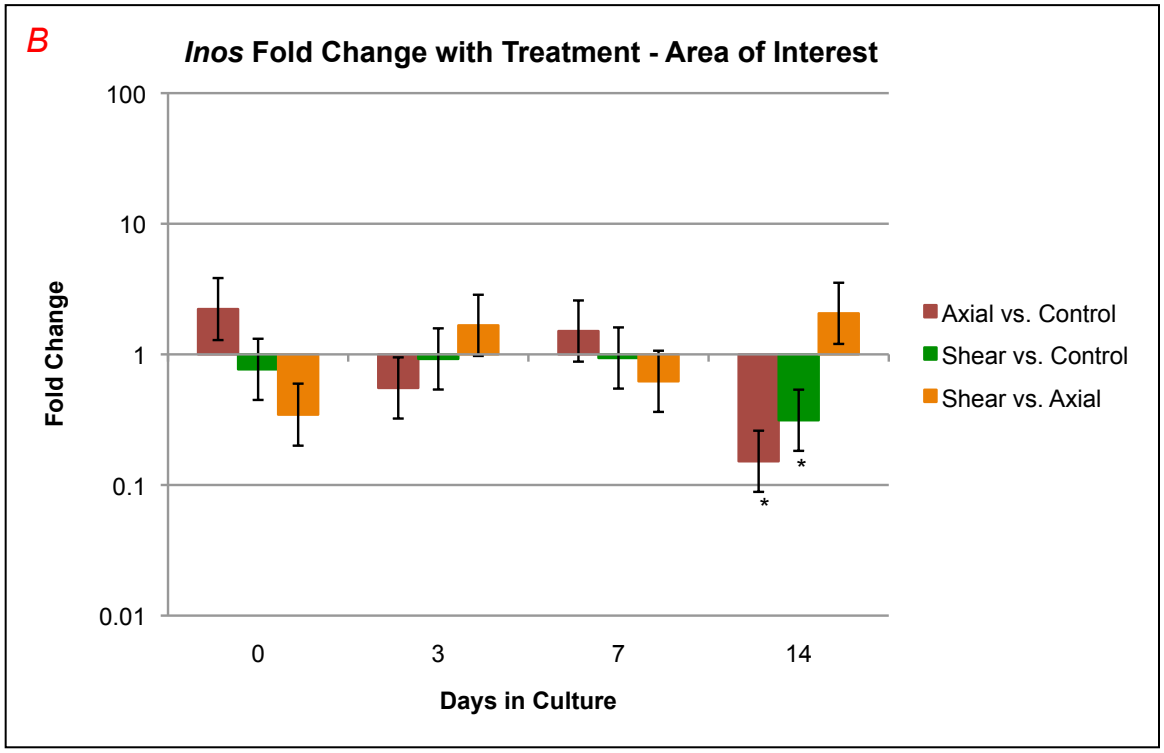
B
Inos Fold Change with Treatment - Area of Interest
100
10
1
0.1
0.01
Fold Change
*
*
0
3
7
14
Days in Culture
Axial vs. Control
Shear vs. Control
Shear vs. Axial

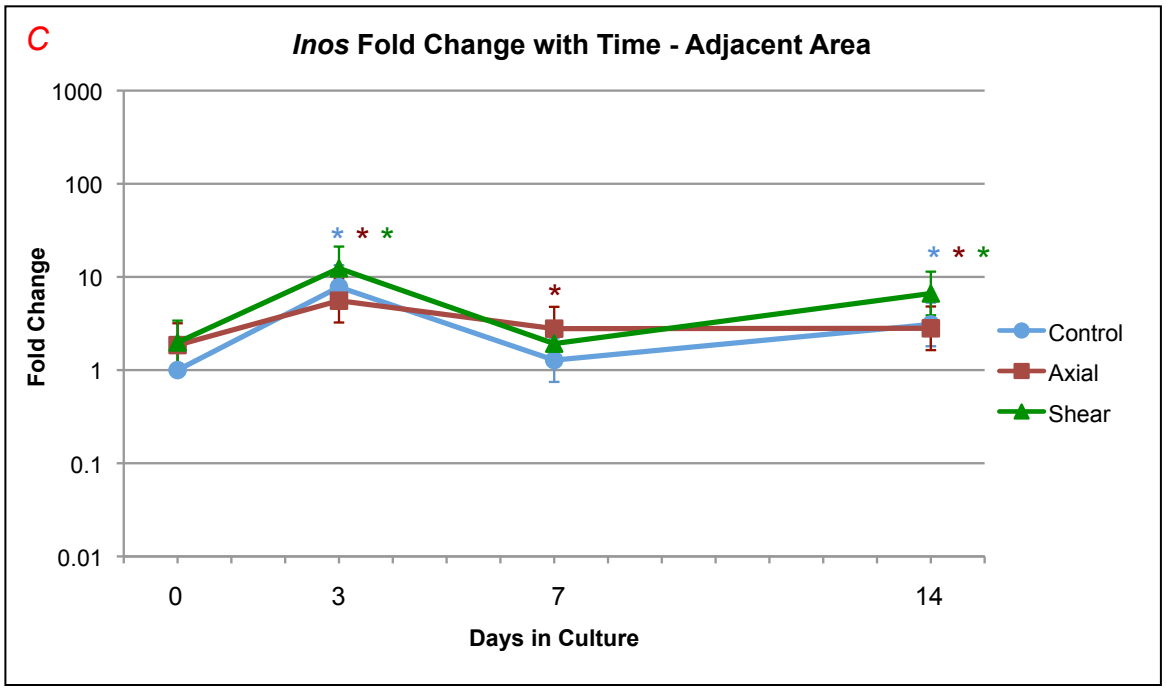
C
Inos Fold Change with Time - Adjacent Area
1000
100
10
1
0.1
0.01
Fold Change
0
3
7
14
Days in Culture
Control
Axial
Shear

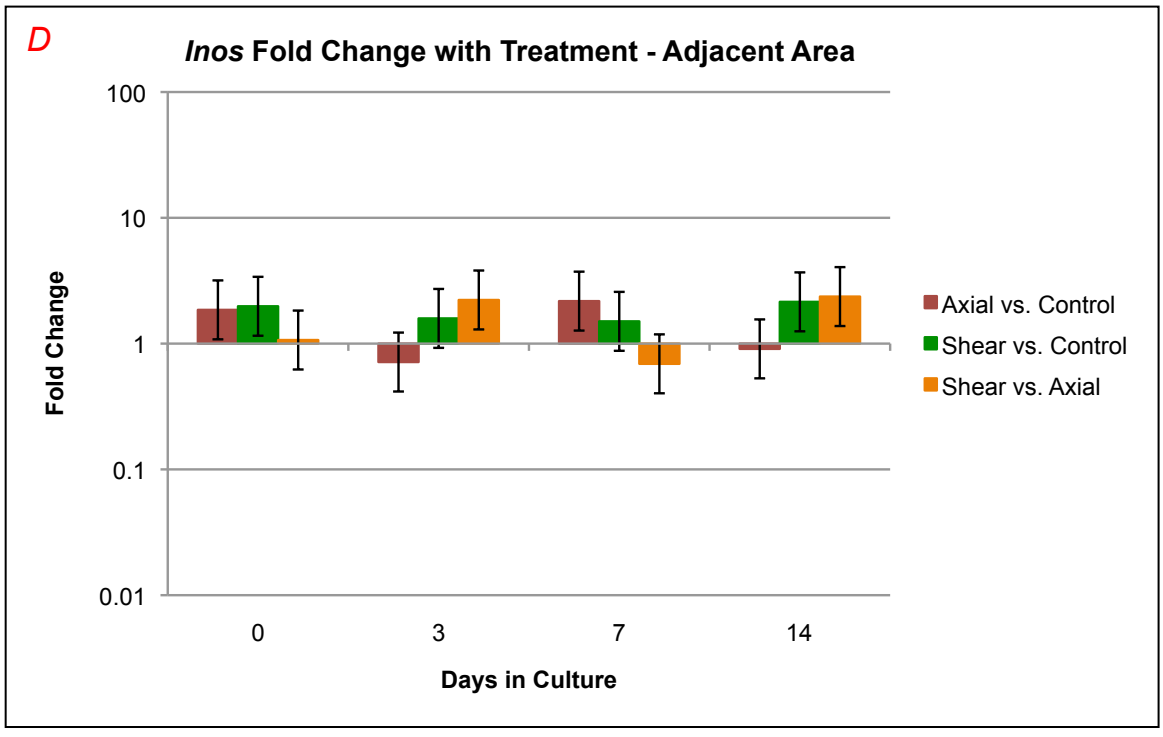
D
Inos Fold Change with Treatment - Adjacent Area
100
10
1
0.1
0.01
Fold Change
0
3
7
14
Days in Culture
Axial vs. Control
Shear vs. Control
Shear vs. Axial

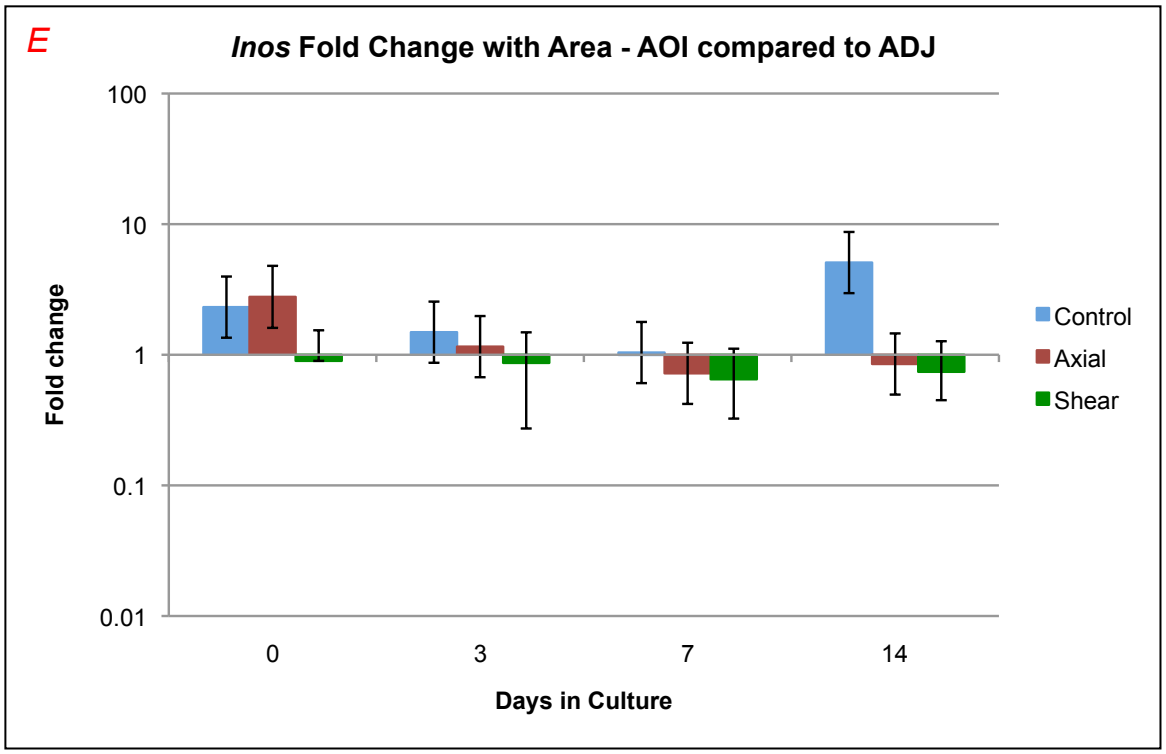
E
Inos Fold Change with Area - AOI compared to ADJ
100
10
1
0.1
0.01
Fold change
0
3
7
14
Days in Culture
Control
Axial
Shear

4.11.4 Results for *Chi3l1*

Fold Change With Time:

The expression of *chi3l1* showed a general rise from day 0 to day 3 and then a leveling off for the remaining time points in both AOI and ADJ specimens. In the control specimens, the expression was higher than day 0 expression at day 3, 7 and 14 (FC = 23.14, $q < 0.01$; FC = 12.80, $q < 0.01$; FC = 21.79, $q < 0.01$) as was axial (FC = 19.51, $q < 0.01$; FC = 14.69, $q < 0.01$; FC = 6.89, $q < 0.01$). For shear specimens, the expression of the AOI specimens was higher than day 0 control at all time points: 0, 3, 7 and 14 (FC = 2.00, $q = 0.17$; FC = 10.61, $q < 0.01$; FC = 15.36, $q < 0.01$; FC = 11.08, $q < 0.01$). The expression of ADJ specimens followed a similar trend and expression was higher at day 3, 7 and 14 in control (FC = 31.70, $q < 0.01$; FC = 16.62, $q < 0.01$; FC = 15.95, $q < 0.01$) and shear specimens (FC = 9.69, $q < 0.01$; FC = 25.28, $q < 0.01$; FC = 12.61, $q < 0.01$). In axial specimens, expression was higher at day 0, 3, 7 and 14 (FC = 2.67, $q = 0.11$; FC = 26.28, $q < 0.01$; FC = 20.29, $q < 0.01$, FC = 7.45, $q < 0.01$).

Fold Change With Treatment:

There were no clear trends in the comparison of treatments at each time point for AOI or ADJ specimens. For the AOI specimens, shear expression was higher than control at day 0 (FC = 2.00, $q = 0.17$) and was lower than control at day 3 and 14 (FC = 0.46, $q = 0.17$; FC = 0.51, $q = 0.17$). Also, the axial AOI expression was lower than control at day 14 (FC 0.32, $q = 0.04$). For the ADJ specimens, axial expression was higher than control at day 0 (FC = 2.67, $q = 0.11$) and lower at day 14 (FC = 0.47, $q = 0.18$). Shear expression

was lower than control at day 3 (FC = 0.31, q = 0.03) as was shear compared to axial (FC = 0.37, q = 0.10).

Fold Change With Area:

When AOI were compared to ADJ specimens, there were no significant differences or trends.

Figures 4.24 A-E. Graphs of *chi3l1* by time point, treatment and area.

Figure 4.24 A. *Chi3l1*: Fold change with time – area of interest. Fold change is shown on the vertical axis as a log scale. Fold changes less than one indicate lowered expression and fold changes greater than one indicate higher expression. Days in culture are shown on the horizontal axis. At each time point, day 0 control specimens are used as the reference or comparative value. Error bars (standard error) are shown for each fold change. Control specimens are plotted in blue, axial are plotted in red, and shear are plotted in green. Significant differences in expression relative to day 0 control are indicated at each time point with an asterisk (*) in the respective color of the plotted treatment.

Figure 4.24 B. *Chi3l1*: Fold change with treatment – area of interest. Fold change is shown on the vertical axis as a log scale, and days in culture is shown on the horizontal axis. The treatments are compared to each other at each time point. Axial vs. Control is shown in red, Shear vs. Control is shown in green, and Shear vs. Axial is shown in orange. Error bars (standard error) for fold change are depicted, and significant differences for the respective comparison are indicated with an asterisk (*).

Figure 4.24 C. *Chi3l1*: Fold change with time – adjacent area. Fold change is shown on the vertical axis as a log scale. Fold changes less than one indicate lowered expression and fold changes greater than one indicate higher expression. Days in culture are shown on the horizontal axis. At each time point, day 0 control specimens are used as the reference or comparative value. Error bars (standard error) are shown for each fold change. Control specimens are plotted in blue, axial are plotted in red, and shear are plotted in green. Significant differences in expression relative to day 0 control are indicated at each time point with an asterisk (*) in the respective color of the plotted treatment.

Figure 4.24 D. *Chi3l1*: Fold change with treatment – adjacent area. Fold change is shown on the vertical axis as a log scale, and days in culture is shown on the horizontal axis. The treatments are compared to each other at each time point. Axial vs. Control is shown in red, Shear vs. Control is shown in green, and Shear vs. Axial is shown in orange. Error bars (standard error) for fold change are depicted, and significant differences for the respective comparison are indicated with an asterisk (*).

Figure 4.24 E. *Chi3l1*: Fold change with area – area of interest vs. adjacent area. Fold change is shown on the vertical axis as a log scale, and days in culture is shown on the horizontal axis. The treatment areas are compared to each other within each treatment at each time point. Control is shown in blue, axial is shown in red, and shear is shown in green. Error bars (standard error) for fold change are depicted, and significant differences for the respective comparison are indicated with an asterisk (*).

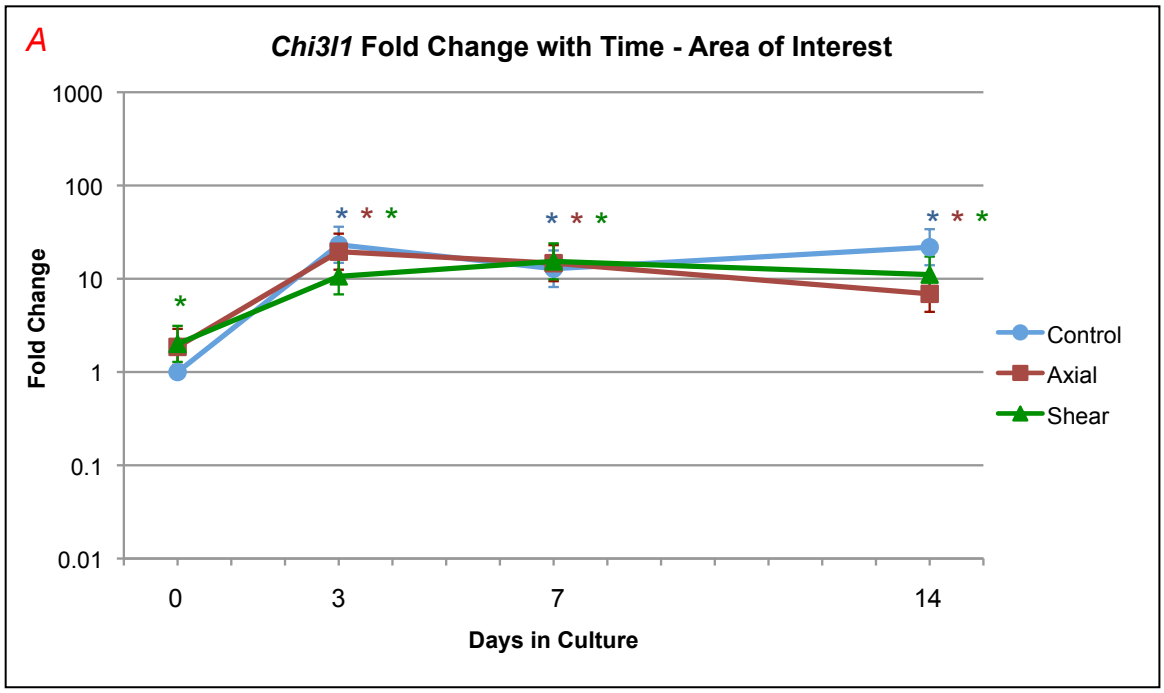
A
Chi3l1 Fold Change with Time - Area of Interest
1000
100
10
1
0.1
0.01
Fold Change
0
3
7
14
Days in Culture
Control
Axial
Shear

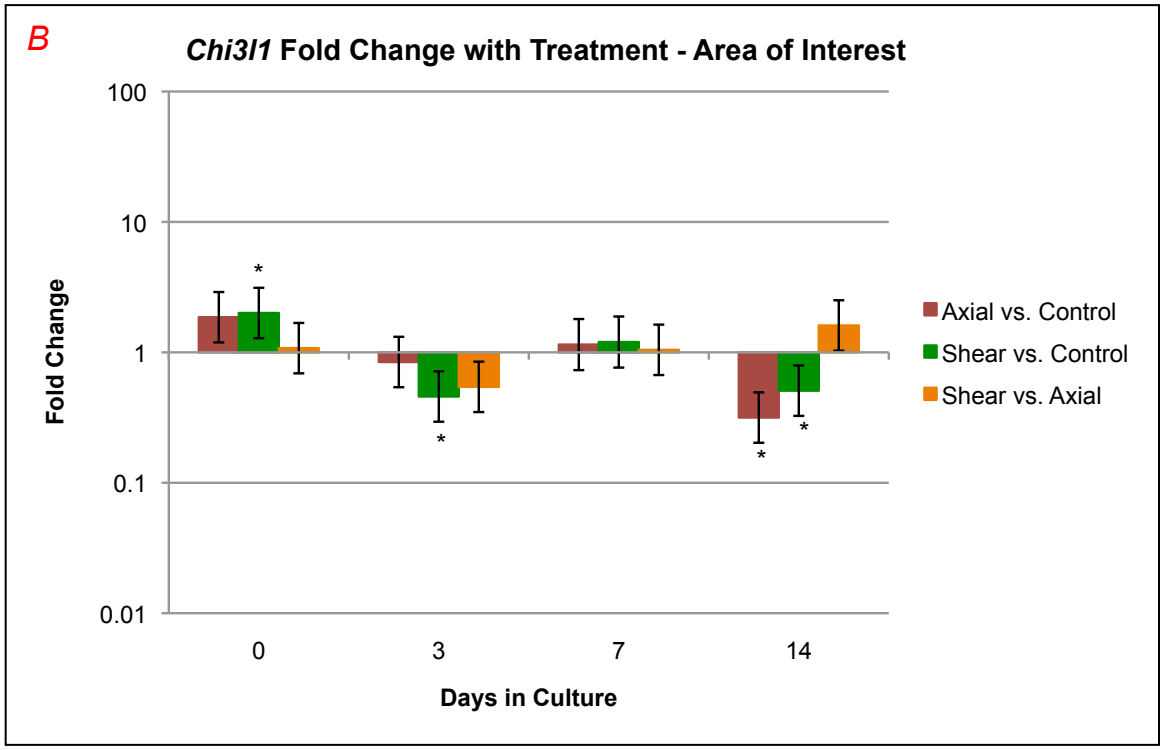
B
Chi3l1 Fold Change with Treatment - Area of Interest
100
10
1
0.1
0.01
Fold Change
0
3
7
14
Days in Culture
Axial vs. Control
Shear vs. Control
Shear vs. Axial

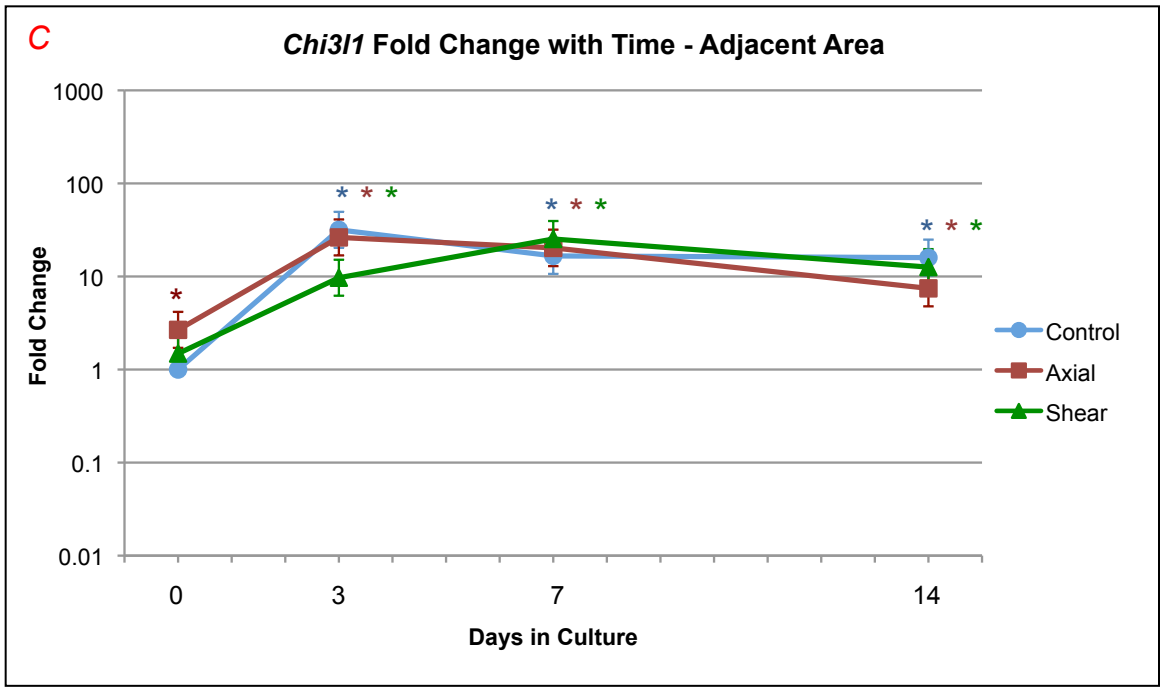
C
Chi3l1 Fold Change with Time - Adjacent Area
1000
100
10
1
0.1
0.01
Fold Change
0
3
7
14
Days in Culture
Control
Axial
Shear

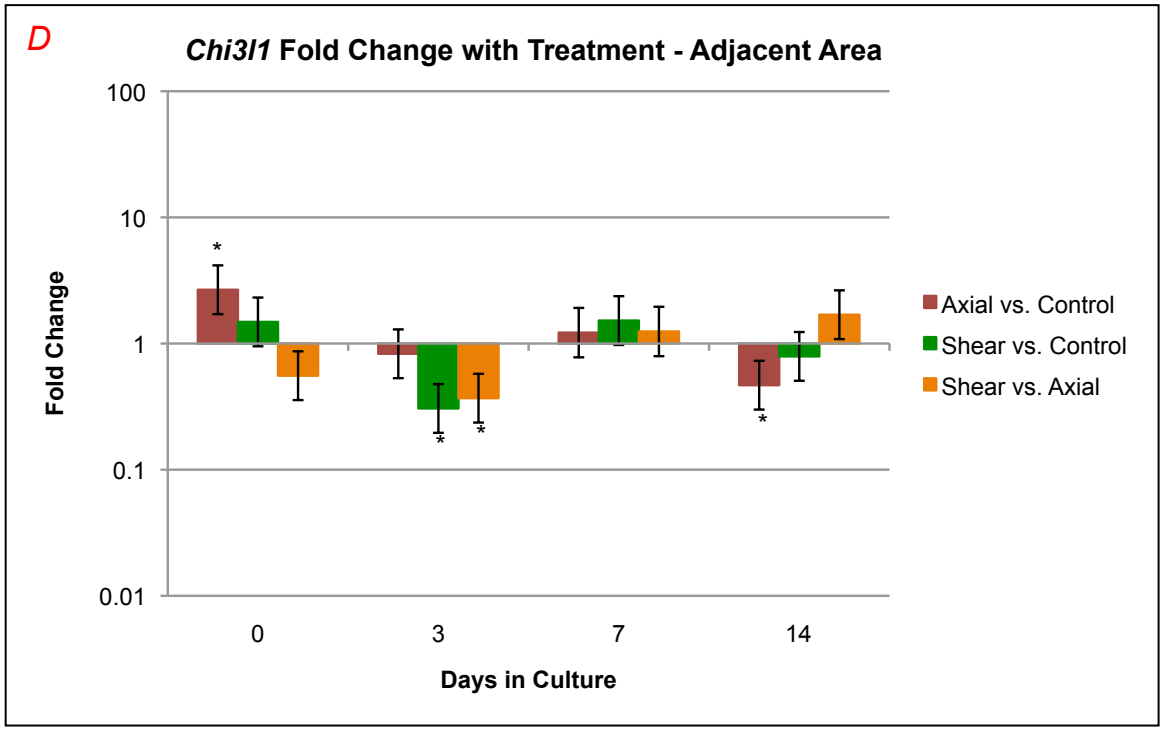
D
Chi3l1 Fold Change with Treatment - Adjacent Area
100
10
1
0.1
0.01
Fold Change
0
3
7
14
Days in Culture
Axial vs. Control
Shear vs. Control
Shear vs. Axial

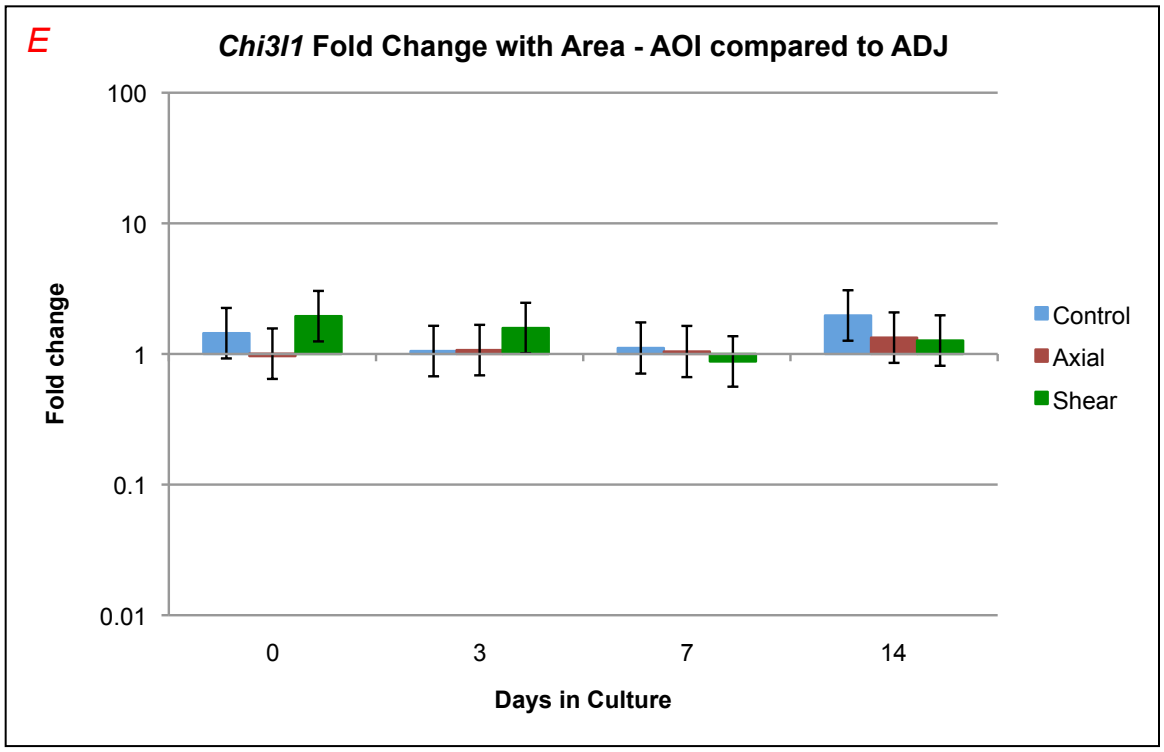
E
Chi3l1 Fold Change with Area - AOI compared to ADJ
100
10
1
0.1
0.01
Fold change
0
3
7
14
Days in Culture
Control
Axial
Shear

Summary of Inflammatory Response and Signaling:

Ihh showed no significant changes or trends over time with the exception of decreased expression in axial AOI specimens compared to ADJ at day 0, 7, and 14. *Tgfb* had relatively consistently lower expression over time in all treatments compared to day 0 control, but was higher at day 3 for axial AOI compared to control. *Tgfb* also had lower expression in shear AOI compared to axial at day 0 and 3, but had higher expression than axial at day 14. *Inos* had generally higher expression over time in all treatments in both AOI and ADJ specimens. In a comparison of treatments however, at day 14, *inos* had lower expression in both shear and axial AOI specimens compared to control. *Chi3l1* showed consistently higher expression over time for all treatments. When treatments were compared though, *chi3l1* had lower expression in both axial and shear compared to control at day 14, but showed higher expression in shear compared to control at the day 0 time point.

Figures 4.25 A-F. Graphs of inflammatory response and signaling genes by time point for AOI and ADJ. Fold change with time – area of interest. Fold change is shown on the vertical axis as a log scale. Fold changes less than one indicate lowered expression and fold changes greater than one indicate higher expression. Days in culture are shown on the horizontal axis. At each time point, day 0 control specimens are used as the reference or comparative value. Graph A and B show changes over time for the control specimens, graph C and D show changes over time for the axial specimens, and graph E and F show changes over time for the shear specimens.

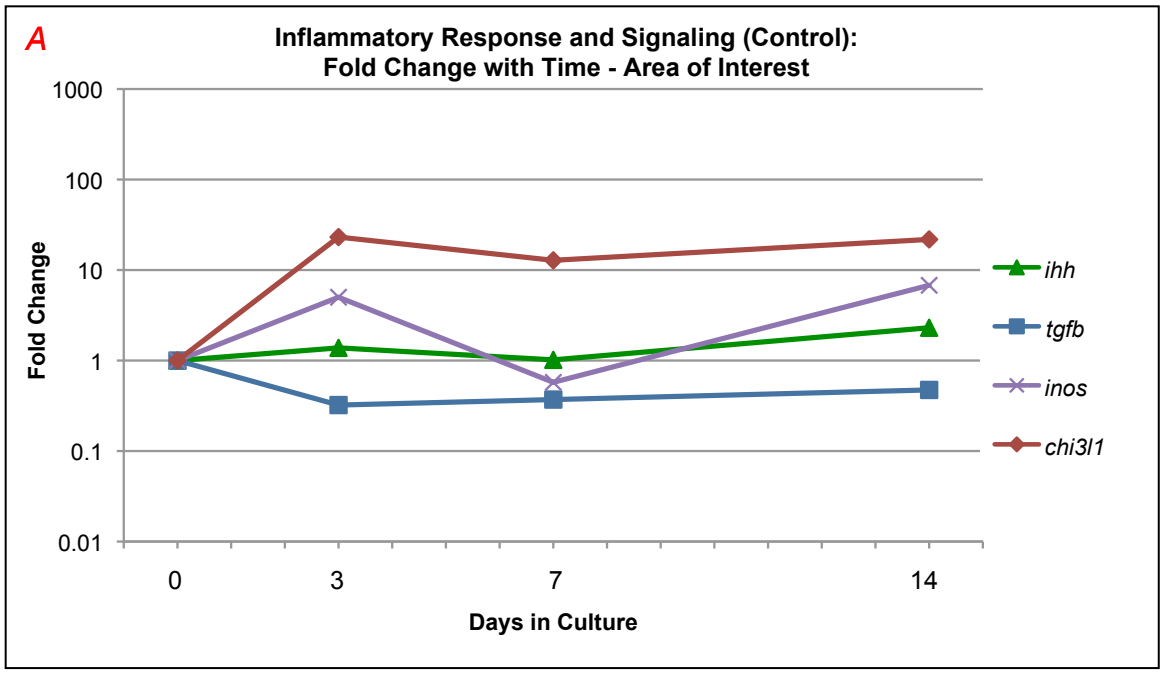
A
Inflammatory Response and Signaling (Control):
Fold Change with Time - Area of Interest
1000
100
10
1
0.1
0.01
Fold Change
0
3
7
14
Days in Culture
ihh
tgfb
inos
chi3l1

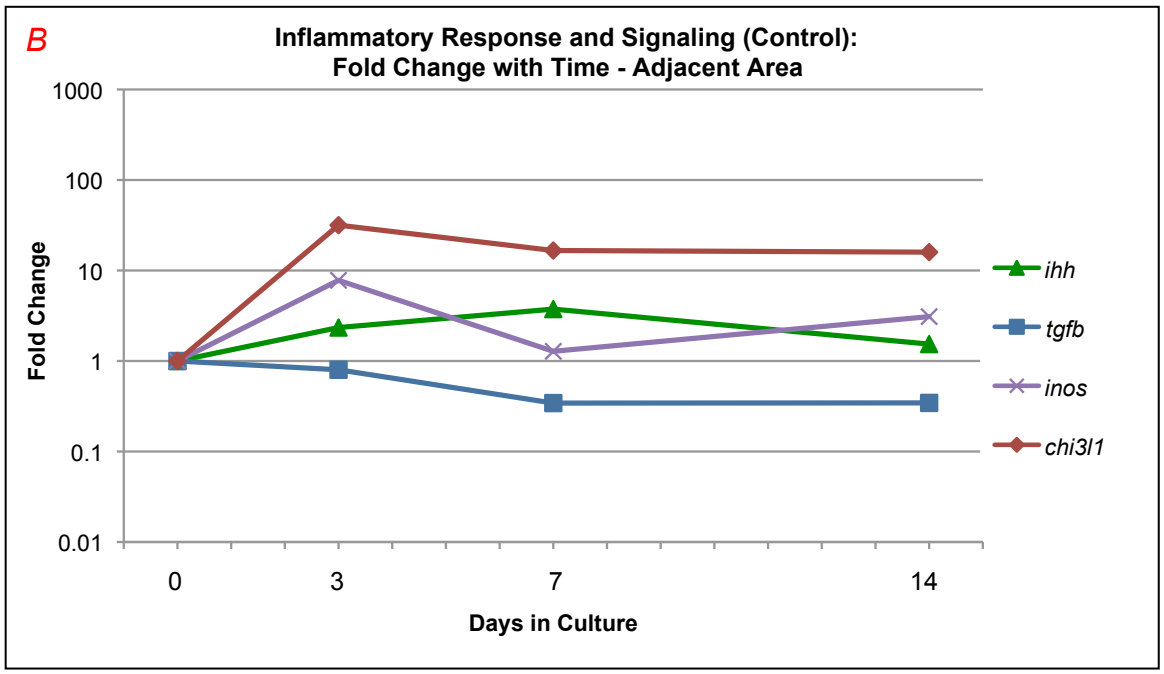
B
Inflammatory Response and Signaling (Control):
Fold Change with Time - Adjacent Area
1000
100
10
1
0.1
0.01
Fold Change
0
3
7
14
Days in Culture
ihh
tgfb
inos
chi3l1

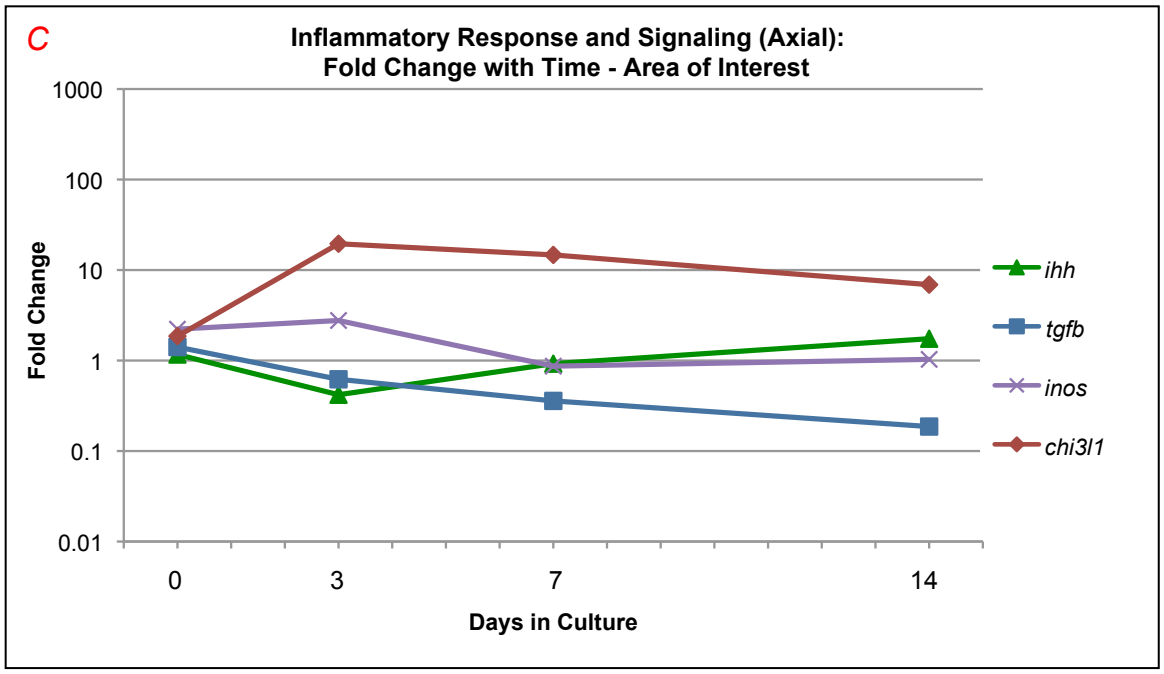
C
Inflammatory Response and Signaling (Axial):
Fold Change with Time - Area of Interest
1000
100
10
1
0.1
0.01
Fold Change
0
3
7
14
Days in Culture
ihh
tgfb
inos
chi3l1

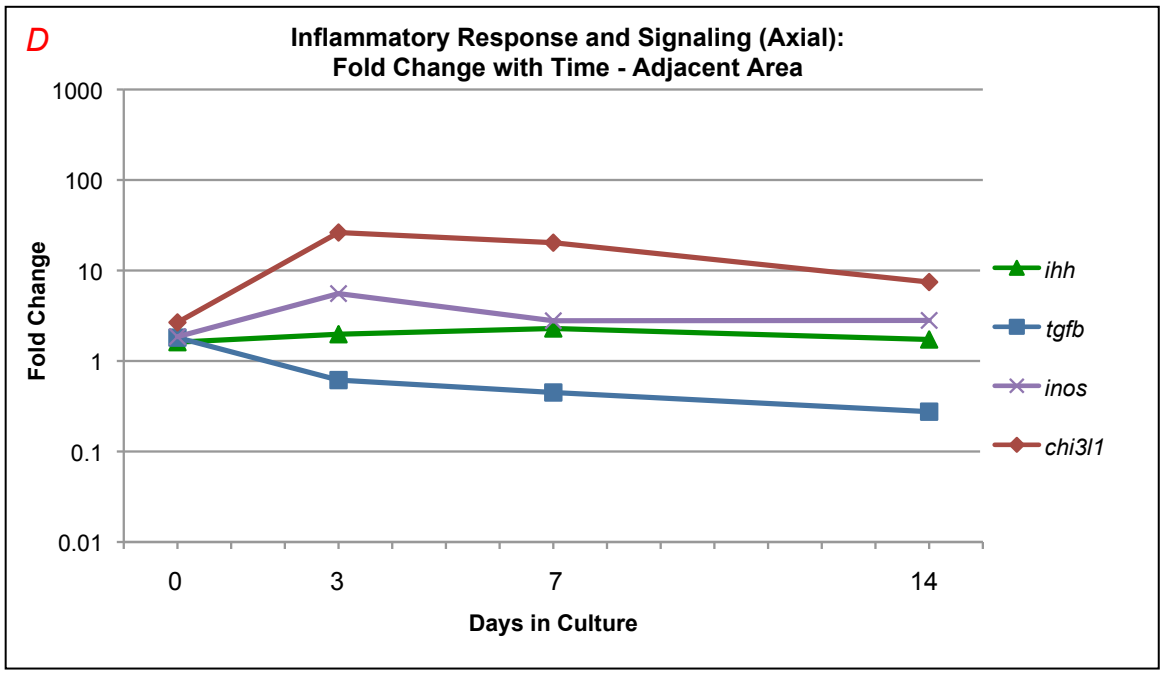
D
Inflammatory Response and Signaling (Axial):
Fold Change with Time - Adjacent Area
1000
100
10
1
0.1
0.01
Fold Change
0
3
7
14
Days in Culture
ihh
tgfb
inos
chi3l1

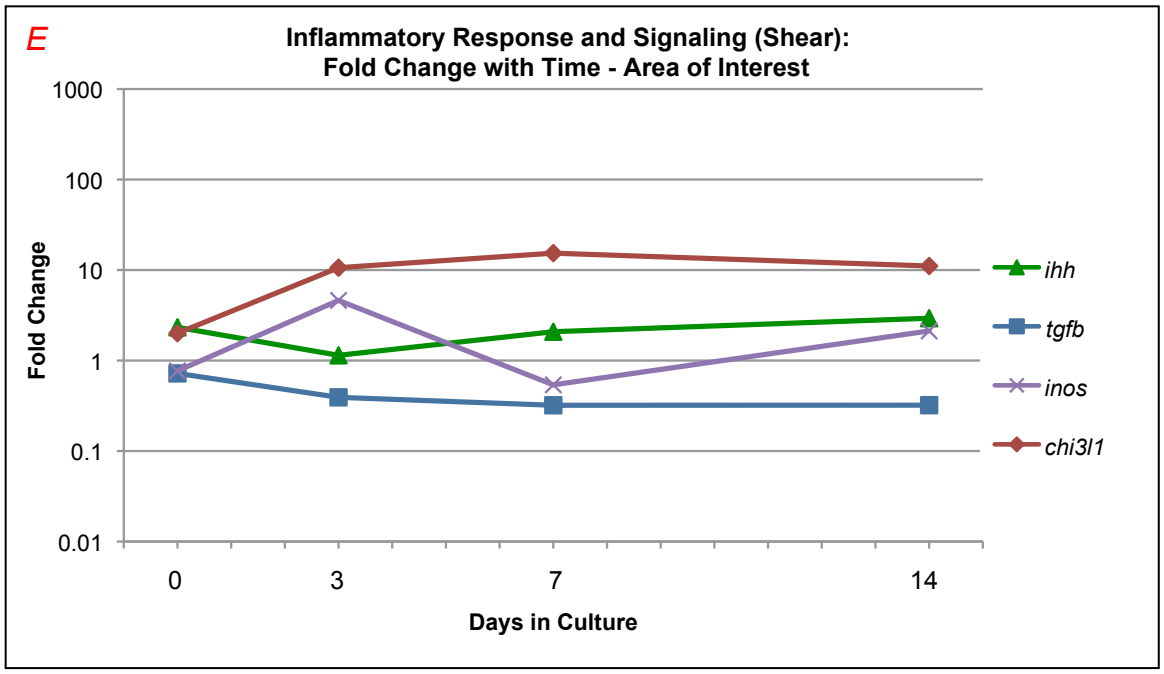
E
Inflammatory Response and Signaling (Shear):
Fold Change with Time - Area of Interest
1000
100
10
1
0.1
0.01
Fold Change
0
3
7
14
Days in Culture
ihh
tgfb
inos
chi3l1

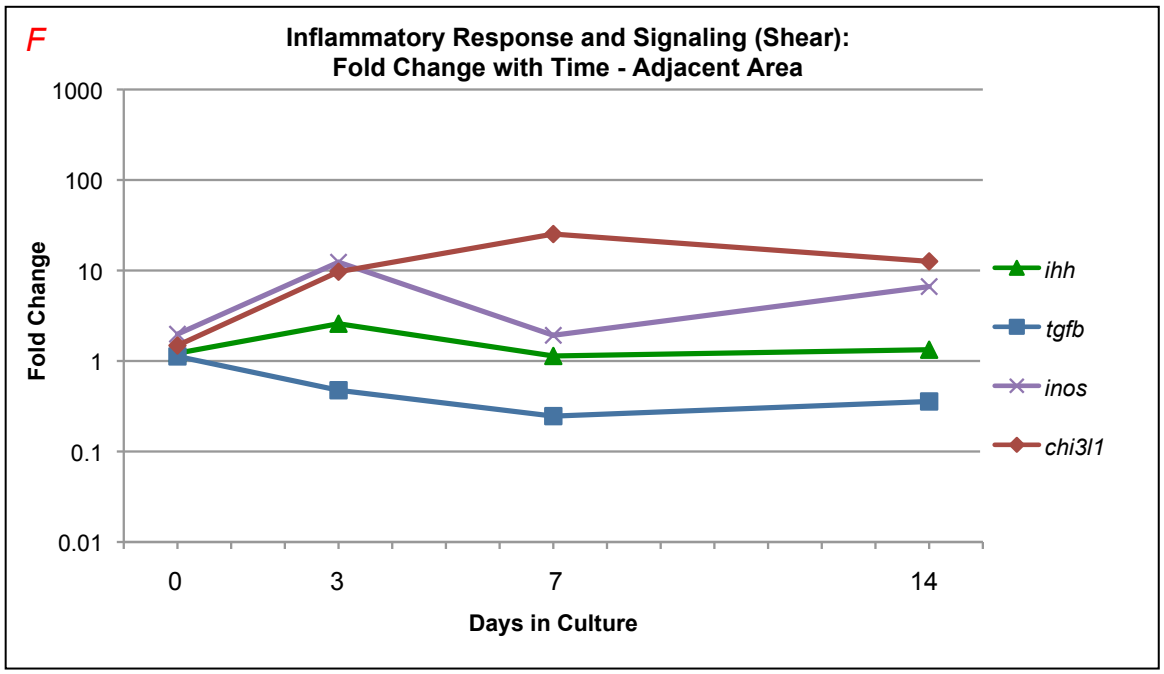
F
Inflammatory Response and Signaling (Shear):
Fold Change with Time - Adjacent Area
1000
100
10
1
0.1
0.01
Fold Change
0
3
7
14
Days in Culture
ihh
tgfb
inos
chi3l1

4.12 Cell Proliferation and Apoptosis

Genes related to cell proliferation and apoptosis (*casp-8, fas*) were evaluated for expression changes over time, differences between treatments, and differences between areas.

4.12.1 Results for *Casp-8*

Fold Change With Time:

For *casp-8* for both the AOI and ADJ specimens, there appeared to be a trend of decreasing expression over time for all treatments. The lowered expression was significant in AOI specimens at day 3, 7 and 14 for control (FC = 0.33, $q < 0.01$; FC = 0.26, $q < 0.01$; FC = 0.24, $q < 0.01$), axial (FC = 0.20, $q < 0.01$; FC = 0.15, $q < 0.01$; FC = 0.10, $q < 0.01$), and shear (FC = 0.23, $q < 0.01$; FC = 0.16, $q < 0.01$; FC = 0.31, $q < 0.01$). For the ADJ specimens the expression was also significantly lower at day 3, 7 and 14 for control (FC = 0.35, $q < 0.01$; FC = 0.47, $q = 0.03$; FC = 0.16, $q < 0.01$) and axial (FC = 0.24, $q < 0.01$; FC = 0.28, $q < 0.01$; FC = 0.30, $q < 0.01$).

Fold Change With Treatment:

A comparison of changes across treatments showed shear AOI specimens compared to axial had very little change until the last time point where there was significantly higher expression in the shear AOI specimens (FC = 2.95, $q = 0.01$). There were no discernible trends in comparing ADJ specimens across treatments.

Fold Change With Area:

AOI specimens were compared to ADJ specimens at each time point for each treatment and control AOI specimens had higher expression than ADJ at day 0, 3, and 14 (FC = 2.14, q = 0.06; FC = 1.99, q = 0.07; FC = 3.13, q = 0.01). Shear AOI expression was higher than axial at day 0 and 14 (FC = 2.00, q = 0.09; FC = 2.58, q = 0.03).

Figures 4.26 A-E. Graphs of *casp-8* by time point, treatment and area.

Figure 4.26 A. *Casp-8*: Fold change with time – area of interest. Fold change is shown on the vertical axis as a log scale. Fold changes less than one indicate lowered expression and fold changes greater than one indicate higher expression. Days in culture are shown on the horizontal axis. At each time point, day 0 control specimens are used as the reference or comparative value. Error bars (standard error) are shown for each fold change. Control specimens are plotted in blue, axial are plotted in red, and shear are plotted in green. Significant differences in expression relative to day 0 control are indicated at each time point with an asterisk (*) in the respective color of the plotted treatment.

Figure 4.26 B. *Casp-8*: Fold change with treatment – area of interest. Fold change is shown on the vertical axis as a log scale, and days in culture is shown on the horizontal axis. The treatments are compared to each other at each time point. Axial vs. Control is shown in red, Shear vs. Control is shown in green, and Shear vs. Axial is shown in orange. Error bars (standard error) for fold change are depicted, and significant differences for the respective comparison are indicated with an asterisk (*).

Figure 4.26 C. *Casp-8*: Fold change with time – adjacent area. Fold change is shown on the vertical axis as a log scale. Fold changes less than one indicate lowered expression and fold changes greater than one indicate higher expression. Days in culture are shown on the horizontal axis. At each time point, day 0 control specimens are used as the reference or comparative value. Error bars (standard error) are shown for each fold change. Control specimens are plotted in blue, axial are plotted in red, and shear are plotted in green. Significant differences in expression relative to day 0 control are indicated at each time point with an asterisk (*) in the respective color of the plotted treatment.

Figure 4.26 D. *Casp-8*: Fold change with treatment – adjacent area. Fold change is shown on the vertical axis as a log scale, and days in culture is shown on the horizontal axis. The treatments are compared to each other at each time point. Axial vs. Control is shown in red, Shear vs. Control is shown in green, and Shear vs. Axial is shown in orange. Error bars (standard error) for fold change are depicted, and significant differences for the respective comparison are indicated with an asterisk (*).

Figure 4.26 E. *Casp-8*: Fold change with area – area of interest vs. adjacent area. Fold change is shown on the vertical axis as a log scale, and days in culture is shown on the horizontal axis. The treatment areas are compared to each other within each treatment at each time point. Control is shown in blue, axial is shown in red, and shear is shown in green. Error bars (standard error) for fold change are depicted, and significant differences for the respective comparison are indicated with an asterisk (*).

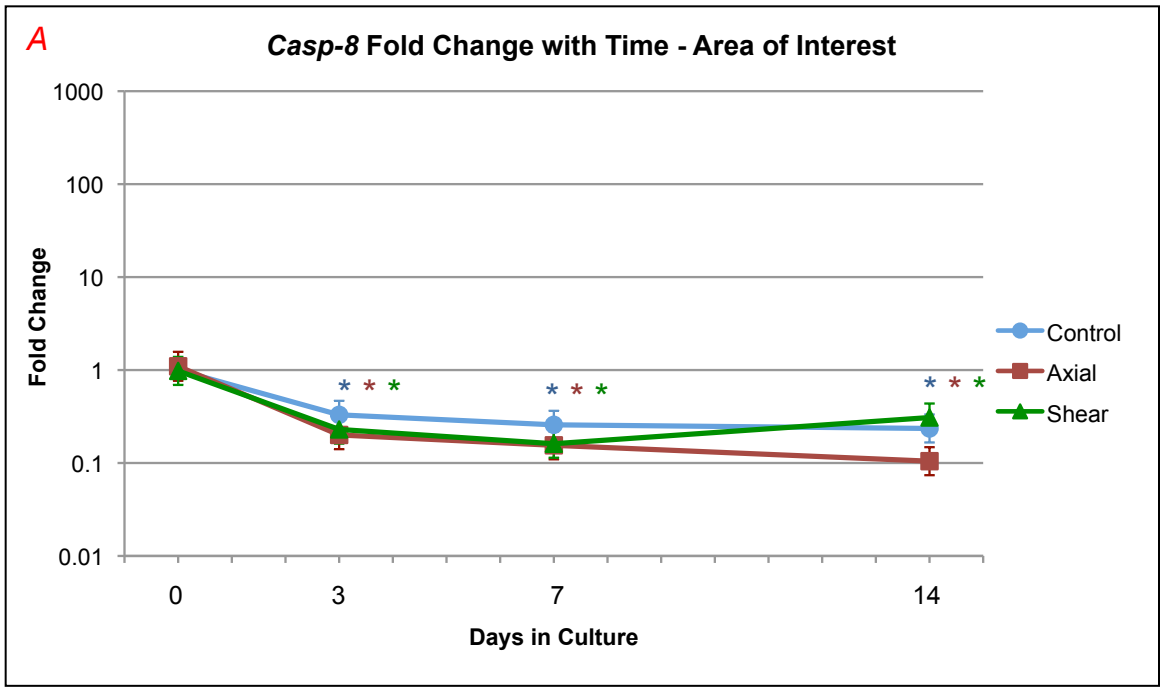
A
Casp-8 Fold Change with Time - Area of Interest
1000
100
10
1
0.1
0.01
Fold Change
0
3
7
14
Days in Culture
Control
Axial
Shear

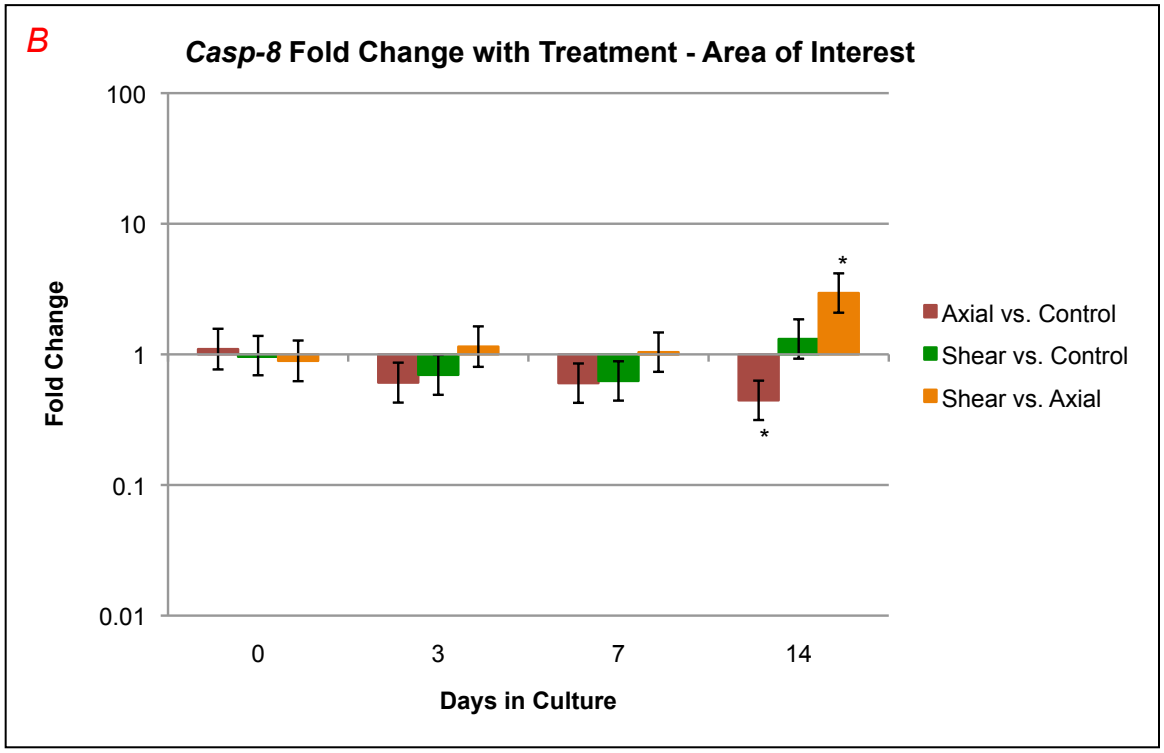
B
Casp-8 Fold Change with Treatment - Area of Interest
100
10
1
0.1
0.01
Fold Change
0
3
7
14
Days in Culture
Axial vs. Control
Shear vs. Control
Shear vs. Axial

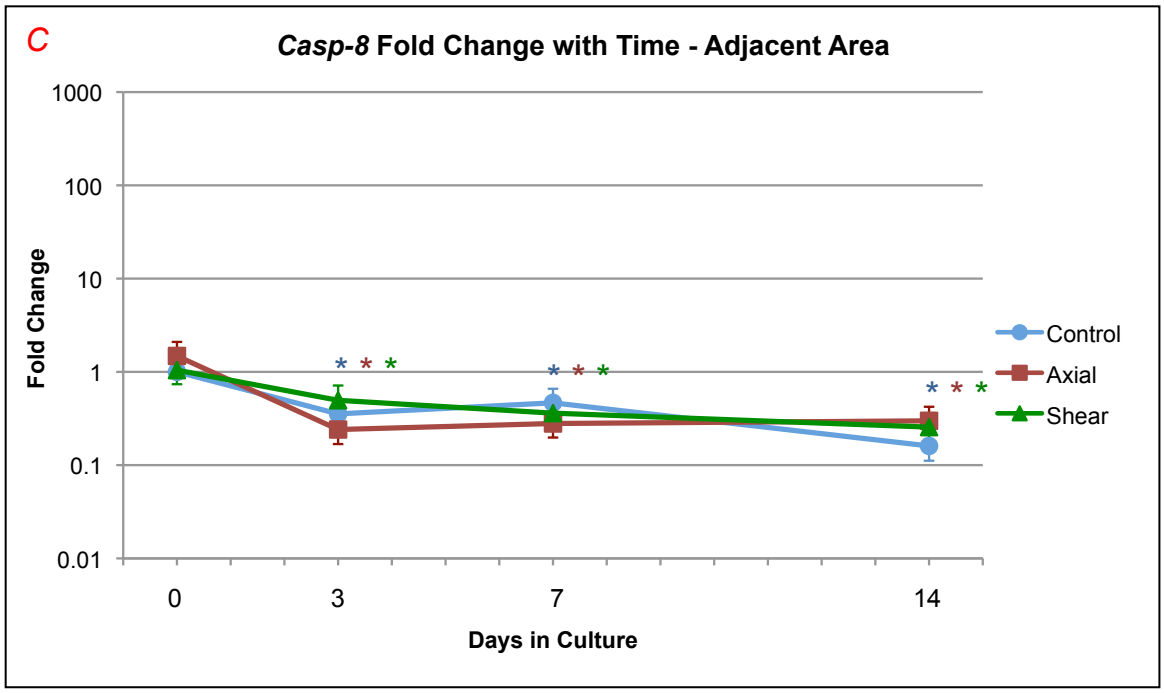
C
Casp-8 Fold Change with Time - Adjacent Area
1000
100
10
1
0.1
0.01
Fold Change
0
3
7
14
Days in Culture
Control
Axial
Shear
* * *
* * *
* * *

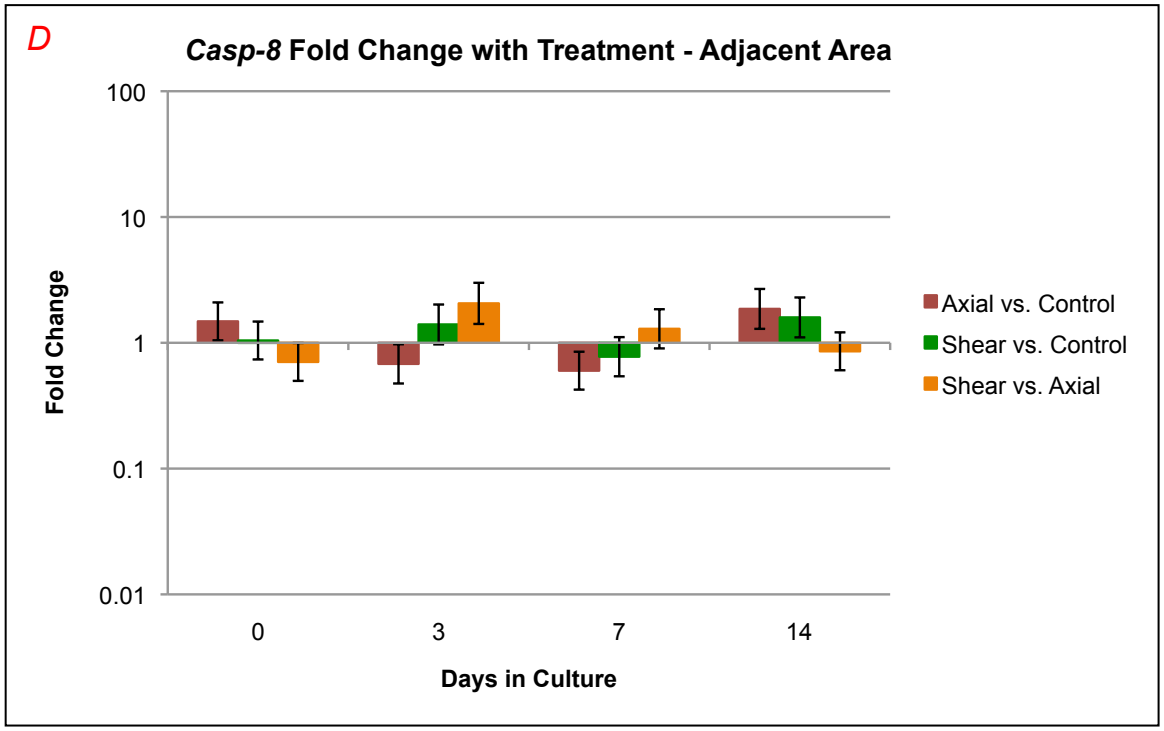
D
Casp-8 Fold Change with Treatment - Adjacent Area
100
10
1
0.1
0.01
Fold Change
0
3
7
14
Days in Culture
Axial vs. Control
Shear vs. Control
Shear vs. Axial

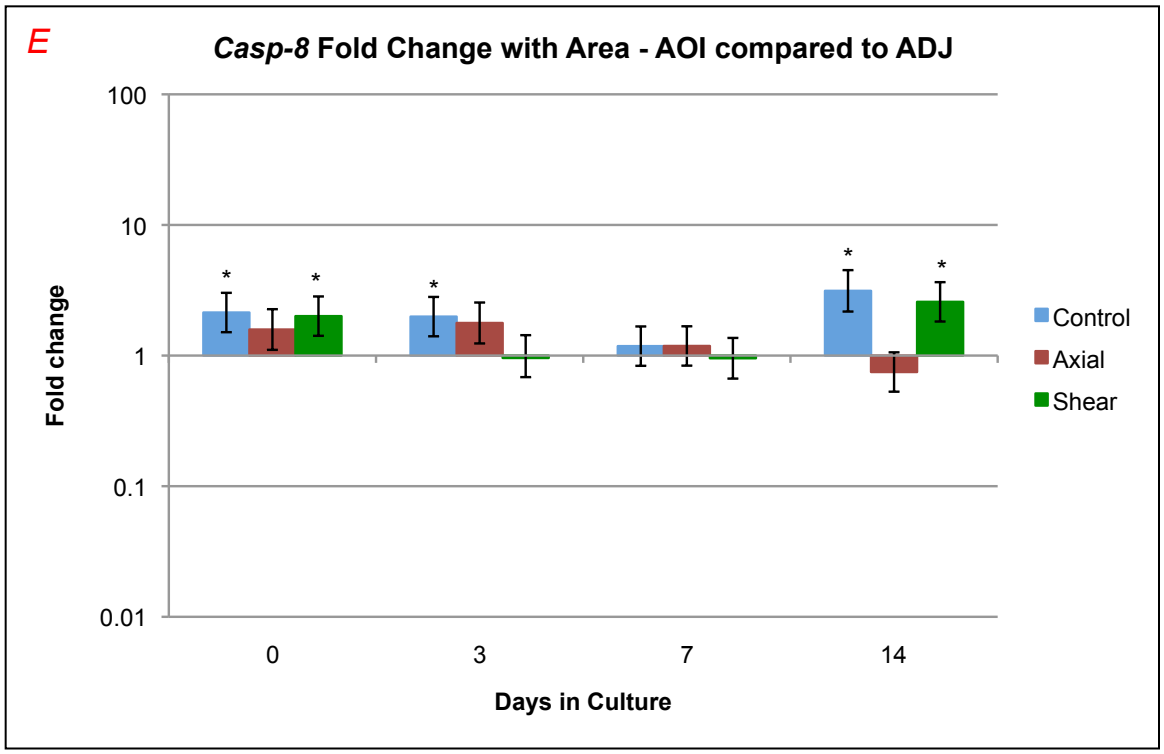
E
Casp-8 Fold Change with Area - AOI compared to ADJ
100
10
1
0.1
0.01
Fold change
0
3
7
14
Days in Culture
Control
Axial
Shear

4.12.2 Results for *Fas*

Fold Change With Time:

For both AOI and ADJ specimens the expression of *fas* remained relatively constant over time for all treatments. However, the expression of axial AOI specimens was significantly lower than day 0 control at day 7 and 14 (FC = 0.30, q = 0.02; FC = 0.40, q = 0.40). The expression of shear was lower than control at day 0 (FC = 0.35, q = 0.06).

Fold Change With Treatment:

For a comparison of treatments, the expression of shear vs. axial AOI specimens was lower initially, and then rose over time, this was significant at day 0 (FC = 0.43, q = 0.19) as well as for shear vs. control (FC = 0.35, q = 0.06). For the ADJ specimens, the expression of shear vs. axial was higher at day 0 and 14 (FC = 2.22, q = 0.15; FC = 2.19, q = 0.15).

Fold Change With Area:

Axial AOI specimens showed higher expression of *fas* at day 0 AOI vs. ADJ (FC = 2.68, q = 0.09).

Figures 4.27 A-E. Graphs of *fas* by time point, treatment and area.

Figure 4.27 A. *Fas*: Fold change with time – area of interest. Fold change is shown on the vertical axis as a log scale. Fold changes less than one indicate lowered expression and fold changes greater than one indicate higher expression. Days in culture are shown on the horizontal axis. At each time point, day 0 control specimens are used as the reference or comparative value. Error bars (standard error) are shown for each fold change. Control specimens are plotted in blue, axial are plotted in red, and shear are plotted in green. Significant differences in expression relative to day 0 control are indicated at each time point with an asterisk (*) in the respective color of the plotted treatment.

Figure 4.27 B. *Fas*: Fold change with treatment – area of interest. Fold change is shown on the vertical axis as a log scale, and days in culture is shown on the horizontal axis. The treatments are compared to each other at each time point. Axial vs. Control is shown in red, Shear vs. Control is shown in green, and Shear vs. Axial is shown in orange. Error bars (standard error) for fold change are depicted, and significant differences for the respective comparison are indicated with an asterisk (*).

Figure 4.27 C. *Fas*: Fold change with time – adjacent area. Fold change is shown on the vertical axis as a log scale. Fold changes less than one indicate lowered expression and fold changes greater than one indicate higher expression. Days in culture are shown on the horizontal axis. At each time point, day 0 control specimens are used as the reference or comparative value. Error bars (standard error) are shown for each fold change. Control specimens are plotted in blue, axial are plotted in red, and shear are plotted in green. Significant differences in expression relative to day 0 control are indicated at each time point with an asterisk (*) in the respective color of the plotted treatment.

Figure 4.27 D. *Fas*: Fold change with treatment – adjacent area. Fold change is shown on the vertical axis as a log scale, and days in culture is shown on the horizontal axis. The treatments are compared to each other at each time point. Axial vs. Control is shown in red, Shear vs. Control is shown in green, and Shear vs. Axial is shown in orange. Error bars (standard error) for fold change are depicted, and significant differences for the respective comparison are indicated with an asterisk (*).

Figure 4.27 E. *Fas*: Fold change with area – area of interest vs. adjacent area. Fold change is shown on the vertical axis as a log scale, and days in culture is shown on the horizontal axis. The treatment areas are compared to each other within each treatment at each time point. Control is shown in blue, axial is shown in red, and shear is shown in green. Error bars (standard error) for fold change are depicted, and significant differences for the respective comparison are indicated with an asterisk (*).

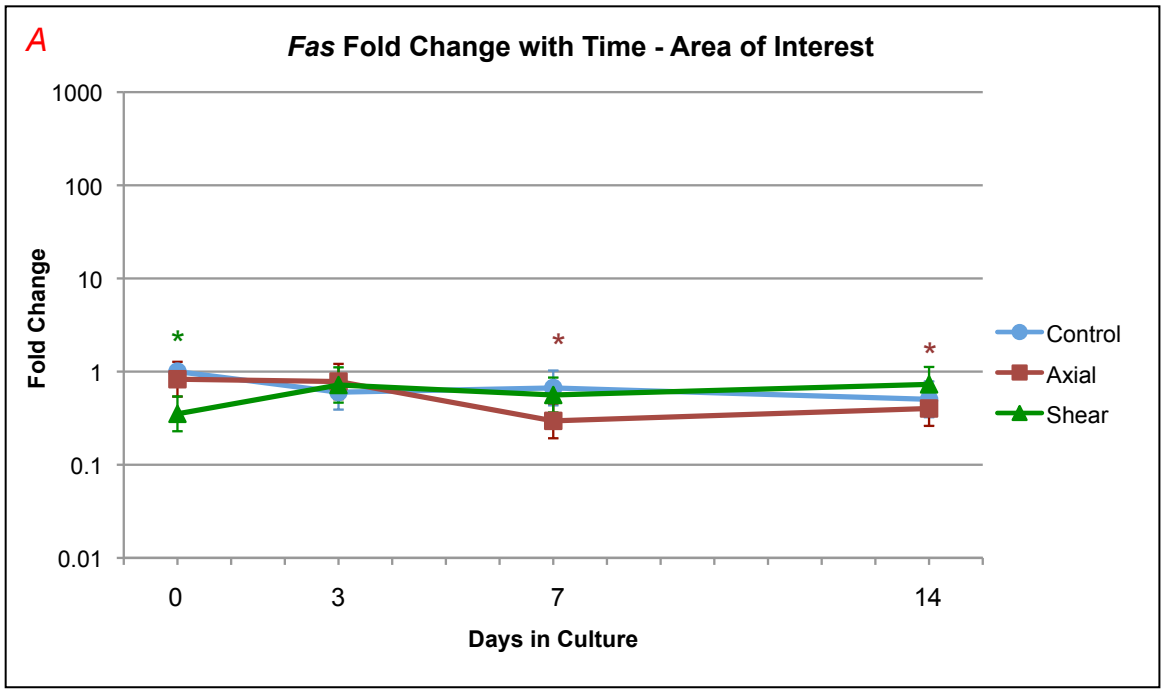
A
Fas Fold Change with Time - Area of Interest
1000
100
10
1
0.1
0.01
Fold Change
0
3
7
14
Days in Culture
Control
Axial
Shear

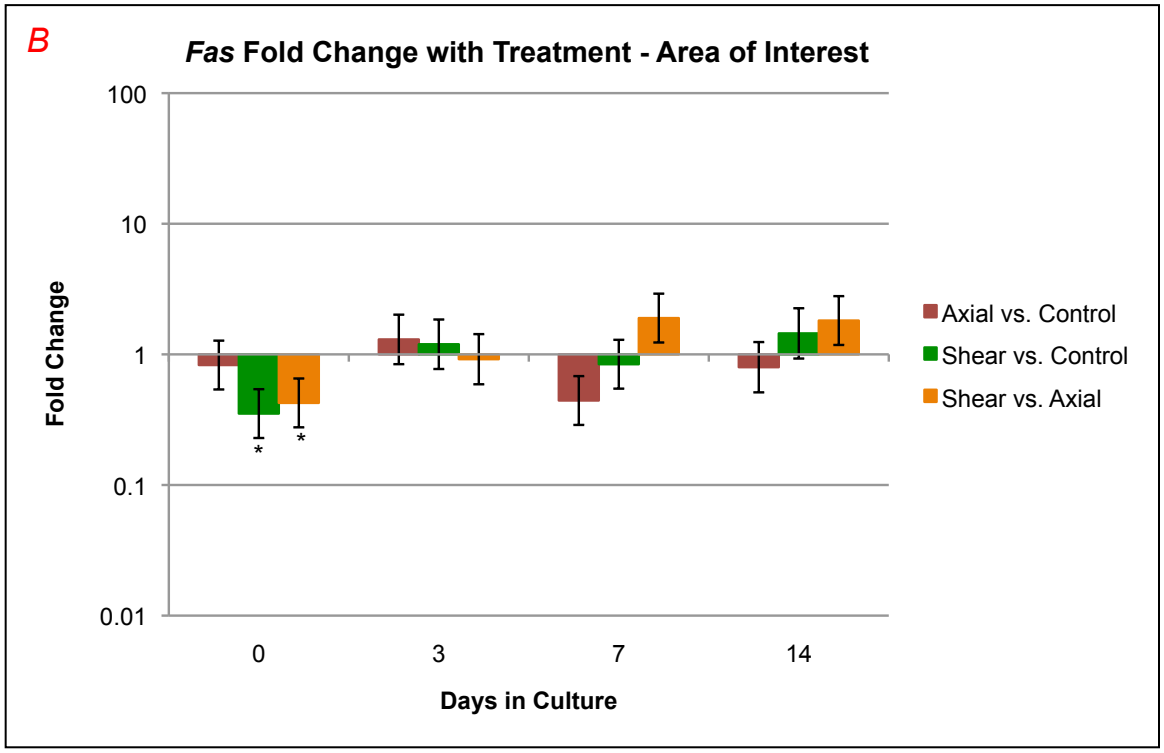
B
Fas Fold Change with Treatment - Area of Interest
100
10
1
0.1
0.01
Fold Change
0
3
7
14
Days in Culture
Axial vs. Control
Shear vs. Control
Shear vs. Axial

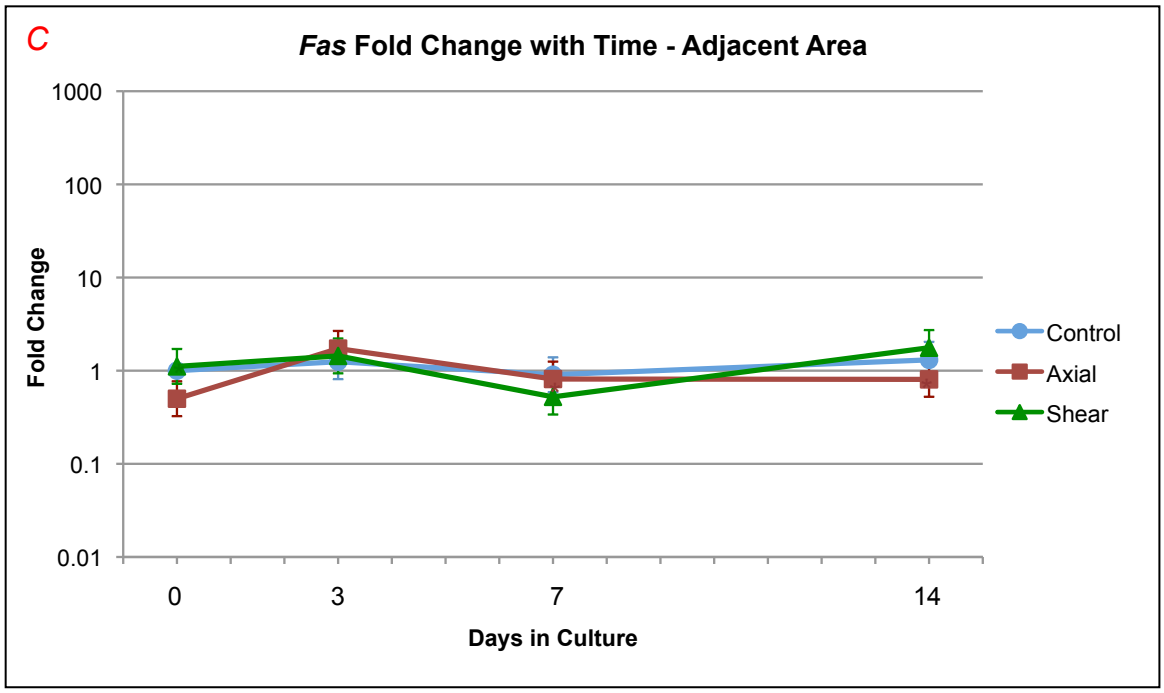
C
Fas Fold Change with Time - Adjacent Area
1000
100
10
1
0.1
0.01
Fold Change
0
3
7
14
Days in Culture
Control
Axial
Shear

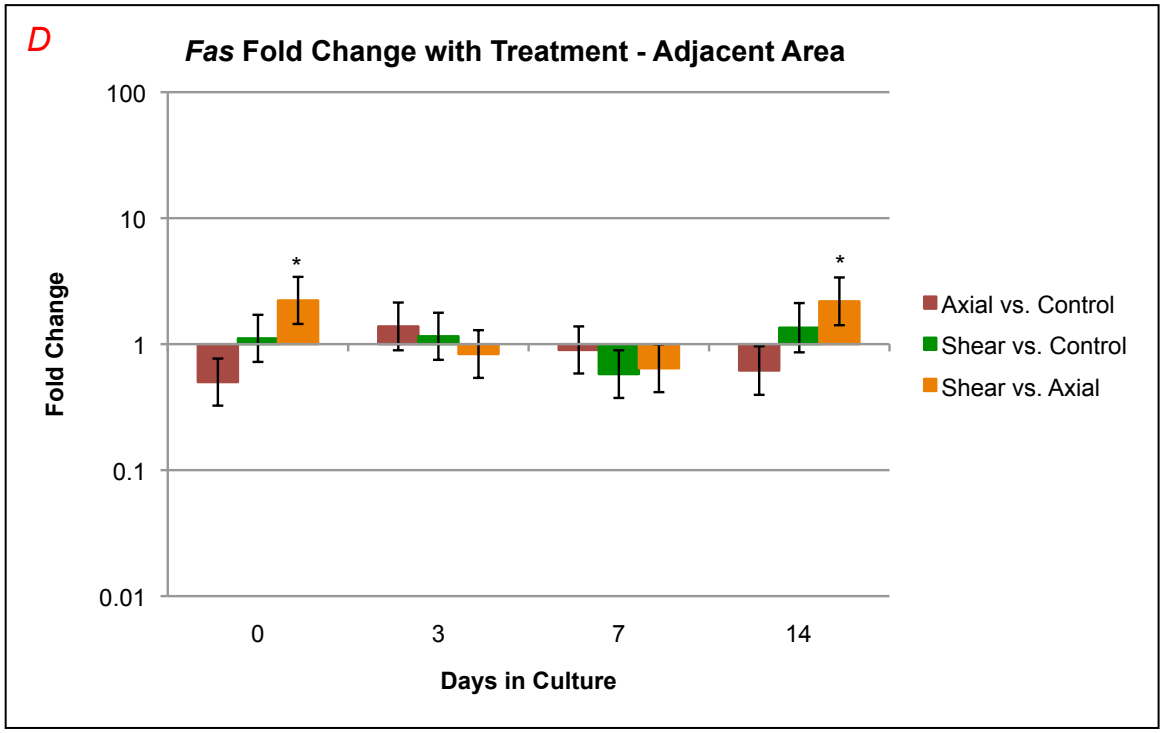
D
Fas Fold Change with Treatment - Adjacent Area
100
10
1
0.1
0.01
Fold Change
*
*
0
3
7
14
Days in Culture
Axial vs. Control
Shear vs. Control
Shear vs. Axial

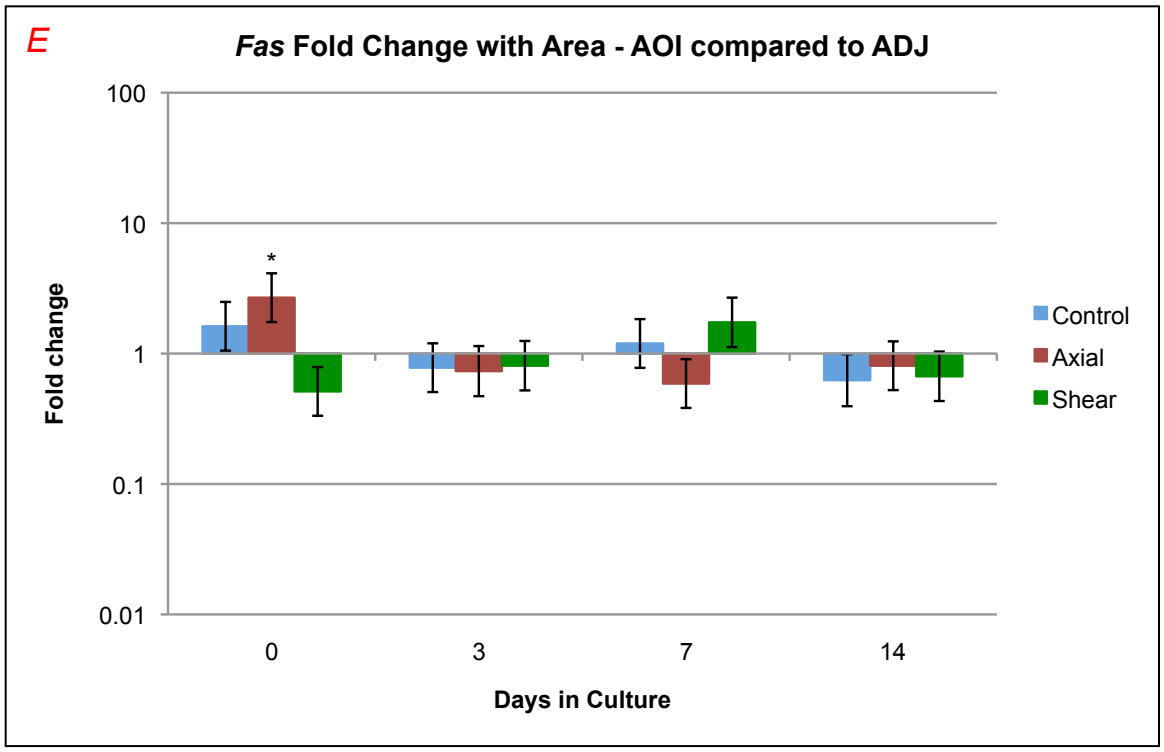
E
Fas Fold Change with Area - AOI compared to ADJ
100
10
1
0.1
0.01
Fold change
*
0
3
7
14
Days in Culture
Control
Axial
Shear

Summary of Cell Proliferation and Apoptosis:

Casp-8 showed lower expression compared to day 0 control for all treatments, and *fas* also showed generally lower expression. *Casp-8* was lower in axial compared to control at day 14, but higher in shear compared to axial at the same time point. Its expression was higher in shear AOI compared to shear ADJ at day 0 and 14. *Fas* expression was lower than day 0 control for axial AOI specimens at day 7 and 14. *Fas* had lower expression in shear vs. axial and shear vs. control at day 0.

Figures 4.28 A-F. Graphs of cell proliferation and apoptosis genes by time point for AOI and ADJ. Fold change with time – area of interest. Fold change is shown on the vertical axis as a log scale. Fold changes less than one indicate lowered expression and fold changes greater than one indicate higher expression. Days in culture are shown on the horizontal axis. At each time point, day 0 control specimens are used as the reference or comparative value. Graph A and B show changes over time for the control specimens, graph C and D show changes over time for the axial specimens, and graph E and F show changes over time for the shear specimens.

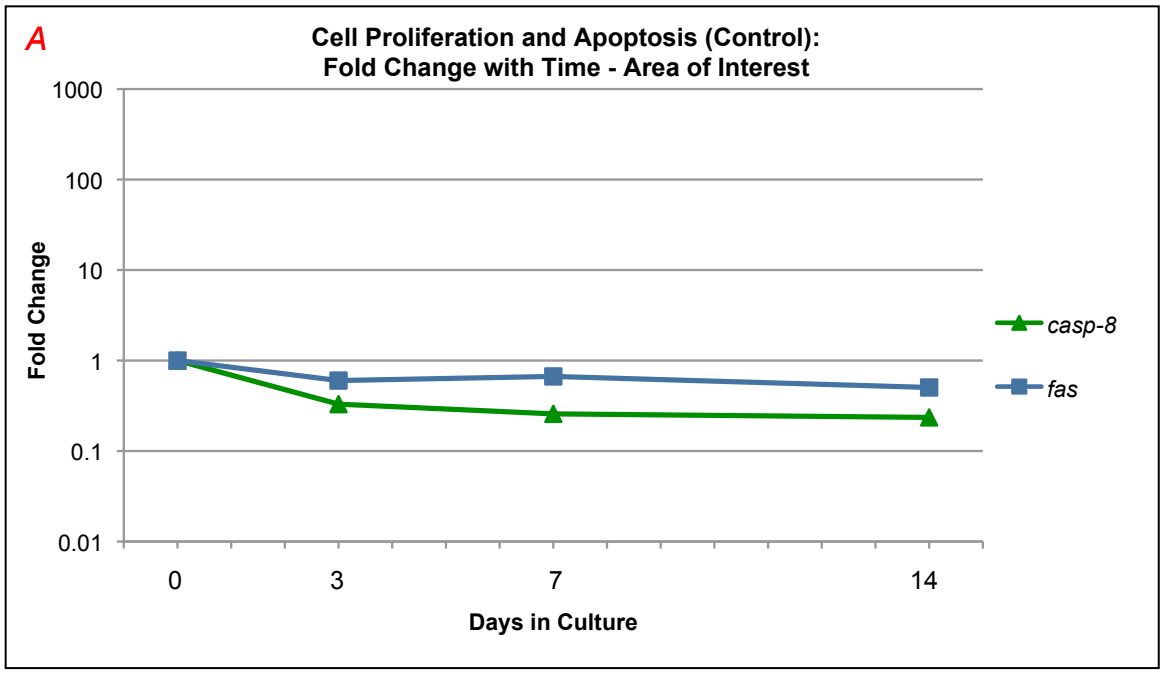
A
Cell Proliferation and Apoptosis (Control):
Fold Change with Time - Area of Interest
1000
100
10
1
0.1
0.01
Fold Change
0
3
7
14
Days in Culture
casp-8
fas

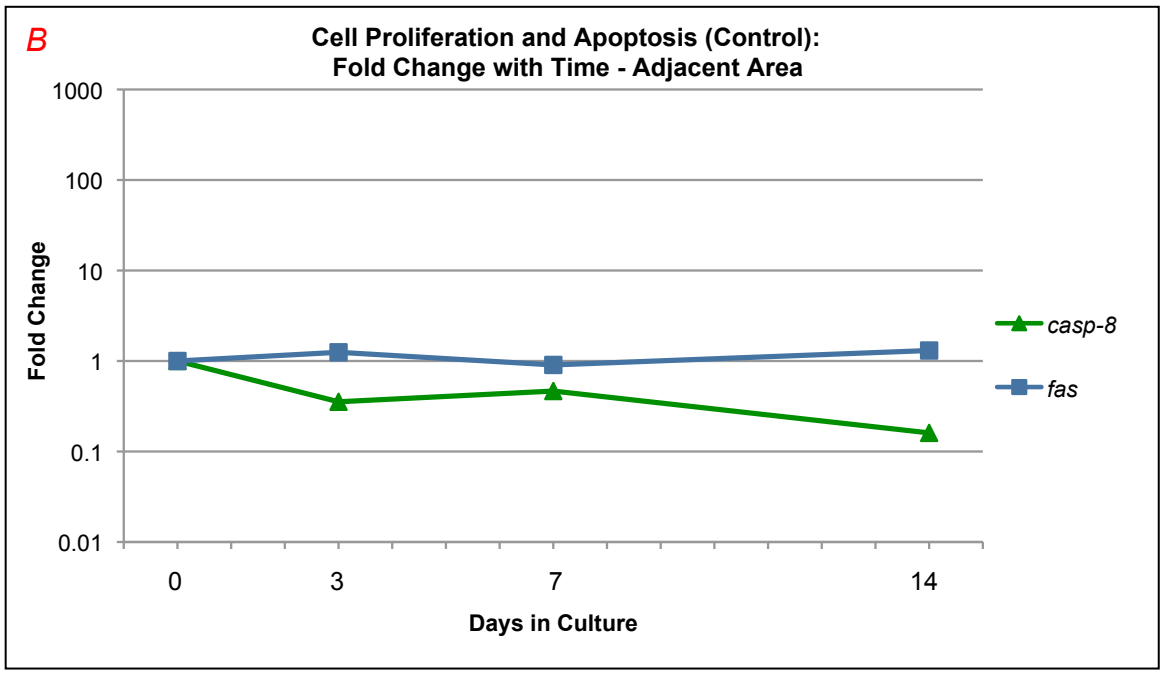
B
Cell Proliferation and Apoptosis (Control):
Fold Change with Time - Adjacent Area
1000
100
10
1
0.1
0.01
Fold Change
0
3
7
14
Days in Culture
casp-8
fas

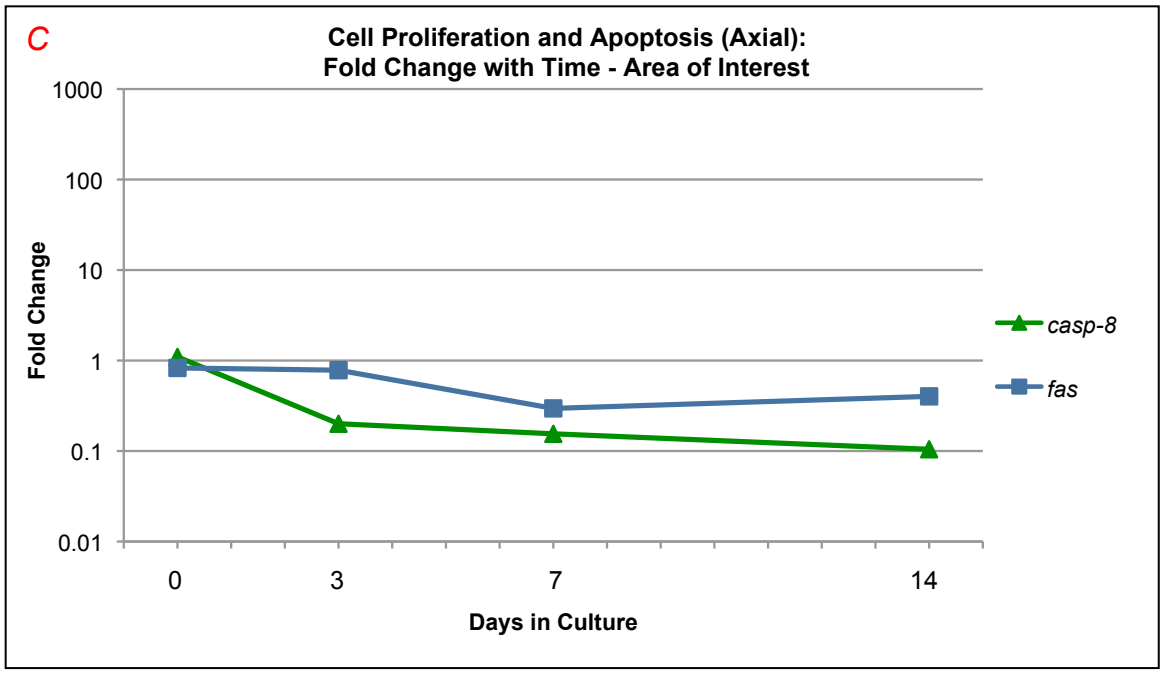
C
Cell Proliferation and Apoptosis (Axial):
Fold Change with Time - Area of Interest
1000
100
10
1
0.1
0.01
Fold Change
0
3
7
14
Days in Culture
casp-8
fas

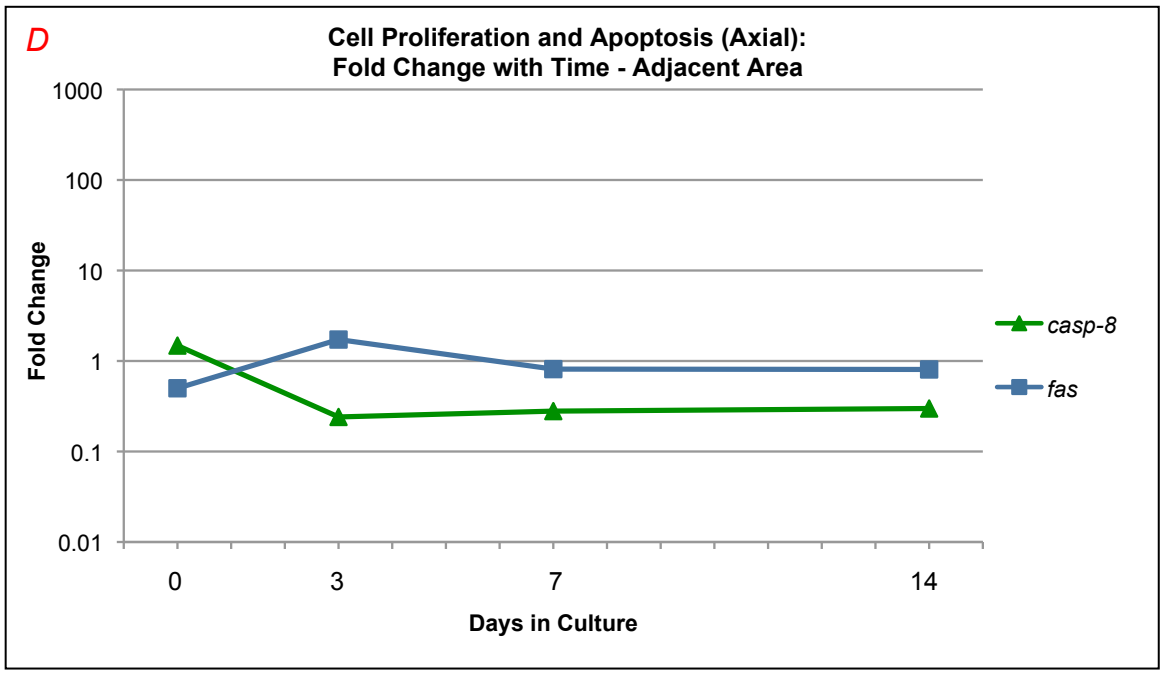
D
Cell Proliferation and Apoptosis (Axial):
Fold Change with Time - Adjacent Area
1000
100
10
1
0.1
0.01
Fold Change
0
3
7
14
Days in Culture
casp-8
fas

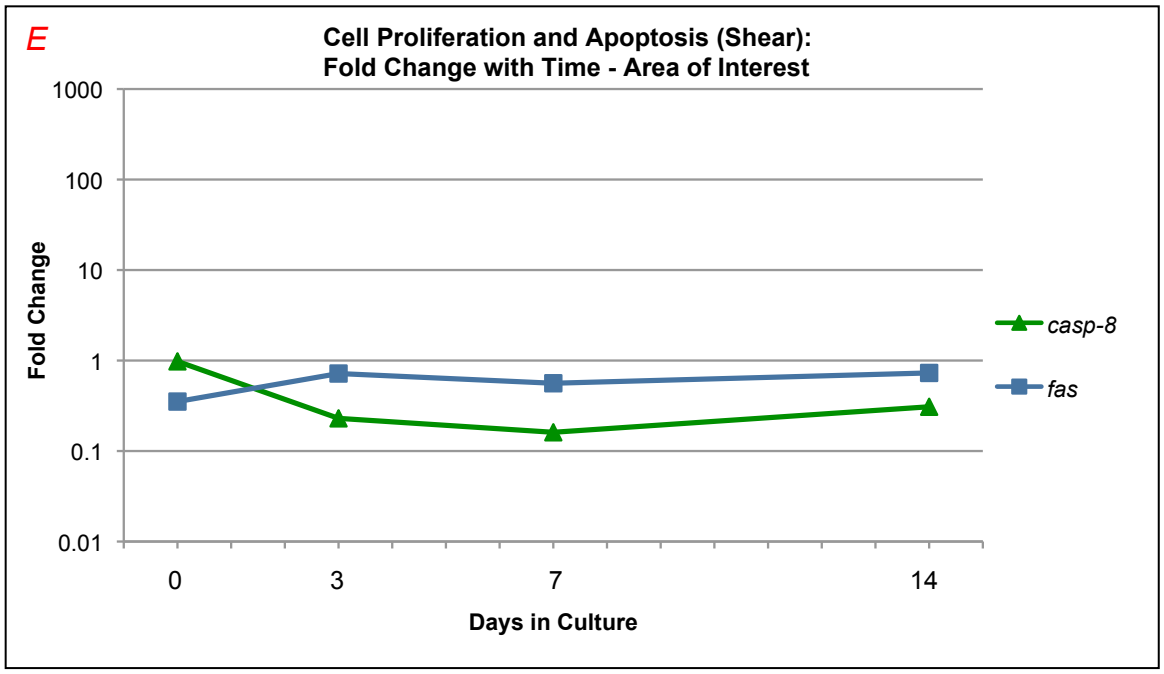
E
Cell Proliferation and Apoptosis (Shear):
Fold Change with Time - Area of Interest
1000
100
10
1
0.1
0.01
Fold Change
0
3
7
14
Days in Culture
casp-8
fas

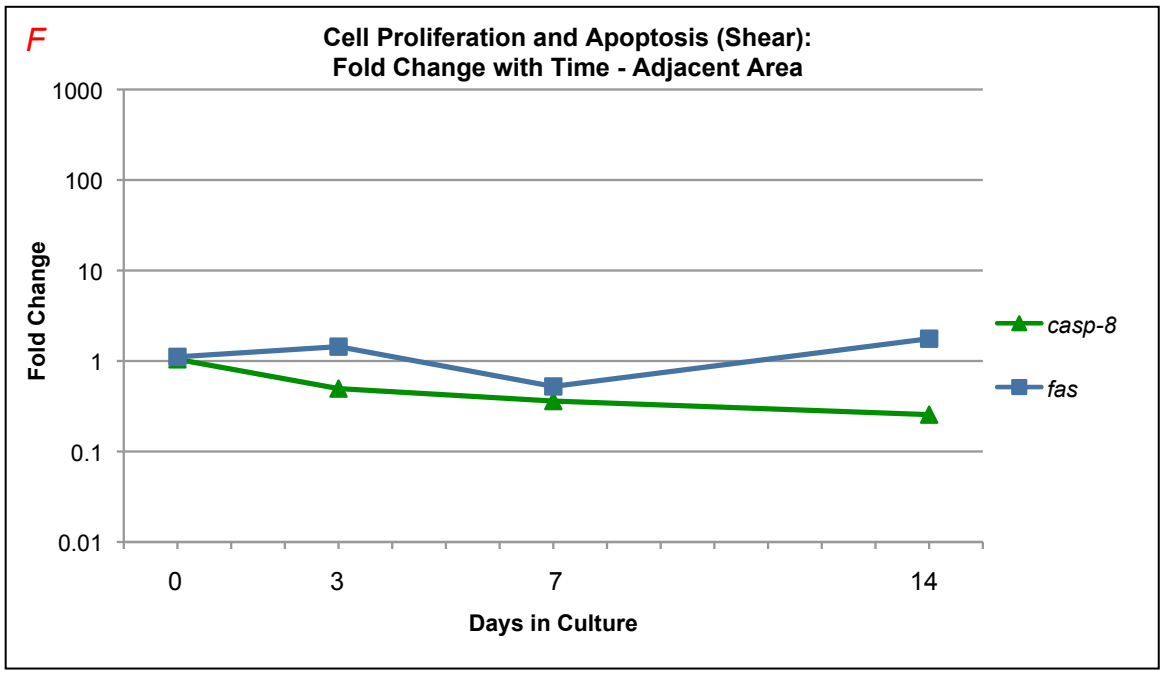
F
Cell Proliferation and Apoptosis (Shear):
Fold Change with Time - Adjacent Area
1000
100
10
1
0.1
0.01
Fold Change
0
3
7
14
Days in Culture
casp-8
fas

5. DISCUSSION

There are an estimated 27 million Americans who suffer from the painful and degenerative effects of OA [1]. Understanding the gene expression changes leading to cartilage degeneration may help identify targets for early-stage intervention to someday slow or halt the progression of OA. In this study an impact injury model was used to study chondrocyte gene expression changes in an early-stage model of OA. Three treatments were evaluated: axial, shear, and a non-impacted control. Gene expression changes were measured over different time points with qRT-PCR, a method that allows precise analysis of the expression levels. As chondrocytes are the only cells in the articular cartilage, it is crucial to understand how they govern their environment following a traumatic injury in order to understand the progression of degenerative changes and to work to identify the potential targets for intervention.

5.1 Impactions

Studying a joint injury as a model for OA is challenging, as a true physiological joint trauma will result in multiple axes of loading. While many studies have sought to load an animal joint *in vivo* [6, 47, 62, 99], the nature of the loading methods used makes it hard to quantify the direction and magnitude of the applied forces and the resulting stresses on the cartilage surfaces. Explant studies are often used to study an impact injury in an *in vitro* setting [66, 68, 70, 72]. A common method involves removing the cartilage from the subchondral bone prior to testing. However, in the methods presented here, an intact

patella was used for testing. This allowed the cartilage to stay attached to the underlying bone and prevented any changes in expression due to cutting the cartilage loose for testing. The full patellae were then kept in culture to maintain the patellae in as close to a natural environment as possible albeit without load.

Impactions were generated in a hydraulic load frame, by impacting the surface with a cylindrical stainless steel impactor tip. The cylindrical shape was chosen to reduce any chances of edge effects from a flat tip such as: gouging of the surface, or localized zones of very high stress at the edges (edge effects). Two types of impactions were used; an axial impaction consisting of a mostly normal (compressive) load, and a shear impaction with a smaller normal load and a tangential displacement to generate shear forces. The axial impactions generated mean peak normal loads of -1966 N ± 237 N, peak radial shear forces of 79 N ± 55 N, and peak longitudinal shear forces of 74 N ± 55 N. The axial impaction did not result in pure normal loads. The patellae were carefully aligned during preparation for the axial impaction to ensure that the surface was perpendicular to the loading direction. Additionally, the impactor was free to rotate about its radial axis to accommodate unevenness in the surface. However, it was not possible to get the patellae perfectly aligned and during the impactions some off-axis (non-perpendicular) loading was generated which was recorded as shear forces in the radial and longitudinal directions. These undesired shear forces were anticipated, but it was desired to have another impaction (shear) that generated significantly higher intended shear forces.

We suspect that shear stresses may play a more significant role in cartilage damage than compressive stress (axial) alone. Therefore a second loading method with increased shear forces was developed. The shear loading impactions generated a mean of peak normal load -1092N ± 205, a peak radial shear force of 198N ± 59 with smaller peak longitudinal shear forces of 60N ± 36. The shear impactions started with a normal load of 500 N applied slowly to the cartilage surface, and then a rapid (200 mm/sec) tangential displacement in the proximal-distal direction along the patella surface (the radial direction relative to the impactor) of 10mm to generate higher radial shear forces. The 500 N axial load allowed the impactor tip to deform the cartilage surface, and with the subsequent tangential displacement, the normal force rose as the impactor had to overcome the deformed cartilage. Any unevenness in the surface of the cartilage, or in the orientation of the patella, also contributed to a rise in the normal force.

The peak normal force generated in the axial impactions was 80% larger than the peak normal force generated in the shear impactions. Conversely, the mean peak radial shear force (the direction of the tangential displacement) in the shear impactions was 151% higher than the mean peak radial forces in the axial impactions. The goal of the two different impaction types was to generate one type of impaction that consisted predominantly of normal force, and a second impaction type that had significantly higher shear forces. These goals were achieved.

The model used in this experiment was an *in vitro* model of OA. An *in vitro* model provides an approximation of what may happen *in vivo*. There are many factors that cannot be replicated in a laboratory setting, therefore any findings will require substantiation with an in depth *in vivo* verification. However, an *in vitro* model does convey numerous advantages. The treatment conditions can be precisely controlled, replicates are more easily and consistently produced, and expense can be reduced.

One of the main advantages of this particular model was that cartilage was maintained attached to the underlying subchondral bone. The entire patella remained intact from the time it was removed from the knee, through impaction, and during culture. The cartilage was only removed during specimen harvesting at the appropriate time point. In a cartilage explant study, cartilage is cut from the surface of the bone and then mechanically injured and cultured. However, it is difficult to identify what expression changes were induced by the impact trauma vs. what changes were induced by cutting the specimen free. This model eliminates the expression effects of cutting the specimen from the bone. The specimens were cut free of the bone at the harvesting time point, but they were immediately flash frozen in liquid nitrogen. One risk with keeping the patella intact is that the bone lost its vascular supply. Signaling molecules and other factors from the bone may have influenced the changes observed in the cartilage. However, a large amount of media was used to fully submerge the patella and the media was changed daily. This would tend to reduce, by dilution, any factors from the bony tissue.

Another challenge of this model is that the patellae are removed from normal loading for the time course of the analysis. Normal, healthy cartilage is loaded repetitively throughout the day. However, the cartilage in this experiment received a singular loading event at the beginning of the experiment and then remained unloaded for up to two weeks. The lack of loading likely contributed to many of the changes observed. In a real joint trauma situation, though, a joint is likely to be subjected to a restricted amount of movement and loading following an injury.

A local slaughterhouse provided the porcine legs utilized for this study. The genetic lines were not controlled, and the knees could have come from a wide range of different lines of varying ages. The potential differences and lack of biological similarity tends to reduce the ability to detect smaller changes. In the human population, there is a wide variance in number of individuals to whom findings must apply. Therefore, using a wide range of differing specimens in this experimental study may prove the findings to be more relevant in translating to humans.

5.2 Tissue culture and RNA extraction

Full-thickness cartilage was harvested at the site of the impaction after either 0, 3, 7, or 14 days in culture (day 0 specimens collected approximately 2 hours after impaction). By evaluating full-thickness slices we effectively averaged the expression levels of the chondrocytes across the three depth layers. It would be desirable to study the layers independently, however the relatively small size of our specimens required use of the

full-thickness to isolate enough RNA for analysis without having to pool samples. The culture medium provides nutrients to help the cartilage cells to continue to function. Chondrocytes are the only cells found in the articular cartilage and are normally not exposed to a vascular supply or neural innervation. Thus, in the body these cells normally get their nutrients through diffusion through the cartilage matrix, and in culture they are also dependent upon diffusion [86]. Infection, or bacterial growth, is a risk of maintaining cartilage in culture for two weeks. Careful sterile removal and testing of the patellae was conducted to minimize any chance of infection, along with daily culture media changes.

Cartilage is very sparsely populated with chondrocytes spread throughout its matrix [86]. The relatively small number of cells are also embedded in a tough proteoglycan/collagen matrix. Extracting RNA from a very few number of cells trapped in a dense medium is challenging. In many, if not most, research scenarios, larger tissue samples would be used to provide more cells, and thus more potential RNA. However, in this study the sample size was dictated by the impactor geometry and resulted in relatively small specimens. In addition to the Tri Reagent, RNA was precipitated first with acetic acid [116], and a second precipitation step with ammonium acetate [139]. Both of these additional steps generated higher purity RNA as measured on a spectrophotometer.

5.3 Housekeeping Analysis

To make accurate comparisons of the genes of interest when studying a tissue, it is important to select the best reference gene(s) for normalizing Ct values. A perfect reference gene would be expressed stably across all treatment regimens for a given tissue. Although a perfect reference gene has not been found, BestKeeper and geNorm provide a method of analyzing a panel of potential genes to select the most stable housekeeping genes. A reference gene is used to control for differences in the amount of starting material, efficiency of amplification enzymes, and differences in expression from cells and the overall level of transcription [133]. Selecting a stable housekeeping gene is therefore inherently challenging. If expression of a particular gene is measured, then variation in its expression may be due to any or all of the afore-mentioned factors as opposed to actual variation in its expression by the cells. This presents a circular problem: determining a stable gene when that gene is expressed differently across samples/tissues. Therefore, both of these programs attempt to provide a measure of stability by evaluating a panel of genes by comparing their individual stability in relation to that of the entire panel.

The results of this study demonstrate that the two programs agree closely regarding the most suitable housekeeping genes. Both programs indicate that the same four genes exhibit the highest stability in porcine cartilage (across our three treatment groups and four timepoints), with only the order differing between the two methods. The most stable genes in order of decreasing stability are *gapdh*, *ppia*, *actb*, and *sdha* (BestKeeper results)

or *ppia*, *sdha*, *gapdh*, and *actb* (geNorm results). The authors of the two programs recommend between 3 and 4 housekeeping genes for an accurate normalization strategy [133, 134]. Each program is easy to use and provides an easily accessible measure of gene stability in a tissue. The two programs agreed on the top 4 most stable genes. The geNorm program provided a simpler more user-friendly interface as it is programmed in Microsoft Visual Basic Language (VBL). This makes geNorm a simpler program to use, however the equations are hidden from the user and missing values for a specimen for a particular gene cannot be accepted; the entire specimen must be removed from analysis. The user is required to calculate a Q value in geNorm, which may be an additional processing step for the user, depending upon the software associated with the qRT-PCR machine in use. BestKeeper doesn't provide as simple an interface, as it is based upon a complex Excel spreadsheet with no VBL. However it allows the user to clearly identify the calculations and steps of the program. Additionally, BestKeeper allows for direct input of Ct values, and can accept missing Ct values for a particular gene. Both programs are easy to use, however, BestKeeper was the slightly preferred method because of its ability to handle missing data, the ease of entering Ct values directly, and the transparency of calculations for each step.

The candidate housekeeping genes that were evaluated for this study (with the addition of *ppia*) were selected from Nygard *et al*. [98]. That study evaluated reference genes in 17 porcine tissues (including: muscle, adipose, skin, heart, etc.), and showed that the ideal reference genes are tissue specific, though they concluded that the ideal reference genes

for the soft tissue they evaluated were *actb, rpl4, tbp, and hprt1*. Therefore, it was important to evaluate a panel of housekeeping genes for our particular tissue and treatment conditions. Their study utilized tissue samples from 3 sibling pigs, and did not include differing treatments. Because our work involves cartilage, the intent of this study was to build on the work of Nygard *et al*. to determine the most appropriate housekeeping genes specifically for porcine articular cartilage in culture. *Ppia* was added because it has been used in previous work in our lab, it has been used as a normalizing gene for other studies examining cartilage [135-138], and it exhibited no differential expression in impacted and control specimens in our previous work [65]. This study found *ppia*, *sdha*, *gapdh*, and *actb* to be the most stable reference genes for porcine articular cartilage across our treatments and timepoints.

In addition to the Nygard *et al*. [98] study, four previous studies have evaluated reference genes for porcine tissue. Erkens *et al*. evaluated ten potential reference genes, and found that *actb*, *tbp* and *top2b* (topoisomerase 2-beta) were stable and that *sdha* appeared to be unstable in the tissues evaluated [146]. The study was conducted in porcine backfat and muscle, both of which can be expected to show different gene expression than articular cartilage. Four housekeeping genes were analyzed by Svobodova *et al*. in seven porcine soft tissues [147]. In contrast to the results of the study outlined in this paper, *gapdh* was found to be relatively unstable while *hprt1* was found to be stable. Kuijk *et al*. studied seven reference genes in different stages of porcine embryonic development [148]. Of the panel of genes, *gapdh*, *pgk1*, *s18* and *ubc* showed high stability. Nygard *et al*. [98],

Svodova *et al*. [147], Piorkowska *et al*. [149], and Erkens *et al*. [146] all showed tissue specific regulation of potential reference genes in porcine tissue. Therefore this study was critical for identifying the best reference genes specifically for porcine articular cartilage.

Gapdh has been previously used as a housekeeping gene for studies of porcine, bovine, goat sheep, and human cartilage [84, 127, 128, 132]. In an analysis of human cartilage with advanced OA, three housekeeping genes (*tbp*, *rpl13a*, and *b2m*) were selected from a panel of genes by Pombo Suarez *et al*., however the differences in selected reference genes with this study may be attributable to the difference in species [130]. Other studies of human OA cartilage have used *gapdh* and *sdha* as housekeeping genes [87, 130]. *Sdha* was also used in a canine OA study [131]. All the genes used as housekeepers in these studies were included in our panel of genes, with the exception of *rpl13a*. However, *rpl4* was included in our analysis, and like *rpl13a*, it encodes for a protein in the 60S subunit of ribosomes. Therefore, this analysis essentially included most commonly used housekeeping genes in porcine tissues and housekeeping genes used in articular cartilage regardless of species. Our findings identify the best reference genes for porcine articular cartilage following impaction treatments.

As proposed by Vandesompele *et al*., each of the best reference genes for a particular tissue can all be used for evaluating the expression levels of genes of interest [133]. This can be accomplished by taking the geometric mean (as compared to the arithmetic mean)

of the selected reference genes. The arithmetic mean is the sum of the individual n values divided by the n (the total number of values), whereas the geometric mean is the n-th root of the product of n numbers. The geometric mean is able to better control for outliers and abundance differences between genes than the arithmetic mean. The most accurate normalization strategy is to use the geometric mean of the top 3 or 4 most stable genes for normalization [133, 134].

5.4 Differential Gene Expression

The progression of OA leads to a wide range of gene expression changes [75, 76, 79, 81, 83, 84, 129, 150, 151]. The aim of this study was to identify differential gene expression changes in a model of early stage cartilage degeneration in an impact injury OA model. A panel of 18 genes believed to be related to OA progression were selected from both literature and previous work in our lab [65]. The selected genes were obtained from four different categories: cartilage matrix constituents, degradative enzymes and their inhibitors, inflammatory response, and cell proliferation and apoptosis. The first category, cartilage matrix, included: *col1a1*, *col2a1*, *agc*, *sox-9*, *opn*, and *comp*. The second category, degradative enzymes and their inhibitors, included: *mmp-1*, *mmp-3*, *mmp-13*, *timp-1*, *timp-2*, and *adamts-5*. The third category, inflammatory response, included: *ihh*, *tgfb*, *inos*, and *chi3l1*. The final category, cell proliferation and apoptosis, included 2 genes: *casp-8* and *fas*. The 18 genes selected for analysis were normalized with the geometric mean of the four reference genes (*gapdh*, *sdha*, *actb*, and *ppia*) [141].

Temporal expression changes were evaluated by measuring changes following a single impact injury from day 0 to 2 weeks. Following sterile removal of the patellae from the porcine knees, the impacts were delivered to the cartilage surface. The patellae were randomized to either a shear impact, or axial impact, or non-impacted control. The impact treatment occurred approximately 2 hours following removal of the patella from the knee. The day 0 cartilage specimens were harvested within approximately 2 hours of the delivery of the impact. Similar timelines were followed for the non-impacted control specimens, to insure consistency and comparability of results. The subsequent 3, 7 and 14 day specimens were collected the requisite number of days later and at approximately the same time of day as the day 0 specimens. It is difficult to harvest all the specimens at the precise time as the day 0 specimens, but small differences in time of harvest over the period of 3, 7 or 14 days likely had negligible effects on the findings.

Three types of analyses were conducted. For each gene, differential expression was evaluated over time within each treatment. For a particular treatment (control, axial, and shear) the expression changes at each time point were evaluated compared to the day 0 control expression. Changes to cartilage gene expression can happen at very early time points following an injury [75, 83, 84, 151, 152]. Therefore it was anticipated that some changes may have begun in the impact specimens during the approximately two-hour delay before tissue harvest. The expression changes at day 0 for the treatment tissue were thus compared to day 0 control, and each subsequent time point was compared to day 0 control as it represented the tissue most closely related to normal cartilage in the porcine

body. The second type of analysis conducted was to evaluate the expression differences between each treatment at each time point. This was important to evaluate whether the changes at a time point were due to culture conditions or due to the impact treatment. Both axial and shear specimens were compared to control, and shear was also compared to axial at each time point. Finally, the under the impactor (AOI) specimens were compared to the surrounding adjacent tissue (ADJ) specimens at each time point for each treatment to identify any differences in expression for the tissue AOI and the ADJ.

Cartilage Matrix

Col1a1 expression increased over the course of the time points in control, axial and shear specimens, while *col2a1* expression decreased over time for all treatments. In the area of interest specimens, *col1a1* was most highly expressed in the axial specimens with a 64 fold change from day 0 control. The rise in expression of *col1a1* may indicate that the chondrocytes are reverting to a more fibroblastic phenotype indicative of their attempt to initiate repairs. However, this is the incorrect collagen for maintenance of the cartilage matrix. However, *col2a1*, the normal collagen found in the matrix, showed lower expression over time in all treatments, indicating that the chondrocytes are not able to maintain normal collagen production, consistent with previous findings [153]. In that study, Natoli *et al*. impacted bovine ulnar cartilage with a drop tower, and evaluated gene expression at 24 hours, 1 week and 4 weeks. *Col1a1* was down-regulated in the high impact specimens (impacted with 2.8 J) at 24 hours, but then rose by 1 week, and then was up 370 fold by 4 weeks. While our time point of 2 weeks falls in between the 1

week and 4 weeks evaluated by Natoli *et al.,* our fold change over time of 64 in the axial specimens is consistent with their findings. Their study also showed a slight increase in *col2a1* expression at 24 hours, consistent with our findings in the day 0 specimens. Additionally, they showed *col2a1* expression dropping at the later time points, again consistent with our findings. Fehrenbacher *et al.* cyclically loaded porcine bone-cartilage plugs in compression with loads up to 6 MPa, attempting to simulate a damaging *in vivo* load, and maintained the explants in culture for 16 hours [83]. The findings showed that collagen I and II levels significantly decreased at 16 hours, this was consistent with the initial drops in *col1a1* and *col2a1* expression that we found. It is believed that chondrocytes may dedifferentiate in OA [67, 69, 154]. These dedifferentiated chondrocytes are of a more fibroblastic phenotype and express *collagen I, III*, and *V* [154], not the type II found in articular cartilage. When the treatments were compared to each other at each time point, *col1a1* was significantly up-regulated at day 3 in shear compared to control, and at day 0 and 3 when shear specimens were compared to axial. However, *col2a1* was also more highly expressed at day 3 in shear compared to axial specimens. Both *col1a1* and *col2a1* tapered in both axial and shear AOI specimens compared to control by day 7. When comparing the ADJ specimens, axial specimens showed an increase in *col2a1* over control at day 14. This may indicate that the tissue in the surrounding area of the axial impaction has triggered a repair process, and is capable of producing normal collagen. The changes in AOI and ADJ specimens may indicate that the shear specimens are attempting a stronger repair effort, but with incorrect matrix constituents.

Agc, *sox-9*, and *comp* all showed lowered expression over time in all treatments. When the treatments were compared to each other, however, *sox-9* was significantly lower at the day 3, 7 and 14 day time points. Additionally, *sox-9* showed higher expression in shear vs. axial at day 14. *Sox-9* encodes the SOX-9 transcription factor for both *agc* and *col2a1* and stimulates the expression and maintenance of the chondrocyte phenotype [13, 81, 91-93, 155], and its lowered expression over time after an injury is consistent with other studies. In one study, Fitzgerald *et al.* slowly compressed bovine cartilage explants to 25 to 50% strain and maintained the strain for time periods up to 24 hours [84]. The expression of *sox-9* was down regulated at 24 hours. *Sox-9* has also been found to be down-regulated in the presence of naturally occurring OA [80]. In this study, Brew *et al*. took samples from OA patients and quantified gene expression changes and found decreased expression of *sox-9*. The higher expression of *sox-9* at day 14 in AOI shear specimens vs. axial may be consistent with the shear specimens attempting to mount repair efforts, and may indicate that the axial impacted specimens are less successful at mounting repairs. *Agc* expression was lowered over time for both axial and shear specimens, and this is consistent with the findings of Fitzgerald *et al.* [84]. However, *agc* was found to be more highly expressed in shear compared to axial in both the AOI and ADJ specimens, consistent with *sox-9* expression. *Comp* expression was significantly lower in the AOI shear specimens compared to axial at the 0 day time point. *Comp* encodes for an abundant extracellular matrix protein, however its function is not fully known [88]. It is a marker for OA progression and generally rises over time in OA [59,

101] with the highest expression being present in late stage OA [103]. In one cyclic tension and hydrostatic pressure study of cultured chondrocytes, alginate constructs seeded with chondrocytes were loaded with tension of 9% strain or hydrostatic pressure up to 5 MPa for 3 days [77]. Gene expression changes were measured afterward, and *comp* was found to be more highly expressed in the cyclic tension model, but unchanged in the compression model. The tension model with the lower level strains, may have more closely represented normal load levels. The compression findings showed no change in *comp* expression, unlike our impact generated compression. However, the differences between cultured chondrocytes in an alginate scaffold and chondrocytes in their native cartilage matrix make exact comparisons difficult. The lowered expression of *comp* in shear compared to axial may be indicative of matrix degradation [20, 59], possibly because the shear specimens experienced more damage during the loading event.

Degradative Enzymes and Inhibitors

Matrix metalloproteinases are enzymes that breakdown the cartilage matrix through degradation of collagen and other matrix proteins. *Mmp-1* and *13* are both collegenases, and *mmp-3* is a stromelysin that breaks down other matrix proteins. *Mmp-1*, *3*, and *13* all showed increased expression over time in all treatments. Likely a large contributing factor is the effects of removing the patellae from the *in vivo* environment and placing them in culture. However, when treatments were compared at each time point, *mmp-1* was lower in shear AOI compared to axial at day 14 and in axial ADJ compared to control, and shear ADJ compared to control. This may be an attempt on the part of the

chondrocytes to maintain the cartilage matrix. *Mmp-3,* on the other hand, was higher in shear AOI compared to control at day 0, and in shear ADJ compared to axial ADJ. *Mmp-13* showed higher expression at day 0 in axial AOI compared to control, but by day 3, *mmp-13* was more highly expressed in shear AOI compared to both control and axial. The higher early *mmp* expression in shear specimens may suggest more repair efforts underway that taper over time. In the high loading model used by Natoli *et al*., *mmp-1* expression was found to be up-regulated in the loaded samples at 24 hours, but the expression then tapered by the later time points [153]. This differs with our findings, however the use of explants by Natoli *et al*., may generate differing responses from our impact loading model where the cartilage remains on the patellae. Fitzgerald *et al.* found both *mmp-3* and *aggrecanase* to have elevated levels in their static compression model where changes were measured at 24 hours [84]. Consistent with our findings, Lee *et al*. also found *mmp-3* levels to be higher at 3 and 24 hours after impaction [81]. Aigner *et al*., in a study of natural OA found *mmp-3* to be up-regulated in early stage OA, and down regulated at later stage [68]. However, *mmp-13* was found to be up-regulated in early stage OA. While the rise in expression of *mmp* levels in this study is consistent with our findings over time, we did see a relative rise in *mmp-13* levels at the day 0 time point compared to control. The elevation at the earliest time point may be due to trauma of the impact, and not necessarily indicative of the progression of OA. *Timp-1* expression was higher across the time points, while *timp-2* expression was lowered across the time points compared to day 0 control. *Timp-1* and *timp-2* are both general inhibitors of mmp action and are not specific to a particular mmp. Natoli *et al.* found elevated

levels of *timp-1* at 24 hours following loading, but the levels then decreased at the later time points of 1 and 4 weeks following impaction [153]. This is not consistent with our findings for *timp-1*, but it may be related to their study being conducted on explants. However, Lee *et al*. found that *timp-1* levels increased up to 12 fold in the 24 hours following an injurious compression, whereas *timp-2* increased by only 2 fold over the same time period [81]. These findings are more consistent with ours. Wong *et al.* found in both their cyclic tension and hydrostatic loading that *timp-1* and *2* demonstrated lower expression [77]. *Timp-1* and *2* were found to be unaffected when Blain *et al.* applied compressive loading to bovine explants and measured the changes over 6 hours [156]. Clearly, the experimental design affects the expression changes measured. When treatments were compared, *timp-2* had lower expression in axial AOI compared to control, but had higher expression in shear AOI compared to axial at day 0 and 3. Timps are general inhibitors (non-specific to a particular *mmp*) of mmp action, and this may be indicative of attempts in the shear specimens to limit matrix breakdown during repair. Finally, *adamts-5*, an aggrecanase, was lower in axial AOI compared to control at day 0, and lower in both shear compared to control and to axial at the later time points. The ADJ specimens for both shear and axial significantly higher expression over time and *adamts-5* was elevated at day 0 in shear ADJ compared to control ADJ. These increases in *adamts-5* are consistent with Fitzgerald *et al*.'s findings of increased expression of another aggrecanase, *adamts-4*, in a compression injury model followed over 24 hours. These changes may indicate that the tissue in the ADJ specimens are undergoing more repair efforts due to their expression of higher levels of *aggrecanase*.

Inflammatory Response and signaling:

Ihh, a signaling molecule associated with chondrocyte proliferation, showed no significant expression changes or trends over time, or for treatment comparisons, with the exception of a decreased expression in axial AOI relative to control at day 3. *Ihh* had higher expression in the shear AOI specimens compared to shear ADJ at day 0, 7 and 14. The decreased expression in axial specimens would be consistent with another OA model, where Kim *et al*. surgically induced OA in a rat ACL transection model and found *ihh* expression decreased over 12 weeks [110]. However, the higher expression seen in the shear specimens (though not significant) is more in line with other studies of early stage OA. Tchetina *et al.* found increases in *ihh* expression in early stage naturally progressing OA in human articular cartilage [93]. *Ihh* was also elevated in more progressed human OA lesions as reported by Swingler *et al.* [87]. *Tgfb* is critical in the inflammatory process which involves the recruitment of white blood cells, fibroblasts and the rebuilding of vascular supply following damage [106]. In our findings, *tgfb* had consistently lower expression over time in all treatments compared to day 0 control, but was higher at day 3 for axial AOI compared to control. *Tgfb* also had lower expression in shear AOI compared to axial at day 0 and 3 but had higher expression than axial at day 14. *Tgfb* may be critical part of the inflammatory process for initiating repairs of the cartilage matrix and aiding cell proliferation, and lack of its expression may coincide with OA development [108]. The increased expression in the axial specimens is consistent with Lee *et al*. who found elevated *tgfb* levels at 24 hours following injurious

compression of bovine cartilage explants [79]. Limiting *tgfb* expression through pharmacological means may prove possible [157]. Another signaling molecule, *inos*, that is part of an inflammatory response and is believed to stimulate production of Prostaglandin E2 [158] which contributes to collagen and aggrecan degradation [159]. *Inos* was generally more highly expressed over time in control, axial and shear and in both AOI and ADJ areas. This may be related to an inflammatory or apoptosis response by the chondrocytes after being placed in culture. When comparing treatments, however, at day 14 *inos* had lower expression in both shear and axial AOI compared to control. Its possible that early rises in *inos* tapered by the later time points as the chondrocytes initiated more thorough attempts at repairs. This is important if the cells are to combat OA progression as *inos* typically is involved in inflammation and in OA development via chondrocyte hypertrophy or inducing apoptosis [73, 115-117]. *Inos* expression may have potential as a target of inhibition via pharmacological treatment [160-162]. Another gene associated with an inflammatory response is *chi3l1*, which is an inflammatory marker whose role is not entirely clear [163], but it may play a role in cartilage remodeling [113]. It showed consistently higher expression over time for all treatments. When treatments were compared however, *chi3l1* had lower expression in both axial and shear compared to control at day 14, but showed higher expression in shear compared to control at the day 0 time point. The lowered expression compared to control at day 14 is consistent with our findings in a SAGE analysis of impacted cartilage at 14 days [65]. Its higher expression initially in the shear specimens may be indicative of early damage and an associated inflammatory response as identified by Volck *et al*. in a study of naturally

occurring OA [112]. Another study also found *chi3l1* levels to increase over 2 weeks in an immobilization model of OA in rat knee cartilage by Trudel *et al.* [164]. *Chi3l1* production also increased in monolayer chondrocytes placed in culture [113]. The expression of *chi3l1* may be related, therefore, with lack of loading when cartilage is placed into culture.

Cell proliferation and Apoptosis:

Casp-8 and *fas*, both linked to cellular apoptosis were evaluated. Over time, both *casp-8* and *fas* showed similar trends and generally lower expression when compared to day 0 control. *Casp-8* was lower in axial compared to control at day 14, but higher in shear compared to axial at the same time point. Its expression was also higher in shear AOI compared to shear ADJ at day 0 and 14. *Casp-8* initiates the caspase apoptosis pathway and higher expression has been linked to OA. In a study of aged rabbits with normal cartilage, Allen *et al.* found increases in *casp-8* expression believed to be a prelude to the development of OA [165]. When OA was induced in an ACL transection model in rabbits by Pennock *et al*., *casp-8* was found to be significantly up-regulated [122]. The higher expression in shear compared to axial at the last time point may be indicative of a higher degree of apoptosis, and more cartilage damage. *Fas*, another gene associated with apoptosis, demonstrated lower expression in shear compared to control at day 0 and in shear compared to axial at day 0. However, shear ADJ specimens had higher expression of *fas* than axial at both day 0 and day 14. *Fas* expression has been found to be region specific in cartilage with the highest expression in the immediate vicinity of

OA lesions [126]. Like *casp-8*, Allen *et al*. found *fas* is also elevated in aged cartilage prior to OA development [165]. The higher relative expression in the shear ADJ tissue is likely due to the trauma induced by hydrostatic pressure buildup in the cartilage matrix during the shearing impaction. Elevated levels of apoptosis correlates with earlier work in our lab that found increased apoptosis compared to control at 14 days [166].

Summary and interpretation of findings:

The aim of this study was to evaluate differential chondrocyte gene expression levels following axial and shear impact injuries to articular cartilage in order to develop an understanding of the early changes that initiate the degenerative process that may lead to OA. The two types of impactions were compared to each other and to a non-impacted control over a two week time period. It was hypothesized first that the impact treatments would cause increased matrix repair efforts, higher degradative enzyme activity, an inflammatory response, and elevated levels of apoptosis. It was also anticipated that the impact with higher shear stresses would show higher levels of degradative enzymes and inflammatory response as compared to the axial specimens. The last hypothesis was that the tissue adjacent to the impact area would suffer more damage in the shear impacted specimens as identified by increased degradation, inflammation, and biological stress signaling.

As this study is an analysis of biological specimens, the interpretation of the findings is complex. However, it is believed that the finding of the first hypothesis is supported.

Col2a1 expression is higher at day 3 in the shear vs. axial specimens indicating a repair effort underway; however there is also a relative rise in *col1a1*, a collagen not normally expressed in articular cartilage, expression indicating the repair efforts in the shear specimens are perhaps not being effectively accomplished. Increased expression of *agc* and *sox-9* at the later time points in shear vs. axial specimens also indicates a repair attempt underway. *Mmp* levels are higher initially in both axial and shear vs. control, but taper by the later time points, indicating the initial matrix breakdown may be tapering off. *Timp-2* was increased in shear vs. axial at the earlier time points, indicating shear specimens were attempting to limit matrix breakdown. Lowered expression levels of genes associated with an inflammatory response in shear and axial vs. control, may indicate that the cells are trying to recover by slowing or halting the inflammatory process. The rise in *casp-8* in shear relative to control indicates more apoptosis in the shear specimens. Therefore, in support of the first hypothesis it is believed that a repair effort is underway in both axial and shear specimens, with a stronger repair effort being attempted by the shear specimens.

When the tissue adjacent to the impact area was evaluated, it was observed that there were initial rises in *col1a1* in both axial and shear vs. control, and increases over time in *col2a1* production. At both day 0 and 7, *col2a1* expression was lower in shear ADJ vs. axial. At the last time point, there was higher expression of *agc* expression in shear relative to axial, indicating a potential stronger repair effort. There was initially higher *mmp-3* levels in shear compared to axial, and elevated *timp-1* levels in the shear ADJ

specimens at the last time point. There was a decreased expression of inflammatory genes at day 3 and 7 in shear vs. axial, and an increase in apoptosis related *fas* at day 0 and 7 in shear specimens. Therefore, the lower expression of *col2a1* in shear specimens, the early rise in *mmp-3*, and the higher expression of *fas* all potentially indicate that more damage may have occurred in the shear ADJ specimens that were subsequently unable to render an effective repair effort. Therefore it is believed that the second hypothesis was supported that the shear injury caused more damage than the axial injury.

5.5 Limitations and Areas of Further Work

With any analysis or experiment, lessons are learned and areas for improvement are identified. Additionally, it is important to identify any limitations of the experiment in relation to conclusions that may be made.

In measuring gene expression levels, the mRNA of chondrocytes was being measured to determine what genes were being differentially expressed based upon our treatments. These measurements were from the living chondrocytes in the matrix at the time of tissue harvesting. However, the size of these cell populations and how they varied from one specimen to another is unknown. It is possible that a particular treatment resulted in higher rates of cell death. For example, the area of tissue directly under the impactor may have had a higher percentage of dead cells compared to the area of tissue adjacent to the impact site. If a higher percentage of cells necrosed prior to the time of specimen collection and associated mRNA analysis, these cells would not contribute anything to

the measured gene expression levels. Therefore, the expression levels that were determined would have been unevenly weighted toward the remaining living cells in the specimen and would not register the changes that occurred to cause the cell death. Results of a histological analysis would identify the relative number of living/dead cells in one specimen compared to another and would aid in interpretation of the accuracy of the gene expression results. Staining for aggrecan and collagen content would also provide an evidence of the physical changes to the cartilage matrix. This could be quite valuable as an indication of the changes wrought by the detected gene expression levels. As part of our ongoing work, a histological analysis of tissue from this study will be conducted at a future date.

Another challenge of this type of *in vitro* analysis is keeping cells in culture. Articular cartilage in the *in vivo* joint is in the presence of synovial fluid that is responsible for providing nutrients. As the joint is exercised, the cartilage is compressed under loading which exudes fluid from the matrix, and then as it relaxes during unloading, proteoglycan charge draws in more nutrient rich fluid for the chondrocytes. This "pumping" action is what both delivers nutrients to the chondrocytes, and removes wastes. However, when cartilage is maintained in culture, the nutrients are required to diffuse from the media through the matrix with no driving force or "pumping" action. This lack of nutrient delivery and associated waste removal likely contributes to the changes observed in gene expression over time. A non-impacted control treatment was kept in culture as well in order to determine which changes in gene expression of the impacted specimens were

due to impact treatment as opposed to culture conditions. In fact, joint immobilization is one model used for studying early-stage OA. With this method, a joint's movement is either minimized or completely inhibited and changes are observed *in vivo*. For example, Hall studied joint immobilization in rats by wiring the femur and tibia together to enforce immobility [30] . He found degeneration in the unloaded cartilage with necrotic tissue and fibrillation of the cartilage surface. One study of immobilized canine knee joints found decreased levels of *timps* (variant not specified) but no changes in matrix metalloproteinase -3 (*mmp-3*) [167]. Two other *mmps*, *mmp-8* and *mmp-13,* were found to be up-regulated in rats with immobilized knee joints after 4-weeks [168]. The knees were immobilized with an internal fixator. These findings are similar to ours, in that we found relatively small changes in both *timp-1* and *2* over time, and a relatively small change in *mmp-3* over time in comparison to *mmp-13*.

However, it would be desirable to develop a system for future experiments to deliver reasonable, physiologically relevant loads in culture on a daily basis during the course of the culture period. This would allow the experiment to more closely approximate an *in vivo* study. It is believed that applying a load across the surface of the cartilage while in culture on a daily basis (or more frequently depending on the experiment) may provide a pumping action of sorts, to aid in diffusion of the nutrients through the articular cartilage matrix. This would potentially reduce the changes observed in gene expression due to culture conditions.

The time points chosen in this experiment were based on previous work in our lab and literature findings. In this analysis however, changes were observed at the day 0 time point which was approximately 2 hours after load delivery. It would be valuable to identify changes perhaps on an hourly basis following the mechanical insult. Additionally, the development of OA may take years to progress to the point of full thickness lesions or debilitation. Therefore, following changes over the first 2 weeks after an impact is potentially representative of only the very earliest stage of OA progression. It would be desirable to keep cartilage in culture for longer periods of time, however the challenge of keeping the cells alive for longer periods of time would possibly prove prohibitive. If a loading method, as described above, were used in culture, it may be possible to effectively extend the time that chondrocytes may be maintained viable in an *in vitro* environment.

It would be desirable in future work to obtain cartilage from a group of similar animals from the same genetic background and same age as much as is possible. This does necessarily increase the complexity and cost of the experiment. However, the ultimate aim of any basic research study is to have clinical relevance. A carefully controlled population of animals could contribute to reducing undesired errors or variability in the results and would potentially allow for clearer conclusions to be drawn. It is believed, though, that the findings here are relevant as they represent animals with a wide range of background, ages, and genetics that is applicable to the similar differences found in the human population.

Finally, the gene expression changes indicate which mRNA is present in the chondrocytes. However, mRNA levels are not conclusive in indicating what actions are occurring in the cells. The mRNA must be translated to protein to carry out actions in the cell, and these ultimate protein levels were not evaluated. Ongoing work is being conducted to measure the changes in protein following a mechanical injury.

6. CONCLUSION

The OA model used in this analysis aimed to initiate OA progression through an *in vitro* mechanical injury. While previous impact studies have used an impact normal to the cartilage surface, it was the aim of this study to evaluate both a load normal to the surface and a shear load delivered tangential to the surface. Gene expression changes were evaluated on the day of impact, and 3, 7, or 14 days after the mechanical injury.

A panel of 18 genes related to cartilage matrix constituents, degradative enzymes and their inhibitors, inflammatory response and signaling, and cell proliferation and apoptosis were evaluated for differential expression over time and compared to a non-impacted control. The relative rise of *col2a1* at day 3 in the shear specimens and the increased expression of *agc* and *sox-9* at the later time points may indicate that the shear specimens are mounting a stronger repair effort. However the increased expression of *col1a1* in the shear specimens may indicate a less effective repair. The decreased expression of degradative enzymes at the later time points may indicate less breakdown of the matrix, supporting the theory of a repair attempt being underway and an attempt at matrix preservation. This is corroborated by lowered expression of genes related to an inflammatory response at the later time points.

The findings from this study indicate that an impaction with higher shear forces may cause the chondrocytes to initiate more repair efforts than an impaction with primarily

normal forces. The shear treatment used may be more physiologically relevant to the study of early stage OA. It is hoped that the findings of this study will contribute to a greater understanding of the complex progression of cartilage breakdown during OA, and may aid future researchers in identification of targets for therapeutic intervention to slow or halt OA development.

7. REFERENCES

1. NIAMS. Osteoarthritis. In: NIAMS Ed. NIH, vol. 06-4617 2006.

2. Sharma L, Kapoor D, Issa S. Epidemiology of osteoarthritis: an update. Current Opinion in Rheumatology 2006; 18: 147.

3. Buckwalter J, Lane N. Athletics and osteoarthritis. The American Journal of Sports Medicine 1997; 25: 873.

4. Repo R, Finlay J. Survival of articular cartilage after controlled impact. The Journal of Bone and Joint Surgery 1977; 59: 1068.

5. Buckwalter JA, Brown TD. Joint Injury, Repair, and Remodeling: Roles in Post-Traumatic Osteoarthritis. Clinical Orthopaedics and Related Research 2004; 423: 7-16

6. Newberry W, Zukosky D, Haut R. Subfracture insult to a knee joint causes alterations in the bone and in the functional stiffness of overlying cartilage. Journal of Orthopaedic Research 1997; 15: 450-455.

7. Tomatsu T, Imai N, Takeuchi N. Experimentally produced fractures of articular cartilage and bone. Journal of Bone & Joint Surgery, British Volume 1992: 457-462.

8. Thompson R, Oegema T, Lewis J, Wallace L. Osteoarthrotic changes after acute transarticular load. An animal model. The Journal of Bone and Joint Surgery 1991; 73: 990.

9. Donohue J, Buss D, Oegema T, Thompson R. The effects of indirect blunt trauma on adult canine articular cartilage. The Journal of Bone and Joint Surgery 1983; 65: 948.

10. Mckinley M, O'Loughlin D. Human Anatomy. 2nd Edition., McGraw-Hill 2008.

11. Stockwell R, Scott J. Biology of Cartilage cells. Cambridge, UK, Cambridge University Press 1979.

12. Eyre D. Articular cartilage and changes in Arthritis: Collagen of articular cartilage. Arthritis Research 2002; 4: 30.

13. Knudson C, Knudson W. Cartilage proteoglycans. Seminars in Cell & Developmental Biology 2001; 12: 69-78.

14. Roth V, Mow V. The intrinsic tensile behavior of the matrix of bovine articular cartilage and its variation with age. The Journal of Bone and Joint Surgery 1980; 62: 1102.

15. Hultkrantz W. Ueber die Spaltrichtungen der Gelenkknorpel. Verh Ant Ges 1898; 12: 248-256.

16. Kahane J, Kahn A. India ink pinprick experiments on surface organization of cricoarytenoid joints. Journal of Speech, Language and Hearing Research 1986; 29: 544.

17. Wang Y, Ding C, Wluka AE, Davis S, Ebeling PR, Jones G, et al. Factors affecting progression of knee cartilage defects in normal subjects over 2 years. Rheumatology 2006; 45: 79.

18. Widuchowski W, Widuchowski J, Trzaska T. Articular cartilage defects: study of 25,124 knee arthroscopies. The Knee 2007; 14: 177-182.

19. Anderson J, Felson D. Factors associated with osteoarthritis of the knee in the first national Health and Nutrition Examination Survey (HANES I): evidence for an association with overweight, race, and physical demands of work. American Journal of Epidemiology 1988; 128: 179.

20. Dieppe P, Lohmander L. Pathogenesis and management of pain in osteoarthritis. The Lancet 2005; 365: 965-973.

21. Roos E. Joint injury causes knee osteoarthritis in young adults. Current opinion in rheumatology 2005; 17: 195.

22. Peyron J, Altman R. The epidemiology of osteoarthritis. Philadelphia, WB Saunders Co. 1992.

23. Yamada K, Healey R, Amiel D, Lotz M, Coutts R. Subchondral bone of the human knee joint in aging and osteoarthritis. Osteoarthritis and Cartilage 2002; 10: 360-369.

24. Hunziker E. Articular cartilage repair: basic science and clinical progress. A review of the current status and prospects. Osteoarthritis and Cartilage 2002; 10: 432-463.

25. Setton L, Elliott D, Mow V. Altered mechanics of cartilage with osteoarthritis: human osteoarthritis and an experimental model of joint degeneration. Osteoarthritis and Cartilage 1999; 7: 2-14.

26. Barnes E, Edwards N. Treatment of osteoarthritis. Southern Medical Journal 2005; 98: 205.

27. McAlindon T, LaValley M, Gulin J, Felson D. Glucosamine and chondroitin for treatment of osteoarthritis: a systematic quality assessment and meta-analysis. Jama 2000; 283: 1469.

28. Ameye L, Young M. Mice deficient in small leucine-rich proteoglycans: novel in vivo models for osteoporosis, osteoarthritis, Ehlers-Danlos syndrome, muscular dystrophy, and corneal diseases. Glycobiology 2002; 12: 107R.

29. Jurvelin J, Kiviranta I, TAMMI M, HELMINEN JH. Softening of Canine Articular Cartilage After Immobilization of the Knee Joint. Clinical Orthopaedics and Related Research 1986; 207: 246-252.

30. HALL M. Cartilage changes after experimental immobilization of the knee joint of the young rat. The Journal of Bone and Joint Surgery 1963; 45: 36.

31. Pritzker K. Animal models for osteoarthritis: processes, problems and prospects. Annals of the rheumatic diseases 1994; 53: 406.

32. Gelber A, Hochberg M, Mead L, Wang N, Wigley F, Klag M. Joint injury in young adults and risk for subsequent knee and hip osteoarthritis. Annals of Internal Medicine 2000; 133: 321.

33. Cooper C, Inskip H, Croft P, Campbell L, Smith G, Mclearn M, et al. Individual risk factors for hip osteoarthritis: obesity, hip injury and physical activity. American Journal of Epidemiology 1998; 147: 516.

34. Nelson F, Billinghurst R, Pidoux I, Reiner A, Langworthy M, McDermott M, et al. Early post-traumatic osteoarthritis-like changes in human articular cartilage following rupture of the anterior cruciate ligament. Osteoarthritis and Cartilage 2006; 14: 114-119.

35. Marshall KW, Chan AD. Bilateral canine model of osteoarthritis. J Rheumatol 1996; 23: 344-350.

36. Yoshioka M, Coutts RD, Amiel D, Hacker SA. Characterization of a model of osteoarthritis in the rabbit knee. Osteoarthritis and Cartilage 1996; 4: 87-98.

37. Suter E, Herzog W, Leonard T, Nguyen H. One-year changes in hind limb kinematics, ground reaction forces and knee stability in an experimental model of osteoarthritis. Journal of Biomechanics 1998; 31: 511-517.

38. Kamekura S, Hoshi K, Shimoaka T, Chung U, Chikuda H, Yamada T, et al. Osteoarthritis development in novel experimental mouse models induced by knee joint instability. Osteoarthritis and Cartilage 2005; 13: 632-641.

39. Brandt KD, Myers SL, Burr D, Albrecht M. Osteoarthritic changes in canine articular cartilage, subchondral bone, and synovium fifty-four months after transection of the anterior cruciate ligament. Arthritis Rheum 1991; 34: 1560-1570.

40. Vilensky J, O'Connor B, Brandt K, Dunn E, Rogers P, Delong C. Serial kinematic analysis of the unstable knee after transection of the anterior cruciate ligament:

temporal and angular changes in a canine model of osteoarthritis. Journal of Orthopaedic Research 2005; 12: 229-237.

41. Brandt KD, Schauwecker DS, Dansereau S, Meyer J, O'Connor B, Myers SL. Bone scintigraphy in the canine cruciate deficiency model of osteoarthritis. Comparison of the unstable and contralateral knee. J Rheumatol 1997; 24: 140-145.

42. Quinn T, Allen R, Schalet B, Perumbuli P, Hunziker E. Matrix and cell injury due to sub-impact loading of adult bovine articular cartilage explants: effects of strain rate and peak stress. Journal of Orthopaedic Research 2001; 19: 242-249.

43. Brandt K, Dieppe P, Radin E. Etiopathogenesis of osteoarthritis. Rheumatic Disease Clinics of North America 2008; 34: 531-559.

44. Smith R. Mechanical Loading effects on articular cartilage matrix metabolism and osteoarthritis. In: Osteoarthritis, Inflammation and Degradation: A Continuum., Buckwalter JA Ed.: IOS Press 2007:14-23.

45. Furman BD, Olson SA, Guilak F. The Development of Posttraumatic Arthritis After Articular Fracture. Journal of Orthopaedic Trauma 2006; 20: 719-725.

46. Newberry WN, Zukosky DK, Haut RC. Subfracture insult to a knee joint causes alterations in the bone and in the functional stiffness of overlying cartilage. Journal of Orthopaedic Research 1997; 15: 450-455.

47. Ewers B, Weaver B, Sevensma E, Haut R. Chronic changes in rabbit retro-patellar cartilage and subchondral bone after blunt impact loading of the patellofemoral joint. Journal of Orthopaedic Research 2002; 20: 545-550.

48. Haut R, Ide T, De Camp C. Mechanical responses of the rabbit patello-femoral joint to blunt impact. Journal of biomechanical engineering 1995; 117: 402.

49. Mente P. Analytic and In-vivo study of dynamic joint loading. In: Biomedical Engineering, vol. PhD. Evanston, IL: Northwestern University 1994.

50. Mente P, Lossing J, Dinola N, Chandler E. Chondrocyte necrosis and proliferation in mechanically impacted articular cartilage. In: Transactions of the 51st annual meeting of the Orthopedic Research Society. 2005.

51. Mente P, Lewis J, Oegama T, Jr., Thompson R, Jr. Damage after blunt trauma to a joint surface. In: Transactions of the 2nd Combined Meeting of Orthopedic Research Societies of USA, Japan, Canada and Europe, vol. 2 1995:125.

52. Mente P, Lossing J, NE D. Quantification of Chondrocyte Necrosis in Mechaically impacted articular Cartilage. In: Transactions of the 5th Combined Meeting of the Orthopedic Research Societies of USA, Japan, Canada, and Europe 2004.

53. Newberry W, Mackenzie C, Haut R. Blunt impact causes changes in bone and cartilage in a regularly exercised animal model. Journal of Orthopaedic Research 1998; 16: 348-354.

54. Jeffrey J, Brodie J, Aspden R. The effects of a single fast impact load compared with slow severe loading on articular cartilage in vitro. Osteoarthritis and Cartilage 2006; 14: S81.

55. Torzilli P, Grigiene R, Borrelli Jr J, Helfet D. Effect of impact load on articular cartilage: cell metabolism and viability, and matrix water content. Journal of biomechanical engineering 1999; 121: 433.

56. Flachsmann E, Broom N, Oloyede A. A biomechanical investigation of unconstrained shear failure of the osteochondral region under impact loading. Clinical Biomechanics 1995; 10: 156-165.

57. Ficklin T, Thomas G, Barthel J, Asanbaeva A, Thonar E, Masuda K, et al. Articular cartilage mechanical and biochemical property relations before and after in vitro growth. Journal of Biomechanics 2007; 40: 3607-3614.

58. Hashimoto S, Nishiyama T, Hayashi S. Shear stress induced apoptosis of human chondrocytes via p53 pathway. In: ICRS. Warsaw, Poland 2007:B138.

59. Salzmann G, Nuernberger B, Schmitz P, Anton M, Stoddart M, Grad S, et al. Physicobiochemical Synergism Through Gene Therapy and Functional Tissue Engineering for In Vitro Chondrogenesis. Tissue Engineering Part A 2009; 15: 2513-2524.

60. Waldman S, Couto D, Grynpas M, Pilliar R, Kandel R. Multi-axial mechanical stimulation of tissue engineered cartilage: review. Eur Cell Mater 2007; 13: 66-73.

61. Wilson W, van Burken C, van Donkelaar C, Buma P, van Rietbergen B, Huiskes R. Causes of mechanically induced collagen damage in articular cartilage. Journal of Orthopaedic Research 2006; 24: 220-228.

62. Radin E, Martin R, Burr D, Caterson B, Boyd R, Goodwin C. Effects of mechanical loading on the tissues of the rabbit knee. Journal of Orthopaedic Research 1984; 2: 221-234.

63. Chen Q. Mouse models and new therapeutic targets for OA. J Musculoskelet Neuronal Interact 2008; 8: 311-312.

64. Ewers B, Dvoracek-Driksna D, Orth M, Haut R. The extent of matrix damage and chondrocyte death in mechanically traumatized articular cartilage explants depends on rate of loading. Journal of Orthopaedic Research 2001; 19: 779-784.

65. Ashwell M, O'Nan A, Gonda M, Mente P. Gene expression profiling of chondrocytes from a porcine impact injury model. Osteoarthritis and Cartilage 2008; 16: 936-946.

66. Clements K, Bee Z, Crossingham G, Adams M, Sharif M. How severe must repetitive loading be to kill chondrocytes in articular cartilage? Osteoarthritis and Cartilage 2001; 9: 499-507.

67. Aigner T, Dudhia J. Genomics of osteoarthritis. Current Opinion in Rheumatology 2003; 15: 634-640.

68. Aigner T, Zien A, Hanisch D, Zimmer R. Gene expression in chondrocytes assessed with use of microarrays. The Journal of Bone and Joint Surgery 2003; 85: 117.

69. Zwicky R, Baici A. Cytoskeletal architecture and cathepsin B trafficking in human articular chondrocytes. Histochemistry and Cell Biology 2000; 114: 363-372.

70. Yager T, Dempsey A, Tang H, Stamatiou D, Chao S, Marshall K, et al. First comprehensive mapping of cartilage transcripts to the human genome. Genomics 2004; 84: 524-535.

71. Dell'Accio F, De Bari C, Eltawil N, Vanhummelen P, Pitzalis C. Identification of the molecular response of articular cartilage to injury, by microarray screening. Arthritis & Rheumatism 2008; 58: 1410-1421.

72. Macsai C, Hopwood B, Zannettino A, Scherer M. Micro-CT and micro-array analyses of growth plate cartilage injury responses and bony repair. Bone 2009: 1090.

73. Wang W, Guo X, Duan C, Ma W, Zhang Y, Xu P, et al. Comparative analysis of gene expression profiles between the normal human cartilage and the one with endemic osteoarthritis. Osteoarthritis and Cartilage 2009; 17: 83-90.

74. Buckley M, Gleghorn J, Cohen I, Bonassar L. Depth dependence of shear properties in articular cartilage. Transactions of the 53rd Annual Meeting of the Orthopaedic Research Society 2007.

75. Fitzgerald J, Jin M, Grodzinsky A. Shear and compression differentially regulate clusters of functionally related temporal transcription patterns in cartilage tissue. Journal of Biological Chemistry 2006; 281: 24095.

76. Meng J, Ma X, Ma D, Xu C. Microarray analysis of differential gene expression in temporomandibular joint condylar cartilage after experimentally induced osteoarthritis. Osteoarthritis and Cartilage 2005; 13: 1115-1125.

77. Wong M, Siegrist M, Goodwin K. Cyclic tensile strain and cyclic hydrostatic pressure differentially regulate expression of hypertrophic markers in primary chondrocytes. Bone 2003; 33: 685-693.

78. Giannoni P, Siegrist M, Hunziker E, Wong M. The mechanosensitivity of cartilage oligomeric matrix protein (COMP) Biorheology 2003; 40: 101-109.

79. Lee C, Grad S, MacLean J, Iatridis J, Alini M. Effect of mechanical loading on mRNA levels of common endogenous controls in articular chondrocytes and intervertebral disk. Analytical biochemistry 2005; 341: 372-375.

80. Brew C, Clegg P, Boot-handford R, Andrews G, Hardingham T. Gene expression in human chondrocytes in late OA is changed in both fibrillated and intact cartilage without evidence of generalised chondrocyte hypertrophy. British Medical Journal 2008.

81. Lee J, Fitzgerald J, DiMicco M, Grodzinsky A. Mechanical injury of cartilage explants causes specific time-dependent changes in chondrocyte gene expression. Arthritis Care & Research 2005; 52: 2386-2395.

82. Karlsson C, Dehne T, Lindahl A, Brittberg M. Genome-wide expression profiling reveals new candidate genes associated with osteoarthritis. Osteoarthritis and Cartilage 2010: 1102.

83. Fehrenbacher A, Steck E, Rickert M, Roth W, Richter W. Rapid regulation of collagen but not metalloproteinase 1, 3, 13, 14 and tissue inhibitor of metalloproteinase 1, 2, 3 expression in response to mechanical loading of cartilage explants in vitro. Archives of Biochemistry and Biophysics 2003; 410: 39-47.

84. Fitzgerald J, Jin M, Dean D, Wood D, Zheng M, Grodzinsky A. Mechanical compression of cartilage explants induces multiple time-dependent gene expression patterns and involves intracellular calcium and cyclic AMP. Journal of Biological Chemistry 2004; 279: 19502.

85. Natoli R, Scott C, Athanasiou K. Temporal Effects of Impact on Articular Cartilage Cell Death, Gene Expression, matrix biochemistry, and biomechanics. Annals of Biomedical Engineering 2008; 36(5): 780-792.

86. Mow VC, Huiskes R. Basic Orthopedic Biomechanics and Mechano-Biology 3rd edition. Lippincott, Williams, and Wilkins: 2005.

87. Swingler T, Waters J, Davidson R, Pennington C, Puente X, Darrah C, et al. Degradome expression profiling in human articular cartilage. Arthritis Research & Therapy 2009; 11: R96.

88. Shen Z, Heinegård D, Sommarin Y. Distribution and expression of cartilage oligomeric matrix protein and bone sialoprotein show marked changes during rat femoral head development. Matrix Biology 1995; 14: 773-781.

89. Grad S, Lee C, Gorna K, Gogolewski S, Wimmer M, Alini M. Surface motion upregulates superficial zone protein and hyaluronan production in chondrocyte-seeded three-dimensional scaffolds. Tissue Engineering 2005; 11: 249-256.

90. Martel-Pelletier J, Boileau C, Pelletier J, Roughley P. Cartilage in normal and osteoarthritis conditions. Best Practice & Research Clinical Rheumatology 2008; 22: 351-384.

91. Sekiya I, Tsuji K, Koopman P, Watanabe H, Yamada Y, Shinomiya K, et al. SOX9 enhances aggrecan gene promoter/enhancer activity and is up-regulated by retinoic acid in a cartilage-derived cell line, TC6. Journal of Biological Chemistry 2000; 275: 10738.

92. Ijiri K, Zerbini LF, Peng H, Otu HH, Tsuchimochi K, Otero M, et al. Differential expression of GADD45β in normal and osteoarthritic cartilage: Potential role in homeostasis of articular chondrocytes. Arthritis & Rheumatism 2008; 58: 2075-2087.

93. Tchetina E, Squires G, Poole A. Increased type II collagen degradation and very early focal cartilage degeneration is associated with upregulation of chondrocyte differentiation related genes in early human articular cartilage lesions. The Journal of Rheumatology 2005; 32: 876.

94. Nakase T, Sugimoto M, Sato M, Kaneko M, Tomita T, Sugamoto K, et al. Switch of osteonectin and osteopontin mRNA expression in the process of cartilage-to-bone transition during fracture repair. Acta Histochem 1998; 100: 287-295.

95. Martin I, Jakob M, Schäfer D, Dick W, Spagnoli G, Heberer M. Quantitative analysis of gene expression in human articular cartilage from normal and osteoarthritic joints. Osteoarthritis and Cartilage 2001; 9: 112-118.

96. Yagi R, McBurney D, Laverty D, Weiner S, Horton W. Intrajoint comparisons of gene expression patterns in human osteoarthritis suggest a change in chondrocyte phenotype. Journal of Orthopaedic Research 2005; 23: 1128-1138.

97. Pullig O, Weseloh G, Gauer S, Swoboda B. Osteopontin is expressed by adult human osteoarthritic chondrocytes: protein and mRNA analysis of normal and osteoarthritic cartilage. Matrix Biology 2000; 19: 245-255.

98. Nygard A, Jørgensen C, Cirera S, Fredholm M. Selection of reference genes for gene expression studies in pig tissues using SYBR green qPCR. BMC molecular biology 2007; 8: 67.

99. Radin E, EHRLICH M, Chernack R, Abernethy P, PAUL I, ROSE R. Effect of repetitive impulsive loading on the knee joints of rabbits. Clinical Orthopaedics and related research 1978; 131: 288.

100. Wong M, Carter D. Articular cartilage functional histomorphology and mechanobiology: a research perspective. Bone 2003; 33: 1-13.

101. Vilim V, Olejarova M, Macháek S, Gatterova J, Kraus V, Pavelka K. Serum levels of cartilage oligomeric matrix protein (COMP) correlate with radiographic progression of knee osteoarthritis. Osteoarthritis and Cartilage 2002; 10: 707-713.

102. Salminen H, Perälä M, Lorenzo P, Saxne T, Heinegård D, Säämänen A, et al. Up-regulation of cartilage oligomeric matrix protein at the onset of articular cartilage degeneration in a transgenic mouse model of osteoarthritis. Arthritis & Rheumatism 2000; 43: 1742-1748.

103. Koelling S, Clauditz T, Kaste M, Miosge N. Cartilage oligomeric matrix protein is involved in human limb development and in the pathogenesis of osteoarthritis. Arthritis Research and Therapy 2006; 8: 56.

104. Aigner T, Haag J, Zimmer R. Functional genomics, evo-devo and systems biology: a chance to overcome complexity? Current Opinion in Rheumatology 2007; 19: 463.

105. Burton-Wurster N, Mateescu R, Todhunter R, Clements K, Sun Q, Scarpino V, et al. Genes in canine articular cartilage that respond to mechanical injury: gene expression studies with Affymetrix canine GeneChip. Journal of Heredity 2005; 96: 821.

106. Wahl SM, McCartney-Francis N, Mergenhagen SE. Inflammatory and immunomodulatory roles of TGF-[beta]. Immunology today 1989; 10: 258-261.

107. Moos V, Sieper J, Herzog V, Müller B. Regulation of expression of cytokines and growth factors in osteoarthritic cartilage explants. Clinical Rheumatology 2001; 20: 353-358.

108. Blaney D, Van der Kraan P. TGF-beta and osteoarthritis. Experimental Rheumatology and Advanced Therapeutics 2007; 15: 597-604.

109. Später D, Hill T, O'Sullivan R, Gruber M, Conner D, Hartmann C. Wnt9a signaling is required for joint integrity and regulation of Ihh during chondrogenesis. Development 2006; 133: 3039.

110. Kim SY, Im GI. The expressions of SOX trio, PTHRP/IHH in surgically-induced osteoarthritis of the rat. Cell Biol Int 2010; 12: 12.

111. Recklies A, Ling H, White C, Bernier S. Inflammatory cytokines induce production of CHI3L1 by articular chondrocytes. Journal of Biological Chemistry 2005; 280: 41213.

112. Birgitte Volck KØ, Julia Johansen, Charly Garbarsch, P.A Price. The Distribution of YKL-40 in Osteoarthritic and Normal Human Articular Cartilage. Scandinavian Journal of Rheumatology 1999; 28: 171-179.

113. Johansen J, Olee T, Price P, Hashimoto S, Ochs R, Lotz M. Regulation of YKL-40 production by human articular chondrocytes. Arthritis & Rheumatism 2001; 44: 826-837.

114. Abramson S. The role of COX-2 produced by cartilage in arthritis. Osteoarthritis and Cartilage 1999; 7: 380-381.

115. Henrotin Y, Bruckner P, Pujol J. The role of reactive oxygen species in homeostasis and degradation of cartilage. Osteoarthritis and Cartilage 2003; 11: 747-755.

116. Amin AR, Attur M, Patel RN, Thakker GD, Marshall PJ, Rediske J, et al. Superinduction of cyclooxygenase-2 activity in human osteoarthritis-affected cartilage. Influence of nitric oxide. Journal of Clinical Investigation 1997; 99: 1231.

117. Scher J, Pillinger M, Abramson S. Nitric oxide synthases and osteoarthritis. Current Rheumatology Reports 2007; 9: 9-15.

118. Pelletier JP, Lascau-Coman V, Jovanovic D, Fernandes JC, Manning P, Connor JR, et al. Selective inhibition of inducible nitric oxide synthase in experimental osteoarthritis is associated with reduction in tissue levels of catabolic factors. J Rheumatol 1999; 26: 2002-2014.

119. Barve R, Minnerly J, Weiss D, Meyer D, Aguiar D, Sullivan P, et al. Transcriptional profiling and pathway analysis of monosodium iodoacetate-induced experimental osteoarthritis in rats: relevance to human disease. Osteoarthritis and Cartilage 2007; 15: 1190-1198.

120. Jeffrey J, Aspden R. Cyclooxygenase inhibition lowers prostaglandin E2 release from articular cartilage and reduces apoptosis but not proteoglycan degradation following an impact load in vitro. Arthritis Research & Therapy 2007; 9: R129.

121. D'Lima D, Hermida J, Hashimoto S, Colwell C, Lotz M. Caspase inhibitors reduce severity of cartilage lesions in experimental osteoarthritis. Arthritis & Rheumatism 2006; 54: 1814-1821.

122. Pennock A, Robertson C, Emmerson B, Harwood F, Amiel D. Role of apoptotic and matrix-degrading genes in articular cartilage and meniscus of mature and aged rabbits during development of osteoarthritis. Arthritis & Rheumatism 2007; 56: 1529-1536.

123. Clements D, Carter S, Innes J, Ollier W, Day P. Gene expression profiling of normal and ruptured canine anterior cruciate ligaments. Osteoarthritis and Cartilage 2008; 16: 195-203.

124. Hashimoto S, Setareh M, Ochs R, Lotz M. Fas/Fas ligand expression and induction of apoptosis in chondrocytes. Arthritis & Rheumatism 1997; 40: 1749-1755.

125. Wei L, Sun X, Wang Z, Chen Q. CD95-induced osteoarthritic chondrocyte apoptosis and necrosis: dependency on p38 mitogen-activated protein kinase. Arthritis Research and Therapy 2006; 8: 37.

126. Kim HA, Lee YJ, Seong SC, Choe KW, Song YW. Apoptotic chondrocyte death in human osteoarthritis. J Rheumatol 2000; 27: 455-462.

127. Flannery C, Little C, Caterson B, Hughes C. Effects of culture conditions and exposure to catabolic stimulators (IL-1 and retinoic acid) on the expression of matrix metalloproteinases (MMPs) and disintegrin metalloproteinases (ADAMs) by articular cartilage chondrocytes. Matrix Biology 1999; 18: 225-237.

128. Darling E, Hu J, Athanasiou K. Zonal and topographical differences in articular cartilage gene expression. Journal of Orthopaedic Research 2004; 22: 1182-1187.

129. Honda K, Ohno S, Tanimoto K, Ijuin C, Tanaka N, Doi T, et al. The effects of high magnitude cyclic tensile load on cartilage matrix metabolism in cultured chondrocytes. European journal of cell biology 2000; 79: 601-609.

130. Pombo-Suarez M, Calaza M, Gomez-Reino J, Gonzalez A. Reference genes for normalization of gene expression studies in human osteoarthritic articular cartilage. BMC Molecular Biology 2008; 9: 17.

131. Ayers D, Clements D, Salway F, Day P. Expression stability of commonly used reference genes in canine articular connective tissues. BMC Veterinary Research 2007; 3: 7.

132. Young A, Smith M, Smith S, Cake M, Ghosh P, Read R, et al. Regional assessment of articular cartilage gene expression and small proteoglycan

metabolism in an animal model of osteoarthritis. Arthritis Res Ther 2005; 7: R852-861.

133. Vandesompele J, De Preter K, Pattyn F, Poppe B, Van Roy N, De Paepe A, et al. Accurate normalization of real-time quantitative RT-PCR data by geometric averaging of multiple internal control genes. Genome biology 2002; 3.

134. Pfaffl M, Tichopad A, Prgomet C, Neuvians T. Determination of stable housekeeping genes, differentially regulated target genes and sample integrity: BestKeeper–Excel-based tool using pair-wise correlations. Biotechnology letters 2004; 26: 509-515.

135. Collins-Racie L, Yang Z, Arai M, Li N, Majumdar M, Nagpal S, et al. Global analysis of nuclear receptor expression and dysregulation in human osteoarthritic articular cartilage Reduced LXR signaling contributes to catabolic metabolism typical of osteoarthritis. Osteoarthritis and Cartilage 2009; 17: 939-949.

136. Fundel K, Haag J, Gebhard P, Zimmer R, Aigner T. Normalization strategies for mRNA expression data in cartilage research. Osteoarthritis and Cartilage 2008; 16: 947-955.

137. Nishimura M, Nikawa T, Kawano Y, Nakayama M, Ikeda M. Effects of dimethyl sulfoxide and dexamethasone on mRNA expression of housekeeping genes in cultures of C2C12 myotubes. Biochemical and Biophysical Research Communications 2008; 367: 603-608.

138. Watson S, Mercier S, Bye C, Wilkinson J, Cunningham A, Harman A. Determination of suitable housekeeping genes for normalisation of quantitative real time PCR analysis of cells infected with human immunodeficiency virus and herpes viruses. Virology Journal 2007 4:130 2007; 4: 130.

139. Geyer M, Grässel S, Straub R, Schett G, Dinser R, Grifka J, et al. Differential transcriptome analysis of intraarticular lesional vs intact cartilage reveals new candidate genes in osteoarthritis pathophysiology. Osteoarthritis and Cartilage 2009; 17: 328-335.

140. Thomson E, Vincent R. Reagent volume and plate bias in real-time polymerase chain reaction. Analytical biochemistry 2005; 337: 347-350.

141. Steibel J, Poletto R, Coussens P, Rosa G. A powerful and flexible linear mixed model framework for the analysis of relative quantification RT-PCR data. Genomics 2009; 94: 146-152.

142. Benjamini Y, Hochberg Y. Controlling the false discovery rate: a practical and powerful approach to multiple testing. Journal of the Royal Statistical Society. Series B (Methodological) 1995; 57: 289-300.

143. Verhoeven K, Simonsen K, McIntyre L. Implementing false discovery rate control: increasing your power. Oikos 2005; 108: 643-647.

144. Reiner A, Yekutieli D, Benjamini Y. Identifying differentially expressed genes using false discovery rate controlling procedures. Bioinformatics 2003; 19: 368.

145. Vandesompele J. geNorm User Manual. In: 2008.

146. Erkens T, Van Poucke M, Vandesompele J, Goossens K, Van Zeveren A, Peelman L. Development of a new set of reference genes for normalization of real-time RT-PCR data of porcine backfat and longissimus dorsi muscle, and evaluation with PPARGC 1 A. BMC biotechnology 2006; 6: 41.

147. Svobodová K, Bílek K, Knoll A. Verification of reference genes for relative quantification of gene expression by real-time reverse transcription PCR in the pig. J Appl Genet 2008; 49: 263-265.

148. Kuijk E, du Puy L, van Tol H, Haagsman H, Colenbrander B, Roelen B. Validation of reference genes for quantitative RT-PCR studies in porcine oocytes and preimplantation embryos. BMC Developmental Biology 2007 7:58 2007; 7: 58.

149. Piórkowska K, Oczkowicz M, Rózyck M. Novel porcine housekeeping genes for real-time RT-PCR experiments normalization in adipose tissue: Assessment of leptin mRNA quantity in different pig breeds. Meat Science 2010.

150. Fujisawa T, Hattori T, Takahashi K, Kuboki T, Yamashita A, Takigawa M. Cyclic mechanical stress induces extracellular matrix degradation in cultured

chondrocytes via gene expression of matrix metalloproteinases and interleukin-1. Journal of Biochemistry 1999; 125: 966.

151. Millward-Sadler S, Wright M, Davies L, Nuki G, Salter D, Foundation N, et al. Mechanotransduction via integrins and interleukin-4 results in altered aggrecan and matrix metalloproteinase 3 gene expression in normal, but not osteoarthritic, human articular chondrocytes. Arthritis Care & Research 2000; 43: 2091-2099.

152. Wheeler C, Jafarzadeh S, Rocke D, Grodzinsky A. IGF-1 does not moderate the time-dependent transcriptional patterns of key homeostatic genes induced by sustained compression of bovine cartilage. Osteoarthritis and Cartilage 2009; 17: 930-938.

153. Natoli R, Scott C, Athanasiou K. Temporal effects of impact on articular cartilage cell death, gene expression, matrix biochemistry, and biomechanics. Annals of Biomedical Engineering 2008; 36: 780-792.

154. Sandell L, Aigner T. Articular cartilage and changes in arthritis. An introduction: cell biology of osteoarthritis. Arthritis Res 2001; 3: 107-113.

155. M. J. Seibel SPR, John P. Bilezikian. Dynamics of bone and cartilage metabolism. Elsevier, Inc. 2006.

156. Blain EJ, Gilbert SJ, Wardale RJ, Capper S, Mason DJ, Duance VC. Up-regulation of matrix metalloproteinase expression and activation following cyclical compressive loading of articular cartilage in vitro. Archives of biochemistry and biophysics 2001; 396: 49-55.

157. Hung KY, Chen CT, Huang JW, Lee PH, Tsai TJ, Hsieh BS. Dipyridamole inhibits TGF-&bgr;–induced collagen gene expression in human peritoneal mesothelial cells. Kidney International 2001; 60: 1249-1257.

158. Van den Berg W, Van de Loo F. Animal models of arthritis in NOS2-deficient mice. Osteoarthritis and Cartilage 1999; 7: 413-415.

159. Attur M, Al-Mussawir HE, Patel J, Kitay A, Dave M, Palmer G, et al. Prostaglandin E2 exerts catabolic effects in osteoarthritis cartilage: evidence for signaling via the EP4 receptor. The Journal of Immunology 2008; 181: 5082.

160. Ryu YS, Lee JH, Seok JH, Hong JH, Lee YS, Lim JH, et al. Acetaminophen Inhibits iNOS Gene Expression in RAW 264.7 Macrophages: Differential Regulation of NF-[kappa] B by Acetaminophen and Salicylates. Biochemical and Biophysical Research Communications 2000; 272: 758-764.

161. Wang WW, Smith DLH, Zucker SD. Bilirubin inhibits iNOS expression and NO production in response to endotoxin in rats. Hepatology 2004; 40: 424-433.

162. Wu F, Tyml K, Wilson JX. Ascorbate inhibits iNOS expression in endotoxin-and IFN [gamma]-stimulated rat skeletal muscle endothelial cells. FEBS letters 2002; 520: 122-126.

163. Eurich K, Segawa M, Toei-Shimizu S, Mizoguchi E. Potential role of chitinase 3-like-1 in inflammation-associated carcinogenic changes of epithelial cells. World Journal of Gastroenterology : WJG 2009; 15: 5249.

164. Trudel G, Recklies A, Laneuville O. Increased Expression of Chitinase 3-like Protein 1 Secondary to Joint Immobility. Clinical Orthopaedics and Related Research 2007; 456: 92-97.

165. Todd Allen R, Robertson C, Harwood F, Sasho T, Williams S, Pomerleau A, et al. Characterization of mature vs aged rabbit articular cartilage: analysis of cell density, apoptosis-related gene expression and mechanisms controlling chondrocyte apoptosis1. Osteoarthritis and Cartilage 2004; 12: 917-923.

166. Siravuri K. Quantification of Chondrocyte Apoptosis in Mechanically Impacted Articular Cartilage. In: Biomedical Engineering, vol. MS: North Carolina State University 2007.

167. Haapala J, Arokoski J, Ronkko S, Agren U, Kosma V, Lohmander L, et al. Decline after immobilisation and recovery after remobilisation of synovial fluid IL1, TIMP, and chondroitin sulphate levels in young beagle dogs. British Medical Journal 2001; 60: 55.

168. Ando A, Hagiwara Y, Tsuchiya M, Onoda Y, Suda H, Chimoto E, et al. Increased Expression of Metalloproteinase-8 and-13 on Articular Cartilage in a Rat Immobilized Knee Model. The Tohoku Journal of Experimental Medicine 2009; 217: 271-278.